Design, Synthesis and Biological Evaluation of Novel Dopamine D_2/D_3 Receptor Ligands

Inaugural dissertation

for the attainment of the title of doctor
in the Faculty of Mathematics and Natural Sciences
at the Heinrich Heine University Düsseldorf

presented by

Cristian Di Biase
from Campobasso, Italy

Düsseldorf, August 2024

from the Institute for Pharmaceutical and Medicinal Chemistry
at the Heinrich Heine University Düsseldorf

Published by permission of the
Faculty of Mathematics and Natural Sciences at
Heinrich Heine University Düsseldorf

Supervisor: Univ. Prof. Dr. Dr. h.c. Holger Stark

Co-supervisor: Univ. Prof. Dr. Constantin Czekelius

Date of the oral examination: 08.01.2025

Affidavit

I declare under oath that I have produced my thesis independently and without any undue assistance by third parties under consideration of the 'Principles for the Safeguarding of Good Scientific Practice at Heinrich Heine University Düsseldorf'.

Cristian Di Biase

Table of Contents

1 Introduction 1

1.1 Dopamine 1

1.1.1 Dopamine receptor subtypes 4

1.1.2 Dopamine D_2/D_3 receptor ligands 16

1.2 Schizophrenia 33

2 Project description and objectives 38

3 Chemistry 41

3.1 Sulphur-based dopamine D_2/D_3 receptor ligands 42

3.2 Dopamine D_2/D_3 receptor ligands with aromatic linker variations 65

3.3 Substituted-anilino-ethyl linker-based dopamine D_2/D_3 receptor ligands 71

4 Pharmacology and SAR 85

4.1 Pharmacological Evaluation 85

4.2 Drug-likeness analysis 89

4.3 Sulphur-based dopamine D_2/D_3 receptor ligands 91

4.4 Dopamine D_2/D_3 receptor ligands with aromatic linker variations 97

4.5 Substituted-anilino-ethyl linker-based dopamine D_2/D_3 receptor ligands 104

5. Summary 117

6 Experimental Section 120

6.1 Chemistry 120

6.1.1 General Methods 121

6.1.2 Synthesis Procedures 124

6.2 Pharmacological Assays 183

6.2.1 Cell culture and membrane preparation of CHO cells expressing the human dopamine D_{2s} and D_3 receptors 183

6.2.2 Radioligand displacement assays at the human D_{2s} and D_3 receptors 183

7 References 184

List of Abbreviations

ACN	acetonitrile
Ac_2O	acetic anhydride
AcOH	acetic acid
ADHD	attention deficit/hyperactivity disorder
Ar	aryl-moiety
Ar-Bmd	benzamide and benzensulfonamide moieties
Ar-Pip	aryl-piperazine
Ar-Ur	aromatic urea moieties
BBB	blood brain barrier
cAMP	cyclic adenosine monophosphate
CNS	central nervous system
DARPP-32	dopamine and cAMP regulated phosphoprotein
DAT	dopamine transporter
DCM	dichloromethane
DCE	dichloroethane
DIBALH	diisobutylaluminium hydride
DIPEA	*N,N*-diisopropylethylamine
DMF	dimethylformamide
DMP	Dess-Martin periodinane
DMSO	dimethylsulfoxide
DOPAC	*3,4*-dihydroxyphenylacetic acid
ECL	extracellular loop
EDG	electron donating group

EPS	extrapyramidal side effects
ERK	extracellular signal regulated kinase
Et_2O	diethylether
EtOAc	ethyl acetate
EtOH	ethanol
EWG	electron withdrawing group
FDA	U.S. Food and Drug Administration
FGAs	first generation antipsychotics
GABA	γ-aminobutyric acid
GIRKs	G-protein-coupled inwardly rectifying potassium channels
GPCRs	G-protein-coupled receptors
GRKs	G-protein-coupled receptor kinases
GSK_3	glycogen synthase 3
GTP	guanosine triphosphate
HATU	hexafluorophosphate azabenzotriazole tetramethyl uronium
HOMO	highest occupied molecular orbital
HVA	homovanillic acid
HWE	Horner-Wadsworth-Emmons reaction
iPrOH	isopropanol
K_i	inhibition constant
LUMO	lowest unoccupied molecular orbital
MAPK	mitogen activated protein kinase
m-CPBA	*meta*-chloroperbenzoic acid
MeOH	methanol
NH_2	aniline

NMDA	*N*-methyl-*D*-aspartate
OBS	orthosteric binding site
OC	oxalyl chloride
PD	Parkinson's disease
PDC	pyridinium dichromate
PET	positron emission tomography
PKA	protein kinase A
PKC	protein kinase C
PLC	phospholipase C
PP	primary pharmacophore
PSA	polar surface area
RGS	regulators of G-protein signalling
Ro5	Lipinski's rule of five
SAR	structure activity relationships
SBP	second binding pocket
SBP_2	additional second binding pocket
SGAs	second generation antipsychotics
$SONH_2$/CONH	sulphonamide or amide
SP	secondary pharmacophore
TEA	triethylamine
TGAs	third generation antipsychotics
TGA/SGA	therapeutic association with second and third generation antipsychotics
THF	tetrahydrofuran
TM	transmembrane helix
VTA	ventral tegmental area

1 Introduction

1.1 Dopamine

Dopamine is one of the endogenous neurotransmitters in human body and it belongs to the group of catecholamines. Firstly described by Carlsson in 1958,[1] dopamine is considered the major monoamine transmitter, as it is involved in crucial mechanisms of human brain such as motion, cognition, emotions, reward and reproductive behaviours.[2] Biosynthesis of dopamine starts from aromatic amino acid L-tyrosine and occurs in the presynaptic terminals of dopaminergic or adrenergic neurons, in central and peripheral tissues. However, L-tyrosine can be obtained from phenylalanine through the enzyme phenylalanine hydroxylase, representing an alternative beginning for biosynthesis of dopamine.[3] Two reactions are responsible of conversion from L-tyrosine to dopamine: hydroxylation and decarboxylation catalysed respectively by tyrosine-3-monooxygenase commonly known as tyrosine hydroxylase and aromatic L-amino acid decarboxylase, also known as DOPA decarboxylase. Once synthetized in dopaminergic neurons, dopamine is collected into acidic lumen of synaptic vesicles thanks to vesicular monoamine transporter 2[4] and it is released in the synaptic cleft under an action potential. On the other hand, in adrenergic and noradrenergic neurons, dopamine undergoes two additional reactions because it is the biochemical precursor of norepinephrine and epinephrine. The sequential modifications are catalysed by dopamine-β-hydroxylase and phenylethanolamine *N*-methyltransferase (Figure 1).[5,6]

The acidic environment of storage vesicles has the further function of preventing dopamine from its degradation.[7] Indeed, the metabolism of dopamine starts in the cytosol of neuronal cells with an oxidative deamination catalysed by monoamine oxidase B (MAO-B) and to a lesser extent by monoamine oxidase A (MAO-A). As a result, 3,4-dihydroxyphenylacetaldehyde (DOPAL) is obtained and it is converted into 3,4-dihydroxyphenylacetic acid (DOPAC) by the enzyme aldehyde dehydrogenase. Subsequently, 3-O-methylation of DOPAC leads to formation of homovanillic acid (HVA) which is one of the main catabolites of dopamine. The latter reaction is performed by catechol-O-methyltransferase that generally transfers methyl groups from S-adenosylmethionine to hydroxy groups of catecholamines.[8] Moreover, dopamine and its metabolites can be converted to phase II conjugates before excretion. This might occur in the brain and in the peripheral nervous system. For instance, O-sulfatation is catalysed by phenolsulfotransferases that transfer a sulphate unit from 3'-phosphoadenosine-5'-phosphosulfate to phenolic hydroxyls. Both 3- and 4-sulfates are generated, but

the 3-sulfates are predominant. Whereas, *O*-glucuronidation is performed by uridine diphosphoglucuronosyltransferases transferring glucuronic acid from uridine diphosphate glucuronic acid to dopamine in position 3-OH and 4-OH. So, the major excretion products of dopamine metabolism are HVA, DOPAC and their corresponding sulfates and glucuronides.[9] Nevertheless, dopamine, like the other catecholamines, can undergo a minor oxidative pathway that leads to production of quinone by-products. These short-lived toxic species form a multitude of reactions that generate harmless derivatives such as neuromelanin that is a dark pigment found in neurons of *substantia nigra pars compacta* or salsolinol, an endogenous neurotoxin that causes oxidative stress and mitochondrial damage by inhibition of the electron transport chain.[10] Generally, biosynthesis and degradation processes may be considered pharmaceutical targets for treatments of dopamine-related disorders such as Parkinson's´ or Alzheimer's´ diseases, because amounts of dopamine metabolites like HVA are correlated to diseases progression.[11,12]

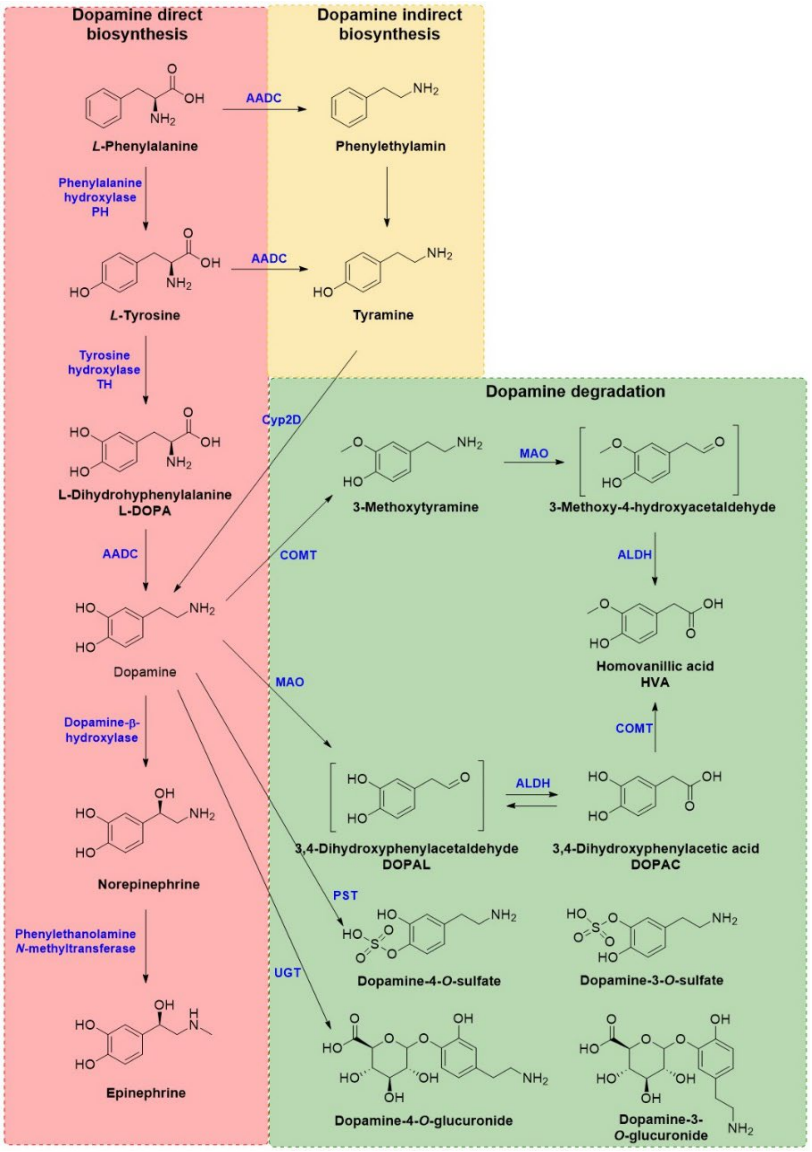

Figure 1. General scheme of synthesis and degradation of dopamine. In red background it is showed the direct synthesis of transmitter with its derivatives (norepinephrine and epinephrine), while in yellow background the alternative synthetical pathway is depicted. In green background, the metabolism of dopamine is described. Adapted from Meiser *et Al*.[9]

In human brain, dopaminergic neurons are characterized by cells that are different in the structure and functionality; they are distributed within the diencephalon, mesencephalon, and the olfactory bulb. For example, the largest cluster of dopaminergic cells is situated within the ventral region of the mesencephalon, including roughly 90% of the overall population of dopaminergic cells.[13]

Dopamine neurons are projecting and forming four axonal pathways: 1) nigrostriatal, 2) mesocortical, 3) mesolimbic and 4) tuberoinfundibular (Figure 2). Obviously, these pathways are involved in dopaminergic transmission as well as in human brain disorders because it depends on which way and in what extent a dysregulation is found within these axons.[14]

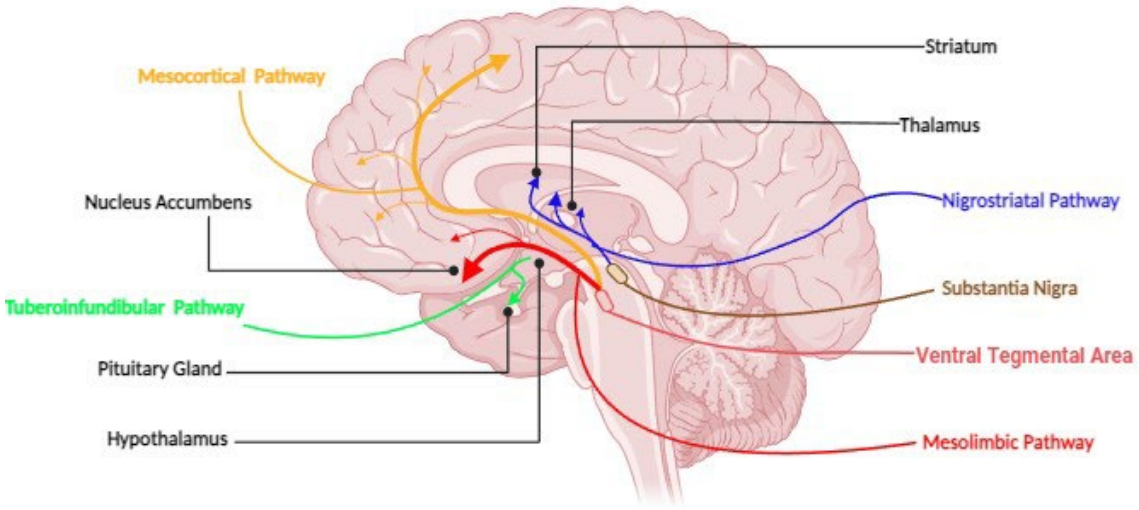

Figure 2. Graphic overview of dopaminergic pathways in the central nervous system. The neurons projecting from *substantia nigra* to *striatum* belong to nigrostriatal pathway (blue). The orange and red arrows are showing the mesocortical and mesolimbic systems respectively, originating together from VTA. Tuberoinfundibular pathway (green) is formed by dopamine neurons that start from hypothalamic nuclei to the pituitary gland. Created with Biorender.com

The nigrostriatal pathway is characterized by neurons projecting from *substantia nigra* to the *striatum*. This pathway is involved in the control and coordination of movement as it projects to dorsal basal ganglia areas, where behavioural and cognitive habits are learned and stored,[15] in fact overactivity in the nigrostriatal pathway is implicated in psychosis,[16] while an underactivity can lead to "Parkinsonism" effects.[17] Dopaminergic neurons, originated in ventral tegmental area (VTA), project to different areas of prefrontal cortex via mesocortical pathway and to *nucleus accumbens* or olfactory tubercle via mesolimbic system. Mesocortical system has a role in mechanisms of learning and memory, while mesolimbic is responsible for positive reward, motivation and sensation-seeking behaviours. These two systems are commonly described together as a mesocorticolimbic system, because there is a significant overlap among VTA cells converging the dopaminergic neurons.[18] It has been reported that a low activity in the mesocorticolimbic system might be linked to negative symptoms of schizophrenia and depressive or drug-seeking tendencies.[19] Finally, tuberoinfundibular

pathway connects cells of periventricular and *arcuate nuclei* of hypothalamus with median eminence and anterior pituitary gland, where released dopamine acts with lactotrophs to inhibit the release of prolactin. This effect has to be removed during lactation, via changes on release of dopamine otherwise a dam does not have proper physiological responses to pup suckling.[20]

1.1.1 Dopamine receptor subtypes

Entire dopaminergic signalling is based on interaction between dopamine and its receptors. This interaction occurs in the synaptic cleft among the dopaminergic neurons. After the release, dopamine can bind to either a postsynaptic or presynaptic receptor, or it can be reabsorbed by transporters near the synaptic junction on the presynaptic neuron. The dopamine active transporter (DAT), located exclusively on presynaptic cells, is responsible of the dopamine reuptake (Figure 3). DAT undergoes post-translational modifications and it is the target of addictive substances such as cocaine or amphetamine that prolong the presence of dopamine in the synaptic cleft by inhibiting this transporter.[21] Reuptake, release, and storage of dopamine are tightly regulated processes and any alterations to these processes can have an impact on neurological disorders. In addition, the release of dopamine can be regulated by phasic or tonic transmission mechanisms. Phasic dopamine release is triggered by action potentials within dopamine-containing cells, leading to a rapid and transient raise in dopamine concentrations near the presynaptic terminal. In contrast, tonic transmission involves the release of dopamine without presynaptic action potentials, thus it is regulated by the activity of other neurons and neurotransmitter reuptake. Tonic release produces more attenuated and spatially broader peaks of extracellular dopamine, when compared with the abrupt and localized nature of phasic release. In fact, phasic rush can reach millimolar ranges of dopamine concentration, while tonic transmission creates a nanomolar concentration.[2,22]

Five dopamine receptor subtypes have been reported, they all belong to the G-protein-coupled receptors superfamily (GPCRs), more precisely to the rhodopsin-like class A. The receptor subtypes are divided into two subfamilies: $D_{1\text{-like}}$ and $D_{2\text{-like}}$. The first one includes dopamine D_1 and D_5 receptors, whereas D_2, D_3, D_4 receptors belong to the second class. The classification and characterization of all dopamine receptors is available thanks to the scientific effort that has been made in the last two decades and it has started with cloning studies of dopamine receptors at the beginning of 90s. The first dopamine receptor to be cloned was D_2 in 1988; it showed a great level of similarity with adrenergic β_2 receptor whose gene fragment was used as control.[23] Afterwards, human dopamine D_1 and D_3 receptors were cloned in 1990 using the gene fragment of D_2 receptor as

reference.[24,25] Accordingly, human D_4 and D_5 were cloned in 1991, showing similarities to D_2/D_3 gene sequences and to D1 one, respectively.[26,27] Taken these findings together, the cloning of receptors has provided new methodologies to perform further studies that demonstrated that all 5 receptors share a high level of homology within their structures. For example, many similarities have been identified in their seven α-helical transmembrane domains, three extracellular loops and three intracellular loops, even though the dopamine receptors feature different biochemical responses, pharmacological properties and locations in the brain.[28]

D_1 and D_5 receptors are generally expressed in *substantia nigra*, *nucleus accumbens*, amygdala, hypothalamus and thalamus (D_5 receptors with lower density than D_1 ones), they are located as post-synaptic receptors in neuronal cells promoting a downstream signal that causes inhibition of dopamine release.[29] On the other hand, D_2, D_3 and D_4 receptors are found mostly in olfactory tubercle and in *nucleus accumbens* (D_2), in the limbic area and islands of Calleja (D_3), in hippocampus, amygdala, hypothalamus and thalamus (D_4 with lower intensity than $D_{1\text{-like}}$). They are located simultaneously in pre and post-synaptic position within dopamine signalling, thereby they are auto-receptors that modulate biosynthesis and release of dopamine through a negative feedback mechanism and a high-stream signal, see figure below.[30]

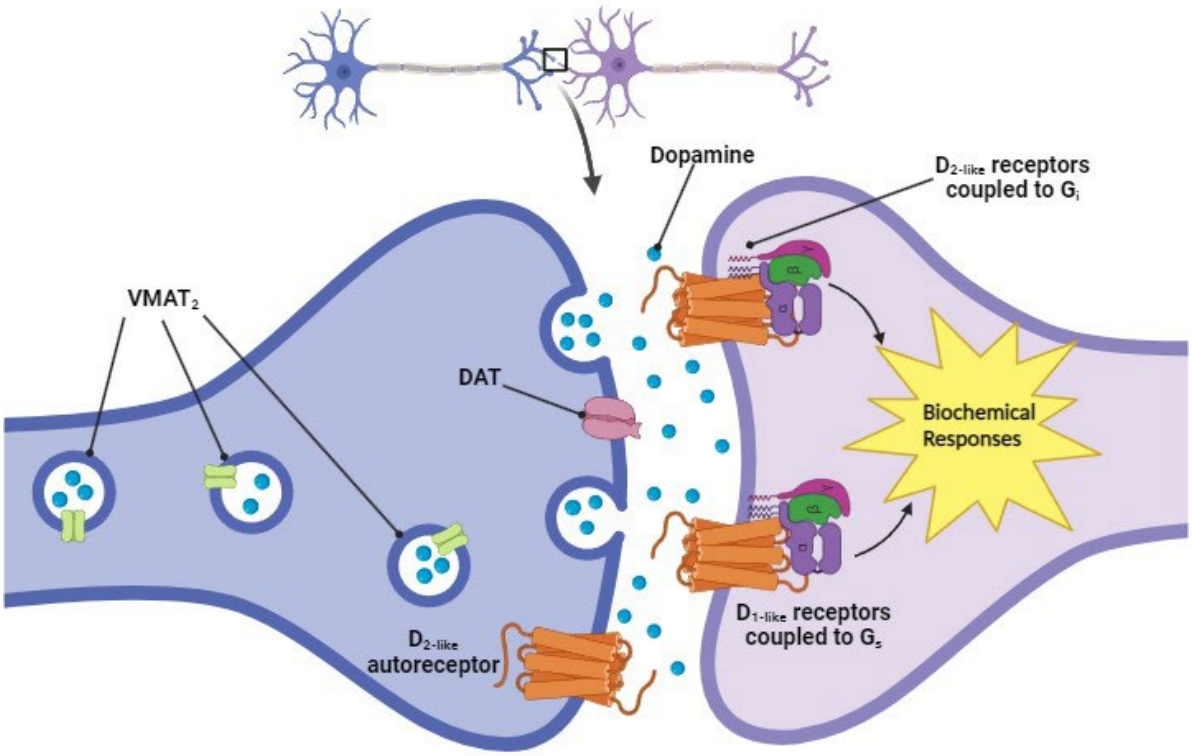

Figure 3. General representation of dopamine release, reuptake and interaction with dopaminergic receptors in the synaptic cleft. DAT, dopamine transporter responsible of dopamine reuptake. $VMAT_2$, vesicular monoamine transporter 2 responsible of dopamine storage. Created with Biorender.com

Receptors, belonging to the same subfamily, share high levels of structural homology; for instance, D_1 and D_5 receptors share 80% of identity in their transmembrane domains, while D_2 have a 79% and 53% identities with D_3 and D_4 receptors respectively, D_3/D_4 homology is about 51%.[31] Differences arise between diverse subfamilies, the COOH-terminal is seven times longer in $D_{1\text{-like}}$ receptors than in $D_{2\text{-like}}$; it has many serine and threonine residues and it contains a cysteine that is conserved in all G-protein-coupled receptors. Indeed, in $D_{1\text{-like}}$ receptors, the cysteine residue is situated next to the beginning of the COOH-terminus. Whereas, in $D_{2\text{-like}}$ receptors, the COOH-terminal concludes with the above-mentioned cysteine residue and it does not have any residues of serine and threonine which could be potential sites of receptor kinases.[32] Similarly to all G-protein-coupled receptors, dopamine receptors feature two cysteine residues in extracellular loops 2 and 3 (ECL2 and ECL3), thought to create an intramolecular disulphide bridge for stabilizing the receptor structures.[33] The intracellular loops 1 and 2 present a high degree of conservation among the dopamine receptors, while the sequences of third intracellular loop exhibit various divergences in combination with the COOH terminus. Especially for D_1 and D_5 receptors, structural discrepancies among these receptors could be related to variations in the third cytoplasmic loop and the COOH-terminal tail. Regarding the NH_2-terminal, a variable number of *N*-glycosylation sites is observed. Both D_1 and D_5 receptors have two sites: one in the NH_2 terminal and another in the second extracellular loop. In contrast, the D_2 receptor presents four potential glycosylation sites, the D_3 has three, and the D_4 possesses only one.[34] On the other hand, there are many other sites that are conserved within the five dopamine receptors, since a broad number of amino acids are conserved in all catecholamine receptors. For instance, the main example is the catecholamine binding site which is represented by a residue of aspartate and two residues of serine, located respectively in the third and fifth transmembrane domains. The exact position of these amino acids is the only detail that changes in every dopamine receptor. In details, aspartate is acting as counterion in a salt-bridge bond to the protonated basic centre of catecholamine, while serine residues are forming hydrogen bonds with the hydroxy groups of the catechol structure.[23–27] Other conserved sites are the ones dedicated to the phosphorylation mediated by protein kinase C (PKC) for dopamine $D_{1\text{-like}}$ receptors and protein kinase A for $D_{2\text{-like}}$ class. Although the process is different, the phosphorylation sites are found to be in the third cytoplasmatic loop for all five receptors.

$D_{1\text{-like}}$ and $D_{2\text{-like}}$ receptor subfamilies diverge in their genetic sequences as well. The coding regions of D_1 and D_5 receptor genes lack introns, whilst the genes for D_2, D_3, and D_4 receptors contain six, five, and three introns, respectively (Table 1). The genetic arrangement of the $D_{2\text{-like}}$ class facilitates the creation of receptor splice variants. Although splice variants for D_3 receptor have been identified, their characterization is still under investigation. Recently, two single nucleotide polymorphisms of

D_3 have been evaluated as diagnostic marker for opioid use disorder.[35] The identification of these nucleotide variations has opened the doors to possible therapeutical instruments for opioid use disorder and heroin dependence.[36,37] Regarding D_2 receptors, alternative splicing encodes a 29 amino-acids insertion in the putative intracellular loop 3 of dopamine D_2 receptor, generating two isoforms with different lengths: D_{2S} (short) and D_{2L} (long). D_{2S} receptor is expressed mostly in presynaptic neurons and thus being involved in autoreceptor functions, while D_{2L} is found predominantly as postsynaptic receptor.[28,30,38]

The D_4 receptor gene has numerous variations in its coding sequence and the most significant variation is found in exon 3.[39] This region encodes the third intracellular loop of the protein and consists of a variable number of tandem repeats, where a 48 base pair sequence is repeated 2 to 11 times. The three most prevalent variants contain 2, 4, and 7 repeats, known as $D_{4.2}$, $D_{4.4}$, and $D_{4.7}$.[40] These variations of the D_4 receptor have been associated with different functional implications. For instance, the common 4-repeat ($D_{4.4}$) and 2-repeat ($D_{4.2}$) variants can create functional heteromers with the short isoform of the dopamine D_2 receptor (D_{2S}), while the 7-repeat allele ($D_{4.7}$) cannot. Activation of the D_2 receptor in the D_{2S}-$D_{4.2/4.4}$ heteromer enhances D_4 receptor-mediated mitogen activated protein kinase (MAPK) signalling in transfected cells and in the *striatum*. This enhancement is not observed in cells expressing $D_{4.7}$, as mentioned before. In the *striatum*, D_4 receptors are situated in cortico-striatal glutamatergic terminals, where they modulate selectively glutamatergic neurotransmission by interacting with D_{2S} receptors.[41] The interaction $D_{4.2}$- $D_{4.4}$-D_{2S} is an example of another peculiar ability found in all GPCRs: dimerization.

Dopamine receptors can form macromolecular complexes within each other or with different receptors, creating homodimers and heterodimers. Receptor oligomerization influences significantly the structure and functionality of dopamine receptors, impacting aspects such as receptor trafficking, signalling, and pharmacological properties. This characteristic has led to the development of more sophisticated models to understand the physiological roles of these receptor heteromers, highlighting their dynamic nature in receptor-ligand interactions and their implications in biochemical responses.[42] Among dopamine receptors, other oligomers have been reported: D_1-D_2 and D_1-D_3 heteromers. D_1-D_2 have been found to be a unique heteromeric protein complex, whose activation triggers a calcium pathway mediated by phospholipase C (PLC),[43] while D_1-D_3 complexes, once activated, provoke a combination of the respective mechanisms, demonstrating also possible functional selectivity triggered by allosteric modulations within the oligomer.[44] Additionally, more heteromers of D_2 receptor have been described like D_2-D_3,[45] featuring own functional properties and D_2-D_5, having similar expression and function to D_1-D_2 heteromers.[46]

The crystal structures of $D_{2\text{-like}}$ receptors have been obtained before the ones belonging to $D_{1\text{-like}}$, because important research efforts have been made on D_2, D_3, D_4 receptors rather than D_1 and D_5, as the first ones are considered the main pharmaceutical targets for psychiatric disorders and their subtype differences might have enormous potential in the development of novel therapies. Consequently, the crystal structure of human D_3 receptor was the first one to be obtained in 2010, thanks to the use of a selective subtype antagonist eticlopride which has been the most suitable ligand to favour the thermal stability for the receptor.[47] Then, the crystal structure of dopamine D_4 receptor in its inactive state has been achieved in 2017, because another antagonist was used: nemonapride (Table 1).[48] The structure of human D_2 receptor has been obtained in its inactive state, using firstly the inverse agonist risperidone (2018)[49] and then another antipsychotic drug: haloperidol (2020).[50] The differences across the two crystal structures have highlighted crucial determinants for D_2 subtype selectivity as it has occurred for dopamine D_3 and D_4 receptor from the corresponding structures. Ultimately, dopamine D_1 receptor has been the last one to be analysed from the structural viewpoint; its crystal structure has been determined in complex with a non-catechol-agonist, shedding light on alternative mechanisms of receptor activation and development of possible subtype ligands.[51] D_5 receptor is the only one with no detailed reports about structural insights, meaning that more studies on this receptor are still needed. In conclusion, the first structures of dopamine D_2, D_3, and D_4, all in the antagonist-bound states, have been listed in the table 1 together with the agonist-bound analysis of D_1 receptor.

Table 1. General overview of dopamine receptors with their characteristics. The representations of crystal structures have been adapted from the related references.

Dopamine receptor	**D_1**	**D_2**		**D_3**	**D_4**	**D_5**
Cloning	1990[24]	1988[23]		1990[25]	1991[26]	1991[27]
Introns	no	six		five	three	no
G-protein coupled	$G\alpha_S$	$G\alpha_i$		$G\alpha_i$	$G\alpha_i$	$G\alpha_S$
Main signalling pathway	↑cAMP	↓cAMP		↓cAMP	↓cAMP	↑cAMP
Crystal structure	2021[51] 	2018[49] 	2020[50] 	2010[47] 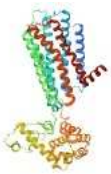	2017[48] 	/

However, the first structural resolution of D_1 receptor boosted other analyses, recently described, that allowed to have more detailed data concerning the interaction points between ligands and receptor of interest.[52,53] Regarding the $D_{2\text{-like}}$ class, an additional description of D_2 receptor in agonist-bound state has been reported in 2020,[54] but the scientific community was still missing examination for the D_3 receptor in its active state. Without a clear understanding of how agonists interact with and activate the D_3 receptor, the comprehension of the underlying mechanisms would have remained incomplete. In this matter, the latest cryo-electron microscopy structures of the human D_3 receptor have solved this scientific gap. The determinations, exerted by Arroyo-Urea *et Al.* and Peiyu Xu *et Al*., have analysed the receptor bound to agonists such as **pramipexole**, **PD128907** or **FOB02-04A**, thus revealing the active state of human D_3 receptor. [55,56] Comparing with D_2 agonist bound-state and D_2/D_3 antagonists-bound structures, the authors have analysed notable differences in the activation processes and in the binding pockets' protrusions between D_2 and D_3 receptors structures, providing new avenues for developing subtype selective ligands, potentially applicable in innovative therapies. For D_4 receptor, no agonist-bound structure has been determined yet, but a second analysis on its inactive state has been described in 2019,[57] providing details of a second binding pocket, which has prompted deeper analyses on structure-activity relationships.[58]

Moreover, comparative reports on agonist/antagonist interactions have revealed distinctions in dopamine affinity between $D_{1\text{-like}}$ and $D_{2\text{-like}}$ receptors. $D_{2\text{-like}}$ receptors exhibit a 10- to 100-fold higher affinity for dopamine than $D_{1\text{-like}}$ receptors 'one, among which D_1 receptor displays the lowest affinity.[59] This variability in dopamine affinity might be attributed to the distinct roles of these receptor subfamilies within dopaminergic signalling, such as the potential existence of tonic and phasic patterns in dopamine neurotransmitter release. It is hypothesized that $D_{1\text{-like}}$ receptors are selectively activated by high concentrations of dopamine during phasic release, while $D_{2\text{-like}}$ receptors are responsible for being detected by tonic low levels of dopamine.[38,60] Anyway, current studies have not determined whether dopamine binding to $D_{2\text{-like}}$ receptors at tonic levels can initiate intracellular signalling responses in vivo, therefore further studies are required.

As it has been mentioned before, dopamine $D_{1\text{-like}}$ and $D_{2\text{-like}}$ receptors are G-protein coupled receptors and they differ from each other in pharmacological properties, because the first ones activate the production of cyclic adenosine-monophosphate and the second ones deactivate it with opposite consequences on dopaminergic response. Before going into details, it is necessary to explain how G-protein is involved in dopamine receptor signalling. Firstly, G-protein is a heterometric protein composed of three subunits: α, β, γ, that are bound together when the GPCR is in its inactive state. As soon as the agonist binds to the receptor, its state changes into active and the trimeric protein dissociates. The α subunit connects with guanosine triphosphate (GTP) and β-γ remain linked forming

the related dimer, both of which are regulators of several biochemical responses. Afterwards, GTP hydrolyses into guanosine diphosphate and G-protein reassociates, forming the trimeric complex again and stopping its activity in order to restart the cycle as soon as the agonist binds again. G-proteins are referred to their corresponding α subunits, in the way that G_s contains $G\alpha_s$, G_i has $G\alpha_i$ etc... G_s proteins stimulate the production of adenylyl cyclase; whereas G_i proteins are responsible of the inhibition of adenylyl cyclase as well as the activation of G-protein-coupled inwardly rectifying potassium channels (GIRKs).[61] Indeed, dopamine $D_{1\text{-like}}$ receptors are coupled to G_s protein, thus they activate adenylyl cyclase and protein kinase pathways, which lead to an increase in cyclic adenosine monophosphate (cAMP, Table 1).[62] The increase of cAMP boosts γ-Aminobutyric acid (GABA) release, which inhibits the release of dopamine in the VTA, *nucleus accumbens* and all the pathways related to pleasure or self-gratification. There are hints that D_5 receptors might have alternative G-protein mechanisms, based on coupling to G_q, which activates PLC. The involvement of this enzyme triggers a signalling pathway that ends with an increased mobilization of intracellular Ca^{2+}. In details, PLC hydrolyses the ester bond between glycerol and phosphate residue of phosphatidylinositol-4,5-bisphosphate, provoking the generation of diacylglycerol and inositol-1,4,5-trisphosphate. These second messengers provoke respectively the activation of PKC pathway and the increase of intracellular Ca^{2+} concentration. On the other hand, dopamine $D_{2\text{-like}}$ receptors are coupled to G_i proteins that induce a decrease of intracellular cAMP level because of inhibition of adenylyl cyclase pathway, thus encouraging high-stream regulation on dopaminergic transmission (Figure 4).[63]

Although dopamine receptors may trigger diverse signalling pathways, they also utilize common molecules to regulate elaborated biochemical pathways. Moreover, when assessing the effects and functions of dopaminergic transmission cascades, factors such as neuronal cell populations, their distribution throughout the central nervous system (CNS), physiological conditions, and the interaction among proteins, enzymes, and receptors should be considered. These elements can lead to distinct physiological responses, even if the performers of biological mechanisms may be the same. For instance, extracellular signal regulated kinases 1 and 2 ($ERK_{1/2}$) are activated by both $D_{1\text{-}}$ and $D_{2\text{-like}}$ receptors with diverse consequences on cell death or growth and on synaptic plasticity. The ERK activation by $D_{1\text{-like}}$ receptors requires the involvement of *N*-methyl-D-aspartate (NMDA) receptors and it has been found to be triggered by drugs addiction in the *striatum*, because increases of ERK_1 and ERK_2 phosphorylation have been observed.[64] The ERK_1 and ERK_2 activation mediated by $D_{2\text{-like}}$ receptors seems to be regulated by G_q and G_i proteins and it occurs in other cells rather than in the brain, enlightening a different possible physiological outcome that is not completely defined yet.[65]

Thereby, ERK_1 and ERK_2 act as enhancers of dopaminergic transmission and represent an alternative biological response to the classical pathway regulated by the activation or not of adenylyl cyclase.

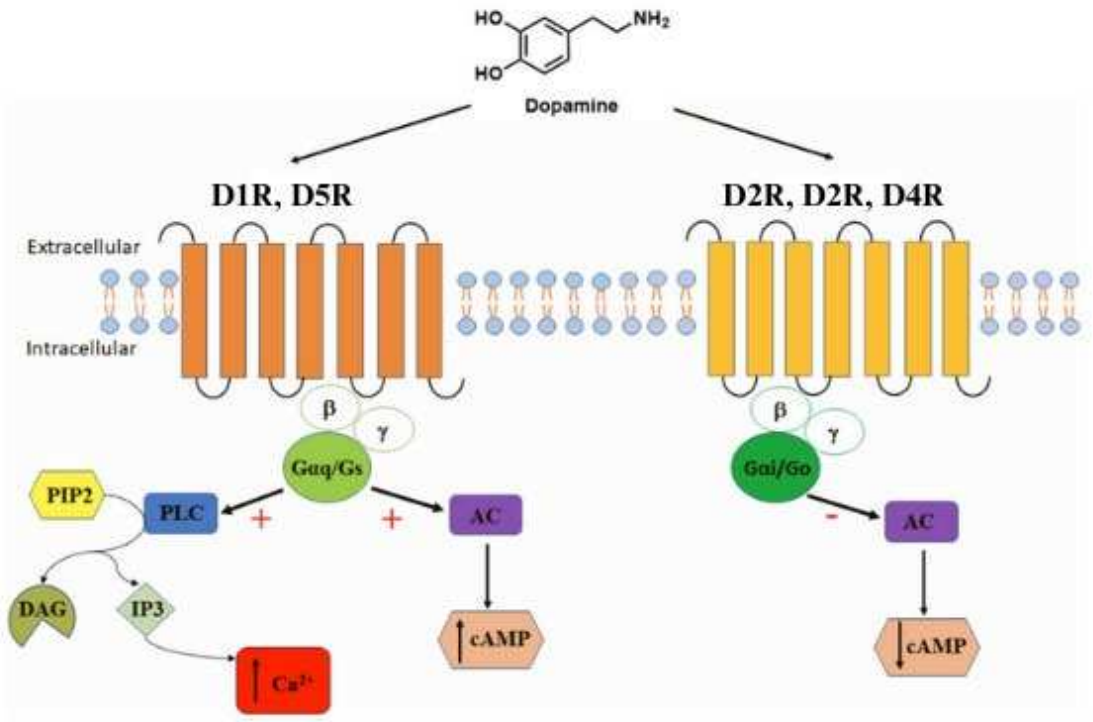

Figure 4. Summary picture of dopaminergic signalling via $D_{1\text{-like}}$ and $D_{2\text{-like}}$ receptors. Ac, adenylyl cyclase; cAMP, cyclic adenosine monophosphate; PLC, phospholipase C; PIP_2, phosphatidylinositol-4,5-bisphosphate; DAG, diacylglycerol; IP_3, inositol-1,4,5-trisphosphate. Picture adapted from Predescu *et Al.* [63]

There are other alternative modulators of dopamine cascades such as the regulators of G-protein signalling (RGS) or G-protein-coupled receptor kinases (GRKs). There are more than 35 types of RGS proteins and they form a family that has inhibitory actions on GPCRs, because they limit the lifetime of GTP bound to G_α state by accelerating greatly the rate of G_α-GTP hydrolysis. Therefore, RGS are negative modulators of GPCRs efficacy in presence of agonists on dopamine receptors.[66] The GRKs regulate GPCR signalling intensity to prevent the receptors from hyperactivation, functioning as dopamine signalling inhibitors. This mechanism is crucial for promoting receptor desensitization during persistent ligand activation or re-exposure of receptor to the ligand after prolonged lack of stimulation.[67,68]

Dopamine receptor functions have been connected not only to cAMP, as a second messenger, but also to protein kinase A. PKA is activated via G-protein mediated transmission by $D_{1\text{-like}}$ receptors and it is deactivated by $D_{2\text{-like}}$ receptors. PKA has a lot of substrates and it amplifies the cascade of signals related to dopamine transmission, as this enzyme represents a further alternative response to dopaminergic signalling. The most important substrate of PKA is a 32-kDA dopamine and cAMP-

regulated phosphoprotein, commonly known as DARPP-32. It is primarily found in medium spiny neurons, it is a versatile phosphoprotein serving as a pivotal integrator in cell signalling modulation in response to various neurotransmitters, like dopamine. Indeed, it has been shown that activation of PKA by dopamine D_1 and D_5 receptors increase the phosphorylation of DARPP-32, while an inhibition of PKA promoted by D_2 receptors stimulate dephosphorylation at the same residue of threonine 34.[69] Nevertheless, PKA, like other kinases that regulate DARPP-32, can be stimulated by other neurotransmitters, different neuropeptides or hormones, demonstrating that this pathway is involved in several signalling modalities. For example, DARPP-32 inhibits protein phosphatase 1 in response to cannabinoids and caffeine, which can affect PKA response to dopaminergic receptors and can regulate dopamine-associated behaviours as well.[70,71]

The biochemical cascades listed before are the core of several human functionalities, in which dopamine and dopaminergic receptors are involved. For instance, it is generally believed that locomotor activity is regulated by dopamine D_1, D_2, and D_3 receptors. The exclusive activation of postsynaptic D_1 receptors stimulates moderately locomotor activity. In contrast, the functions of D_2 and D_3 dopamine receptors are more intricate, due to their expression in both presynaptic and postsynaptic sites, presenting a more intricate regulatory role when compared with D_1 receptors.[31]

Autoreceptors, situated in presynaptic position, work as negative feedback modulators, regulating neuronal firing rate, synthesis, and release of neurotransmitters in response to fluctuations in extracellular neurotransmitter levels. Activation of presynaptic $D_{2\text{-like}}$ autoreceptors induces a reduction in dopamine release, leading to decreased locomotor activity, while activation of postsynaptic receptors promotes locomotion. As $D_{2\text{-like}}$ autoreceptors are triggered by lower concentrations of dopamine agonists than ones necessary to activate postsynaptic receptors, a same agonist can elicit a biphasic effect, causing decreased activity at lower doses and behavioural activation at higher doses. Dopamine D_2 receptors appear to be the primary autoreceptors involved in regulating presynaptic firing rate, dopamine synthesis, and release. Particularly, the splice variants of the D_2 receptor, D_{2L} and D_{2S}, exhibit distinct neuronal distributions, with D_{2S} primarily presynaptic and D_{2L} postsynaptic. Consequently, the differential roles of postsynaptic and presynaptic dopamine D_2 receptors are derived by the unique contributions of these isoforms.[30,72] Furthermore, dopamine D_3 autoreceptors might play a role in regulating tonically released dopamine, joining the function of D_{2S} autoreceptors in controlling neuronal firing rate, dopamine synthesis, and phasic dopamine release. D_3 receptors appear to inhibit moderately locomotion, either acting as autoreceptors or interacting with postsynaptic receptors. On the other hand, the influence of dopamine D_4 and D_5 receptors seems minimal in movement regulation. In conclusion, it is evident that activation of both

postsynaptic dopamine D_{1}- and $D_{2\text{-like}}$ receptors is essential for the complete expression of locomotor activity.[73]

Numerous essential functions rely on the activation of brain dopamine receptors. Particularly, dopamine D_1, D_2, and D_3 receptors have critical roles in reward and reinforcement mechanisms. Various studies have demonstrated that pharmacological or genetic interventions in the dopamine receptor functionalities modulate responses to natural rewards and addictive substances, making dopamine receptors the main focus in addiction research.[74,75] Moreover, D_1 and D_2 receptors are crucial for learning and memory processes, such as working memory that is primarily governed by the prefrontal cortex. Additionally, dopamine D_3, D_4, and eventually D_5 receptors exert a minor modulatory influence on specific aspects of cognitive functions mediated by hippocampal areas.[76] The fact that the majority of effective antipsychotic drugs block D_2 receptors highlights the critical role of these receptors in the psychotic symptoms observed in schizophrenia and bipolar disorder. Furthermore, dopamine receptor subtypes like D_3 and D_4 contribute partially to functions such as affect, attention, impulse control, decision-making, motor learning, sleep, reproductive behaviours, and regulation of food intake.[77] Dopamine receptors localized outside the CNS mediate various functions as well. These include olfaction, vision, and hormonal regulation. For instance, dopamine D_2 receptors in pituitary gland regulate prolactin secretion, dopamine D_1 receptors located in the kidney mediate renin secretion, and D_2 receptors of adrenal gland regulate aldosterone secretion. Dopamine receptors also play roles in regulating sympathetic tone, renal function (through D_1, D_2, and D_4 receptors), blood pressure, vasodilation, and gastrointestinal motility.[78]

Considering that many important functions rely on the interactions between dopamine and its receptors, it's not surprising that dysfunctions of dopaminergic signalling are linked to dysregulations of the receptors, which may provoke development of human brain disorders. *In vivo* imaging investigations employing newly developed radioligands have obtained consistent findings. A recent comprehensive analysis of synaptic function has localized some dysfunctions of dopamine receptor expression in patients affected by mental and affective disorders, by using positron emission tomography (PET) and single-photon emission computer emission tomography.[79] A higher density of dopamine D_2 receptors has been observed in the basal ganglia of schizophrenia patients, when compared with the values of healthy individuals. Patients with depression have been found to have reduction in D_1 receptors binding, while most studies found either unchanged or elevated dopamine D_2 receptor binding in the basal ganglia. Nevertheless, anhedonia connected with depression is thought to be related to a lowering of sensitivity of dopamine D_2 and D_3 receptors in the limbic brain areas.[80] Bipolar disorder patients show mostly no changes in D_1 receptor binding, although it has been reported increased D_2 receptors density.[81] Whereas, a decrease in D_2 receptor binding has been

observed in drug abusers; some comparable findings have been confirmed for Tourette's syndrome patients but not for the individuals with ADHD.[82] Alterations of dopamine D_1 and D_2 receptor binding have been found in patients with Parkinson´s and Huntington´s diseases as well. However, the pattern of changes in dopamine receptors depends on the time-line of disease: at earlier stages of PD there is a light increase of dopamine D_2 receptor binding, which becomes a decrease in the late stages. On the other hand, important reductions of D_1 and D_2 receptor bindings generate a post-synaptic degeneration at the level of GABA-ergic medium spinal neurons in patients affected by Huntington´s disease.[81]

Obviously, the abnormalities, that occur at the level of dopamine receptors, involve also the corresponding biochemical responses. Therefore, research indicates that both protein and mRNA levels of DARPP-32 are decreased in the dorsolateral prefrontal cortex among individuals diagnosed with schizophrenia or bipolar disorder.[83,84] Specifically, a study revealed a reduction of DARPP-32 mRNA in the prefrontal cortex within a limited group of suicide victims, when compared with a control group without mental disorders.[85] Moreover, recent investigations have highlighted a diminished expression of DARPP-32 in the leukocytes of patients diagnosed with schizophrenia and bipolar disorder. This report suggests that a potential deficiency in the DARPP-32-mediated transmission pathways might be associated with these conditions.[86] Other kinases associated with the DARPP-32, such as cyclin-dependent kinase 5 and ERK, have been demonstrated to play a role in dopamine dysfunctions implicated in drug abuse and development of L-DOPA-induced dyskinesia.[87,88] Akt/GSK_3 signalling pathway is another cascade that might have a role in pathogenesis or treatment of psychiatric diseases. An imbalance of GSK_3 transmission has been connected with patients affected by mental disorders as well as a decrease of Akt activity results from a hyperactivation of dopamine $D_{2\text{-like}}$ receptors. Indeed, it has been shown that some antipsychotics of first and second generation could correct these imbalances in their pharmacological action spectrum, also because GSK_3 activity might be regulated by serotonin neurotransmission and thus antipsychotic drugs, that exert an inhibition on serotoninergic receptors, can regulate Akt/GSK_3 network indirectly.[89]

Given the intricate nature of dopamine's functions and its role in the onset of numerous diseases, it's necessary acting on dopamine receptors either directly or indirectly to address the dopamine related diseases. A broad range of selective or non-selective dopamine agonists and antagonists have been employed to treat symptoms associated with Parkinson's disease, hyperprolactinemia, schizophrenia, bipolar disorder, depression and nausea. Another area of interest involves the design of allosteric drugs targeting GPCRs, including dopamine receptors. These drugs can reduce unwanted side effects by binding to allosteric sites that are different from the orthosteric ones; they might influence

downstream pathways in both directions too. It has been suggested that employing allosteric modulators may enhance selectivity for specific GPCR subunits and enhance therapeutic outcomes, especially for dopamine $D_{2\text{-like}}$ receptors.[90] Then, targeting dopamine receptors has demonstrated to be the most effective approach to modulate dopaminergic disfunctions connected to pathological conditions, although several biochemical mechanisms can be involved. Nevertheless, it is important to consider that a receptor-ligand interaction prompts a consecutive activation of multiple pathways exerting a pluridimensional efficacy. Ligands are able to either trigger or stabilize receptors in various bioactive conformations, resulting in the beginning of several signalling pathways. In addition, the ability of a GPCR to form oligomers complicates the development of a therapeutic treatment, because heterodimers of receptors can initiate a broad range of intracellular transmissions. In this context, it could be a mistake classifying ligands based exclusively on one pathway, due to possible different signal cascades activated by a single GPCR. Then, the same ligand might function as a full agonist for one pathway, as an antagonist or inverse agonist for another.[91,92]

Regarding dopaminergic receptor ligands the concept of "biased ligand" has aroused in the recent years. In details, known also as functional selective ligands, biased ligands are designed to target specifically and to activate a single signalling pathway of a receptor, which usually regulates multiple pathways. For example, dopamine D_2 receptor-biased ligands are being developed as potential therapies for schizophrenia, aiming to activate selectively either the cAMP/PKA or β-arrestin-2/Akt downstream signalling pathways. These biased ligands may offer improved therapeutic effects and reduced side effects.[93] In this matter, another big example is represented by **cariprazine**, that is pharmacologically classified as biased agonist, having antagonism and partial agonism properties at dopamine D_2 and D_3 receptors.[94] **Cariprazine** belongs to the newest generation of antipsychotics that feature better pharmacological profiles than the ones exhibited by first and second generations. This is one of great results that research has managed to obtain in the last decades opening new doors in the treatment of psychiatric disorders and in the area of pharmaceutical chemistry related to dopamine D_2/D_3 receptor ligands. This topic will be discussed in major details in the next paragraph as it is the scientific background of the PhD project reported here.

1.1.2 Dopamine D_2/D_3 receptor ligands

Dopamine D_2 and D_3 receptors have been highly investigated in the last decades because of their specific properties and treatment opportunities for psychotic disorders, so they are considered the main pharmaceutical targets. Among dopamine $D_{2\text{-like}}$ receptors, D_2 is the most abundant in dopaminergic projection areas such as *striatum*, limbic areas, hypothalamus; D_2 presynaptic function increases its distribution even more in other areas like *substantia nigra pars compacta* and VTA.[95] However, the broad localization of D_2 receptor has been reported to be counterproductive, because striatal D_2 receptors, that are the predominant dopamine receptors found in this tissue, might be one of the reasons why extrapyramidal side effects (EPS) are triggered in combination with an antipsychotic activity. Particularly in this case, the onset of EPS is observed when the occupancy of striatal D_2 receptors overcome the 80%; that is when more than 80% of these receptors are bound to an antagonist, hampering the possible interaction with dopamine.[96] Additionally, when the striatal D_2 receptor subfamily is blocked, a significant rise in muscle rigidity in rats is observed and it can cause symptoms similar to PD in humans. Another consequence of D_2 receptors blockade might be a quick and substantial increase in prolactin release from the anterior pituitary gland, because the natural dopamine inhibition of prolactin release is hindered.[97] Then, in the development of new scaffolds or structural motifs, more details have been considered such as orientating the activity at limbic/cortical regions rather than *striatum,* or controlling the receptors occupancy with the dose, or the interest around dopamine D_3 receptor has been increased. Despite being few in number, dopamine D_3 receptors are highly concentrated in brain areas linked to emotional and cognitive but not locomotor functions. The *nucleus accumbens* and the islands of Calleja report the highest density of D_3 receptors, where they are predominantly located on the postsynaptic side,[98] suggesting that these receptors could trigger an antipsychotic activity without EPS.

Initially developed to visualize D_2 receptors in the rat brain, **^{11}C-(+)-PHNO** emerged unexpectedly as a valuable ligand for imaging D_3 receptors in live rodent, primate, and human brains.[99] Thanks to its use, it has been possible to discover that distribution of dopamine D_3 receptors is changing across different animal species. For instance, in rats, the highest D_3 expression occurs in specific brain regions like the islands of Calleja, ventromedial shell of the *nucleus accumbens*, VTA, and *substantia nigra*. Conversely, in mice, guinea pigs, and rabbits, elevated D_3 receptor levels are observed in the islands of Calleja, *nucleus accumbens*, and *caudate nuclei*. Among these species, mice exhibit the highest density of hippocampal D_3 receptor expression and the lowest in the frontal cortex. In Rhesus monkeys, D_3 receptors, along with other dopamine receptor subtypes, exhibit prominent mRNA expression in layered pyramidal neurons within the prefrontal cortex.[100–102]

In post-mortem human brains, various radioligands and methods have been employed to map dopamine D_3 receptors. Techniques like in situ mRNA hybridization and receptor quantitative autoradiography have been used, including studies with agonists **^{3}H-7-OH-DPAT**[103] and **^{3}H-PD-128907**[104] or with antagonists such as **^{125}I-epidepride**[105] and **^{18}F-fallypride**[106] (Scheme 1). D_3 receptor mRNA expression displayed a laminated pattern on principal cells in the prefrontal cortex. Although D_3 receptors are abundant in the basal ganglia, there was also a low level of expression observed in cortical areas like the anterior cingulate cortex and various subcortical regions such as the anterior and medial thalamic nucleus, amygdala, mamillary body, *substantia nigra pars compacta*, *locus coeruleus*, *raphe nuclei*, lateral geniculate body, hippocampus. Notably, unlike rats, human studies did not report D_3 receptor mRNA expression in the VTA.[107,108] Dopamine D_3 receptors found in *substantia nigra* may act as autoreceptors, impacting dopaminergic feed-forward loops and affecting theta oscillations, crucial for coordinating neuronal activity.[109]

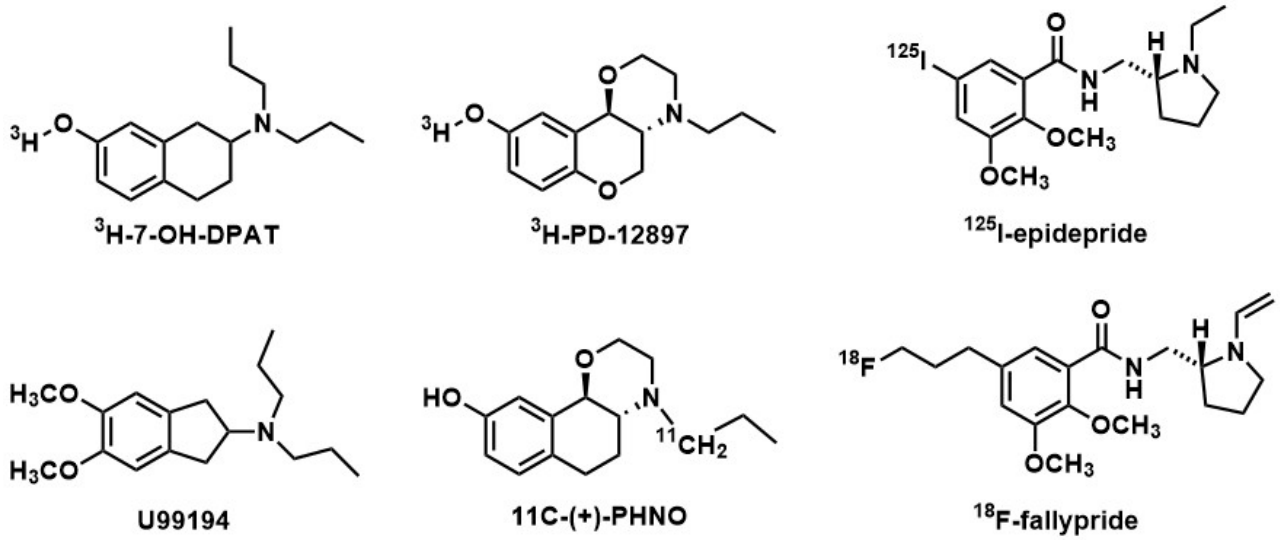

Scheme 1. Structures of D_2/D_3 agonists **(^{3}H-7-OH-DPAT, H-PD-128907, ^{11}C-(+)-PHNO)** and D_2/D_3 antagonists **(^{125}I-epidepride, ^{18}F-fallypride)** used as radiotracers. Compound **U99194,** selective D3 antagonist**,** has been used as modulator of intraocular pressure.

The predominant presence of D_3 receptors in areas governing attention, memory, and emotions implies a potential role for these receptors in regulating cognitive function.[110,111] Indeed, D_3 receptors might regulate cortical control of cognitive functions through their inhibition on mesocortical dopaminergic transmission. It has been reported that D_3 receptors are able to control NMDA receptor signalling by affecting pyramidal cells directly at post-synaptic levels in the *nucleus accumbens* or indirectly at presynaptic levels in the prefrontal cortices.[112] However, further research is still needed for exploring the role of D_3 receptors in normal and abnormal cognition. There are brain regions with low concentrations of D_3 or areas in which D_3 receptors are abundant but D_2 prevail in terms of binding and activity.

Regarding dopamine D_3 receptors, an additional consideration is their presence in peripheral locations. Although the function of D_3 receptors remains largely unexplored in peripheral organs, studies have found these receptors in organs like kidneys[113] and immune cells, indicating a potential role in immune responses.[114,115] Furthermore, D_3 receptors have been detected in the pancreas[116] and human retina,[117] hinting an involvement in insulin secretion and regulation of intraocular pressure; for example, in the ciliary body D_3 receptors form heteromers with melatonin 1 and melatonin 2 receptors.[118] About this, there is a pioneering study, in which **7-OH-DPAT**, a selective D_3 agonist, has decreased intraocular pressure in rabbits while a selective antagonist, **U99194**, reverted its effect (Scheme 1).[119] Consequently, it has been thought that D_3 receptors are located in sympathetic fibres afferent to ciliary body and their activation might block the aqueous humor production that is the main responsible of ocular hypertension which provokes glaucoma.[120]

Human PET studies with **^{11}C-(+)-PHNO** and **^{18}F-fallypride** have been used for assessing *in vivo* the occupancy of D_2 and D_3 receptors by using a given drug treatment, because their down- or up-regulation may be a consequence of the disease as well as a response of the stimulation by a D_2/D_3 ligand used in therapy.[120] In fact, it has been demonstrated that there is a direct relationship between D_3 receptors and cognitive dysfunctions in individuals with psychotic disorders, so in this context preferring D_3 ligands are believed to enhance cognitive performances.[121] Selective D_3 receptor antagonists impact the electrical activity of dopamine neurons in VTA similarly to atypical antipsychotics. They counteract the effects caused by the blockade NMDA glutamate receptors and they increase cortical levels of dopamine, as observed in microdialysis studies. In contrast to the antagonism of dopamine D_2 receptors, D_3 antagonists have a positive effect on social and cognitive behaviours in rodents, including tasks that assess cognitive flexibility and executive function, both of which are commonly impaired in individuals with schizophrenia. Current treatments for schizophrenia focus primarily on dopamine D_2 antagonism, which addresses effectively the disorder's positive symptoms but it fails in treating negative symptoms such as social impairments and cognitive deficits. This differential effect aligns with fewer consequences for extrapyramidal functions mediated by dorsal striatal areas, as mentioned before.[122]

Theoretically, an antagonism on D_2/D_3 receptors with selectivity towards D_3 might be optimal, because it has been found that striatal hyperdopaminergia could be responsible of cognitive and negative symptoms of schizophrenia, and D_3 receptor are not located in the *striatum*. Whereas, in the same brain area, an overstimulation of D_2 and D_3 autoreceptors can lead to a decrease of frontocortical dopaminergic activity, resulting in the inhibition of dopamine release in the *nucleus accumbens* or prefrontal cortex. A D_2/D_3 agonist amplifies these biochemical processes, while a D_2/D_3 antagonist or a partial agonist reverse this scenario, by boosting dopamine release in the mentioned brain regions

and regulating excessive dopaminergic activity. The increased dopamine release triggers the activation of D_1 and D_2 receptors, that are influenced indirectly by D_3 and a cascade effect is observed on postsynaptic D_3 receptors too.[123] In addition to that, it has been proved that D_3 receptor blockade attenuates both rewarding effects of cocaine and cocaine-induced drug-seeking behaviours.[124] Indeed, D_3 receptor antagonists diminish drug-induced motivation, weaken the rewarding effects of drugs, caused by drug re-exposure, environmental cues linked to drug use, or stress. Moreover, the efficacy of different dopamine agonists in reducing cocaine self-administration was found to be linked to their functional potency at D_3 receptors rather than D_2 receptors.[125] This indicates that dopamine agonists targeting D_3 receptors may either imitate or amplify the effects of cocaine, aligning with the concept of using agonist substitution therapy for treating drug dependence.

Continuous administration of levodopa provokes an abnormal increase in D_3 receptor expression in the dorsal striatum through D_1 receptor mediation, resulting in heightened sensitivity to levodopa in rats,[126] drug-induced dyskinesia, and an elevation of D_3 receptors in monkeys.[127] The regulatory mechanism was later discovered to involve brain-derived neurotrophic factor-dependent (BDNF) expression of D_3 receptors.[128] Recent studies have confirmed the role of D_3 receptors in levodopa-induced dyskinesia throughout experiments with D_3 receptor knockout mice[129] and PET imaging studies, showing elevated D_3 receptor binding in dyskinetic patients.[130] The BDNF-dependent expression of D_3 receptors has implications for depression as well. While antidepressant medications target primarily the serotonin and noradrenaline systems, mesolimbic dopamine neurons, that express BDNF, are converging in the targeted systems.[131] Consequently, following stress or chronic antidepressant therapy, alterations in mesolimbic dopamine neuron activity might occur and they can impact the expression of genes, regulated by BDNF in target neurons. In agreement, various antidepressant treatments such as tricyclic antidepressants, selective serotonin reuptake inhibitors, monoamine oxidase inhibitors, and electroconvulsive therapy can increase selectively D_3 receptor expression in the shell region of the *nucleus accumbens*, confirming that these receptors might be beneficial in antidepressant therapies. In fact, the potential use of D_3 receptor ligands in treating depression is found in literature reviews.[132,133]

D_3 agents are also utilized therapeutically in the treatment of PD, due to the fact that dopamine agonists, commonly employed in PD treatment, often exhibit equal or greater affinity at D_3 receptor. This suggests a plausible involvement of the mesolimbic D_3 receptor in providing relief for Parkinsonian symptoms.[134] D_3-preferring agonists such as **pramipexole**[135] and **ropinirole**[136] have been incorporated into therapy to enhance effectiveness in managing PD symptoms[137] and restless leg syndrome,[138] or to decrease the risk of motor complications, even though they cause somnolence as major adverse effect, when compared with **levodopa**[139](Scheme 2). It has been studied with a

rodent model of PD that intraventricular infusion of the dopamine D_3 receptor agonist **7-OH-DPAT**[140] triggered cellular proliferation with a certain neuronal maturity in *substantia nigra pars compacta* of hemiparkinsonian rats.[141] Another report demonstrated that D_2/D_3 agonists with preferential affinity for D_3 receptors (e.g. **quinpirole**[142] and **7-OH-DPAT**) produced neurotrophic changes, especially expansion of dendritic arborization,[143] suggesting a positive outcome in neurodegenerative conditions, where disruptions in dendritic arborization can lead to altered synaptic connectivity, impaired signal integration, and compromised neuronal plasticity. In this work the involvement of D_2/D_3 receptors was investigated at the intracellular level, focusing on the ERK signalling pathways, known to be involved in cell growth and morphogenesis. The expansion of dendritic arborization observed after 3 days of **quinpirole** incubation was antagonized by pre-treatment with one of the three phosphorylation inhibitors known to interfere with D_2/D_3 intracellular pathways such as **sulpiride**.[144]

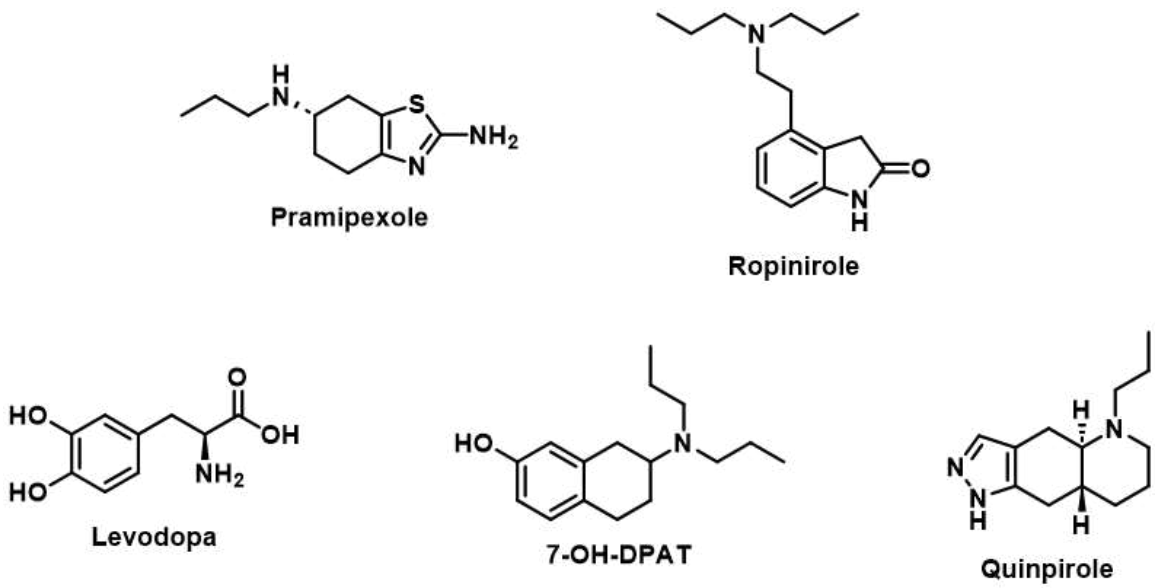

Scheme 2. Chemical structures of D_2/D_3 agonists with selectivity towards D3 receptor.

To summarize, dopamine D_3 receptor has become a pivotal point for development of new antipsychotics for three main reasons:[122]

1) The role of dopamine in psychotic disorders like schizophrenia.
2) The presence of D_3 receptors in limbic brain regions crucial for antipsychotic effects.
3) The higher affinity of many existing antipsychotics for this specific dopamine receptor subtype.

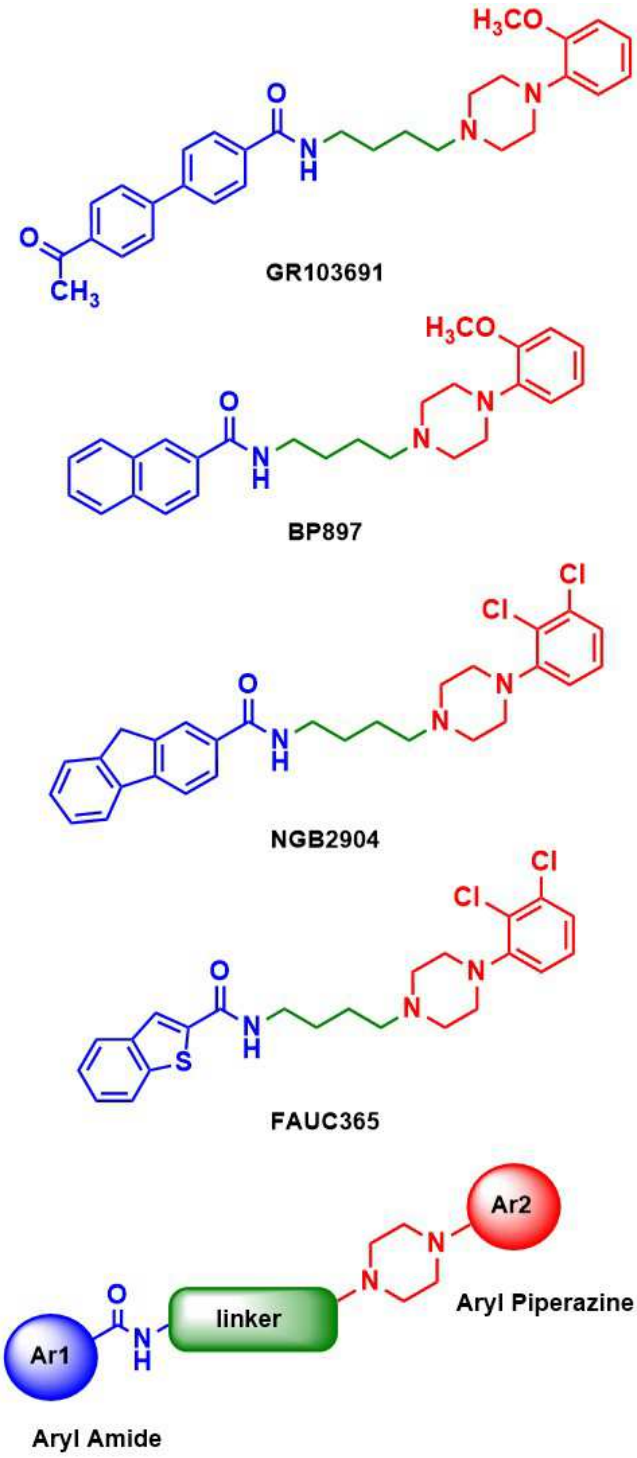

Scheme 3. Chemical structures of D_2/D_3 antagonists with the related pharmacophore model of selective D_3 ligands. The arylpiperazine moieties, represented in red, are the primary pharmacophores, while the arylamides, depicted in blue, are considered the secondary pharmacophores. The spacer is coloured in green.

Moreover, D_3 receptors feature 420-fold higher affinity for dopamine compared with D_2 ones and, unlike D_2 receptors, minor alterations in their number or activity can have severe impacts on synaptic communication.[145] However, it has been a challenging task in the last decades to obtain a highly selective subtype ligand or a drug candidate with a pharmacological profile uniquely on a single receptor among D_2 and D_3, simply because the structures of the two receptors are almost identical. In details, if a structural sequence alignment of wild type receptors is considered, a moderate sequence identity of 50% exists between D_2 and D_3 receptors. When similarity is assessed using the Gonnet250 similarity matrix,[146] the similarity score between D_2 and D_3 increases up to 63%, confirming the initial trend. Furthermore, when focusing on the transmembrane regions as primary interaction sites for ligands, the sequence similarities increase until 80%.[147]

In early 2000s a plethora of structures has been reported in the search for novel D_2/D_3 receptor ligands. Some of them attracted particular attention, because they were claimed as D_3 receptors selective antagonists (or partial agonists). These "early" D_2/D_3 ligands had higher affinity at D_3 receptor, innovative pharmacological characteristics in drug-seeking behaviours, selectivity over off-target receptors. Therefore, the first structure activity relationships (SAR) and pharmacophore model for D_2/D_3 receptor ligands and/or selective D_3-receptor ligands were provided.[97,98] The

compounds are shown in Scheme 3. **GR103691** was an interesting molecule, highly affine at both receptors of interest, displaying activity only in the mesolimbic dopamine system and selectivity over serotoninergic receptors.[148] **BP897** exhibited high potency as a dopamine D_3 receptor ligand with an inhibition constant of 0.92 nM, demonstrating a significant 70-fold selectivity, when compared with D_2 receptor (Scheme 3). It displayed moderate affinity for 5-HT_{1A} receptors (K_i = 84 nM), adrenergic α1 receptors (K_i = 60 nM), and α2 adrenoceptors (K_i = 83 nM). This compound obtained considerable attention, due to its ability to reduce cocaine-seeking behaviour in rats at a dose of 1 mg/kg intra parenteral, without inducing reinforcement on its own.[149,150] Indeed, **BP897** has been taken as one of the lead compounds in this PhD project. Throughout the replacement of the 2-methoxyphenyl group with the 2,3-dichlorophenyl ring attached to the piperazine nitrogen, a new set of potent and selective D_3 ligands was synthesized. Among these compounds, **NGB2904**, a fluorenyl carboxamide-based derivative, firstly reported in 1998,[151] and **FAUC365**[152] stood out. Both of them exhibited a distinct D_3 antagonistic profile with a K_i value of 0.90 nM for **NGB2904** and K_i of 0.50 nM for **FAUC365**, demonstrating exceptional affinity at this receptor subtype and remarkable selectivity, comparing with the other dopamine receptor subtypes.[151,152]

Taking a closer look to the mentioned compounds, it is easy to observe common elements that are referred to the pharmacophore model (Scheme 3): an aryl moiety bearing a H-bond acceptor (amide in blue, scheme 3) connected to a basic moiety, often represented by an arylpiperazine system (in red), throughout a linker that is usually characterized by a *n*-butyl chain (green in scheme 3).[98,153] In addition, Hackling and co-workers identified two more crucial features for a D_3-preferring affinity: linearity and extension.[154] Basically, they performed a comparative study by superimposing selected D_2/D_3 ligands that showed higher affinity for D_3 receptor over D_2 and vice versa within the D_2/D_3 pharmacophore model. The projections have revealed that preferring-D_3 receptor ligands tend to assume an elongated and linear conformation, while preferring-D_2 receptor molecules typically exhibit a more curved orientation as it is depicted in Figure 5.

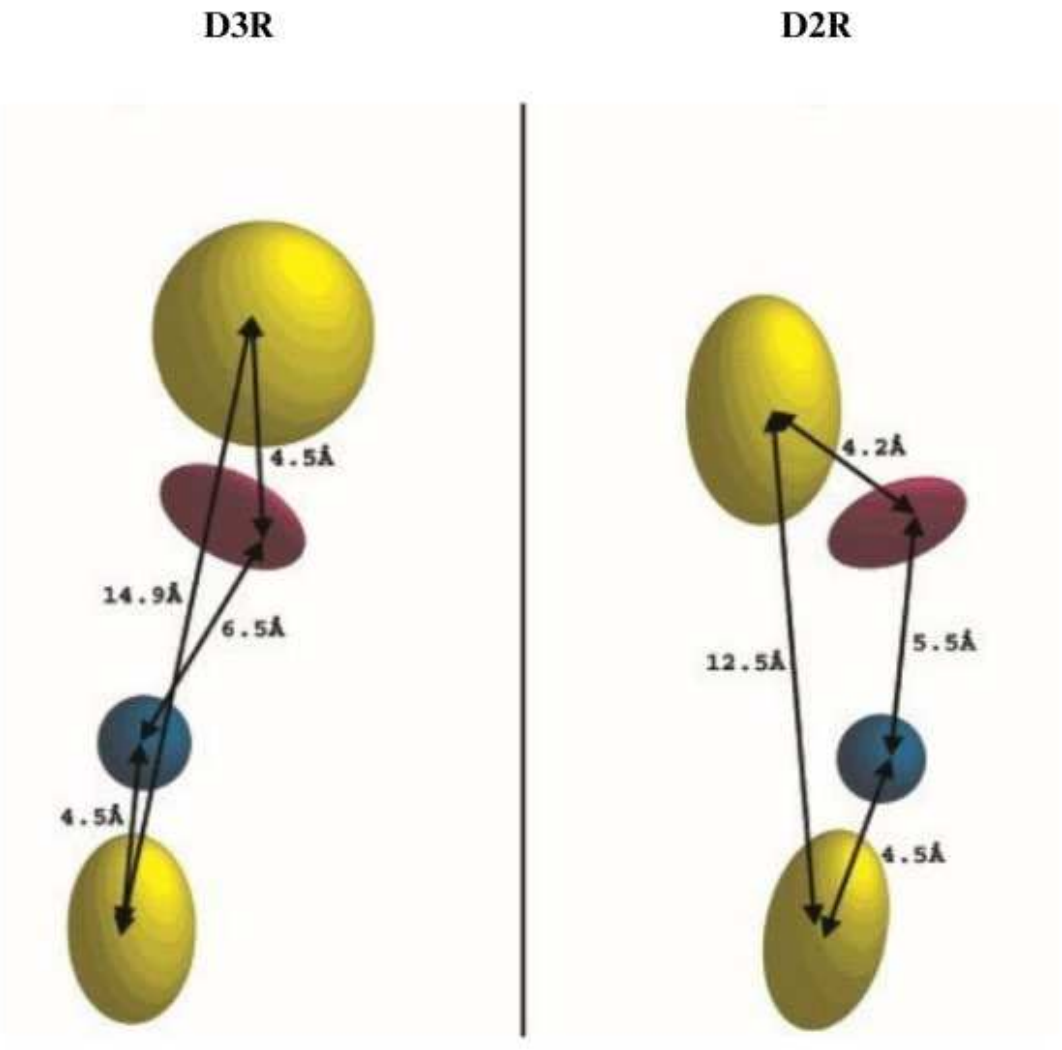

Figure 5. Schematic representation of pharmacophoric points in the D_3 conformation (left side) and D_2 conformation (right side) obtained by superimposition of selected ligands within the pharmacophore model. The pharmacophoric points are shown in yellow for aromatic moieties, violet for hydrogen bond acceptor, blue for basic aliphatic nitrogen atom. The distances are described in Armstrong (Å) and outline the higher length and extension found in preferring D_3 ligands conformation. Picture adapted by Hackling *et Al.*[154]

Following this model, it has been possible to vary and improve structural motifs in terms of affinity towards D_2 and D_3 receptors and selectivity at D_3 over D_2. For example, the lipophilic residue of aryl amide allowed diverse modifications including cycloalkyl, aryl, heteroaryl units, while the arylpiperazine system underwent replacement into piperidine systems or modifications of substitutional patterns in the aromatic ring. In contrast, the linker has been object of minimal modifications such as the insertion of hydroxy group in position 3 of the chain or a double bond, with the purpose of increasing the structural rigidity.[154–160] For the same reason, an ethyl cyclohexyl structure replaced the chain of 4 carbons, producing interesting ligands,[161–163] clinical candidates like **SB-2770011A** with an inhibition constant of 12.7 nM at D_3 receptors and 100-fold selectivity over

D2;[164] **SB-269652** that bears high affinity values at D_2 receptors (K_i = 33.9 nM) and at D_3 (K_i = 1.9 nM);[165] and ultimately a marketed drug, that is **cariprazine,** showing the best pharmacological profile with K_i = 0.7 nM for D_2 and K_i = 0.09 for D_3 receptors[166] (Scheme 4). Even if this structure was developed 20 years after the first use of this type of linker, it obtained the approval by food and drug administration (FDA) in 2015 for treatment against schizophrenia and bipolar disorders under the trade name of Vraylar. But the structural innovation of cariprazine lies in a more rigid linker and in the absence of aryl amide moiety, efficiently replaced by a methylated ureido group in combination with the hydrophobicity of cyclohexyl linker.[97,167] This compound and its innovative design have

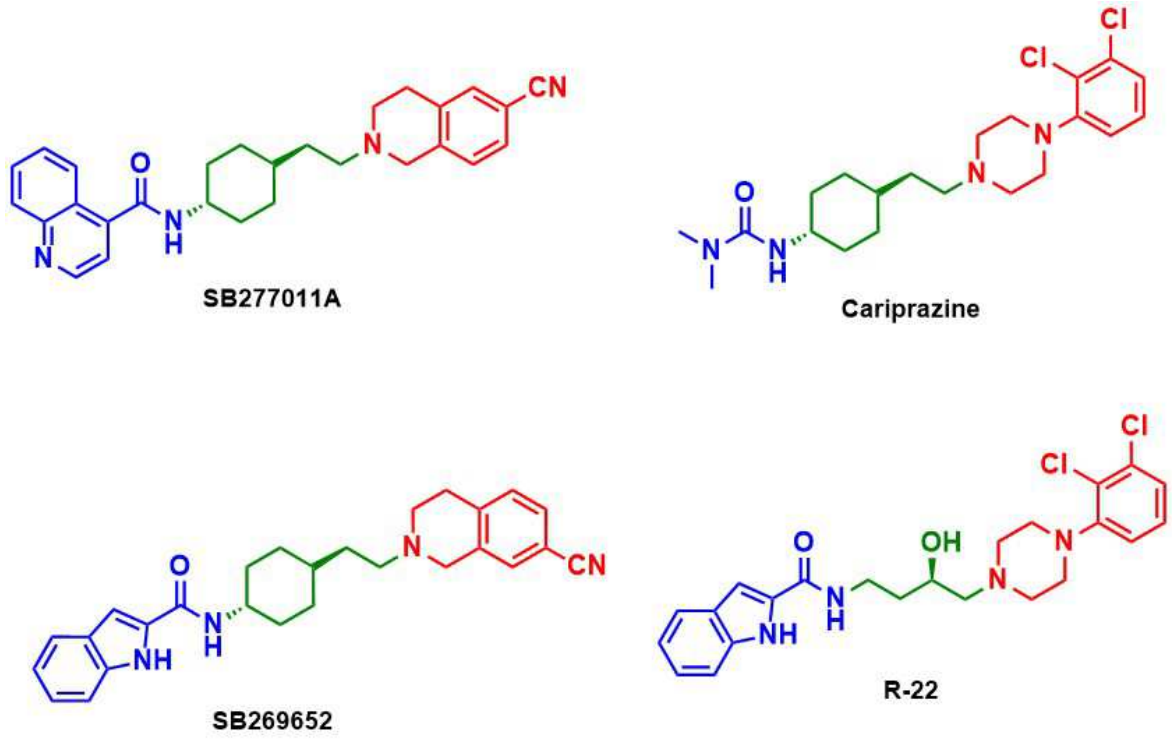

Scheme 4. D_2/D_3 antagonists and partial agonists displaying modifications at linker unit. **SB277011A** and **SB26952** bear an alternative basic moiety, represented by the tetrahydroisoquinoline ring. The compounds shown have a selective D_3 receptor pharmacological profile according to the related references.

been taken as inspiration for the design of the ligands described in this PhD project.

The achievement of the first structures of D_3 receptor in 2010 and D_2 in 2018 have been incredibly helpful; especially after 2010, the research of selective D_3 ligands has boosted up, because putative selectivity criteria have been outlined. Chien *et Al.* provided precise binding points and strengthened previous structure activity relationships for D_3 receptor. For example, at physiological pH, the tertiary amine within the ethyl pyrrolidine ring of eticlopride is likely to be charged and forms a 2.8 Å salt bridge with the carboxylate of $Asp110^{3.32}$, a highly conserved residue in most aminergic receptors including D_2 and D_3. This salt bridge plays a crucial role both structurally and pharmacologically in

facilitating highly effective receptor-ligand interaction and it is positioned within the orthosteric binding site (OBS) of both target receptors. This is the reason why, piperazine or piperidine rings are considered core moieties,[168] keeping in mind that they are protonated at physiological pH like eticlopride.

Another vital feature of eticlopride-based binding mode is an aromatic ring with a substitution connected to the pyrrolidine via amide bond, fitting tightly into a hydrophobic cavity bordered by helices VI, V, III, and ECL2. The presence of polar substituents (e.g., -OH, -OCH_3) in the phenyl ring enables intramolecular hydrogen bonding with both N and O atoms of the amide, maintaining the compound in a nearly planar conformation as evidenced by crystallized structure analysis.[169] In this way, it was demonstrated the necessity of having a carbonyl moiety or acyl-like unit in that area of the receptor.

After having examined the D_3 structure, the authors have conducted a similar analysis between D_3 and D_2 receptors, constructing a homology model of D_2 receptor using the structural framework of D_3 as a reference. In this way they have pointed out that of the 18 eticlopride contact residues in the D_3 structure, 17 are identical in the D_2 ($Val350^{6.56}$ is an isoleucine in D_2). Further, they performed a docking studies with **R-22**[157](compound described by Newman *et Al.* in 2009 that shows a selectivity index over D_3 of 394 with K_i = 502 nM at D_2 receptors and K_i = 1.4 nM at D_3), revealing that 2,3-dichlorophenylpiperazine binds to the OBS, the same pocket where eticlopride binds. Meanwhile, the indole-2-carboxamide terminal is directed towards a binding pocket formed by ECL2/ECL1 and the intersection of helices II, III, and VII, delineating a secondary extracellular binding pocket known as SBP, see Figure 6.

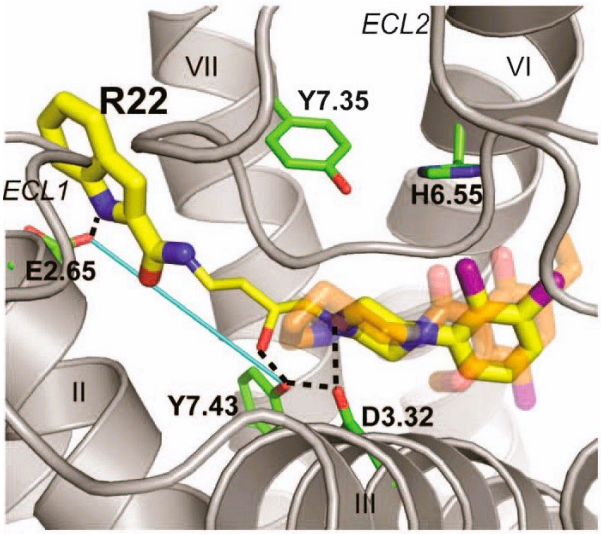

Figure 6. The docking of the most extended conformation of **R-22** is represented in yellow. The 2,3-diCl-phenylpiperazine occupies the same space as bound eticlopride (orange), whereas the indole-2-carboxamide interacts within ECL2 and ECL1. Adapted by Chien *et Al.*[47]

In the particular case of **R-22** another point must be considered, that is the linker which is represented by a butyl chain with -OH in position 3, allowing the ligand to have proper poses and interactions inside SBP (Scheme 4).[157,169] Such docking studies and comparative simulations on D_2 by Chien and colleagues demonstrated that a significant portion (44%) of the extracellular segment of helix I, particularly from positions 1.35 to 1.50, exhibits non-conservation between D_2 and D_3 receptors (Figure 7). This divergence is likely to induce significant alterations in the packing arrangement

within D_2 receptor at the intersection of transmembrane helices I, II, and VII, aligning with findings from prior SAR investigations.[170–172]

Notably, the absence of conservation at $Thr^{3687.38}$ (replaced by Phe in D_2), a residue, that forms a hydrogen bond with the conserved $Tyr^{3657.35}$ backbone in D_3, could contribute to a positional shift between helices I and VII. The differences in the structural arrangement and backbone configuration between D_2 and D_3 receptors, even if they are minor, are thought to influence subtype selectivity. Moreover, the distance between the conserved $Glu^{952.65}$ (located in the second binding pocket, SBP) and $Tyr^{3737.43}$ (situated between the OBS and the SBP) is approximately 1 Å larger in D_3 when compared with D_2 due to the occurrence of unique interactions.[169] These special relations are considered very important in the structural correlation between the OBS and the SBP within D_2 and D_3 receptors, confirming the previous calculations of Hackling and co-workers.[154] Visualization of differences among the two receptors are shown in figure 7 below.

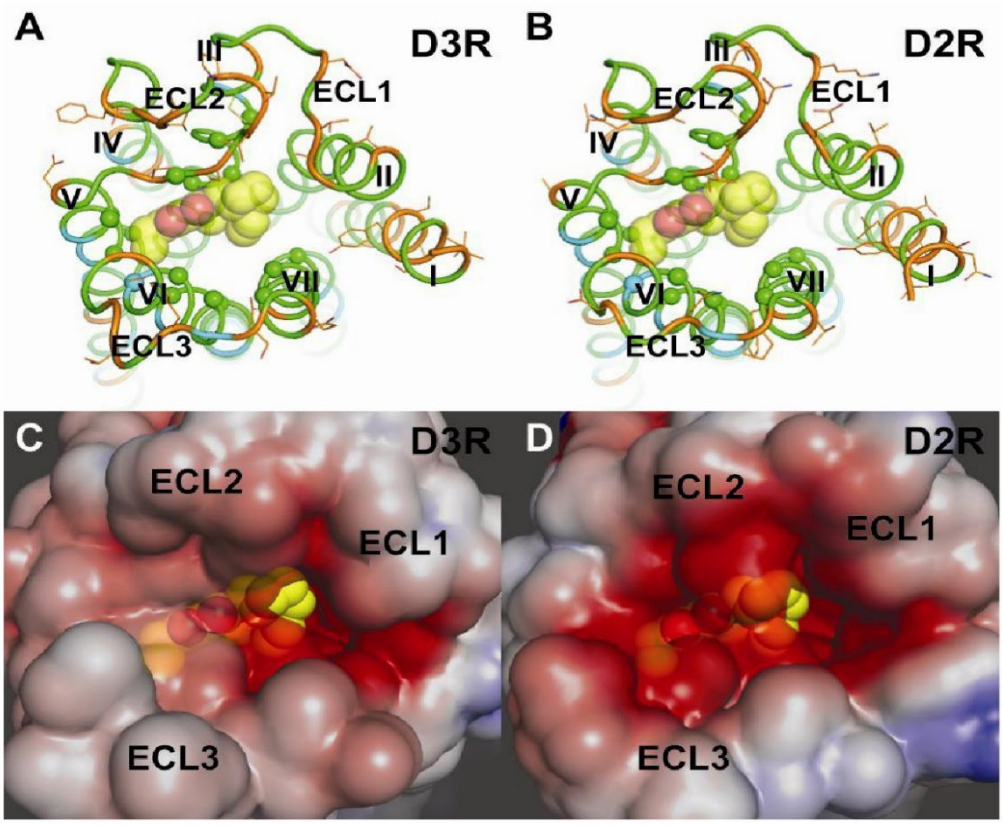

Figure 7. Extracellular viewpoints display the distribution of non-conserved regions in the D_3 receptor (**A**) and D_2 receptor (**B**). Regions with identical residues are highlighted in green, those with similar residues in cyan, non-conserved positions in orange, and the ligand eticlopride represented by red and yellow spheres. Variations in residues within the extracellular loops lead to distinct electrostatic surfaces between the two receptors, as illustrated by D_3 in (**C**) and D_2 in (**D**). Noticeable electrostatic distinctions are evident, particularly in the area responsible for forming the second binding pocket of D_3-selective compounds. Figure reproduced by Chien et Al.[47]

The structure of the D_2 receptor has been the last obtained in chronological order, so the comparison with the known ones of D_3 and D_4 receptors helped even more to outline the structural differences. The first dopamine D_2 structure has been achieved in a bound complex with risperidone which is an inverse agonist, thus the receptor has been analysed in its inactive state. Comparing with D_3 and D_4 receptors, there are subtle differences in extracellular loops ECL1 and ECL2, and in extracellular ends of transmembrane helices V, VI and VII. In the D_2-risperidone structure, the rearrangement of ECL2 creates a small helical turn, where the residues of this section are pointing across the binding pocket to interact with ECL1, instead with the ligand. So, ECL1 and ECL2 are generating a lipophilic area, that is not involved in engaging the ligand. The extracellular tip of transmembrane helix V (TMV) is shifted closer to the transmembrane bundle. Whereas, TMVI and TMVII are more distant from the receptor core, respectively, when compared with the corresponding regions in D_3 and D_4.[49]

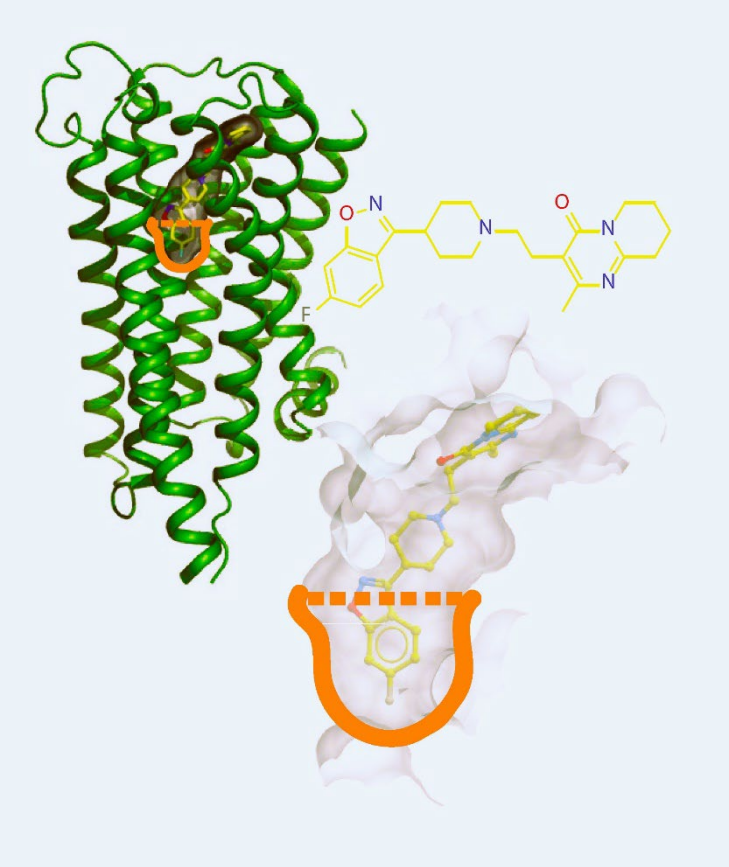

Figure 8. Representation of risperidone and its binding pose within dopamine D_2 receptor. The sub-pocket below OBS is marked in orange. Adapted by Wang *et Al.*[49]

Unlike eticlopride, which has been used for D_3 receptor, risperidone lacks an amide group and instead features a benzisoxazole moiety. This unique motif exhibits a distinct binding mechanism by extending into a deep binding pocket created by the chains of helices III, V, and VI, forming a sub-pocket beneath the orthosteric site (Figure 8), while $Asp114^{3.32}$ forms a salt bridge with the tertiary amine of risperidone. Nevertheless, the most substantial difference has been found in the location and structure of the SBP in D_2. In dopamine D_2 receptor, the SBP extends towards the extracellular region of TMVII and is formed by ECL1 alongside the junction of helixes I, II, and VII.[49] Whereas, in dopamine D_3 receptor, the SBP is formed by the junction of ECL1 and ECL2 involving helix III at the place of helix I. Additionally, the loop of ECL1 is rotated enough to orientate the conserved residue of Trp^{EL1} towards the binding pocket, thus having a unique conformation among the $D_{2\text{-like}}$

receptors, and the extracellular tip of TMVII makes an outward rearrangement that creates additional space in D_2 SBP.[49] Such elements are not found in D_3 SBP.

Furthermore, the second crystal structure of D_2 receptor, obtained by the bound-complex with **haloperidol**, confirmed the residue Asp114$^{3.32}$ as crucial anchoring point within the OBS, because it forms a salt bridge bond with the protonated nitrogen of the piperidine ring, found in haloperidol.[50] On the other hand, the volume of SBP in this D_2 receptor structure is smaller than in the risperidone-bound configuration. This size difference can be attributed to the closer positioning of transmembrane helices II and VII around the ligand. The structural arrangement of haloperidol within the receptor differs from risperidone in two key aspects. Firstly, the chlorobenzene group is positioned nearer to the gap between TMII and TMIII. Secondly, this group extends further towards ECL1. In contrast, the terminal portion of risperidone (benzisoxazole) interacts with TMVI upper turns through aromatic interactions. Examining the structural complex between the D_2 dopamine receptor in its active state**,** Fan *et Al*. have revealed an additional second binding pocket (SBP_2). This pocket is formed by the outward movement of the tryptophan residue at position 100 in the first extracellular loop (Trp100^{EL1}). Notably, the SBP_2 has been found to have two important functions. First, it directly engages with the chlorobenzene moiety of haloperidol. Second, it plays a crucial role in the activation process of D_2 receptor. This newly identified mechanism, combined with the unique positioning of haloperidol within the binding site, may serve as a critical factor in developing potentially selective D_2 ligands over the other dopamine receptors. This additional second binding pocket is disrupted in the risperidone-complex D_2 structure, because the residue Trp100^{EL1} makes an inward rotation.[50]

A similar finding has been achieved with recent reports describing the structure of dopamine D_3 receptor in its active state, thus in agonist-bound state.[53,56] In details, the authors have described the residue H$^{6.55}$ as essential binding point for the agonists used in the studies, because H$^{6.55}$ is forming a stable salt bridge bond with the protonated nitrogen of the ligands (e.g. **pramipexole** and **PD128907**). This residue has not been found in D_2-bound agonist state analyses, rendering it a key determinant for subtype selectivity. In addition to this, Arroyo-Urea *et Al*. have discovered that **FOB02-04A**,[173] the D_3 agonist complexed with the receptor, binds D_3 exploiting the OBS, the established SBP and a new additional second binding pocket (SBP_2), see scheme 5.[55] This SBP_2 is structurally diverse also in aminergic receptors and it could potentially be used to develop subtype-selective ligands. Such molecules could help to improve current treatments targeting the D_3 receptor, as it is target for Parkinson´s disease and other neurological disorders and neuropsychiatric disorders, including substance use disorders.[174–176]

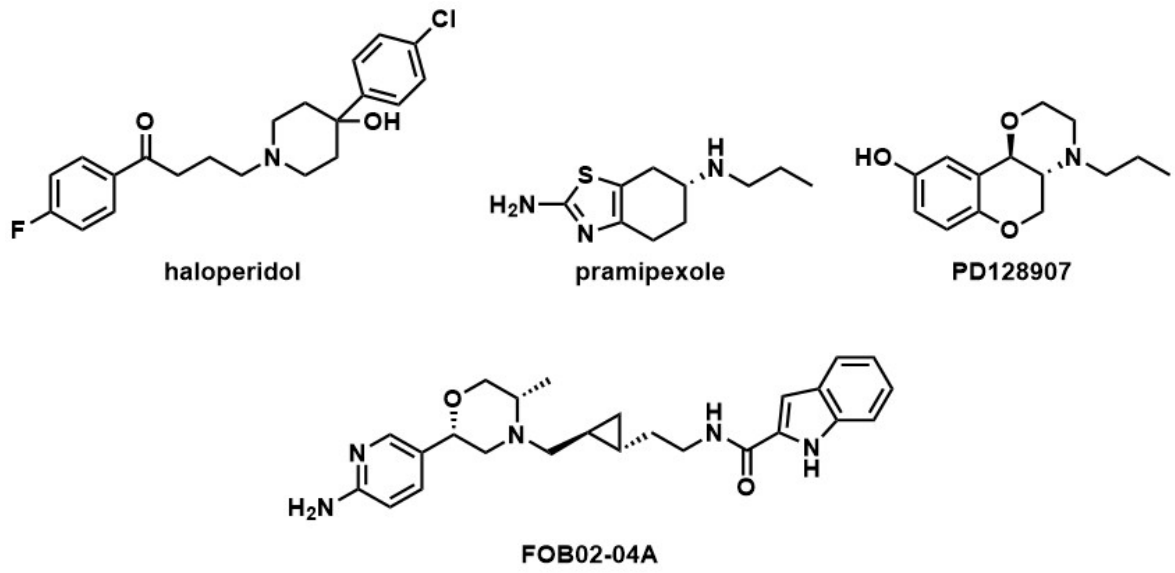

Scheme 5. D_2/D_3 agonists used to obtain the crystal structures of D_2 and D_3 receptors in their active states. [50, 53, 55-56]

The comparison among the structures of D_2 and D_3 receptors have defined groups necessary for binding to OBS (primary pharmacophore, PP) and the ones able to interact with SBP (secondary pharmacophore, SP), providing an upgrade of the previous pharmacophore model for selective D_3 ligands. The upgrade model requires a tertiary amine or protonable nitrogen with minimal variations as PP, because OBS is crucial for ligand-receptor binding in both D_2 and D_3, an apolar linker and lipophilic moiety having an H-bond acceptor unit as SP[123](see Figure 9). An amide group is generally preferred, as the NH might form a critical hydrogen bond with a carbonyl function of residue Cys181 located in the extracellular loop ECL2 of D_3,[177] which plays an important role in the stabilization of the receptor structure. In this way, a selective ligand is effectively anchored at SBP and the secondary pharmacophore might have more opportunities of variation than primary pharmacophore.

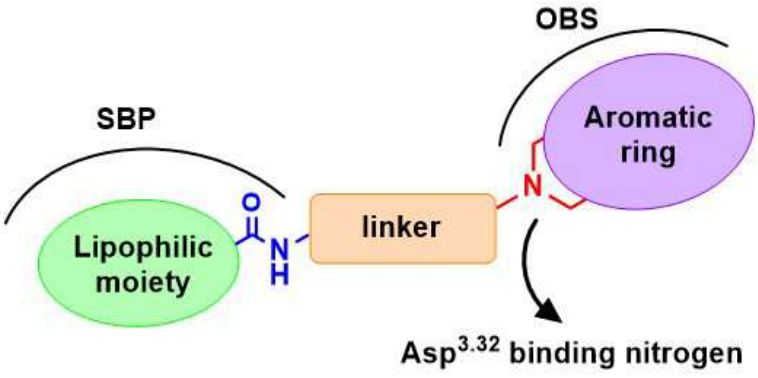

Figure 9. Representation of pharmacophore model of potential selective D_3 ligands characterized by a primary pharmacophore for OBS and a secondary for SBP. The core units are drawn in blue and red.

Since it has turned out that SBP is different between D_2 and D_3 receptors, further studies have been performed exclusively on this binding pocket, because it has considered the main responsible for selectivity towards D_3 over D_2. For instance, Newman and her working team have analysed the SBP of D_2 and D_3 receptors in terms of shape and size. To evaluate the size, they have characterized the volume of the SBP counting the water molecules present in that pocket during molecular dynamics simulations and they have found out a greater number of water molecules in D_3 than D_2.[178] To evaluate the shape, they have run molecular dynamics trajectories with **R-22** and derivatives bound-complexes for both receptors, having the classical butyl linker without 3-OH . Then, the comparison of these trajectories with the bound-complexes of eticlopride has shown conformational rearrangements that occur only in the SBP of D_3.[179] In details, the secondary pharmacophore of **R-22** interacts with D_3 receptor at the interface of TMII, TMIII, ECL1, and ECL2 (Ptm23) while in D_2 the SP is positioned closer to the interface of TMs I, II, and VII (Ptm27). Similar data for both of receptors have been observed with derivatives having butyl chain linker without the OH in position 3. These results are dependant on the conformational flexibility of dopamine D_2 and D_3 receptors, which relies on TMII elasticity that is determined by two factors: 1) a residue of proline that is conserved in both receptors acting as a hinge,[180,181] 2) the configuration of ECL1 which, in turn, regulates the degree of bending at this crucial proline residue. Nevertheless, ECL1 is different between D_2 and D_3, it has one more Glycine residue in D_3, which renders ECL1 flexible enough to allow TMII rearrangement that enhance the optimal accommodation of a ligand in SBP, like it happened for **R-22**.[178] In fact, from these studies TMII, ECL1 and Gly94 have been addressed as the critical determinants for D_3 over D_2 selectivity.[182]

Another important aspect of SBP has been found out: allosteric activity. When SP binds and engages interactions with SBP, an allosteric activity is triggered which, in turn, improves the pharmacological profile of ligand itself by enhancing the affinity between PP and OBS.[183] This condition seems possible only if the linker has particular isomeric conformations within some extended-length molecules, revealing a further determinant for subtype selectivity that is enantioselectivity. Indeed, in their elegant study Moritz *et Al.* found that **(+)-VK04-87** inhibits the D_3 receptor in a mixed non-competitive/allosteric manner, while **(-)-VK04-87** behaves as a purely competitive antagonist (Scheme 5). These findings indicate that bitopic interactions of **(±)-VK04-87** with dopamine D_3 receptor exhibit stereoselectivity naturally, where the allosteric effects are attributed to the **(+)-** isomer. This isomer interacts with the SBP, resulting in a bitopic behaviour. In contrast, the **(−)-VK04-87** enantiomer's SP protrudes away from this pocket, causing lower binding affinity and a competitive mode of action rather than allosteric.[184]

In this matter, another interesting example has been the pharmacological repurposing of **SB269652**, found to be negative allosteric modulator for D_2 and D_3 receptors. Particularly, the binding and functional assays indicated an antagonist behaviour with high concentrations of radioligands or dopamine, but in presence of higher concentrations the molecule had an allosteric profile.[185] In details, **SB269652** is bitopic ligand, bearing a competitive antagonism with receptor monomers and allosteric properties across receptor dimers. Obviously, some SAR have been developed in relation to the structure of this ligand: indole NH as SP and tetrahydroquinoline moiety as PP are crucial for maintaining the allosteric activity (Scheme 4). This type of primary pharmacophore favours the correct orientation of the SP within the SBP. Nevertheless, the choice of linker is influencing the functional activity as well, because a substitution of cyclohexylethyl spacer with the butyl chain, varying lengths of the alkyl spacer, can change the orientation of the SP, leading to a transition from allosteric to competitive pharmacology.[186,187]

Along the lines of these studies, many dopamine D_2/D_3 and some selective D_3 receptor ligands have been demonstrated to be bivalent ligands in nature, because they engage two distinct sites present in both receptors, as explained above. If the allosteric property of SBP is triggered by SP, then the molecule is defined bitopic ligand.[188,189] However, affinity and efficacy of a selective D_3 scaffold is attributed to the PP, while SP is responsible for D_3 selectivity. If the two pharmacophores are taken separately, PP essentially does not show D_3 selectivity over D_2 and SP has virtually no binding affinity to D_3, until these two pharmacophores are linked to each other.[179]

Following this perspective, it is clear that the linker is playing a pivotal role in combining the two pharmacophores. So, the molecule is allowed to have the best conformation in order to bind OBS and SBP, including the possible trigger of allosteric activity. Therefore, the above-mentioned investigations on SBP-SP interactions have given new perspectives and points of variation for the linker as well. Secondary pharmacophores in combination with linkers can influence the selectivity of antagonist activities at D_2 and D_3 receptors. For example, modifications on *trans*-cyclo propyl methyl linker (shown in **(±)-VK04-87**) revealed interactions between binding pockets and relative ligands in bitopic fashion. The observed allosteric effects seem to be facilitated by a bivalent compound of adequate length, where SP is correctly positioned in the secondary binding pocket, which is influenced obviously by the type and structure of the linker. Even minor alterations in the structure and orientation of the linker can result in a transition between allosteric and competitive antagonism, like increasing the length of one, two carbons or adding substituents on the linker.[190]

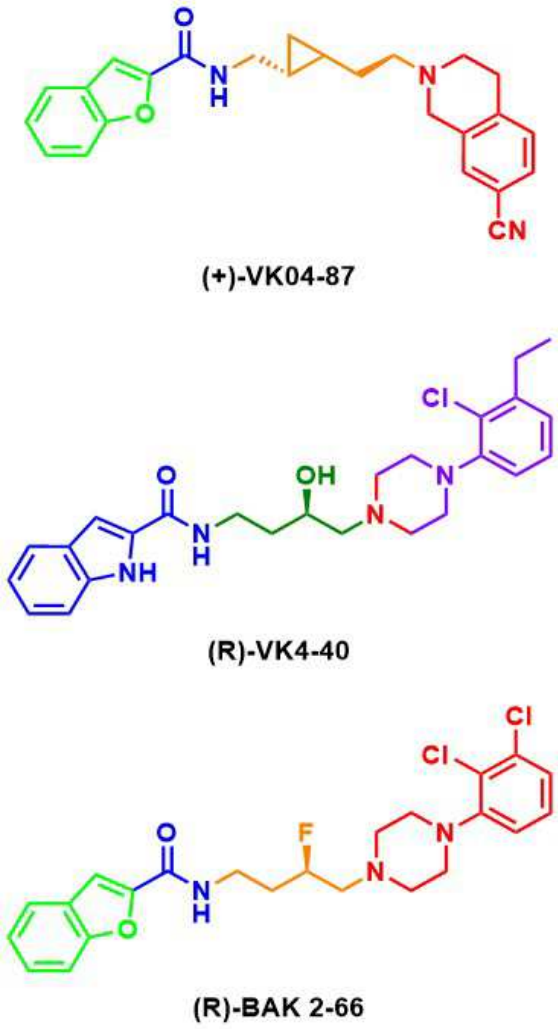

Scheme 6. Dopamine D_2/D_3 ligands bearing a high selective pharmacological profile towards D_3.[184,194,196] These compounds are proved to bind the target receptors in bitopic way. Based on the updated pharmacophore model, new moieties are highlighted in orange for the linker, light green for SP and purple for PP.

Since fluorine (−F) is often regarded as a bio-isostere of a hydroxy group,[191–193] replacement of 3-OH with an atom of fluorine has been evaluated, developing new promising ligands with high D_3 selectivity indices such as **BAK 2-66**, whereby the (R)-enantiomer is the eutomer (Scheme 6).[194–196] The introduction of 3-F in the butyl chain linker has confirmed that the linker is the most influencing part of the pharmacophore model. Little modifications in the linker structure modifies the entire molecule orientation within both binding pockets, obtaining great results. In addition, it has been demonstrated that, like 3-OH, 3-F interacts with ECL2 that contributes to D_3 binding selectivity.[157,195] The introduction of 3-F also resulted in higher permeability through blood brain barrier (BBB), metabolic stability in rat liver microsomes and retention of enantioselectivity, suggesting these derivatives might serve as new lead compounds for further SAR studies and as *in vivo* tools for deeper investigations into the role of D_3 receptor in psychotic disorders.[197] The studies of SBP-SP interactions and linker modifications, that have listed so far, have been used as background for designing the dopamine D_2/D_3 ligands described in this PhD project.

In conclusion, the dopamine D_2/D_3 receptor ligands, described in this section, have been obtained by following a common driving force that is functional selectivity towards D_2 and D_3 or subtype selectivity towards D_3 receptor. The antipsychotic drugs discovery has been characterized by the idea that functional selectivity was believed to be the main solution for the EPS of typical antipsychotics. Nevertheless, alongside this theory, an alternative hypothesis has been developed in late 90s, according to which an antipsychotic drug might exert a biphasic effect in order to manage the symptoms related to schizophrenia. This biphasic effect is matching perfectly with the pharmacological behaviour of a partial agonist whose activity is dose-dependent.[198] Indeed, the biphasic effect idea has led to the third generation of antipsychotic drugs and it may be considered as tool together with functional selectivity for the removal of EPS.[199]

1.2 Schizophrenia

The World Health Organization states that schizophrenia, a persistent and serious mental illness, impacts 20 million individuals globally. This disorder is commonly identified between the late teenage years and the early thirties, with women experiencing symptoms at a later stage. Patients diagnosed with schizophrenia have a mortality rate that is two to three times higher thanthe one of the average populations. Schizophrenia leads to an abnormal perception of reality and a disconnection from it, resulting in significant distress. Symptoms of schizophrenia are generally categorized into three categories:

- **Positive**: disorganized motor behaviours, delusions, hallucinations, disorganized thinking and speech.
- **Negative**: social withdrawal, loss of motivation, lack of enjoyment in daily activities. These symptoms are classified as primary if they are a direct consequence of schizophrenia or secondary if they are triggered by other factors such as depression, drug abuse. The latter symptoms are more difficult to diagnose and they are not targeted effectively by current therapeutic treatments.
- **Cognitive**: lack of attention and of critical thinking, deficiencies in working memory.

A minimum of two of the previous symptoms must be evident for at least one month in order to diagnose schizophrenia, as outlined in the Diagnostic and Statistical Manual of Mental Disorders.[200] Usually, the symptoms are associated with reduced levels of interest in life areas such as work, personal relationships, or self-care. Schizophrenia is a condition that tends to reoccur and necessitates ongoing treatment throughout a person's life, even during periods of remission. Frequently, it is connected to other health conditions like substance abuse, depression, or anxiety.

The cause of schizophrenia remains unknown to date, a putative treatment typically focuses on managing symptoms. Despite this, certain risk factors have been identified, with heritability being a significant one. This concept was first noted by Bleuler in 1910 and subsequent studies have confirmed it, showing up to 83% heritability in twins.[201–203] Individuals with a family history of schizophrenia are at a higher risk of developing the disorder. Over 40 risk genes have been defined so far, including mutations in common inherited and new alleles.[202] Recent advancements in genetic engineering have led to the creation of pluripotent cells capable of differentiating into various cell types, offering insights into the genetic aspects of schizophrenia.[204] Furthermore, environmental factors like migration, substance abuse, neonatal and adult vitamin D deficiency, unemployment, childhood traumas, and prenatal exposure to infections are also considered potential risk factors for

psychosis.[205–210] In addition to the role of the mesolimbic and mesocortical pathways in schizophrenia, recent research has highlighted the importance of the striatal region and the interaction with other neurotransmitters, such as glutamate.[211] This correlation has been supported by evidence showing that NMDA agonists like ketamine can trigger psychosis.[212] Moreover, elevated levels of glutamate can be harmful, leading to toxic effects and enhancing cognitive decline.[213]

Schizophrenia treatment needs a combination of pharmacotherapy and psychotherapy, including individual therapy, social skills training, family therapy, and vocational rehabilitation. The disorder is primarily associated with dopamine dysfunctions, as the dopamine agonists might induce schizophrenia-like symptoms and dopamine antagonists exhibit antipsychotic effects.[214] Antipsychotic drugs, introduced in the second half of the 20th century, remain a pharmacological landmark in curing schizophrenia. These medications are divided in three generations, based on their development timeline and mechanisms of action.

Currently available antipsychotics exhibit D_2 receptor occupancy levels ranging from 60-80%. First generation antipsychotics(FGAs), known as "dirty drugs", lack specificity for dopamine $D_{2\text{-like}}$ receptors and also affect other receptors such as muscarinic, histaminic, and cholinergic. Their non-selectivity causes significant side effects like EPS, that are manifested as tremors, dystonia potentially progressing to tardive dyskinesia, decreased libido and hyperprolactinemia. These unwanted effects are originated from excessive dopamine receptor activation in the nigrostriatal and tuberoinfundibular pathways. FGAs do not address effectively negative symptoms and they include marketed drugs like chlorpromazine, loxapine, haloperidol, perphenazine, and thioridazine (Scheme 7).[215]

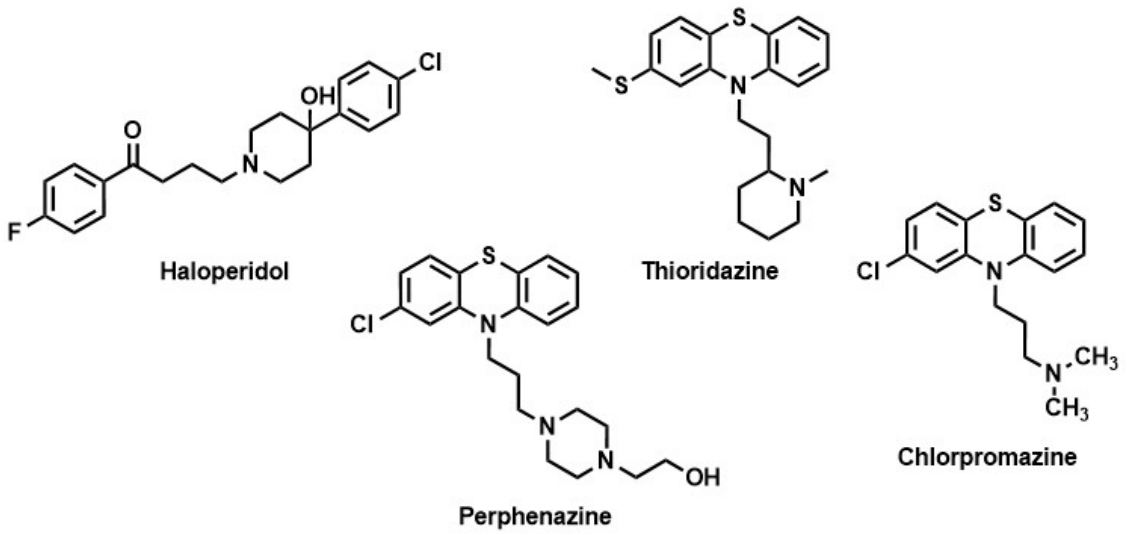

Scheme 7. Some structures belonging to first generation of antipsychotics

The group of second generation antipsychotics (SGAs) consists of drugs such as amisulpride, clozapine, lurasidone, loxapine, olanzapine, sulpiride, quetiapine, risperidone, and ziprasidone, while aripiprazole, brexpiprazole and cariprazine are considered the pioneer drugs of third generation of antipsychotics, as it is shown below in scheme 6.[199] SGAs exhibit greater selectivity compared with the values of FGAs, obtaining reduced side effects and improved patient compliance. They are more effective in addressing negative symptoms and they target serotoninergic 5-HT_{2A} receptors as well.[216] SGAs bind loosely and dissociate more rapidly.[217] However, they are associated with metabolic side effects like weight gain, hyperglycemia and dyslipidemia at a higher frequency than FGAs.[218–220] Clozapine, a notable SGA, is connected to a serious side effect known as agranulocytosis.[221] Second-generation antipsychotics, excluding clozapine, are typically the initial choice for treating schizophrenia.

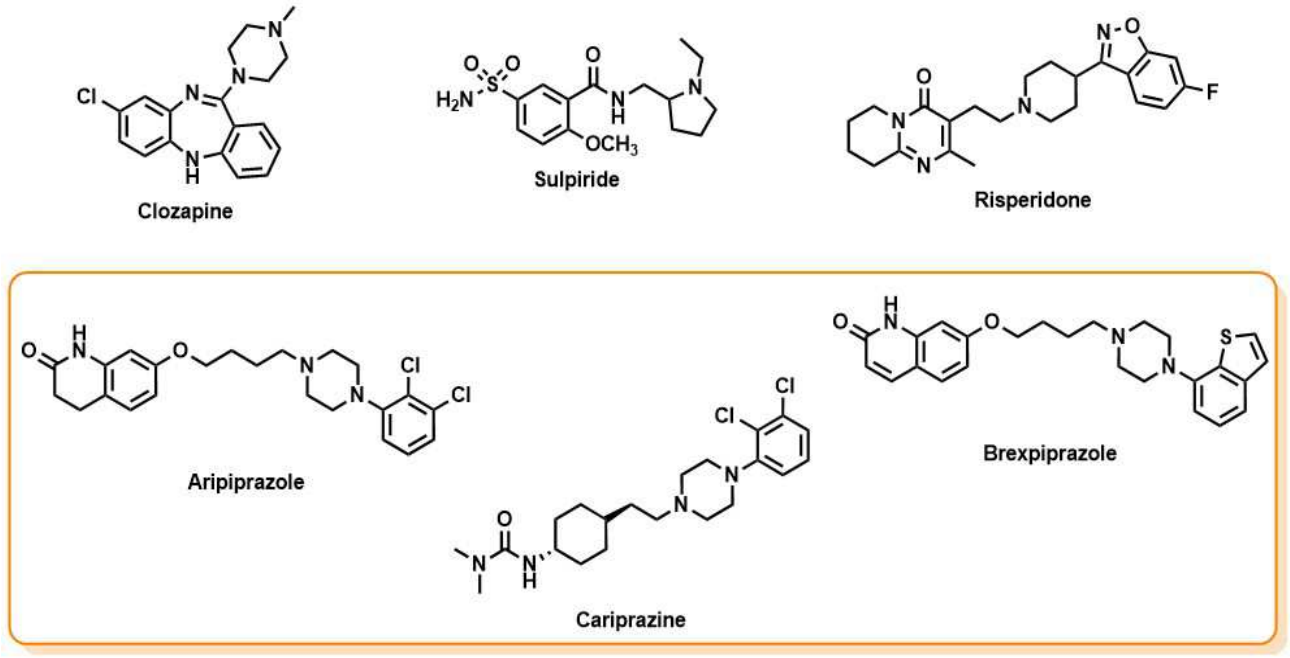

Scheme 8. Representation of some drugs belonging to the second generation of antipsychotics. The ones marked in the orange box are the marketed drugs of third generation.

Novel 4-phenylpiperazine derivatives like aripiprazole, brexpiprazole, and cariprazine have been developed and introduced into the market in order to improve selectivity, to address the side effects associated with traditional FGAs, thus they could be defined as SGA drugs. Nevertheless, they elicit a biphasic effect dose-dependant that make them the so-called "dopamine stabilizers".[222] Aripiprazole, brexpiprazole, and cariprazine are D_2/D_3 partial agonists (Scheme 8).[223–225] These drugs are believed to antagonize excessive dopamine in the striatum, which is linked to the positive symptoms of schizophrenia. At the same time, they show agonist activity by enhancing dopamine release in the mesocortical pathway, which is often low and related to negative symptoms.

As they do not block completely dopamine pathways like the older antipsychotics, the partial agonists might reduce the risk of movement-related side effects and high prolactin levels that are typically seen with the older drugs.[226] On these bases, partial agonism with functional selectivity at D_2 and D_3 receptors represents a innovative approach leading to the newest third generation of drugs, because a single compound may increase or decrease dopaminergic activity according to the state of dopaminergic signalling following the idea of "dopamine stabilization".

The first partial D_2/D_3 agonist approved for the treatment of schizophrenia was aripiprazole in 2002 by FDA. The efficacy of aripiprazole in treating acute exacerbations of schizophrenia and in preventing relapses is well-established and comparable to other antipsychotic medications. In addition, aripiprazole has been approved for treatment of acute bipolar mania and as an adjunctive treatment for major depressive disorder.[227] Whereas, Brexpiprazole has received approval in 2015 to treat schizophrenia in adults and in 2021 for treating major depressive disorder in adults as an adjunctive therapy to antidepressant.[228] Brexpiprazole, like other SGAs, shows high affinity values on serotoninergic receptors 1A and 2A, even though it is very similar to aripiprazole structurally and pharmacologically. Indeed, the total half-life of brexpiprazole is 94 hours, which can be considered identical to 91 h half-life of aripiprazole.[229] When compared with aripiprazole, Brexpiprazole interacts with dopamine receptors in a way that calms rather than stimulates, reducing potentially the likelihood of side effects like agitation and restlessness. It has a lower level of intrinsic activity at the D_2 receptor (around 45%) unlike aripiprazole that has over 60% activity. This means that aripiprazole can activate dopamine receptors even at low doses, but it requires higher doses to block them. In contrast, brexpiprazole competes with dopamine in order to produce calming effect rather than stimulation.[230,231]

Cariprazine, a selective D_3 receptor partial agonist, is particularly effective in managing negative symptoms, it obtained the approval for treating schizophrenia and acute episodes associated with bipolar I disorder in 2015, and it received FDA approval as an adjunctive therapy for treating major depressive disorder in 2022.[232,233] Its metabolism via CYP3A4 produces active metabolites (desmethyl and didesmethyl cariprazine), resulting in a total half-life of 3 days for cariprazine.[234,235] This extended duration improves efficacy, prolongs the time to relapse and mitigates symptoms exacerbation.[236] Given the significant impact of negative symptoms on quality of life, cariprazine is recommended as first treatment option.[237] Indeed, in the pharmaceutical treatment of schizophrenia, the initial approach requires a third-generation antipsychotic as a standalone therapy. If this monotherapy proves ineffective, combining it with another SGA should be considered. FGAs are

reserved for cases where TGA/SGA therapy has not yielded satisfactory outcomes. Detailed guidelines for schizophrenia treatment are outlined in the accompanying figure 10.[238]

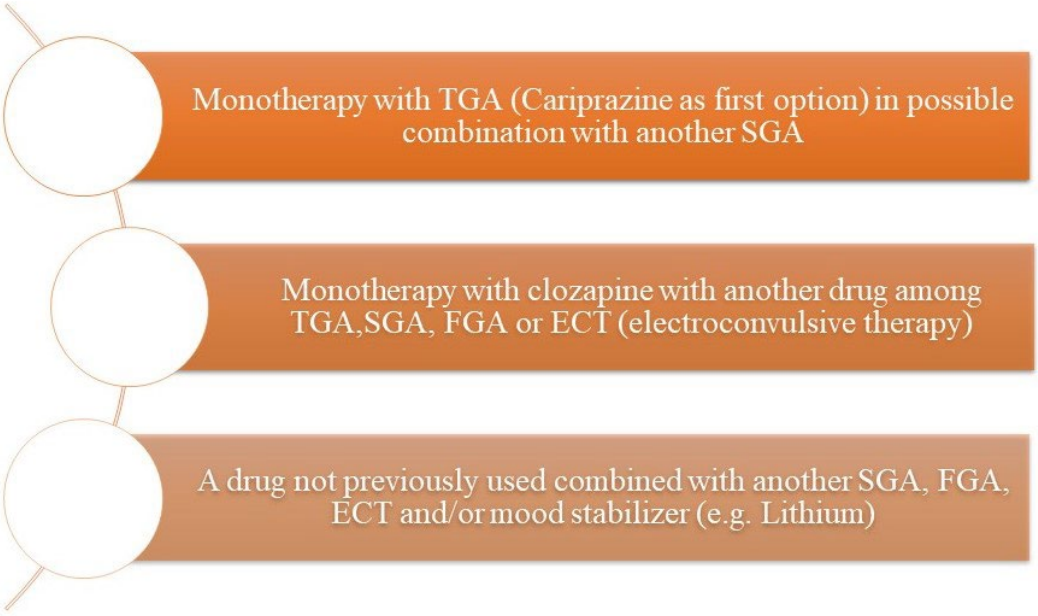

Figure 10. Guidelines for treatment of schizophrenia**,** adapted by Patel *et Al*.[227]

2 Project description and objectives

In recent decades, the crystal structures of the D_2 and D_3 dopamine receptor subtypes have been resolved, providing valuable insights into their structural properties. This has offered important information to guide the design and synthesis of novel, selective dopamine D_2/D_3 ligands. However, no molecules with pharmacological profiles exclusively at dopamine D_2/D_3 (or towards D_3) have yet made it to the market. Among currently available antipsychotic drugs, the lack of selectivity can lead to severe side effects and reduced patient adherence. Moreover, the existing drug regimes often fail to address adequately the negative symptoms of schizophrenia. This leaves significant room for improvement in the field. The D_3 receptor subtype presents an intriguing target, due to its limited localization in the brain and its implications in serious neurological conditions such as schizophrenia and addictive behaviours. Targeting selectively the D_3 receptor could offer therapeutic benefits not seen until now. In summary, the development of selective dopamine ligands remains an ongoing challenge, while progress has been made in understanding dopamine receptors structure. Overcoming this challenge may produce more effective and better-tolerated treatments for neurological and psychiatric disorders.

Over the years, the focus has been on designing selective ligands for D_2 and D_3 receptors, with particular interest on the second ones; indeed, **BP897** was the first selective ligand described, initiating the development of substituted *N*-phenylpiperazine based ligands. Therefore, 1-(2-methoxyphenyl)piperazine, displayed by this compound, served as primary pharmacophore for the entire set of molecules described here. Based on the pharmacophore model of selective D_3 ligands shown in section 1.1.2 (Figure 9), the main objective of this PhD project was synthetizing and evaluating dopamine D_2/D_3 receptor ligands; introducing different linkers in combination with variations of SP moieties. Doing so, it was possible to investigate and explore SAR interactions within the second binding pocket of target receptors, since the SBP is considered a crucial determinant for selectivity. In this way, exploring the chemical space of this binding site gave interesting insights to obtain possibly better binding properties within the receptors of interest.

As first step of the project, sulphur-based replacements of arylamide unit were applied due to comparable H-bond donor/acceptor properties. Therefore, the sulphur group was inserted in the "classical linkers": butyl and cyclohexylethyl (e.g. **BP897** and **cariprazine**), an aromatic ring was used to link the evaluated sulphur units to 2-methoxyphenylpiperazine with the purposes of increasing the structural rigidity and following the concepts of extension and linearity. So, an initial set of

sulphur-based novel dopamine D_2/D_3 ligands was produced, showing modest nanomolar affinity values at both receptors (Figure 11).

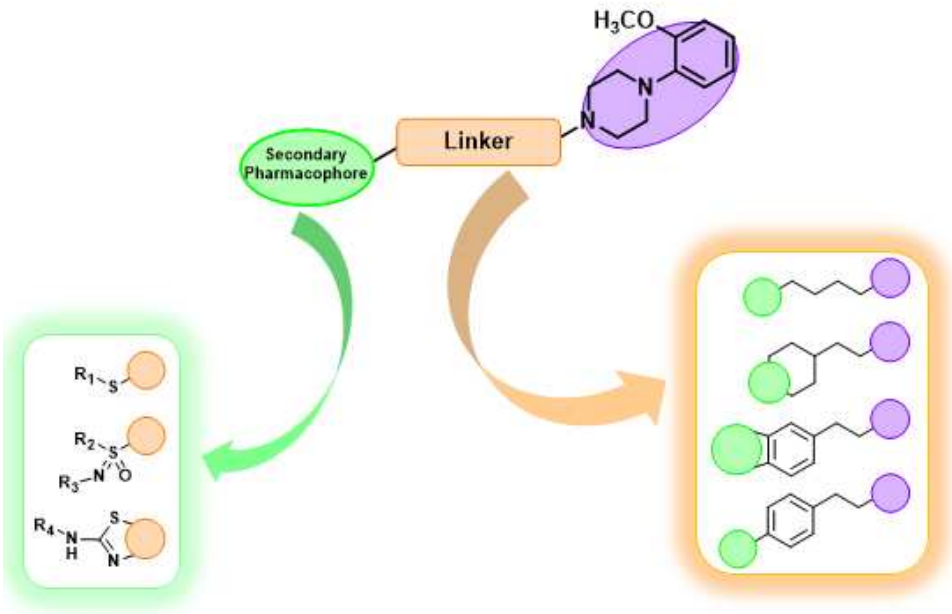

Figure 11. Rational design of sulphur-based dopamine D_2/D_3 ligands described in the research project. The linker modifications are listed in the orange box while the SP variations are grouped in the green box.

Following the structural innovation brought by the development of **cariprazine**, in which the lipophilicity of aryl amide moiety (SP) had been replaced by the linker and being inspired by the results of sulphur ligands, the aromatic linker application was investigated in deep. Firstly, two variations were examined: phenylmethyl and phenylethyl. For each variation, the substitution patterns in *ortho*, *meta* and *para* positions were considered in order to understand which conformation would be the most effective in binding the target receptors. The evaluation was performed combining the aromatic linker with 1-(2-methoxyphenyl)piperazine and methylamide on the opposite sides of phenyl ring. Secondly, it was analysed whether manipulation of electronic properties of aromatic ring would have an impact on affinity values by changing the functional groups attached to it, as it is shown in figure 12. A second set of conformationally restricted dopamine D_2/D_3 ligands with nanomolar affinity was synthetized, developing an innovative 4-aniline-ethyl linker that was used as main scaffold for the third part of PhD project.

The great advantage of 4-aniline-ethyl linker was the presence of aniline group at the western end of the molecule (figure 12), which gave the possibility to apply several modifications, to experiment diverse substitution pathways and to alternate structural motifs. In this way, a more expanded evaluation of SP moieties was executed in order to optimise the pharmacological profile shown by the developed scaffold. Thereby, several residues were applied to the phenylethyl linker such as alkyl,

cycloalkyl, aryl, heteroaryl or biphenyl substituents, increasing the size and molecular weight of the scaffold alongside the hydrophilicity by replacing the amide function with urea. Ultimately, a large set of 4-aniline-ethyl linker-based amides and ureas with different variations were synthetized showing interesting affinity values at both dopamine D_2 and D_3 receptors.

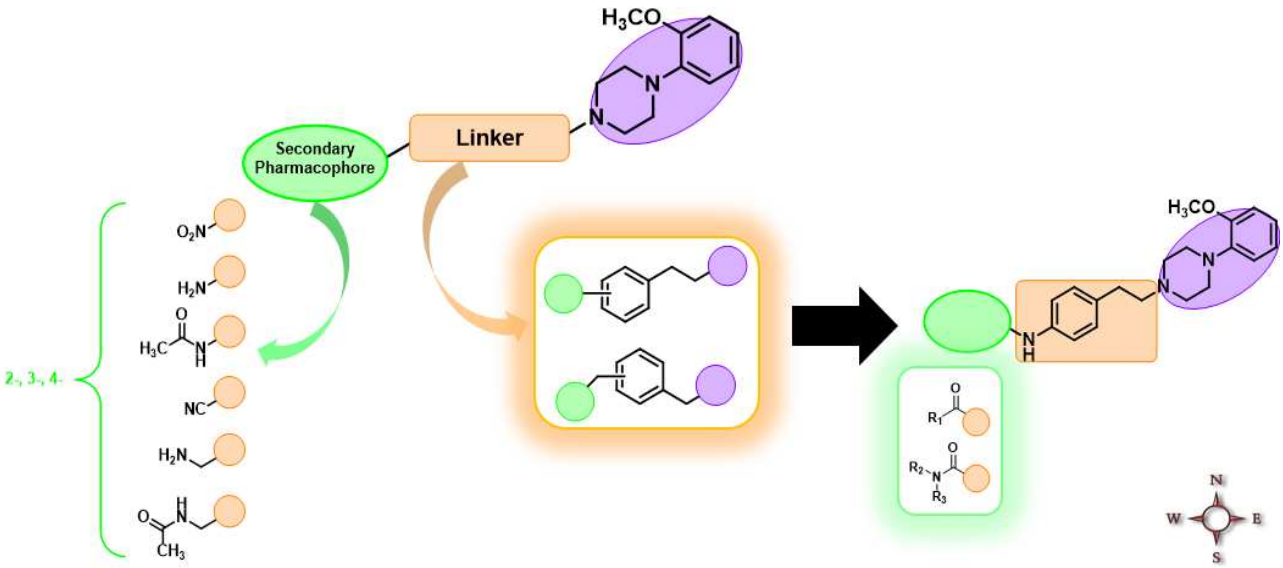

Figure 12. Rational design of second set of ligands described in this project. The variations of aromatic linker are represented in the orange box. The substitution patterns with corresponding functional groups are listed in green box. The black arrow indicates the obtaining of 4-aniline ethyl linker scaffold, which was used as blueprint for the development of amides and ureas, produced in the last part of the PhD project.

To conclude, a library of 93 novel dopamine D_2/D_3 ligands was rationally designed, synthetized and screened in pharmacological assays. A SAR investigation was performed focusing on linker modifications combined with secondary pharmacophore variations. An innovative scaffold was developed and further analysed by evaluating interactions with the binding pockets of target receptors.

The described derivatives were synthetized and characterized following state-of-art procedures. The related analytical data were obtained using APCI-MS, HPLC-MS, HPLC-HRMS, HPLC-DAD, ^{1}H-NMR and ^{13}C-NMR. Major details for analytics are listed in the experimental part (see section 6) as well as for pharmacological assays described in section 4. The synthetical routes and the chemical procedures are described in the next chapter.

3 Chemistry

The main objective of this PhD project is the rational design and synthesis of dopamine D_2/D_3 ligands to develop small molecules. These ligands could be further used in providing innovative details within subtype selectivity or in treating neurological diseases. In this chapter, the main chemical routes and reaction mechanisms for the synthesis of desired ligands will be described. *In silico* studies, determination of pharmacological properties, and SAR investigations will be explained in chapter 4. Synthesis description follows the experimental timeline of the PhD project, with overlap of few works that are mentioned and explained in corresponding sections. This chapter is divided in three parts, based on the three sets of ligands that were produced.

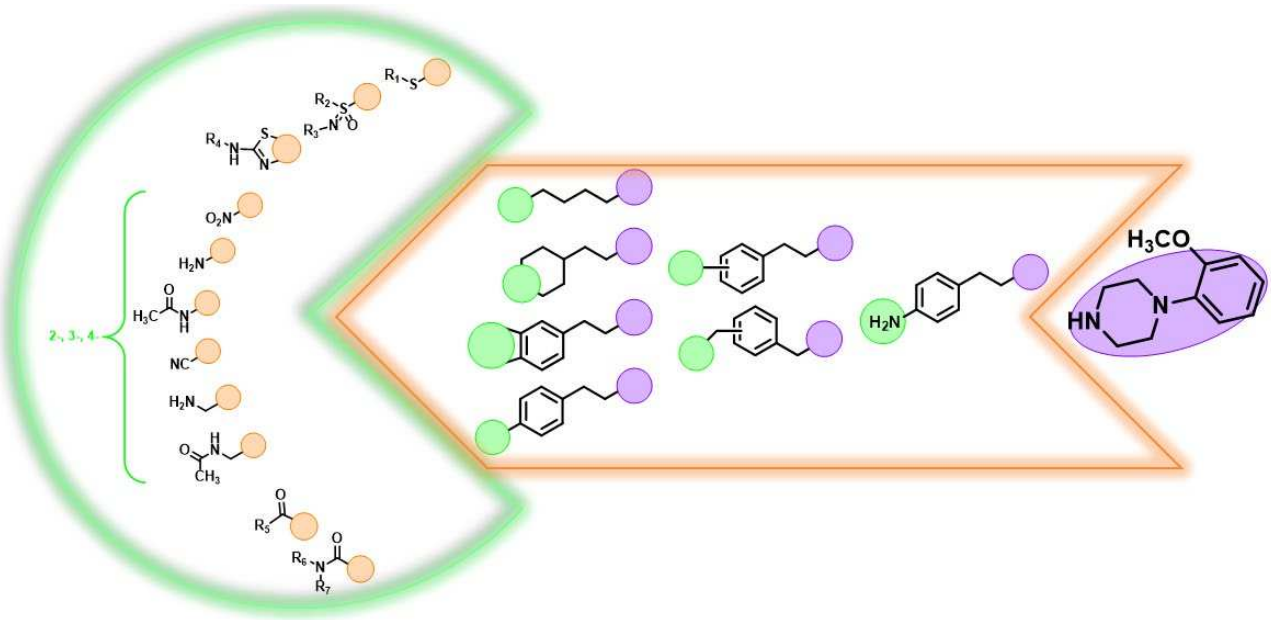

Figure 13. General overview of the structural variations executed in this PhD project. The moieties, grouped in the green sphere, represent the modifications applied as secondary pharmacophores. The different linkers evaluated in the project are listed in the orange arrow, in which 4-aniline-ethyl scaffold is the ultimate spacer. 1-(2-Methoxyphenyl)piperazine is highlighted in purple as primary pharmacophore.

3.1 Sulphur-based dopamine D_2/D_3 receptor ligands

N-Phenylpiperazine derivatives acting as antagonists and partial agonists of the dopamine D_3 receptor have shown promising for treating substance abuse and various neuropsychiatric conditions. Nonetheless, the achievement of lead selective D_3 structures has proven difficult, due to the significant sequence similarity between D_3 and D_2 receptors. In this effort, the SBP has found to be the main structural difference, thus it has been considered a key determinant for intrinsic affinity and subtype selectivity. It is possible to modulate the affinity and efficacy of an extended D_2/D_3 ligand, by changing SP motifs combined with modifications on apolar linkers.[222] Indeed, interactions across SP and SBP might influence the orientation of the linker and the position of PP within the orthosteric binding site, which results in fine-tuning the entire pharmacological behaviour of a molecule towards the receptors of interest.[123]

Based on the pharmacophore model (Section 1.1.2), the linker and PP are represented by a lipophilic moiety and a protonable nitrogen like *N*-phenylpiperazine, respectively. Whereas, the most suitable unit for SBP is an amide thanks to its H-bond acceptor/donor properties. It may contain a lipophilic residue that tolerates diverse substituents such as cycloalkyl, aryl, heteroaryl or biphenyl groups. In addition, modifications of this area provide alterations of physicochemical properties, being determining factors for drug-likeness and for bioavailability of drug candidates.

Following these scaffolds, preferring dopamine D_3 partial agonists such as **BP897** and **cariprazine** served as blueprints for synthetizing the first set of dopamine D_2/D_3 ligands described in the PhD project (Figure 14); this group consists of 17 compounds that display a sulphur unit as replacement of carbonyl moiety for the SBP. Lately, sulphur based functional groups like sulphonamide or 2-aminothiazole rings have been widely used in this matter, because they have similar H-bond donor/acceptor properties and they are mimicking bioisosterically the aryl-amide group in the interactions with SBP.[239] In fact, these moieties combined to *N*-phenylpiperazines as basic centres have allowed to get interesting bitopic D_2 and D_3 receptor ligands.[145,239–242]

Figure 14. BP897 and **cariprazine**, blueprints for the first set of synthetized ligands.

Accordingly, to investigate the role of sulphur, a simple thioether and the corresponding oxidation derivatives were evaluated. To accomplish this, benzenethiol was attached to the chosen 1-(2-methoxyphenyl)piperazine through the "classical" butyl linker. 1-bromo-4-chlorobutane was used as alkylating agent to perform a double alkylation, obtaining the first derivative in one pot reaction. Precisely, a nucleophilic substitution was executed firstly by benzenethiol and then by 1-(2-methoxyphenyl)piperazine, based on the reactivity of halides (I > Br > Cl > F) and S_N2 mechanism. Being aromatic thiol, benzenethiol features high grade of nucleophilicity, thus the total consumption of nucleophilic agent was obtained after 1 hour and half using acetonitrile as aprotic polar solvent and sodium phosphate as base. Subsequently, *N*-alkylation was performed in the same conditions obtaining acceptable yields. Therefore, compound **4** was used as substrate for oxidations to have the corresponding sulfoxide and sulphone analogues. The related synthetic route is represented in scheme below.

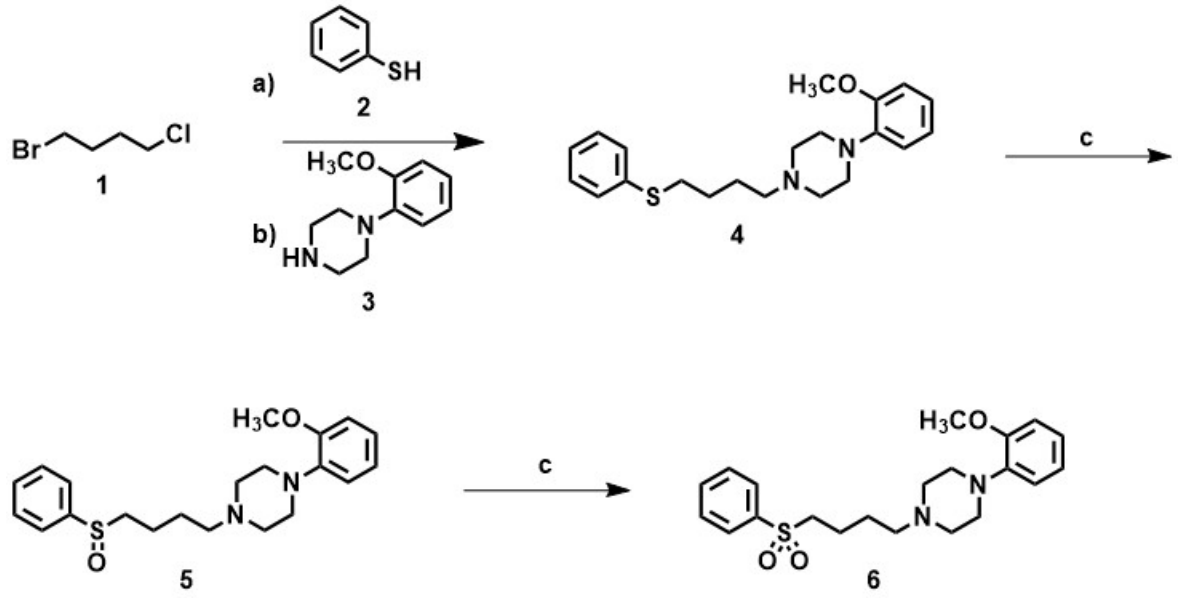

Scheme 9. Synthesis of sulphur-based ligands **4**,**5** and **6**. Reagents and conditions: (a) benzenethiol **2**, Na_3PO_4, acetonitrile, reflux, 1.30 h; (b) 1-(2-methoxyphenyl)piperazine **3**, Na_3PO_4, acetonitrile, reflux, 20 h; (c) *m*-CPBA 75%, DCM, R.T., 2 h.

The chosen oxidizing reactant was *meta*-chloroperbenzoic acid that is the most employed chemical for oxidation of sulphides to sulfoxides and sulfones,[243–245] or for epoxidation of alkenes.[246–248] *m*-CPBA belongs to the group of organic peracids, it is easy to handle and its commercial grade is up to 75%. Furthermore, *m*-CPBA is used in lots of reactions such as BAEYER-VILLIGER oxidation,[249,250] MEISENHEIMER rearrangement,[251] COPE elimination,[252–254] RUBOTTOM oxidation.[255,256] Its unique chemistry is characterized by a weak O-O bond and a nucleophilic OH group. The peroxide bond (O-

O) facilitates the transfer of an oxygen atom to electron-rich substrates, while the nucleophilic attack of *m*-CPBA on ketones and aldehydes leads to the insertion of an oxygen atom into carbonyl carbon.[257]

A putative mechanism of the sulphur oxidations, executed in this project, has been thought to be an electrophile addition of oxygen atom to sulphur, similar to the one that occurs in the epoxidation of alkenes. In details, the formation of epoxide bond is the result of interaction between the orbital π of the double bond C-C and the orbital σ^* of the peroxidic bond O-O, that are highest occupied molecular orbital (HOMO) and lowest unoccupied molecular orbital (LUMO), respectively. The electronic configuration of sulphur in sulphides and sulfoxides may have similarities with the one of alkenes. The lone electron pairs of sulphur might attack in a nucleophile manner the weak bond O-O, thus behaving as HOMO in the formation of the new C-S bond, as it happens in the generation of epoxydic structure. Scheme 10 clarifies this theory by showing the HOMO-LUMO interaction, epoxidation mechanism and a plausible comparison with sulphur oxidations.[258]

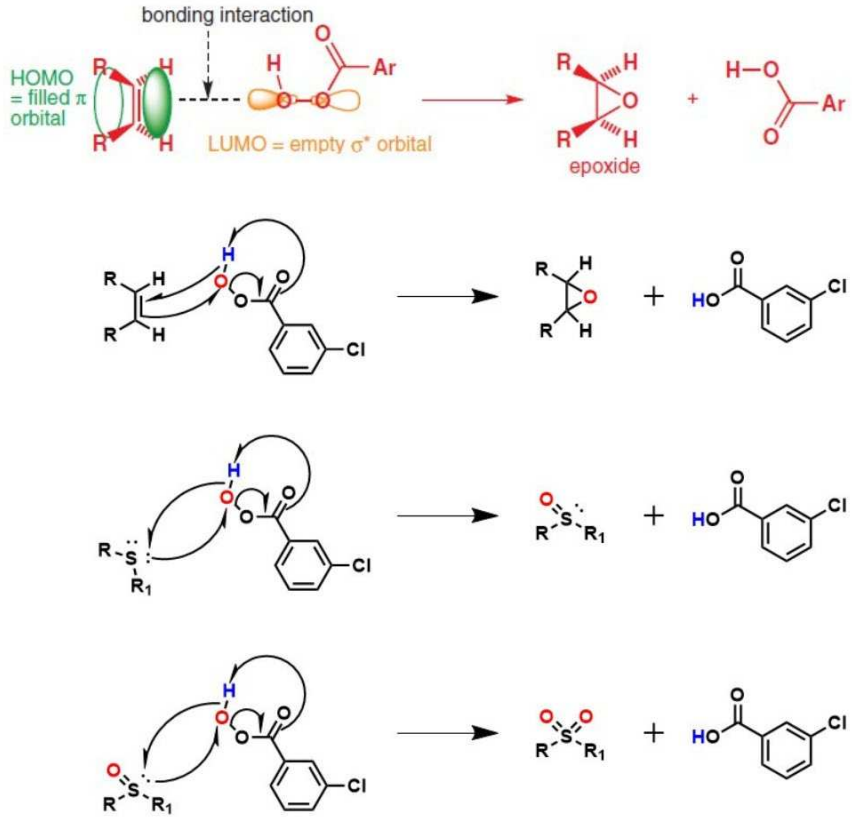

Scheme 10. The first row shows the interaction HOMO-LUMO, that occurs in the epoxidation of alkenes catalysed by *m*-CPBA. The second row represents the detailed mechanism of epoxidation. Below, a plausible mechanism of sulphur oxidation is displayed for sulphides and sulfoxides, illustrating chemical similarities with oxidation of double bond. Image adapted by Clayden *et Al.*[258]

The idea was to get the oxidative derivatives **5** and **6** performing one reaction in order to reduce the costs and time of synthetic route. Hence, many conditions were tested by changing solvent, temperature and equivalents of *m*-CPBA. According to the experiments shown in table 2, the best conditions were 1.1 equivalents of *m*-CPBA, dichloromethane and room temperature. Surprisingly, it was found out that a high excess of *m*-CPBA led to the disruption of desired products, supported by a correlating decrease of yields.

It had been hypothesized that a side-reaction occurred, that is a COPE elimination-type where a *N*-oxide intermediate of 1-(2-Methoxyphenyl)piperazine (**3**) provoked a rearrangement leading to *N*-hydroxy piperazine and vinyl sulfoxide or sulfone, thus disrupting the desired products. Indeed, this kind of application of COPE elimination has been described by Griffin *et Al.* to afford specific vinyl sulfones in presence of basic centres like piperidine ring and high excess of *m*-CPBA.[259] At the end, the oxidations were exerted one by one, isolating exclusively the corresponding product which served as substrate for the following reaction. So, the sulfoxide was produced by oxidation on sulphide, while the sulfone was obtained by oxidizing the sulfoxide. In this way, the oxidation derivatives were obtained with higher yields: 48% for **5** and 32% for **6**.

Table 2. Overview of the conditions tested in order to establish the best synthetical route for the sulphur oxidation. The chosen conditions are marked in **bold**. Although the sulfone was obtained with a yield of 9%, a further oxidation was performed on sulfoxide, which was more efficient.

Substrate	Solvent	Eq. m-CPBA	Temperature	Time (h)	Yield Sulfoxide	Yield Sulfone
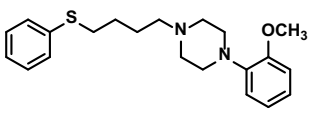	$CHCl_3$	1.5	-30°C → r.t	12	42%	11%
	$CHCl_3$	2.2	-30°C → r.t	24	19%	20%
	$CHCl_3$	4.4	-10°C → r.t	24	-	-
	$CHCl_3$	6	-10°C → r.t	6	-	-
	DCM	1.5	0°C → r.t	6	36%	5%
	DCM	**1.1**	**r.t.**	**2**	**48%**	**9%**
	DCM	2.2	r.t	4	13%	12%
	DCM	3.5	r.t.	1	11%	-
	DCM	5	r.t	2	-	-

The sulphur investigation continued by inserting the sulphur atom in an aliphatic ring, getting inspired by cyclohexylethyl linker supported by **cariprazine**. Therefore, sulphur-based ligands having a tetrahydrothiopiran-ethyl linker were obtained. The synthetic route started with tetrahydrothiopyran-4-one, that was the substrate for HORNER-WADSWORTH-EMMONS (HWE) reaction[260–262] to produce the corresponding unsaturated ester **8**. This type of olefine reaction was performed under inert conditions with a phosphonate ester, that must be activated by strong base to provide the typical ylide used for HWE. Then, the oxaphosphetane intermediate is formed, driving the formation of sodium phosphonate as by-product and the α,β-unsaturated ethyl ester.[263] Detailed mechanism of the reaction is shown in scheme 11.

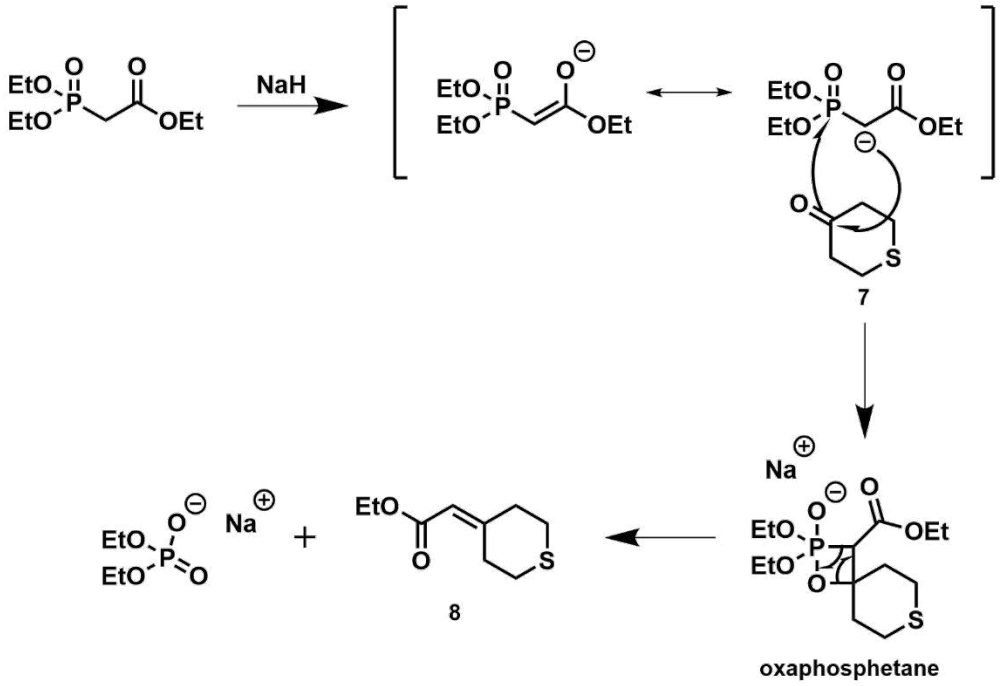

Scheme 11. Detailed mechanism of Horner-Wadsworth-Emmons reaction applied in the first synthetical step of sulphur-based ligands with tetrahydropyran-ethyl linker. The resonance structures of ylide are shown in brackets.

Afterwards, it was designed that the unsaturated ester should have been converted into alcohol in order to perform the alkylation with **3** through the activation of OH function. Considering that presence of sulphur might have poisoned Pd/C,[264,265] the initial synthetical approach to reduce the α,β-unsaturated ethyl ester (**8**) was the utilization of $NaBH_4$-$NiCl_2$-MeOH system. The combination of sodium borohydride ($NaBH_4$) with a catalytic amount of nickel(II) chloride ($NiCl_2$) in presence of methanol generates a highly reactive nickel boride species in situ. This system has found extensive application for reducing functional groups that are typically inert to sodium borohydride alone.[266] Numerous research groups have employed it to reduce the carbon-carbon double bonds of α,β-unsaturated esters, enabling the synthesis of various natural and unnatural bioactive molecules.[267–269] Moreover, the $NaBH_4$-$NiCl_2$ system has proven valuable for reducing aliphatic nitro groups or nitroarenes to amines,[270,271] or converting α-amino acids to 1,2-amino alcohols.[272] This reduction system is particularly attractive due to its low cost, simple handling (tolerant to air and moisture), non-pyrophoric nature, and rapid reaction times (typically requiring only a few minutes). Thereby, $NaBH_4$-$NiCl_2$-MeOH was used to reduce the double bond and $NaBH_4$-MeOH system for the carboxyl function of ethyl ester obtaining **10**.

However, the alcohol was obtained with larger presence of saturated methyl ester of **9**, finding out that a transesterification was preferred with the reductive system $NaBH_4$-MeOH (Scheme 12). As a consequence, methanol was substituted with ethanol, removing the saturated methyl ester as impurity

and transesterification as side-reaction. In spite of this improvement, the overall yield related to the alcohol was too low to execute the rest of synthetical pathway, as **10** was drawn up to be the crucial precursor of planned derivatives. Then, the reduction steps were improved by changing the reductive agents. The double bond in α-β position was reduced by hydrogenation exerted with the catalyst PtO_2 in basic conditions (TEA) under H_2 atmosphere, while the ester function was reduced in high excess of hydrogen donor $LiAlH_4$ under inert atmosphere in THF. This additional change optimized the overall yield of **10** from 12% to 50%. (See scheme 12).

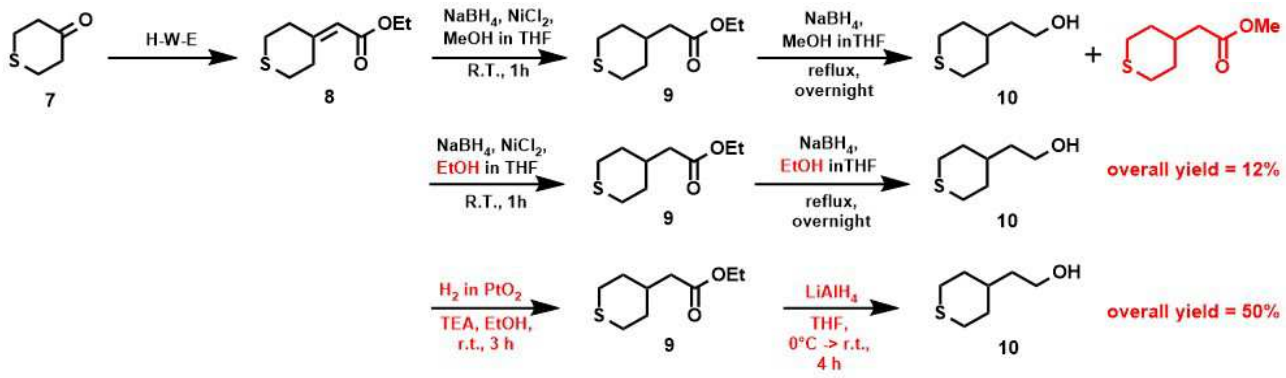

Scheme 12. Detailed overview of reductions optimization to obtain the alcohol **10.** All attempted conditions are listed here. The applied changes to the synthetical steps with the corresponding results are marked in red. The reactions that gave an overall yield of 50% were chosen as definitive steps in the general synthesis of the described sulphur-based ligands.

Once the alcohol was yielded in larger amounts, it was converted into mesylate, activating that side of the molecule and the alkylation with 1-(2-Methoxyphenyl)piperazine (**3**) was performed, gaining the required derivative **12**. On the other hand, the mesylated intermediate **11** was used for the oxidation into sulfoxide **13** which, in turn, was oxidized to have **15**. These oxidized intermediates with mesylate (**13** and **15**) were used in the alkylation with piperazine **3** and Na_3PO_4 to achieve **14** and **16**, respectively. The complete synthesis is described in the scheme 13.

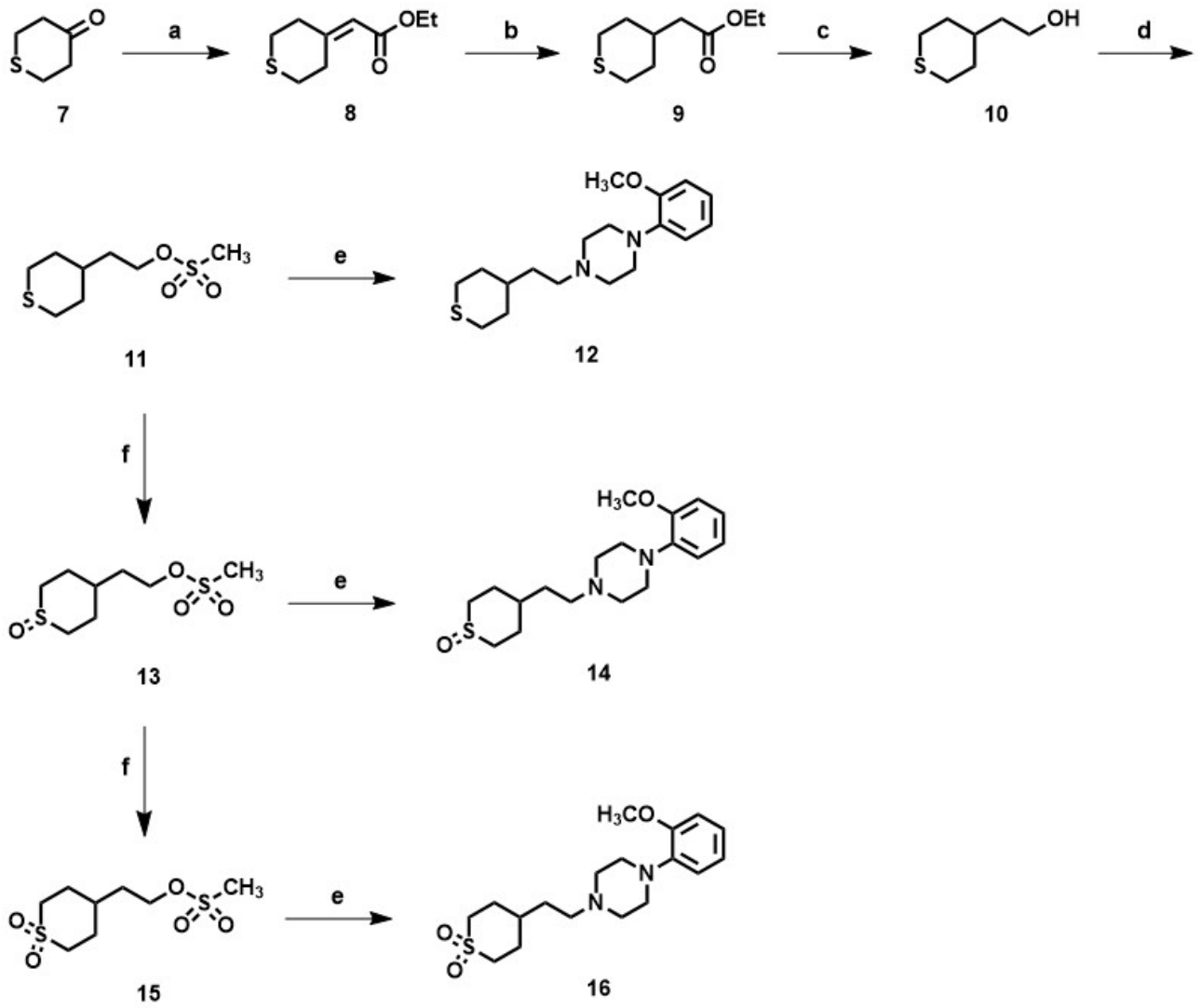

Scheme 13. Synthesis of sulphur-based ligands with tetrahydrothiopiran-ethyl linker **12**, **14**, **16**. Reagents and conditions: (a) NaH, $(EtO)_2OPCH_2COOEt$, THF, 0°C → R.T., 4 h; (b) PtO_2, TEA, H_2, EtOH, R.T., 3 h; (c) $LiAlH_4$ 2 M, THF, 0°C → R.T., 4 h; (d) methane sulfonyl chloride, TEA, DCM, 0 °C, 15 min; (e) **3**, Na_3PO_4, ACN, reflux, 20 h; (f) *m*-CPBA 75%, DCM, R.T., 1 h.

After successful syntheses of products **4-6** and **12,14,16**, the concept of a sulphur atom inserted in a rigid structure was expanded. The aliphatic ring displayed by **12**,**14** and **16** was replaced by an aryl one, providing a phenylethyl linker. Using a phenyl ring as spacer was a crucial tool in the entire PhD project, because it gave the possibility of exploring the chemical space of SBP with a wide range of substitution patterns. The first one was the application of 2-aminothiazole moiety attached to the phenyl ring, inspired by a work previously described in our working group[241] and by the structure of **pramipexole**, which is a dopamine D_3 receptor preferring partial agonist.[135] It was marketed in 1997, since then, it has become a reference structure for *in vitro* and *in vivo* studies, as well as standard therapeutic agent for PD, being a valuable alternative of levodopa.[139] So, 2-aminothiazole moiety was evaluated by analysing the interactions of the heteroaromatic ring within SBP of target receptors. In

this context, the aromatic thiazole structure was chosen as sulphur-based unit for two specific purposes:

- Investigation of thiazole and aminothiazole moieties as bio-isosteric replacements of carbonyl function in combination with the aromatic linker and 1-(2-Methoxyphenyl)piperazine.
- Evaluation of 2-aminothiazole ring as a part of aromatic linker itself, due to the position 2-NH_2 that offers opportunities of further modifications.

Therefore, a set of sulphur-based derivatives was produced having an aromatic linker with variations at the thiazole structure, as it is presented in figure 15.

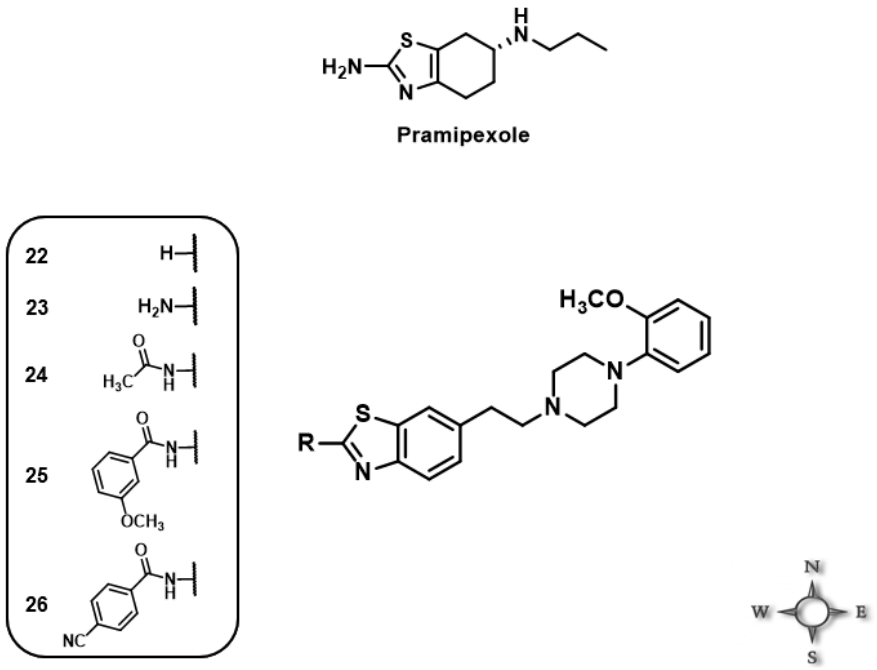

Figure 15. General structure of sulphur-based ligands that show variations on a thiazole ring attached to phenylethyl linker and 1-(2-Methoxyphenyl)piperazine. Marketed drug **pramipexole** is shown above.

The chemical 2-(4-nitrophenyl)ethan-1-ol (**17**) was purchased to start the synthetic route for this group of derivatives. The first reaction was the reduction of nitro group, using the catalyst Pd/C 10% under H_2 atmosphere. Once the corresponding aniline **18** was obtained, the synthesis of 2-aminothiazole was carried out. In details, **18** was treated with ammonium thiocyanate to form the related thiourea, which was not isolated. Subsequently, insertion of bromine dropwise in situ at 0°C favoured the ring closure of 2-aminothiazole, producing intermediate **19**. Afterwards, APPEL reaction[273] was used to convert the OH function into chloride in order to obtain **20.** The following step reaction was a deamination on 2-aminothiazole chloride, executed with isopentyl nitrite in order

to exchange the amino group with a simple hydrogen in position 2. Then, deaminated intermediate **21** was used to perform the usual nucleophilic substitution on **3**, achieving the first sulphur-based ligand having 2-*H*-thiazole as variation.

In this case, the chosen conditions of the *N*-alkylation were based on FINKELSTEIN exchange, that required KI, K_2CO_3 in acetone.[274] It is an equilibrium reaction, but the driving force for completion is the different solubility of halide salts in acetone. Theoretically speaking, KI is the only soluble salt in acetone and in presence of an alkyl chloride (R-Cl like **20** and **21**) the exchange is driven towards the formation the desired alkyl iodide (R-I). Whereas, KCl, just formed, precipitates due to insolubility in acetone, thus favouring the S_N2 reaction and the wanted alkylated product. In this way, it is necessary a small catalytic amount of iodide, because the anion is regenerated and starts the exchange again. However, the traditional FINKELSTEIN conditions worked with low yields, problem that was solved by using acetonitrile as solvent and high excess of KI (4 eq.) and K_2CO_3 (6 eq.), increasing the yields up to 43%. The difference of solubility among halide salts did not occur with acetonitrile, thereby the reason of this optimization was thought to be connected to the polarization and solvency effects exerted by acetonitrile, or to the high excess of KI and K_2CO_3 that represented a new driving force in the optimized reaction environment.[275]

Following the same alkylation conditions, **20** provided 2-aminothiazole product **23** that served as precursor for acylated analogues **24, 25,** and **26**. Same *N*-acylation conditions were used for every derivative except for the acylating agent, whereby acetic anhydride was used for **24**, 3-OCH_3 and 4-CN benzoyl chlorides were used for **25** and **26** respectively. The general synthetical pathway is represented in scheme 14 and particular reaction steps (e.g. aminothiazole ring formation, APPEL and deamination) are described in more details below.

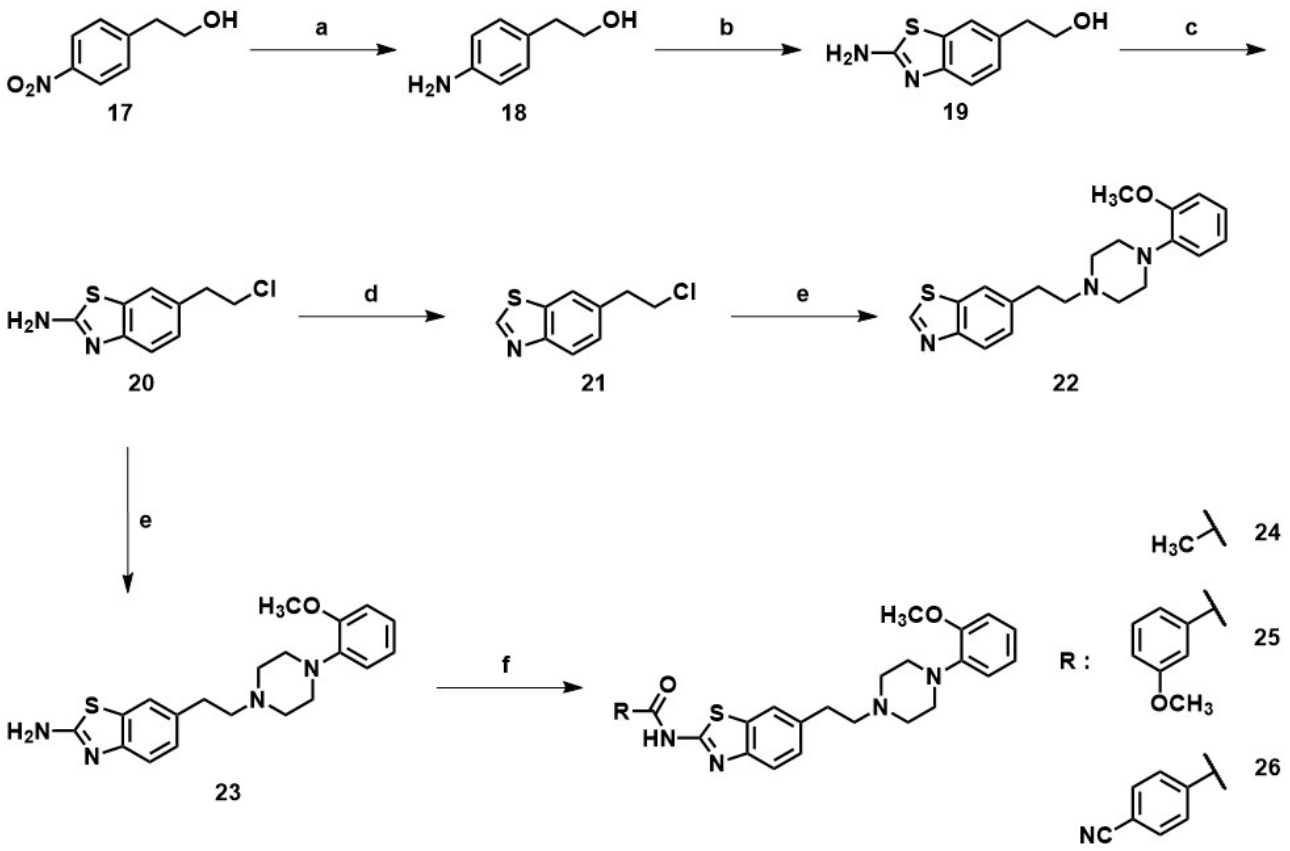

Scheme 14. Synthesis of sulphur-based derivatives **22-26**. Reagents and conditions: (a) Pd/C 10%, H_2, MeOH, R.T., 18 h; (b) NH_4SCN, Br_2, EtOH, 0°C → R.T., 4 h; (c) Ph_3P, $Bu_4N^+I^-$, DCE, 80°C, 12 h; (d) Isopentyl nitrite, THF, R.T. → reflux, 4 h; (e) **3**, KI, K_2CO_3, acetonitrile, reflux, 20 h; (f) Ac_2O for **24**, 3-OCH_3 benzoyl chloride for **25**, 4-CN benzoyl chloride for **26**,TEA , DCM, reflux, 3 h.

Generally, the synthetical pathway allowed to have the desired final products with satisfactory yields, but some crucial reactions must be considered in major details. For example, the synthesis of 2-aminothiazole ring was exerted by performing two synthetical steps in one reaction. Specifically, the first step was a nucleophilic attack of aniline **18** at the carbon of thiocyanate anion in ethanol, which generated a rearrangement of protons that led to the formation of thiourea **A**, as it is depicted in scheme 15. Subsequently, the addition of elemental bromine triggered an aromatic nucleophilic substitution in the mixture of reaction, going through the classical addition-elimination mechanism typical of this type of reactions. Thereby, the aryl bromide with Br in *ortho* position was formed. Since Br is a good leaving group, **B** underwent a second nucleophilic aromatic substitution, in which the lone pair of sulphur attacked the ortho position. Following the addition-elimination mechanism and consequent rearrangement of electron density, the 2-aminothiazole synthesis was afforded producing **19** with high yields. The entire proposed mechanism is shown below.

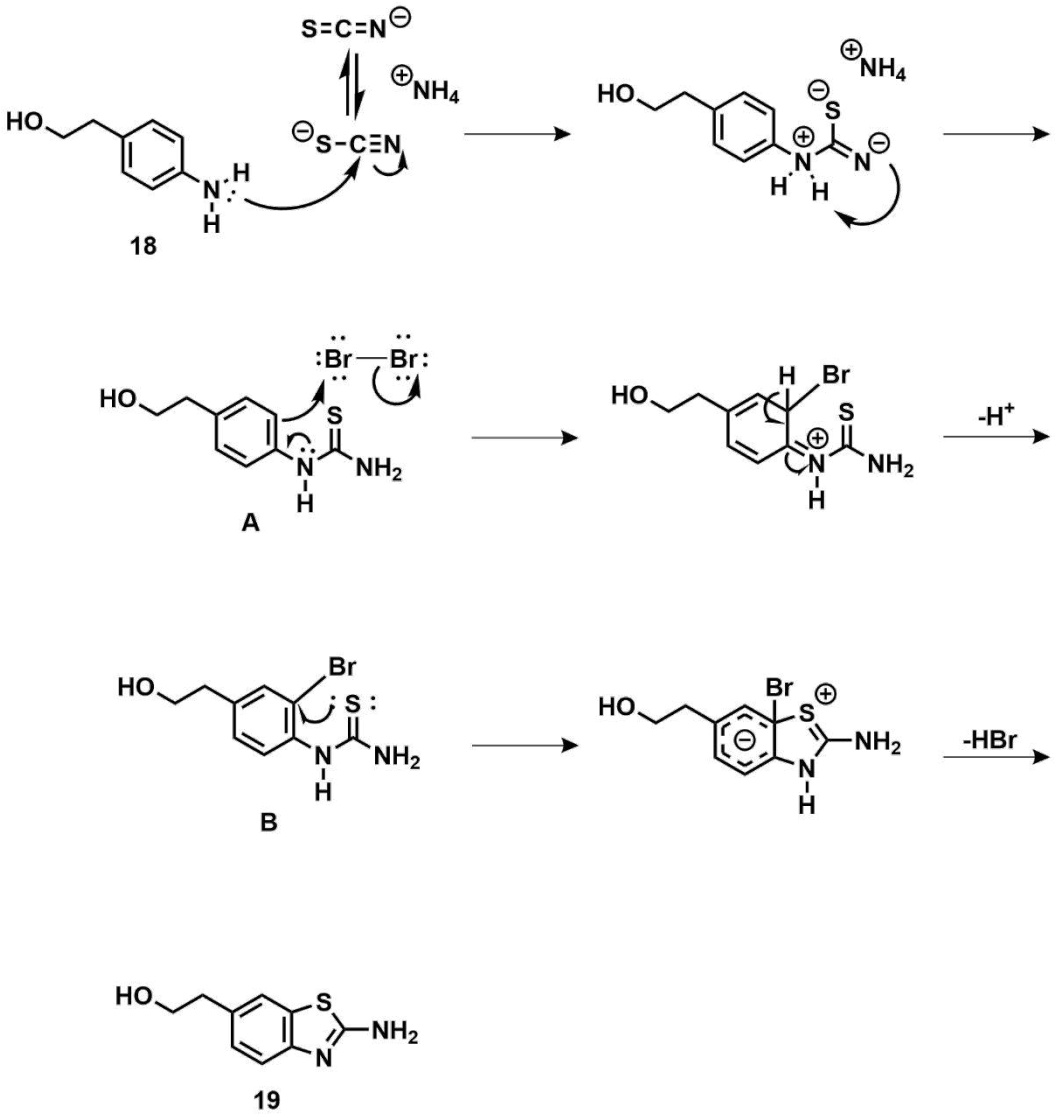

Scheme 15. Proposed mechanism for the 2-aminothiazole ring synthesis. Two synthetical steps occurred in one reaction, in which the thiourea **A** was firstly generated by nucleophilic attack and protons rearrangement. Then, the addition of elemental bromine drove the formation of brominated intermediate **B** and then it led to the obtaining of the desired product **19** through addition-elimination, typical mechanism of nucleophilic aromatic substitution.

Once **19** was synthetised, it was necessary to activate the hydroxy function in order to couple 1-(2-Methoxyphenyl)piperazine **3** and thiazole phenylethyl substrate. Since the 2-NH_2-benzothiazole is a reactive substrate that could form diverse side reactions and by-products, the idea for the coupling was to use a selective and mild reaction such as reductive amination or APPEL. Nevertheless, the attempted oxidations on **19** did not work out very well, because many side products were produced in this reaction environment, making the isolation of wanted aldehyde difficult or the desired product was not formed at all, as it is described in the table 3. According to the listed results, it was chosen to convert the alcohol in halide, taking advantages of the phosphorus chemistry, that is used in APPEL halogenation. Indeed, the P=O bond, with its bond energy of 575 kJ mol^{-1}, is one of the strongest

double bonds in chemistry, and the APPEL reaction is driven forward by the formation of this P=O bond.[258]

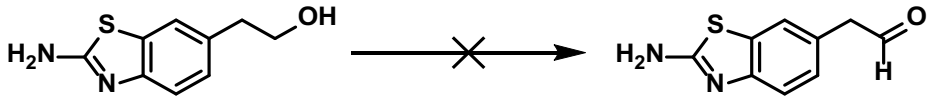

19

Table 3. General outlook of attempted oxidations on substrate **19**.

Reagent (eq.)	Solvent	T (°C)	Time (h)	Results
PDC 1.5	DCM in THF	R.T	24	Formation of product not observed
PDC 2	DCM in THF	R.T	12	7%
DMP 1.1	DCM in THF	R.T	8	10% but isolated with impurities
DMP 1.5	DCM in THF	R.T	14	Formation of product not observed
DMP 2	DCM in THF	R.T	6	Formation of product not observed
DMSO 3,9, OC 1.98, TEA 5, [a]	DCM in THF	-78°c → R.T.	1	Isolated with impurities
DMSO 3, OC 1.5, TEA 3.6, [a]	Toluene	-78°C → R.T.	1	Formation of product not observed

[a], Swern oxidation.

In details, APPEL is a deoxyhalogenation of primary or secondary alcohols and aldehydes, promoted by a trivalent phosphorus catalyst and an electrophilic halogen-containing agent; it is considered one of the most effective synthetical strategies to insert a halogen. However, the electrophilic halogen-containing agents, usually used for this reaction, like tetrahalomethanes and *N*-halo compounds were not used here due to toxicity reasons. As a consequence, a recently described reagent system for APPEL was used, characterized by $Ph_3P/Bu_4NI/Cl\text{-}CH_2\text{-}CH_2\text{-}Cl$, in which dichloroethane worked simultaneously as solvent and halogen source.[276] Although the iodide anion was present in the reaction environment, no iodination by-product was observed, possibly because chlorination was faster than iodination due to the stronger C−Cl bond.

A detailed mechanism of the halogenation system used on substrate **19** is described in scheme 14. For the $Ph_3P/Cl\text{-}CH_2\text{-}CH_2\text{-}Cl$ system, halide exchange occurs, providing $I\text{-}CH_2\text{-}CH_2\text{-}Cl$ that is followed by the release of ethylene. In this way, molecular iodine is produced, which, in turn, reacts with triphenylphosphine to afford iodophosphonium salt **A**. The alcohol **19** is activated by salt **A** to form intermediate **B**. The nucleophilic attack of the halide is following a S_N2 process that affords the deoxyhalogenation product **20** (Scheme 16).

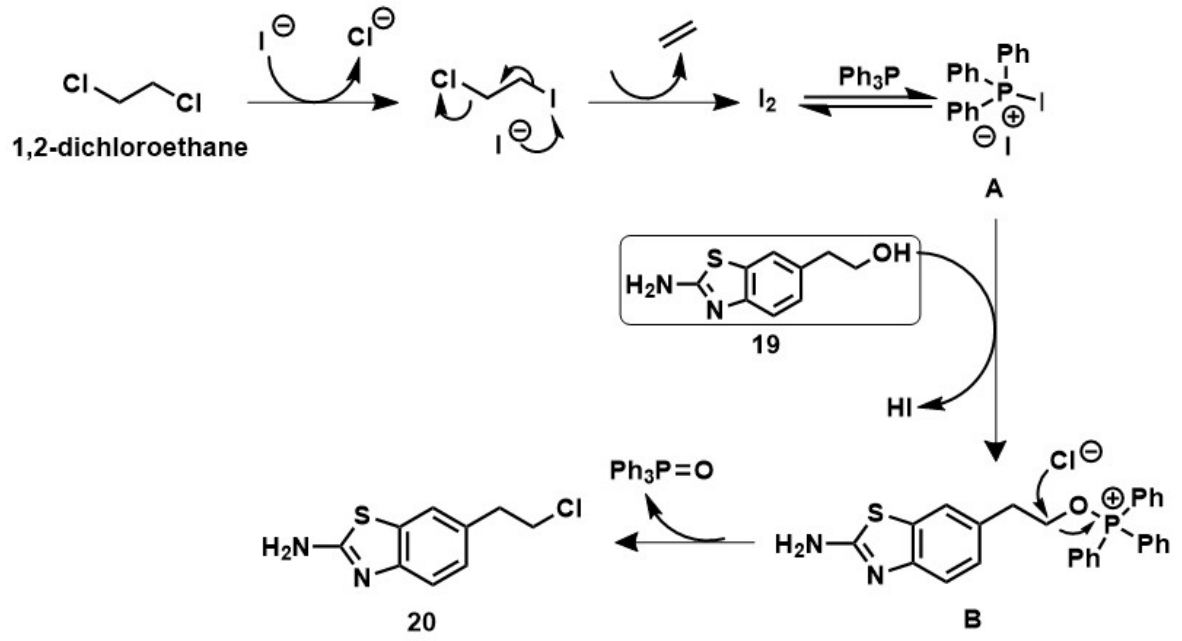

Scheme 16. Detailed mechanism of deoxy-halogenation exerted on **19** to the obtain the related alkyl chloride **20**. Adapted from Chen *et Al.*[276]

The following step reaction was a deamination on 2-aminothiazole chloride **20**, executed with isopentyl nitrite in order to exchange the amino group with a simple hydrogen in position 2. The plausible radical mechanism of this reaction by Doyle et Al. and Röder et Al. is shown in Scheme 15.[277,278] The reaction between substrate **20** and isopentyl nitrite generates an intermediate that undergoes rearrangements, followed by elimination of isopentanol, that forms intermediate **A**. However, nitrosamine **A** is in equilibrium with its hydroxy form **B** which is more preferred. Under thermal decomposition achieved with refluxing the solvent, **B** produced the diazonium species **C**. After the elimination of nitrogen, the carbene intermediate **D** executes a hydride abstraction from tetrahydrofuran, that is the chosen solvent for this reaction, producing ultimately the wanted product **21** with satisfactory yields, as it is depicted in scheme 17. The versatility of this reaction allowed to have the desired final product **22** facilitating the synthetical workflow.

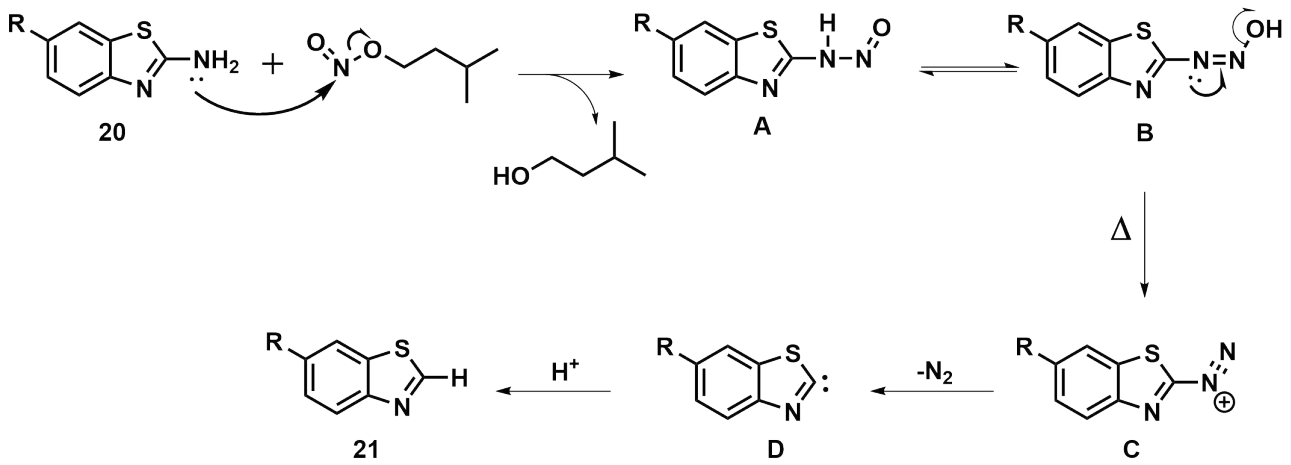

Scheme 17. Putative mechanism for the formation of the diazonium species **B** that led firstly to the formation of heteroaryl carbene **D** and then to the generation of hydrogenated intermediate **21**.

According to the synthetical pathway and particular reactions explained above, sulphur-based novel dopamine D_2/D_3 receptor ligands were synthetized. They had a phenyl ring as lipophilic linker, whereby a thiazole ring was attached; it represented a challenging but interesting function and it worked well as prolongation of the phenylethyl linker. Therefore, following the idea of aromatic linker, a second sulphur-based moiety was attached to the phenyl ring/spacer: methylthio ether. It was examined under the same two viewpoints used for the compounds with 2-aminothiazole variations:

- As bio-isosteric replacement of acyl-like function required by pharmacophore model (Section 1.1.2)
- As a further modification and prolongation of the aromatic linker developed in the project.

Consequently, a fourth list of sulphur-based ligands was synthetized, featuring the classical 1-(2-Methoxyphenyl)piperazine and the phenylethyl linker combined with methylthio ether. The sulphur atom inserted in this configuration was analysed throughout its oxidation states (as it was done for derivatives **4-6**, **12**, **14** and **16**) and further modification, that was sulfoximine, obtained by a synthetical method recently described. The sulfoximine group was obtained synthetically from methyl sulfoxide and it was evaluated as possible part of the aromatic linker, as it was performed for ligands **22-26**. At this point, a historical background and a general description about sulfoximine must be given.

Sulfoximines are isoelectronic with sulfones and the presence of nitrogen offers an additional point for substitution, metal ion coordination or salt formation,[279] and unique H-bond donor/acceptor properties.[280,281] Particularly, the sulphur-bound heteroatoms (via S=O) are H-bond acceptors, while *N*-unsubstituted sulfoximines may serve as H-bond donors and acceptors (via NH).[281]

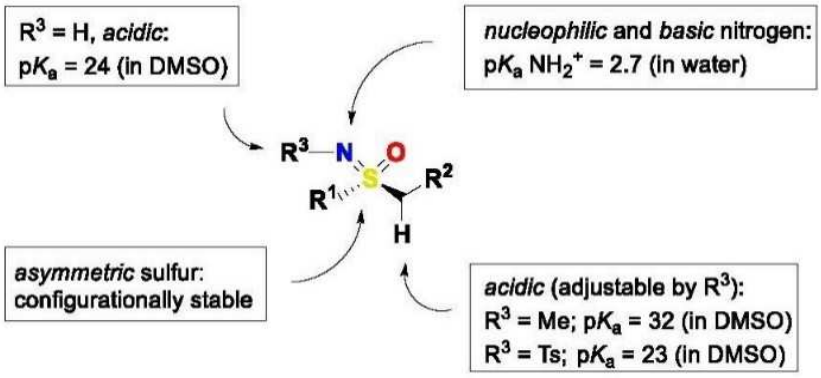

Figure 16. General structure of sulfoximine. As it is shown, the pKa values can be manipulated by changing the groups in position **R²** and **R³**. Whereas, **R¹** is an unreactive moiety that is usually represented by an aromatic ring. Figure adapted by Lücking *et Al.*[290]

Sulfoximines have been used as chiral auxiliaries, organocatalysts and agrichemicals.[282,283] Based on NMR spectroscopic studies, the overall unit of sulfoximine is more electron-withdrawing than the sulfone and it might have three reactivity patterns such as C-nucleophile, electrophile and chiral ligand.[284] In addition, sulfoximines are chemically and configurationally stable,[284] have high solubility in protic solvents like water or alcohols[285] and feature high chemical versatility[286], hence in the last years sulfoximine group has been used as isostere or bio-isostere of sulphonamides, sulfones, alcohols or amines[287–289] to improve physicochemical and pharmacodynamic characteristics, obtaining promising outcomes (Figure 16).[290,291] For instance, the first sulfoximine based compound was approved in the drug market in 2013, that is Sulfoxaflor®, an insecticide used for sap-feeding insect control,[292] while other molecules bearing sulfoximine function (roniciclib,[287] atuveciclib,[288] AZD6738[293]) have entered clinical trials for cancer treatment in the last ten years.[294]

Nonetheless, sulfoximines were discovered in the early 1950s, when several research groups were addressing a problem originated by using a flour bleaching chemical "Agene", that was nitrogen trichloride (NCl_3). This process generated a by-product that caused illness in dogs that ate treated grains. The entire episode had gone down in history as "dog hysteria". This effect was caused by a chemical substance, methionine sulfoximine, which was formed in wheat through oxidation and subsequent imination of the natural amino acid *L*-methionine. In 1949, Bentley and Whitehead succeeded in isolating *L*-methionine-*R,S*-sulfoximine as the first sulfoximine.[295,296] Later on, the active stereoisomer, *L*-methionine-*S*-sulfoximine, was found to act as a mimetic of glutamate and to reduce glutathione biosynthesis by inhibiting γ-glutamyl cysteine synthetase and glutamine synthetase.[297,298] This mechanism of action was thought to be effective against tumors that overexpress glutathione (e.g., hepatocarcinoma); in fact the discovery of methionine sulfoximine led

to the development of buthionine sulfoximine that proved to be well-tolerated fore this type of cancer in preliminary studies.[299] Furthermore, *L*-methionine-*R,S*-sulfoximine was isolated from *Cnestis palata*, a tropical woody plant belonging to the *Connaraceae* family. Species within this plant family are renowned for their toxic properties. The identification in *Cnestis palata* provided evidence that sulfoximines, including this specific compound, can be classified as natural products.[300,301]

The sulfoximine function was inserted in this set of sulphur-based molecules not only for the purposes described above, but also to investigate whether hydrophilicity can have an impact on binding behaviours towards D_2 and D_3 receptors. As the developed scaffold (phenylethyl linker combined with 1-(2-Methoxyphenyl)piperazine) is quite lipophilic, it was thought to balance it with a novel hydrophilic moiety such as sulfoximine. Thereby, three sulfoximine-based ligands were synthetized and added to the group of sulphur-based ligands having methyl sulphide and sulfoximine variations, that are shown in the figure below.

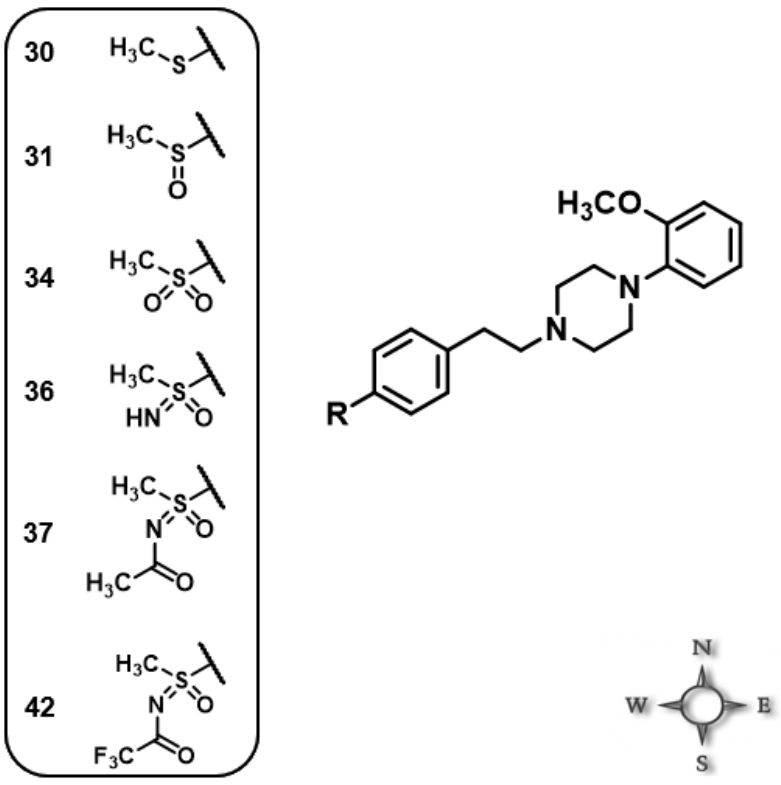

Figure 17. General overview of the chemical structures related to sulphur-based ligands with phenylethyl linker combined to methyl sulphide and methyl sulfoximine variations respectively. Methylthio ether derivatives are **30-31,34** and sulfoximine ligands are **36-37, 42**.

To afford the ligands with methylthio ether and sulfoximine variations together with phenylethyl linker, the synthesis started by purchasing the starting material 2-(4-(methylthio)phenyl)acetic acid **27** that underwent a reduction into the corresponding alcohol **28**. The reduction was exerted with a borane-dimethylsulphide complex solution under N_2 atmosphere, achieving quantitative yields. 2-(4-(methylthio)phenyl)ethan-1-ol **28** was converted into mesylate in order to perform the alkylation with 1-(2-Methoxyphenyl)piperazine **3** and to obtain the first methylthio ether derivative **30**. To have the related sulfoxide **31**, an oxidation with *m*-CPBA was executed on sulphide **30**. Nevertheless, the sulfoxide was obtained with a yield of 19%, which was considered inefficient for achieving the other compounds, because **31** was supposed to be the precursor of the other derivatives. The low yield was a consequence of COPE elimination type, that occurred in presence of piperazine as side reaction. It provoked the disruption of desired product, already observed in the synthesis of derivatives **4-6**. Despite having used a small excess of *m*-CPBA (1.1 eq.), the unwanted reaction took place more intensely with the substrate **30**. The piperazine **3** was attached to the C in β position from the phenyl ring, which was a more reactive and suitable centre for the COPE-type reaction. This was the reason why 1-(2-methoxyphenyl)piperazine was added always in the final step of the synthetic routes to afford compounds **34**, **36**, **37** and **42**. The synthesis of derivatives **30** and **31** is depicted below.

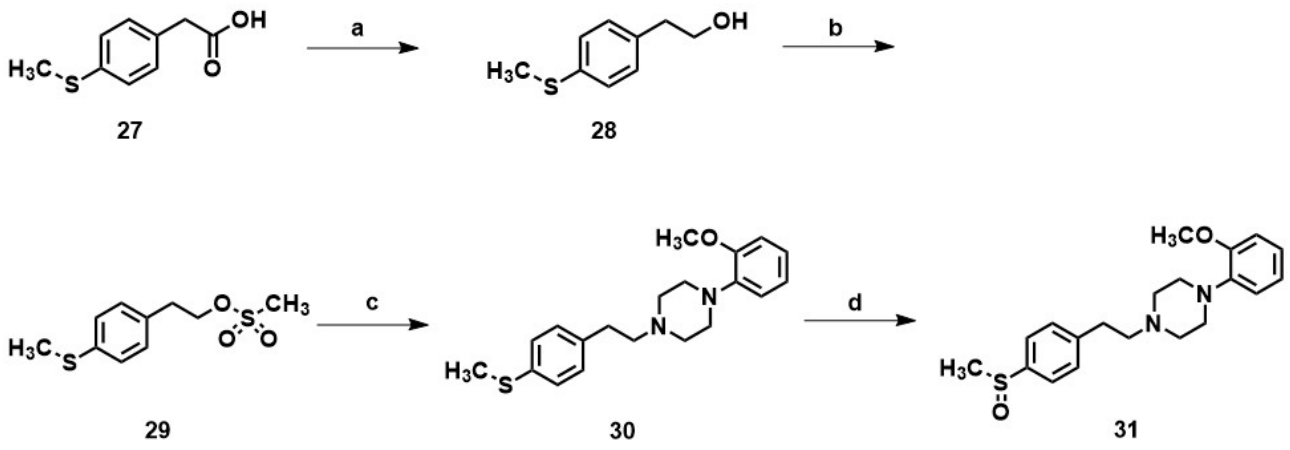

Scheme 18. Synthesis of sulphur-based derivatives **30** and **31**. Reagents and conditions: (a) $BH_3 \cdot S(CH_3)_2$ in THF 2 M, THF, R.T., 4 h; (b) methane sulfonyl chloride, TEA, DCM, 0 °C, 15 min; (c) Piperazine **3**, Na_3PO_4, ACN, reflux, 20 h; (d) *m*-CPBA 75%, DCM, R.T., 1 h.

Based on what mentioned before, a different synthetic pathway was executed at the place of the one showed in scheme 18. Then, the mesylated intermediate **29** was oxidized first into sulfoxide (**32**) and then into sulphone (**33**), performing a double oxidation with *m*-CPBA in DCM and high yields (up to 80 %). 1-(2-methoxyphenyl) piperazine **3** alkylated the mesylate with sulfone **33** in acetonitrile

(ACN) and Na_3PO_4 to obtain **34**. Whereas, the mesylate with sulfoxide (**32**) was used as substrate for BOLM imination[302] to afford the corresponding sulfoximine with mesylate function on the other side of molecule (**35**). The BOLM reaction of sulfoximines requires phenyl- λ^3-iodanediyl diacetate as nitrene precursor[303] thanks to hypervalent chemistry of iodine,[304] trifluoroacetamide as nitrogen source, rhodium acetate as catalyst and magnesium oxide, that is optimal to remove acetic acid (AcOH), produced in the reaction, which is detrimental to catalytic activity of rhodium complexes. A detailed description of this reaction is provided below. So, **35** was used in combination with **3** to perform the alkylation obtaining **36** with free NH of sulfoximine. Cleavage of trifluoro acetyl function was observed in this step, because CF_3COO-NH was found to be instable in basic conditions that were used in the *N*-alkylation. Ultimately, two reactions were combined in one allowing to have free NH of sulfoximine ready for further variations. Indeed, the following step was the acylation of **36** with acetic anhydride, TEA and DCM to afford **37**. The reaction steps just described are depicted in the scheme below:

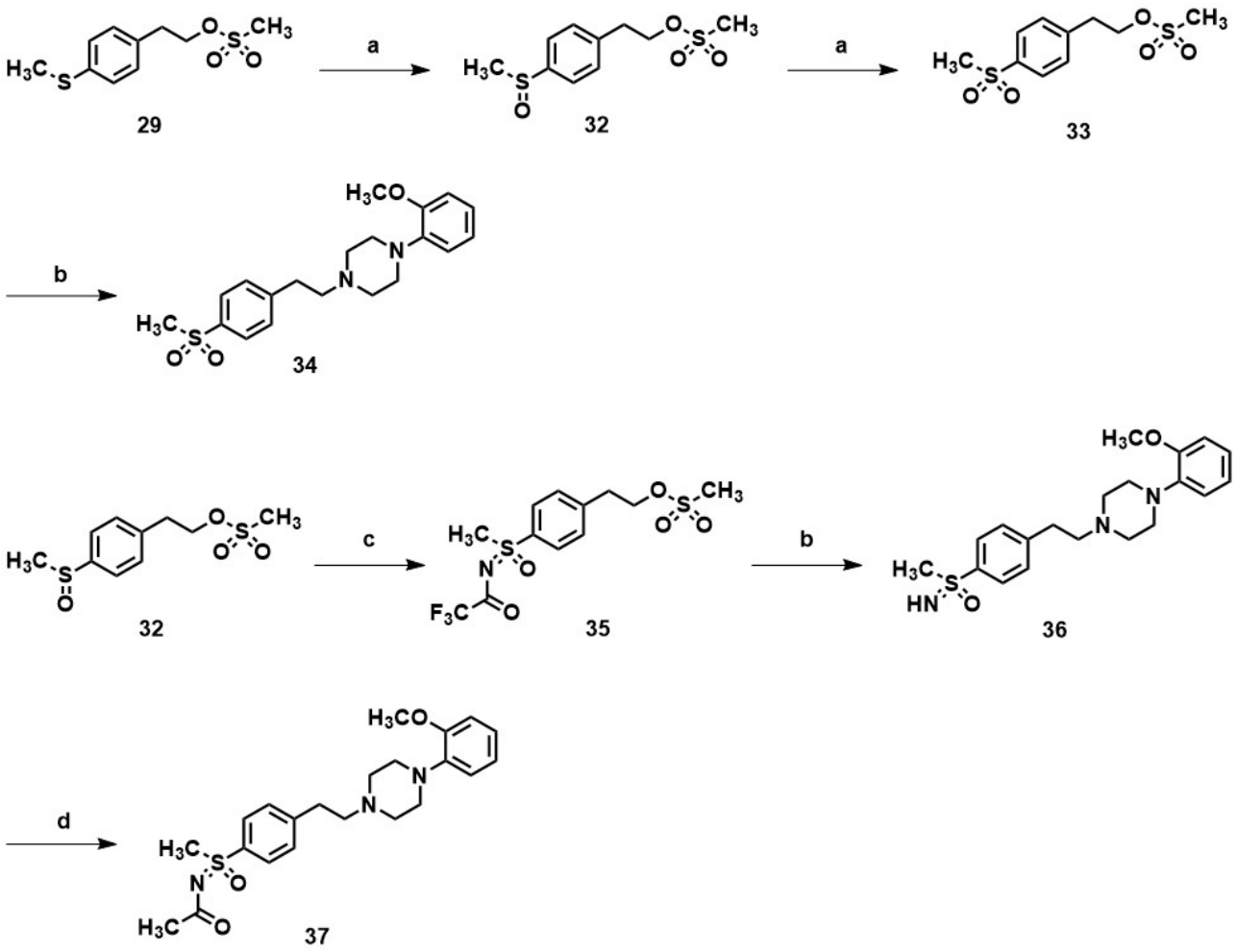

Scheme 19. Synthesis of compounds **34**,**36** and **37**. Reagents and conditions: (a) *m*-CPBA 75%, DCM, R.T., 1 h; (b) Piperazine **3**, Na_3PO_4, ACN, reflux, 20 h; (c) CF_3COONH_2, $Rh_2(OAc)_4$, $PhI(OAc)_2$, MgO, DCM, R.T., 16 h; (d) Ac_2O, TEA, DCM, reflux, 6 h.

Since the trifluoro acetyl group arose interest, CF_3COO-derivative was added as desired compound within the group of sulphur-based ligands bearing the phenylethyl linker. Keeping in mind that trifluoro acetyl is a base-labile moiety, a different synthetic pathway was drawn up to have CF_3COO-derivative **42.** The chosen reaction for attaching the piperazine was reductive amination that features acidic conditions and requires an aldehyde. As a consequence, the new synthetic route was exerted by performing an esterification with thionyl chloride in MeOH on **27**. The obtained ester **38** was first oxidized into sulfoxide **39** with the usual *m*-CPBA oxidation and then it was reduced to have the corresponding aldehyde **40,** performing a partial reduction with the reductive agent diisobutylaluminium hydride. Afterwards, the BOLM imination was performed on sulfoxide **40**, but the presence of aldehyde on the eastern side of the molecule had an impact on the reaction environment. It was observed a worsening of the yields (16 %), when compared with those of reaction performed on mesylate **32** (75%). However, the required aldehyde with *N*-substituted sulfoximine (**41**) was afforded and it was treated with the classical piperazine **3**, $NaBH(OAc)_3$, AcOH in DCE under N_2 atmosphere, which are the typical conditions of a reductive amination. In this way, the desired product **42** was obtained and its related synthetic route is shown in scheme 20.

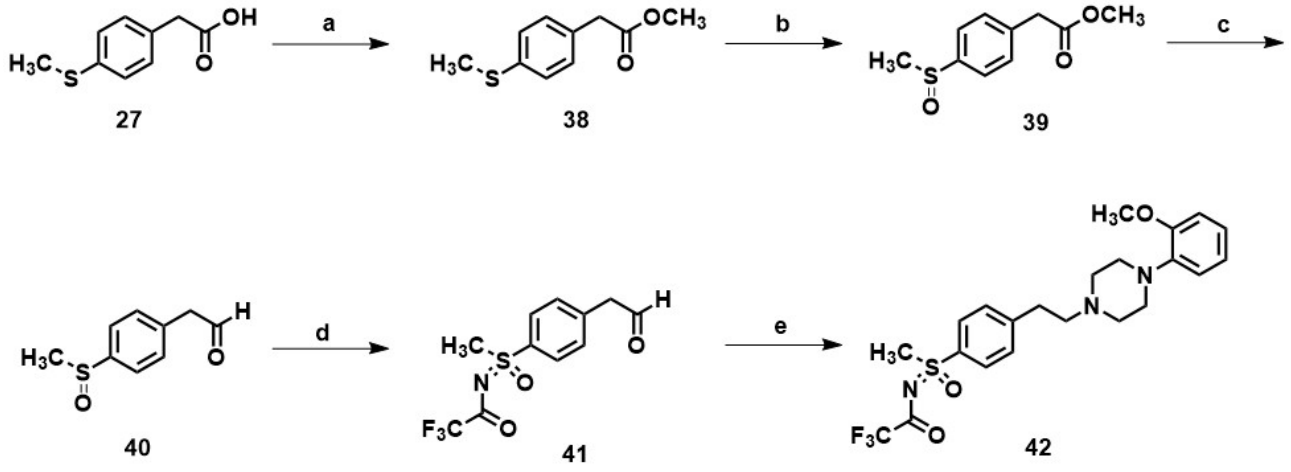

Scheme 20. Synthesis of derivative **42**. Reagent and conditions: (a) $SOCl_2$, MeOH, R.T., 1 h; (b) *m*-CPBA 75%, DCM, R.T., 1 h; (c) DIBAL in toluene 1 M, toluene, -78°C, 14 h; (d) CF_3COONH_2, $Rh_2(OAc)_4$, $PhI(OAc)_2$, MgO, DCM, R.T., 16 h; (e) Piperazine **3**, $NaBH(OAc)_3$, AcOH, DCE, R.T., 16 h.

The turning points of the described synthetical pathways are the obtaining of free sulfoximine with removal of trifluoro acetyl moiety and the reductive amination, which allowed to have the most interesting structures (**36-37, 42**) among this group of sulphur-based dopamine D_2/D_3 receptor ligands. Anyway, the applied BOLM imination is one of the several methods to access sulfoximine function. Since this moiety has got a lot of interest in the recent years, many reaction environments with different reactants were developed.[305–313] Usually the production of sulfoximines goes through either imination of sulfoxides or oxidation of sulfimines, which are obtained by oxidizing or iminating the sulphides respectively. So, basically it is a combination of oxidation/imination or vice versa. As it is shown before, the path oxidation/imination was chosen and the imination is observed in major details here.

The first synthetical protocol of the imination used hydrogen azide, which is produced *in situ* from sodium azide with concentrated sulfuric acid.[314,315] However, since hydrogen azide is toxic, highly volatile and explosive, reagents such as *O*-Mesitylenesulfonylhydroxylamine,[316,317] organic azides like tosyl azide[318,319] have been increasingly used, also N-tert-butoxycarbonyl azide,[320] chloramine-T or hypervalent iodine compounds (PhI=N-Ts)[321] are used in combination with copper or iron salts under milder conditions.[322,323] Electrochemical methods might be used as well; they can still represent a promising alternative for the synthesis of sulfoximines on an industrial scale. Furthermore, enantioselective imininations of sulphides have been made possible by the methods of Carreira[324] and Katsuki,[325] which produce enantiomerically enriched sulfimines with enantiomeric excesses up to 99% through the use of chiral ruthenium and manganese complexes.

Okamura and Bolm developed an efficient and mild variant of metal-catalysed imination, which allowed the conversion of sulphides and sulfoxides to NH-sulfimines and sulfoximines in high yields, using rhodium acetate as a catalyst and the trifluoroacetamide-iodobenzene/acetate-magnesium oxide system as imination reagent.[302] The novelty of this method lies in the avoidance of isolating the intermediate iminoiodane; the nitrene transfer occurs immediately after the formation of iminating reagent. Another advantage is the use of trifluoroacetamide, because this group requires milder conditions to be removed than moieties like N-carbossibenzylamide or N-tert-butoxycarbonyl amide, which are other electron-withdrawing functions used as nitrene sources. Therefore, the BOLM imination was chosen for synthetizing the sulfoximine derivatives reported here.

In details, the formation step of sulfoximine is an insertion of nitrene within the sulphur atom of sulfoxide. The nitrene must be stabilized by an electron-withdrawing group that is trifluoro acetyl moiety in this case. This is the reason why CF_3COONH_2 is considered the nitrene source. $PhI(OAc)_2$ is an oxidizing agent that works by using the iodine hypervalent chemistry. Indeed, the iodine achieves a *decet* structure which is called λ^3-iodane. The most important characteristic of this

structure is the capability of being a very good leaving group. The leaving process is called reductive elimination, where λ^3-iodanyl function eliminates with energetically preferable reduction into univalent iodides like Ph-I. In this way, thanks to λ^3-iodanes, it is possible to generate highly reactive species such as carbenes, nitrenes, arynes under mild conditions or to oxidise a wide range of functionalities such as alcohols, amines, sulphides and carbonyl compounds.[304] For instance, λ^3-iodanes like $PhI(OAc)_2$ are used in presence of metal catalysts such as rhodium, iron and cupper to execute aziridination of olefines.[326,327] In similar way, $PhI(OAc)_2$ is used in the conversion from sulfoxide to sulfoximine as nitrene precursor, managing to produce a metal-nitrene complex intermediate. The catalyst used is $Rh_2(OAc)_4$, whereby rhodium coordinates between the reactive nitrene and the sulphur, forming a metal-catalysed transitional state that drives the entire reaction. By doing this, the catalyst triggers the formation of acetic acid which is also produced by $PhI(OAc)_2$. Surprisingly, AcOH is detrimental to catalytic activity of rhodium complexes, therefore it is used a high excess of magnesium oxide which has been found to be optimal to neutralize AcOH.

Based on what has just explained, a putative mechanism of sulfoxide imination performed on **32** and on **40** is described in scheme 21. Phenyl- λ^3-iodanediyl diacetate interacts with trifluoro acetamide forming the nitrene precursor **A**, that is stabilized by the resonance structures and by the presence of trifluoro acetyl group. In this configuration it is possible to observe the *decet* structure of λ^3-iodane that releases iodobenzene and the species nitrene, stabilized by electron withdrawing moiety. Afterwards, rhodium forms a coordination dimer between sulfoxide (**32**, **40**) and nitrene in order to favour the insertion of reactive species into sulphur, generating the desired sulfoximine (**35**,**41**).

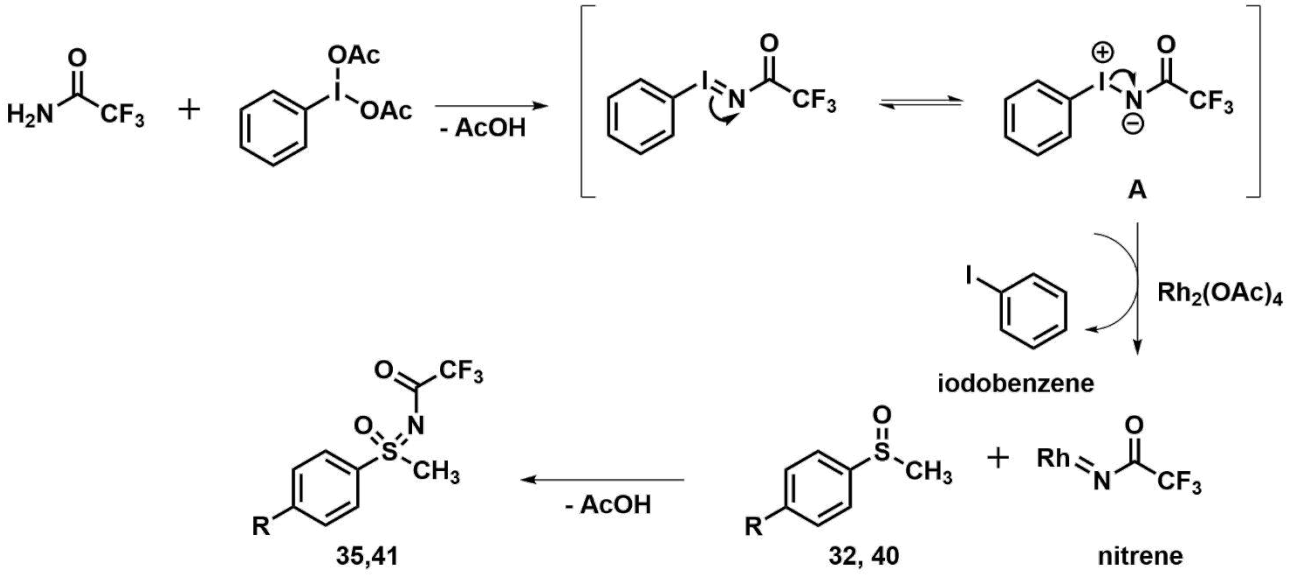

Scheme 21. Proposed mechanism of Bolm imination used for producing sulfoximines **35** and **42** from the respective sulfoxides **32** and **40**.

According to literature,[302] the cleavage of *N*-trifluoro acetyl sulfoximine is performed right after the imination of sulfoxide, as second synthetical step. The used conditions are methanol and high excess of potassium carbonate, due to the instability of CF_3COONH_2 in basic environments. The authors performed a methanolysis to have unsubstituted NH-sulfoximines in high yields. The *N*-alkylation, exerted for sulfoximine **36**, has similar basic conditions, represented by sodium triphosphate and acetonitrile, but the hydroxy anion, which is the main responsible of CF_3COO-removal, is missing because no protic solvent is used. Nevertheless, the difference was the excess of 1-(2-methoxyphenyl)piperazine (1.5 eq.), which was believed to recreate basic environment enough to remove the group. However, the obtaining of free NH-sulfoximine in one pot reaction was a crucial turning point in the synthesis because it optimized the workflow.

Amine synthesis is frequently accomplished through reductive amination, a rapid and efficient organic chemistry technique where aldehydes or ketones undergo reaction with corresponding amines, frequently catalysed by acids.[328] While reductive amination can employ palladium,[329] sodium cyanoborohydride,[330] or sodium borohydride,[331] these reagents exhibit limitations like high toxicity, functional group incompatibility, complex purification, cyanide residue impurities, or prolonged reaction times. Conversely, sodium triacetoxyborohydride emerges as a mild and selective reducing agent, providing higher product yields,[328] thus rendering it the chosen reducing agent for the reductive amination conducted to obtain sulfoximine **42** (Scheme 22). The initial step is the formation of the carbinol amine intermediate. This hemiaminal produces the iminium ion under acidic conditions due to the elimination of water. Then, it undergoes reduction by triacetoxyborohydride in order to afford corresponding amine (**42**).

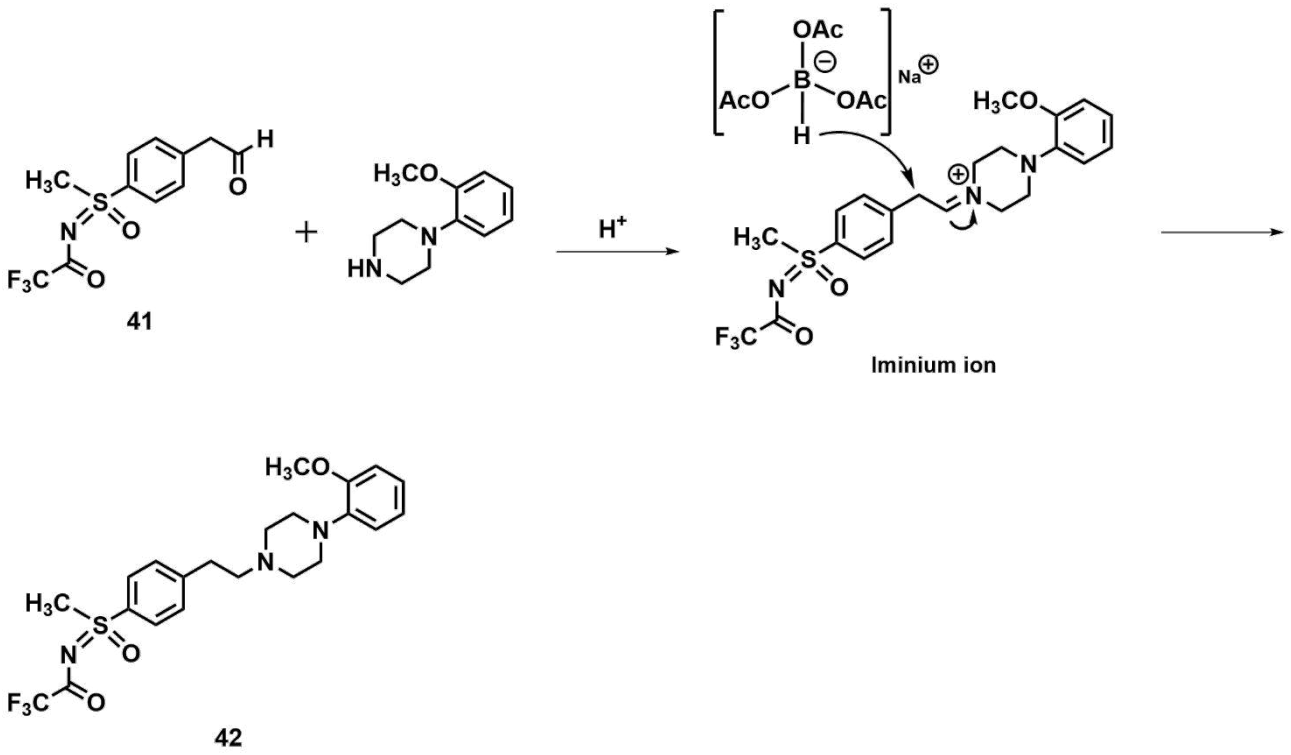

Scheme 22. Mechanism of reductive amination on the example of 2,2,2-trifluoro-N-(methyl(oxo)(4-(2-oxoethyl)phenyl)-λ^6-sulfaneylidene)acetamide (**41**).

3.2 Dopamine D_2/D_3 receptor ligands with aromatic linker variations

After the successful syntheses of sulphur-based dopamine D_2/D_3 receptor ligands (**4-6**, **12**, **14**, **16, 22-26, 30, 31, 34, 36, 37, 42**), the research project addressed the intriguing aromatic linker that was developed and evaluated with the sulphur-based compounds above described. According to the pharmacophore model of substituted *N*-phenylpiperazine based ligands and to the dopamine D_2/D_3 ligands developed in the last decades (See section 1.1.2), a simple alkyl chain of four carbons seems to be the best suitable structure to respect the two most important requirements for optimal D_2/D_3 receptor binding properties: linearity and extension. Single point modifications have been applied such as hydroxy or fluoride substituents with the purpose of directing the butyl chain to engender an efficient conformation of the ligand inside binding pockets. However, the obtaining of clinical candidates like **SB277011A** or **SB26952** and a marketed drug such as **cariprazine** have demonstrated that a variation of butyl chain is possible and can lead to a further optimization of D_2 and D_3 receptor binding properties. The novelty of these molecules lies in this core structure: the 1,4-disubstituted cyclohexyl unit used as a linker. This modification is the result of a conformational restriction that reduces the overall number of possible conformations and, as a consequence, favors the molecular recognition by the target receptor,[332] in this case D_2 and D_3 receptors.

Inspired by this type of lead optimization a set of conformationally restricted 1-(2-methoxyphenyl) piperazine derivatives is described here. The compounds were designed as aromatic analogues of **cariprazine,** having piperazine **3** and a simple methylamide group as PP and SP, respectively. The methylamide was chosen because it is well known to be bioisosterically similar to urea supported by cariprazine.[333] So, the evaluation of the aromatic linker used for sulphur-based ligands was continued and expanded by adding a second aryl variation: phenylmethyl. For each phenyl spacer, substitution patterns in *ortho*, *meta* and *para* were investigated in order to analyse which conformation is respecting the linearity concept of C4-chain linker. Additionally, further modifications of amide group have been examined, using nitro or cyano as electron-withdrawing group; aniline, methanamine and acetanilide as electron-donating group in different positions thanks to changeable western end position of the investigated linkers. In this context, two objectives were established:

1) whether variations of aromatic linkers might influence the binding properties towards D_2 and D_3 receptors.
2) whether an electronic depletion or enrichment might have an impact on the electron density of the phenyl rings, used as spacers, in terms of affinity at the target receptors.

Accordingly, to stick with the established objectives, a synthetic procedure with three steps of reaction was carried out to obtain the derivatives bearing the phenylethyl linker as it is presented in scheme 23. The first step is the coupling between the bromide substrates (**43** and **44**) and 1-(2-methoxyphenyl)piperazine, performed in microwave reactor with DMF to afford the first two compounds **45-46**, which served also as precursors of the anilino and acylated analogues (**47-50**). The reduction of nitro group was exerted with catalytic hydrogenation using palladium on activated carbon for the related aniline intermediates, while the acylation was executed with a mild acylating agent such as acetic anhydride.

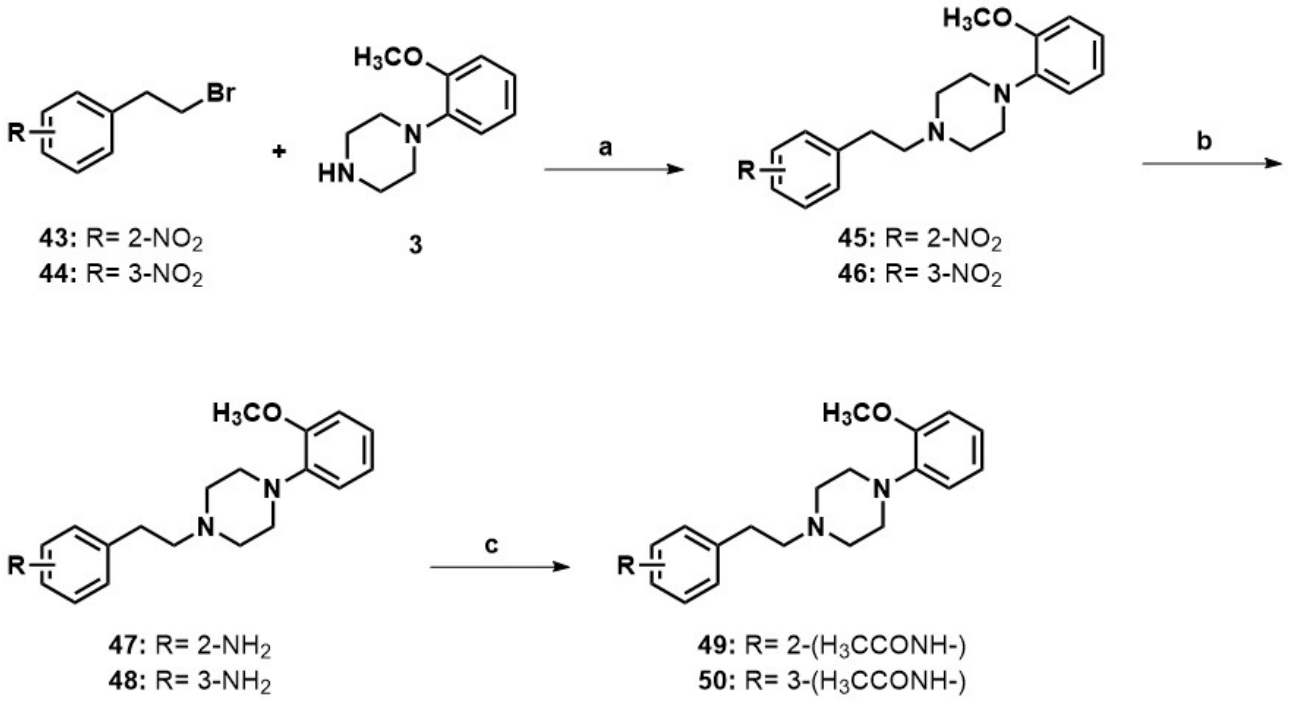

Scheme 23. Synthesis of ligands **45-50**. Reagent and conditions: (a) Na_3PO_4, DMF, 130 °C, 5 min, μW; (b) Pd/C 10%, H_2, MeOH, R.T., 18 h; (c) Ac_2O, TEA, DCM, reflux, 3 h.

However, the conditions for the *N*-alkylation used in this synthetic route were the result of an optimization that was necessary due to the competition between S_N2 and E_2. The substrates *ortho* and *meta*-nitro-phenethyl bromides are suitable moieties for elimination bimolecular mechanism as well. Initially, the *ortho* and *meta*-nitro-vinyl benzenes were obtained with higher yields than desired alkylated products. Thereby, it was necessary to modify the initial conditions in order to drive the reaction towards the nucleophilic substitution rather than the elimination. Different conditions were attempted in the coupling between piperazine **3** and substrate **43** and they are summarized in table 4. Taking a closer look at the results, slight but important improvements of nucleophilic substitution product were obtained by using FINKELSTEIN exchange, or DMF and Na_3PO_4 instead of ACN and K_2CO_3. Ultimately, the highest increase of the yields was achieved with the involvement of

microwave reactor, especially combined with DMF and Na_3PO_4. Consequently, these conditions were the chosen ones for obtaining **45** and **46**. By doing this, the alkylation step was improved and the synthetical workflow was facilitated. Being slightly more polar than acetonitrile, DMF increased the yields because it enhanced efficiently the reactivity of transitional state within the nucleophilic substitution mechanism. Furthermore, the carbonyl oxygen of DMF is able to interact through electrostatic forces with cations, thus leaving the anions not solvated and making them much more reactive in the reaction environment.[334]

Table 4. Overview of the optimization attempts performed in the N-alkylation in order to obtain ligands **45** and **46**.

Reagent (eq.)	Solvent	T (°C)	Time (h)	Yield S_N2 product (%)
TEA 1.5	ACN	25	24	23
K_2CO_3 1	ACN	25	24	30
KI, K_2CO_3 1.5 [a]	Acetone	reflux	24	39
KI, K_2CO_3 1.5 [a]	ACN	reflux	20	42
K_2CO_3 1.5	ACN	reflux	16	31
Na_3PO_4 1.5	DMF	reflux	10	36
K_2CO_3 1.5	ACN	130 in μW	0.08	49
Na_3PO_4 1.5	**DMF**	**130 in μW**	**0.08**	**60**

Reagent: TEA, triethylamine, [a] FINKELSTEIN conditions. Solvent: ACN, acetonitrile; DMF, dimethylformamide; μW, microwave reactor

Besides, 1-(2-methoxyphenyl)piperazine can act either as nucleophilic agent or as a base that takes out the hydrogen in *β*-position, provoking the formation of the double bond in α,β (Figure 18). This double activity is caused by the chemical structure of piperazine itself, where 2-methoxyphenyl ring enriches the electron density of piperazinyl ring exerting an inductive effect. According to HSAB theory and Pearson's original softness definition,[335] this effect makes the piperazine **3** more polarizable and softer. In addition, Méndez *et al*. have proved through kinetic studies that substrates like *p*-nitro-phenethyl bromide holds two soft centres.[336] The results of the work have pointed out that *β*-hydrogen atom is even softer than the C in α-position (See Figure 18). Consequently, a soft nucleophile like 1-(2-methoxyphenyl)piperazine has lower attraction toward C_α (soft property) than H_β (softer property), so there will be always a competition between S_N2 and E_2 with a major preference for the elimination mechanism, despite changing and trying several reaction conditions. Keeping these considerations in mind, the temperature was assumed to be the crucial determinant that changed the outcome of the *N*-alkylation step, which is theoretically in contrast to the knowledge that elimination mechanism is favoured

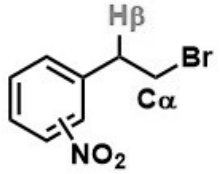

Figure 18. Outlook of the two soft centres in **43** and **44**. Adapted by Mendez et Al.[336]

by an increase of temperature. In this context, the microwave reactor application must be considered in major details.

Microwave reactions have gained broad utility in the last decades as powerful tool for obtaining rapid ed efficient syntheses of various compounds. As stated, microwave irradiation is an electromagnetic irradiation in the frequency range of 0.3 to 300 GHz; microwave reactors usually operate at a particular frequency of 2.45 GHz.[337] The great innovation brought by means of these devices is microwave heating, which is uniform throughout the reaction mixture. The microwave radiation passes through the walls of the vessel and heats only the particles of reactants and solvent. Consequently, the temperature increase will be uniform through the sample, which can lead to less by-products and/or decomposition products and no consumption of energy, as it happens in conventional heating methods like oil and sand baths.[338,339]

The mechanism behind microwave heating is an electromagnetic field generated by the irradiation; as a consequence, polar molecules are the ideal material because they align themselves with the oscillating field. On the other hand, intermolecular forces might induce polar molecules to oppose the field, triggering random motion, rotation or friction that dissipate as internal homogenous heating.[338,340] The effects of microwave radiation are dependent on the polarizability of molecules involved. In terms of reactivity and kinetics, Loupy and co-workers have demonstrated through their investigations that microwave effects should be considered referring to reaction mechanism and how the polarity of the system is altered during the progress of the reaction.[341] Then, the transitional state of reaction gains certain importance in microwave study viewpoint. For instance, the transitional state of S_N2 reactions involves a combination of anions with delocalized charge, conferring an increase of polarity in the medium of reaction. Logically, this means that the transitional state of S_N2 reactions has the right polarizability to achieve the uniform microwave heating, responsible of enhancing reaction rate. In fact, this is what is thought to happen in the *N*-alkylation analysed and optimized here. Basically, the microwave heating combined with polarizability of reaction system between **43**, **3** and DMF induced an increase in molecular vibrations that, in turn, lowered the activation energy of reaction, speeding up the reaction time and favouring the kinetic control of reaction.[342,343] In this way, the nucleophilic substitution mechanism prevailed over the elimination one and the kinetic product, that is *N*-alkylated one (**45**), was obtained with improved yields of 60% and same situation was reproduced with compound **46**.

In the meantime, no problems occurred for the synthesis of *para* substituted derivatives with phenylethyl linker, simply because the starting material was different and therefore different conditions were required. Instead of using from *p*-nitro-phenethyl halide, the chemical route started from 2-(4-nitrophenyl)ethan-1-ol (**51**) that was converted into mesylate **52** in order to perform the *N*-

alkylation with piperazine **3** in ACN and Na_3PO_4 at reflux. Once obtained the nitro compound with high yields, the reduction and the acylation steps were carried out in the same way of ligands **45-50**. The synthetical pathway is shown in the scheme below.

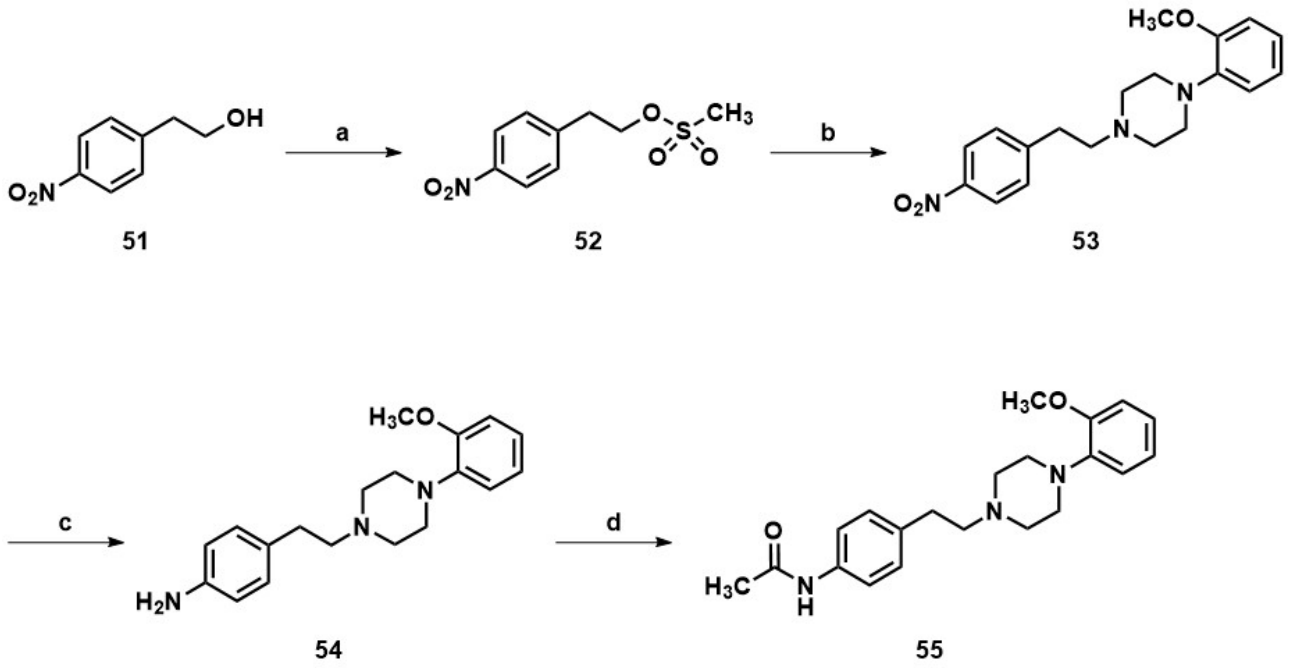

Scheme 24. Synthesis of ligands **53-55**. Reagents and conditions: (a) TEA, DCM, 0 °C, 15 min; (b) **3**, Na_3PO_4, ACN, reflux, 16 h; (c) Pd/C 10%, H_2, MeOH, R.T., 18 h; (d) Ac_2O, TEA, DCM, reflux, 3 h.

Regarding the desired compounds with phenylmethyl linker, the synthetical pathway was characterized by the same reaction steps but with slight modifications due to the different configuration and moieties. In the following route no competition between nucleophilic substitution and elimination was observed, because the structure of phenylmethyl ring avoided the formation of double bond. According to the established purposes, the purchased starting materials featured -CN instead of $-NO_2$, therefore a different reductive agent and conditions were used to obtain the methanamine intermediates. The related benzonitrile halides were coupled to 1-(2-methoxyphenyl)piperazine **3** with Na_3PO_4 in ACN at reflux to obtain without any problems the ligands **59-61**, that served as precursors for the reduced analogues **62-64** in order to elongate the structure. The reduction of cyano group was performed in autoclave by using the catalyst Raney-Ni and ammonia in methanol, leading to the formation of primary amines, which were acylated with acetic anhydride and triethylamine to gain phenylmethyl linker derivatives **65-67**. The synthetical pathway is represented in scheme 25.

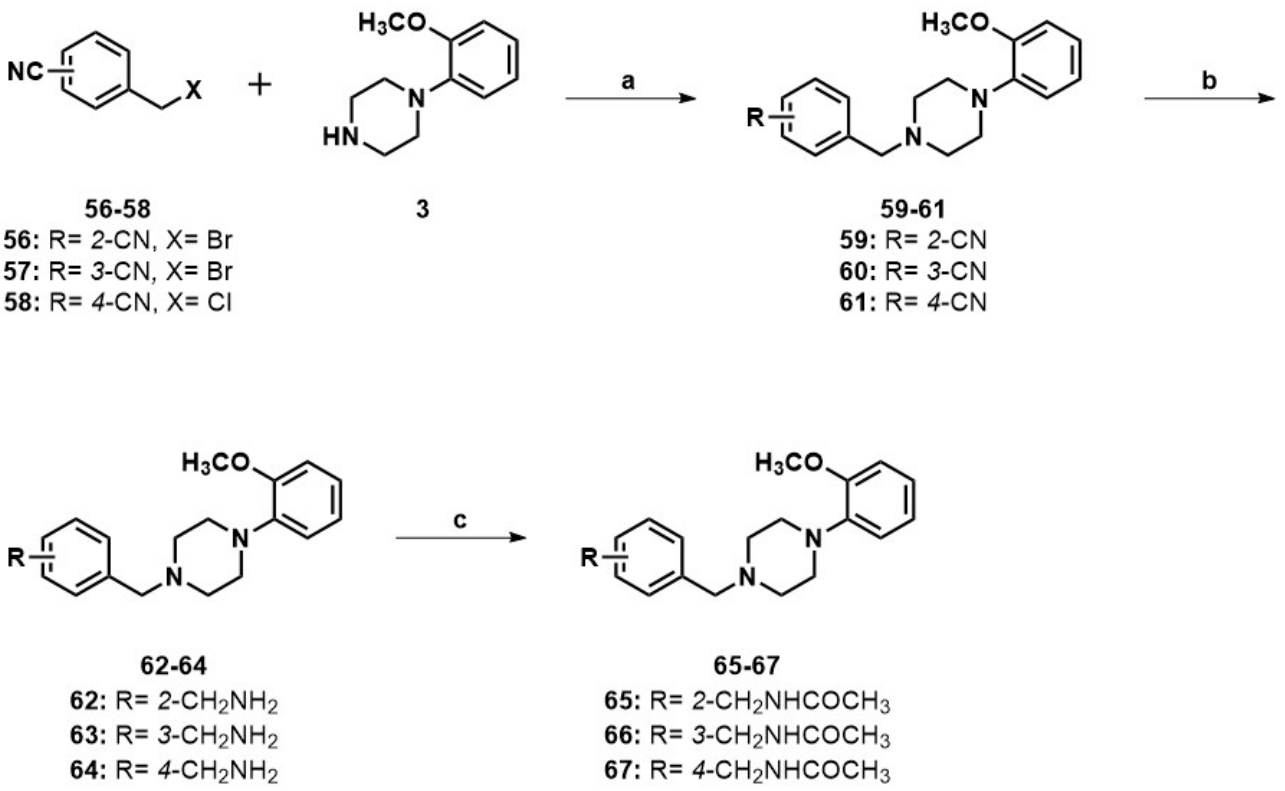

Scheme 25. Synthesis of compounds with phenylmethyl linker **59-67**. Reagents and conditions: (a) Na_3PO_4, acetonitrile, reflux, 3 h; (b) Raney-Ni, NH_3/MeOH, H_2 5 bar, 40°C, 16 h; (c) Ac_2O, Et_3N, CH_2Cl_2, reflux, 3 h.

The dopamine D_2/D_3 ligands with aromatic linker variations were obtained as free base derivatives and crystallized preferentially as hydrochlorides (**45-46**, **53**, **55**, **59-60**, **65** and **67**). To comply this, a standard procedure was adapted by literature[344] and applied using Et_2O as a solvent to solubilize the free base compounds and adding a solution of HCl in dioxane (2M). Compounds **47-50, 54**, **61** and aliphatic primary amines **62-64** were obtained as free base solids in Et_2O due to their insolubility properties. Derivative **66** featured to have problems with the obtaining of hydrochloride, the reason might be related to its *meta* orientation, therefore oxalic acid was used to form the corresponding crystallized salt according to the previous literature.[345]

3.3 Substituted-anilino-ethyl linker-based dopamine D_2/D_3 ligands

The results obtained by the modifications of aromatic linkers drove the third and final step of this PhD project. The dopamine D_2/D_3 ligands with different aromatic linker combinations demonstrated that the most suitable conformation is the *para* acetanilide phenylethyl linker, displayed by compound **55**. Consequently, the aniline derivative **54**, that has the free NH_2, was chosen as pivotal scaffold to perform the final study of this research project. A broad variety of functionalities and substitution patterns were linked to the free NH_2; in this way, the versatility of the developed linker was evaluated in combination with different moieties as secondary pharmacophores. Therefore, novel dopamine D_2/D_3 ligands with the innovative spacer were prepared with the purpose of exploring a possible application for future clinical candidates.

Based on the structure of products **54-55** and following the pharmacophore model of substituted *N*-phenylpiperazine D_2/D_3 ligands (Section 1.1.2), the first modifications applied to the scaffold were the insertion of one, two or three more carbons in order to elongate the acyl function. Then, a cyclic substitution pattern was applied producing 4-aniline-ethyl amides with aliphatic rings from 3 up to 6 members. This latter concept was executed also by changing the acyl function from amide into urea, synthetizing different cyclic urea derivatives with 5 or 6 membered rings.

Moreover, aromatic moieties were applied to the 4-aniline ethyl scaffold, increasing the size and lipophilicity of the structure in order to have a better overview in term of affinity at the target receptors related to the SPs. Therefore, one or two aromatic rings differently substituted were connected to the scaffold with amide and urea bonds, keeping the H-bond donor/acceptor characteristics, required in that area of the molecule. Among these, various positions of attachment (*ortho*, *meta*, *para*) to the phenyl ring were evaluated as well, checking if the manipulation of electron density might have an impact on the binding behaviour of studied ligands. Additionally, heteroaromatic rings were inserted within the aromatic modifications, fused or not to another benzene ring and attached into different positions.

In conclusion, 58 acylated-anilino-ethyl linker derivatives were designed and synthetized in this part of the PhD project, featuring the scaffold investigated previously and different substitution patterns studied as SPs thanks to the changeable western part of the aniline scaffold. Since the synthesis was developed and optimized for the previous ligands, the workflow was quite immediate and effective. The amide synthesis and urea formation are the reactions explored in this study with the related mechanisms.

To synthetize the scaffold, compound **54**, the same synthetical pathway was used and scaled up: 2-(4-nitrophenyl)ethan-1-ol (**51**) was converted into mesylate **52** in order to perform the *N*-alkylation with piperazine **3** in ACN and Na_3PO_4 at reflux. The nitro derivative (**53**) was obtained and reduced exerting the catalytic hydrogenation with palladium on carbon. Once the scaffold (**54**) was obtained, different conditions of acylation were applied, depending on which acylating agent was used and which final product was established. For instance, if the acylating agent was an acyl chloride or anhydride, DIPEA, THF were used, while temperature and time were adjusted accordingly. If carboxylic acid was used as acylating agent, the chemical HATU was used with the same solvent and base. Regarding the urea formation, the aniline **54** was treated with diphosgene, leading to the formation of isocyanate **68**, which underwent nucleophilic addition by the amine having the wanted substitution pattern. In this way, amides and ureas bearing 4-aniline-ethyl linker (**69**-**126**) were synthetized and the steps are shown in the scheme 26.

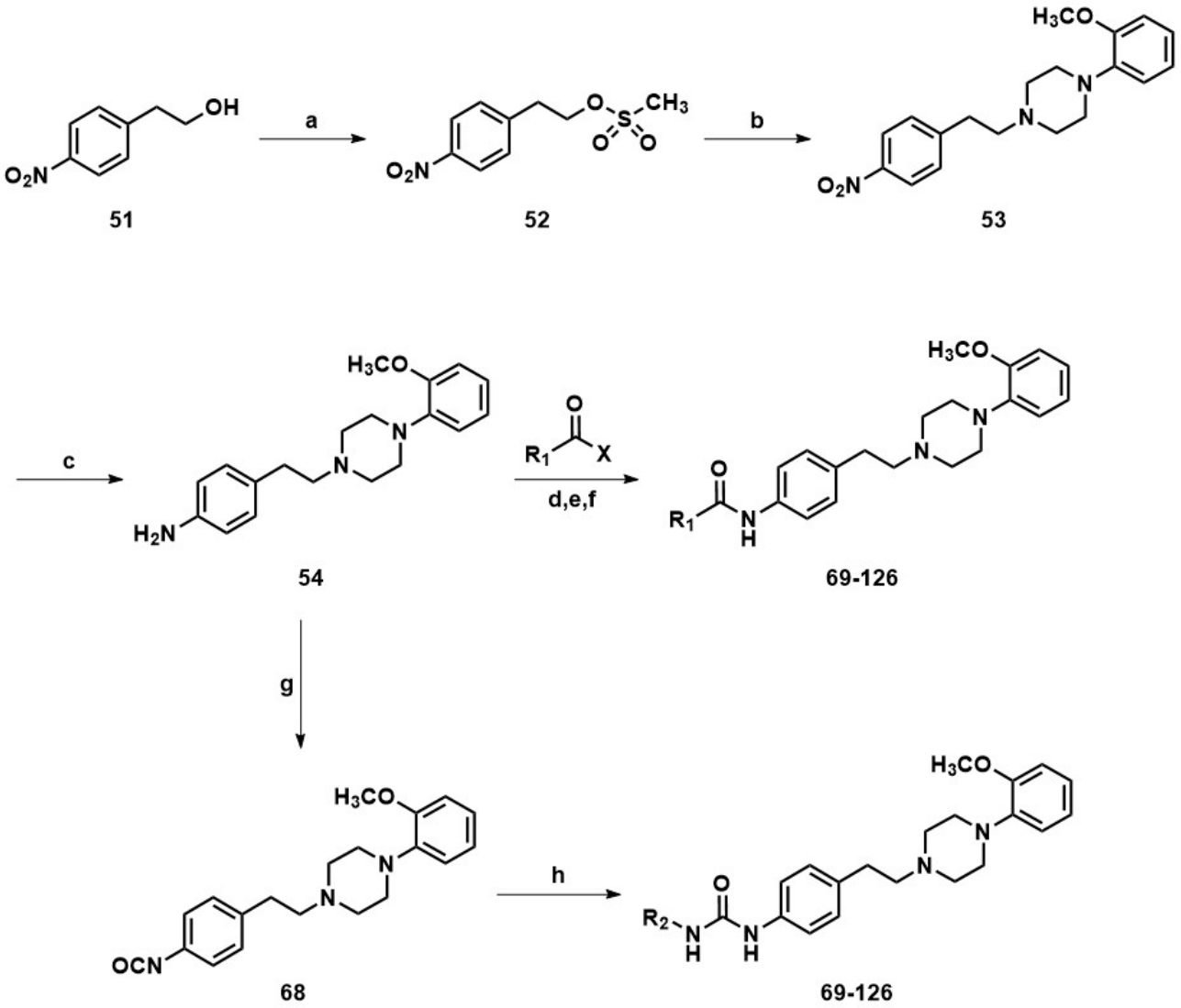

Scheme 26. Synthesis of ligands **69-126**. Reagents and conditions: : (a) TEA, DCM, 0 °C, 15 min; (b) **3**, Na_3PO_4, ACN, reflux, 16 h; (c) Pd/C 10%, H_2, MeOH, R.T., 18 h; (d) **X = Cl**, DIPEA, THF, r.t → reflux, 3-6 h; (e) **X = OR´**, DIPEA, THF, reflux, 3-6 h; (f) **X = OH**, DIPEA, HATU, DMF, R.T., 16 h; (g) diphosgene, dioxane, reflux, 2h; (h) **R_2**-NH_2, ACN, reflux 10 h.

As it has been mentioned before, the synthetical workflow did not face any particular difficulties or problems, all the derivatives (**69-126**) were achieved with high yields. The products **71**, **79**, **84-85**, **91**, **97**, **108**, **118**, **121**, **123**, **125**, **126** were obtained as free base derivatives and crystallized preferentially as hydrochlorides. To comply this, a standard procedure was adapted by literature[344] and applied using Et_2O as a solvent to solubilize the free base compounds and adding a solution of HCl in dioxane (2M). The additional synthetical steps of the chemical route are characterized by the amide synthesis and urea formation, whose general mechanisms are described.

Amide bond formation is an important synthetic approach in medicinal chemistry. The amide bond is broadly present in macromolecules such as proteins, as well as in numerous preclinical and clinical candidates and commercially available drugs. This functional group is a valuable tool due to its resistance to hydrolysis and high temperatures. It can form hydrogen bonds or π-interactions within an active site of target receptor.[346] Amides are typically formed from carboxylic acids and corresponding amines. However, this reaction does not occur spontaneously and requires high temperatures, which can lead to low yields, complex purification, and racemization. To avoid these difficulties, carboxylic acids need to be activated.[347]

Among the oldest and still very common activation methods, one is converting carboxylic acids to halides (mostly chlorides) using thionyl chloride, oxalyl chloride, or triphenylphosphine. Carboxylic acids can also be converted to anhydrides, azides, acyl imidazoles, or esters. The main goal of activation is forming a better leaving group, leading to an unstable tetrahedral intermediate. Indeed, one of the amide preparations used here, required acetic chloride or symmetric anhydride. The mechanism is based on a simple nucleophilic addition of aniline **54** towards the electrophilic carbon belonging to the acylating agent used. Then, rearrangement and proton transfer lead to the formation of the corresponding desired product. Whereas, hydrochloride or the corresponding carboxylic acid are produced in presence of acetyl chloride or anhydride, respectively as by-products. The mechanism of reaction is depicted in the following scheme 27, where "R" groups generally the substitution patterns applied on the scaffold **54**. [348]

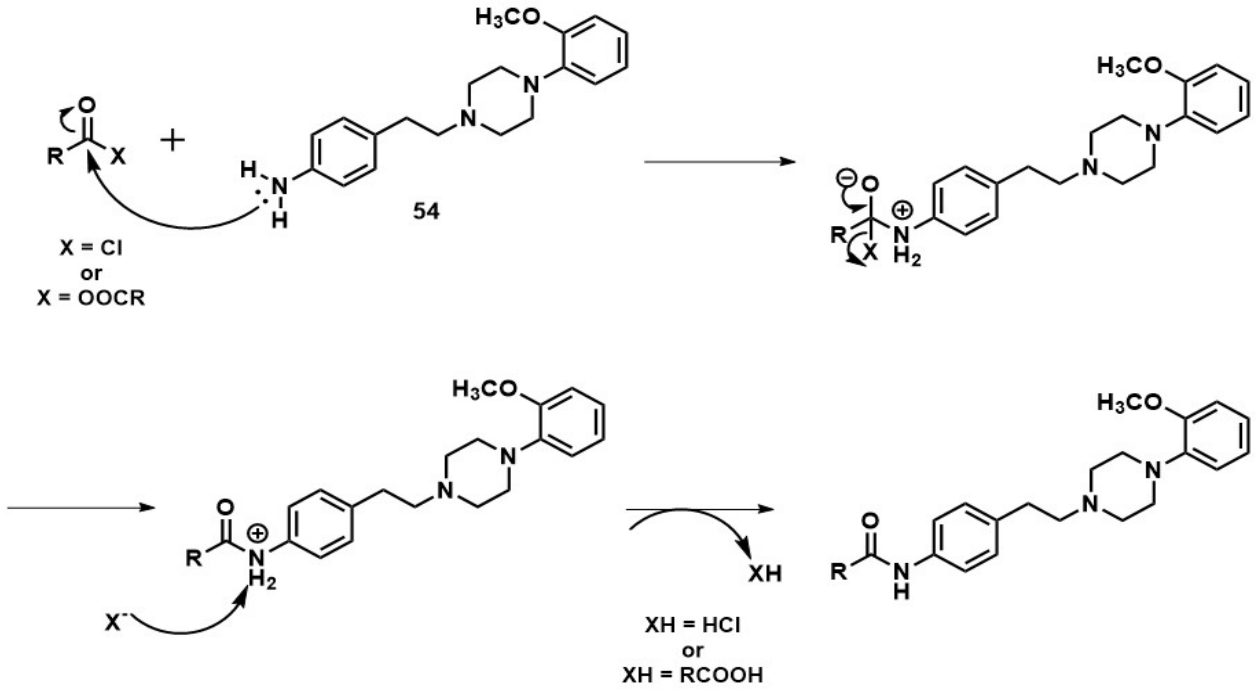

Scheme 27. Mechanism of amide preparation with acyl chloride or anhydride on aniline **54**, adapted by Montalbetti *et Al.*[348]

The amide synthesis using HATU is going through a different mechanism. Once the carboxylic acid is deprotonated by DIPEA, the carboxylate anion **A** attacks HATU to form the unstable O-acyl(tetramethyl)isouronium salt **(B)** (Scheme 26). The 1-Olate-7-azabenzotriazole anion (OAt) rapidly attacks **B**, affording the OAt-active ester **C** and liberating tetramethyl urea as by-product. The benzotriazole ring is rendering the carboxyl carbon more electrophile and more reactive to the nucleophilic addition of aniline **54**. Therefore, the addition of **54** results in the formation of desired anilide. The general mechanism of this amidation is represented in scheme below.[349]

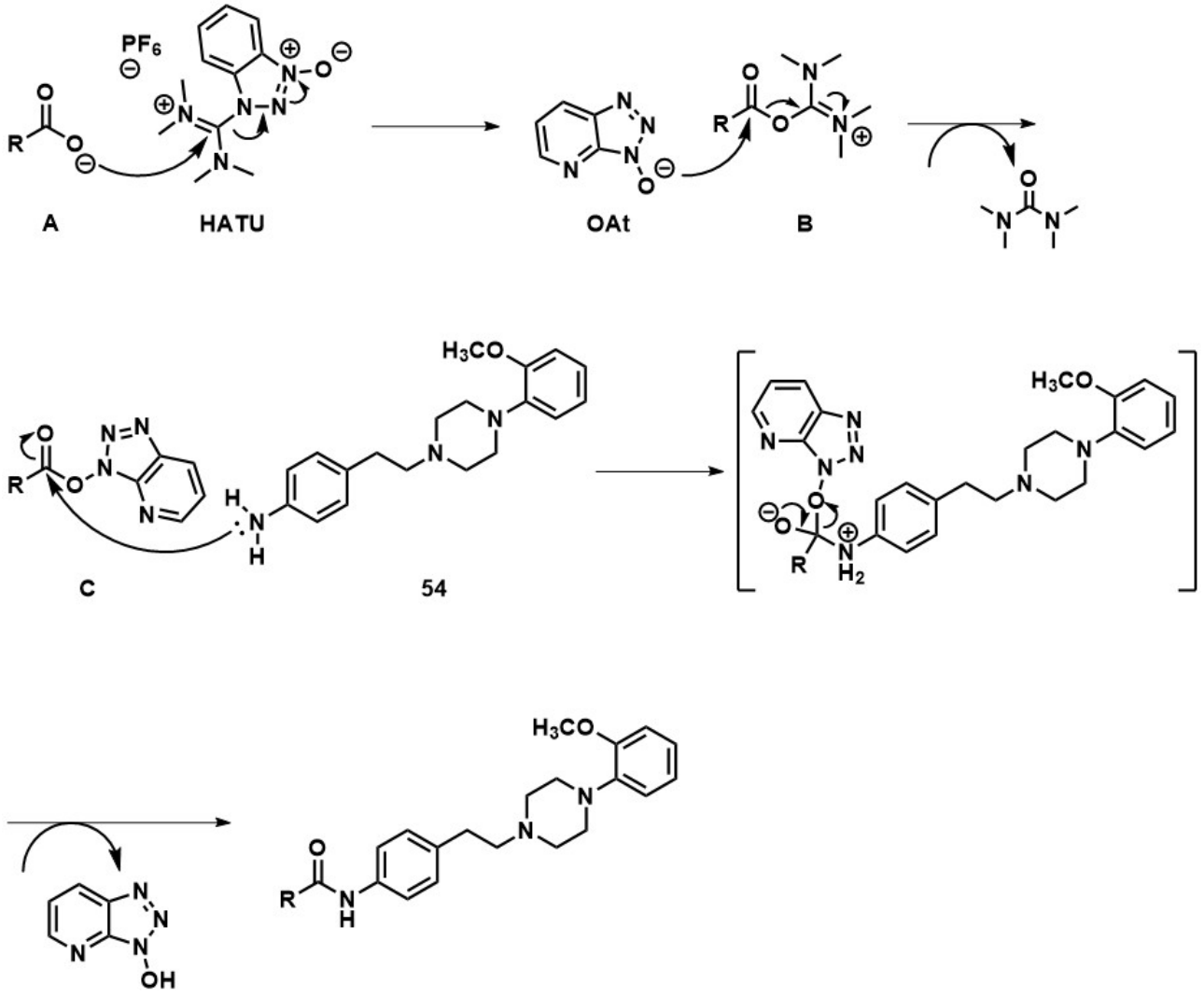

Scheme 28. General mechanism of one-pot amidation using HATU. Adapted by Vrettos *et Al.*[349]

The urea and its derivatives occupy a central position in drug development and medicinal chemistry due to the remarkable capability of forming multiple stable hydrogen bonds with protein and receptor targets. These drug-target interactions are the driving force of specific biological activities, therapeutic actions, and desirable properties exhibited by urea-based compounds. Consequently, it is

not surprising that a large number of urea derivatives finds extensive applications across lots of medicinal domains. The strategic incorporation of the urea serves as a powerful tool for modulating drug potency, enhancing selectivity, and optimizing the overall properties of promising structures during the drug development process.[350,351] The presence of urea exerts a profound influence on a drug's aqueous solubility and permeability, owing to its unique dual nature as both hydrogen bond donor and acceptor. For drugs intended to act on the CNS, a moderate level of lipophilicity is crucial, as it facilitates passive diffusion across the BBB.[352] The hydrogen bond ability together with ionization, polar surface area, and flexibility affects drug transport throughout the BBB. These properties, carefully modulated by the efficient application of the urea, play a pivotal role in optimizing the pharmacokinetic profile and ensuring effective CNS penetration of therapeutic agents.[353] In this matter, the best example is **cariprazine**, that is a urea-containing marketed drug and it is one of the leading compounds of the project reported here.

The urea bond exhibits a distinct degree of conformational restriction, a characteristic that is represented by the presence and delocalization of electron lone pair on the nitrogen atoms into the adjacent carbonyl group. This phenomenon of electronic delocalization, which extends across the entire urea moiety, introduces a planar geometry and inherent rigidity to the molecular framework.[354] Accordingly, three resonance structures can be drawn for ureas (namely **A**, **B**, **C**; figure 19). Due to the importance of urea derivatives and the broad utility of this function, several methods have been developed for their syntheses.[355,356]

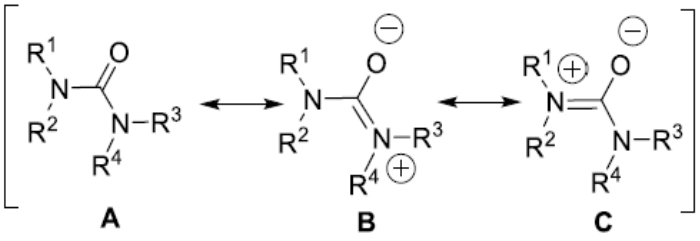

Figure 19. Possible resonance structures for the urea moiety, reproduced by Ghosh *et* Brindisi.[351]

The most traditional methodology is the reaction of amines with diphosgene. It is commonly used for producing symmetric ureas, but unsymmetrical derivatives can be prepared as well. In general, amines react with diphosgene to provide the required isocyanate intermediates.[357,358] Subsequent reactions of the isocyanates with diverse amine nucleophiles provide the desired unsymmetrical urea derivatives. Indeed, this synthetical method was executed in order to obtain the urea-containing dopamine D_2/D_3 ligands represented here. Since aniline **54** was the precursor, all the compounds are unsymmetrical ureas. The proposed mechanism is depicted in scheme 29. The aniline **54** exerts a nucleophilic addition at the electrophile carbon of diphosgene, producing an instable carbamate which leads to the formation of isocyanate **68** under heating. Subsequently, the second amine with proper

substitution pattern is performing a second nucleophilic addition, that generates the desired urea derivative through a proton rearrangement.

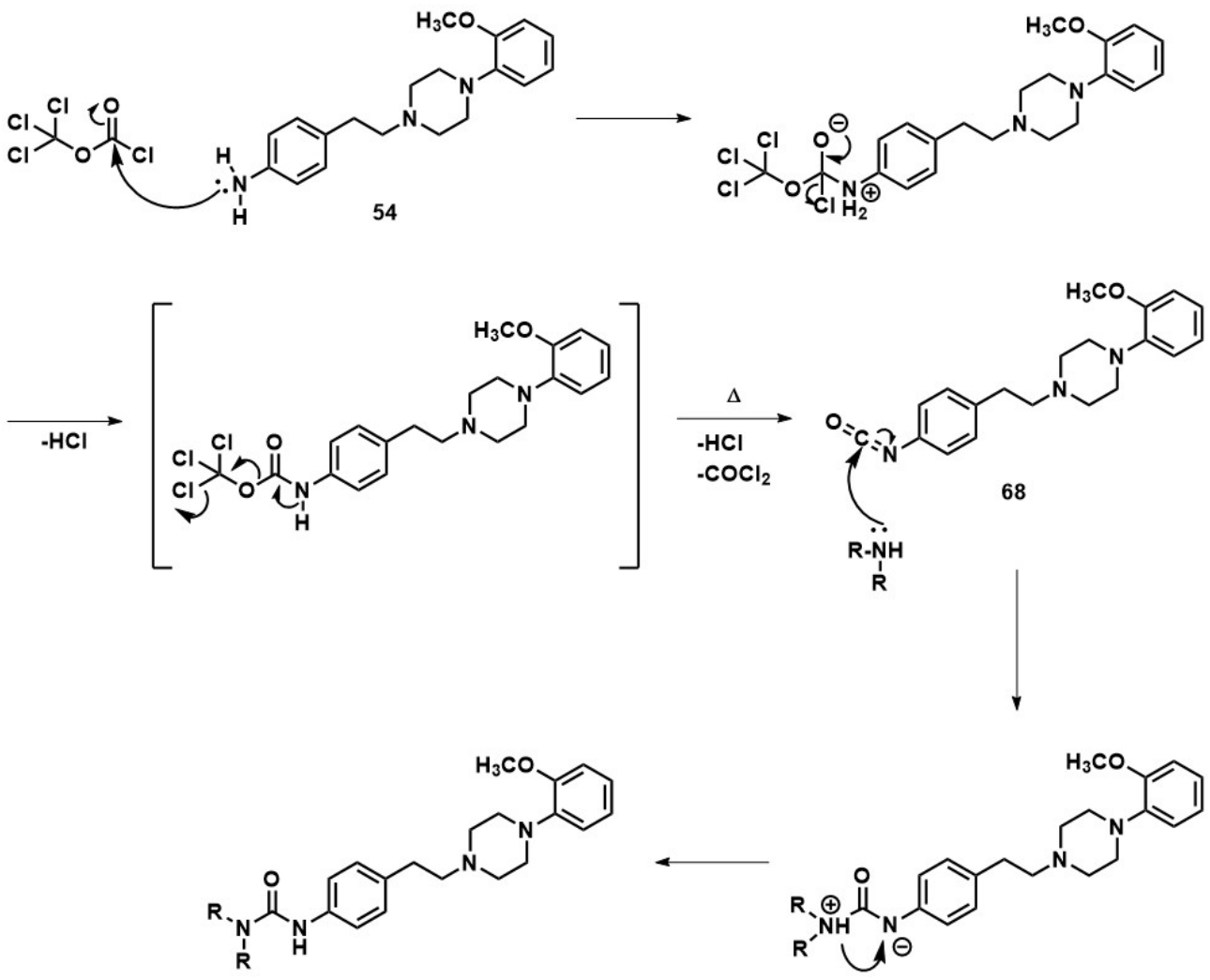

Scheme 29. Putative mechanism of urea synthesis using diphosgene and isocyanate as reactive intermediate. The synthetical method has been employed to afford the urea derivatives presented in the PhD project. Mechanism adapted by Ghosh *et* Brindisi.[351]

Following these synthetical methods, the 58 amide- and urea-containing dopamine D_2/D_3 receptor ligands are listed in different tables, depending on the type of modification applied to the scaffold 4-aniline ethyl linker. In table 5 the amide derivatives with aliphatic modification are represented. The aliphatic modification consists of the elongation of acyl function by inserting one, two or three more carbon atoms and the application of cyclic substitution pattern. Indeed, it is possible to notice a gradual increase of the size and the chain attached to amide bond.

Table 5. Overview of the structures of ligands **69-79**.

Compound	R	Compound	R
69		**76**	
70	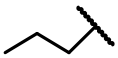	**77**	
71		**78**	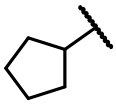
72		**79**	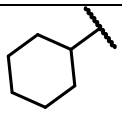
73			
74	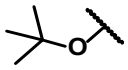		
75	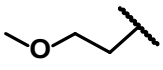		

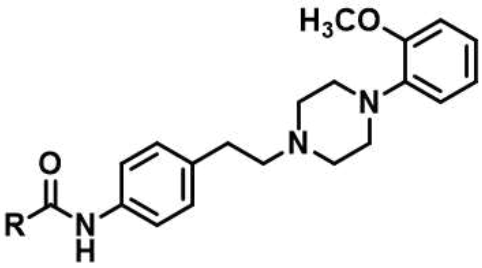

Once compounds **69-79** were successfully afforded, the modifications continued by changing the amide bond into its bioisostere urea and by modifying the chemical unit attached to the second nitrogen. Urea derivatives with aliphatic and aromatic rings (**80-88**) were synthetized, see table 6. Compound **80** displays a (1-ethylpyrrolidin-2-yl)methanamine ring which was attached to the second nitrogen of urea (Table 6). This moiety is featured by two important marketed drugs: **amisulpride** and **sulpiride**, that were taken as reference to develop some structures in the SP investigation described here (Figure 20). Both of them are atypical antipsychotics and they belong to the class of substituted benzamides. They act antagonizing the dopamine D_2 and D_3 receptors and they are indicated for the treatment of positive and negative symptoms of schizophrenia.[359,360] Particularly, **amisulpride** has a unique dose-dependent mechanism of action and it is available in intra venous formulation, while **sulpiride** is primarily used orally and has been explored for its prolactin-releasing properties.[361–364] Given the interest towards these drugs, their structures were used to design ligands in combination with the scaffold developed. Afterwards, a pyrrolidine ring (**81**) and 6-membered aliphatic rings variously substituted were linked to 4-aniline-ethyl linker (**82-84**). Subsequently, simple aromatic rings were attached to the scaffold along the lines of the previous aliphatic modifications (**85-88**).

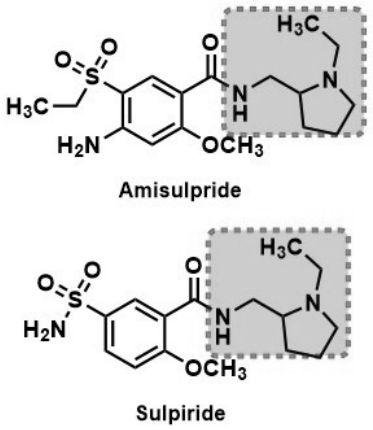

Figure 20. Structures of marketed drugs **amisulpride** and **sulpiride**. The chosen moiety for urea modifications is highlighted in grey.

Table 6. List of urea containing dopamine D_2/D_3 ligands **80-88**.

Compound	R	Compound	R
80	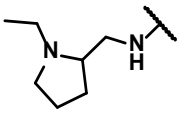	**85**	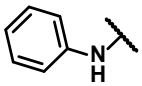
81	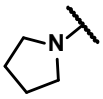	**86**	
82	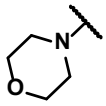	**87**	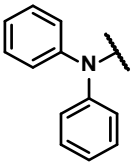
83	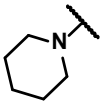	**88**	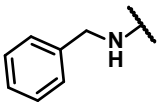
84	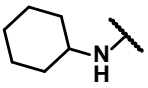		

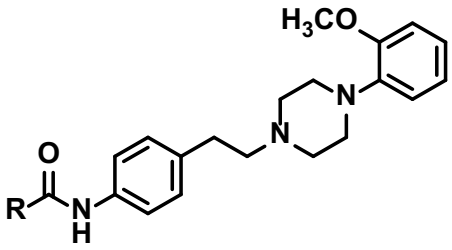

The aromatic urea-containing ligands (**85-88**) have given the idea to apply this type of substitutions to the amide function. In this case, the substituted phenyl rings displayed by **amisulpride** and **sulpiride** were added to the scaffold as it has been done for compound **80**, see above. Additionally, a third framework has been taken to expand the investigation, that is *3*-methoxybenzamide, see figure 21. This amide moiety has been deeply explored by Leopoldo and co-workers, obtaining promising dopamine D_2/D_3 ligands.[155] In their study they demonstrated that *3*-methoxybenzamide moiety is influencing the binding properties of ligands at D_2 and D_3 receptors, thanks to the intramolecular bond between amidic hydrogen atom and the oxygen of methoxy group.[155,365] Thereby, the *3*-methoxybenzamide was added to the *4*-aniline-ethyl linker to produce compound **90** and the methoxy group was analysed in different positions or as di- and tri-substituted function into phenyl ring, as it is depicted in table 7.

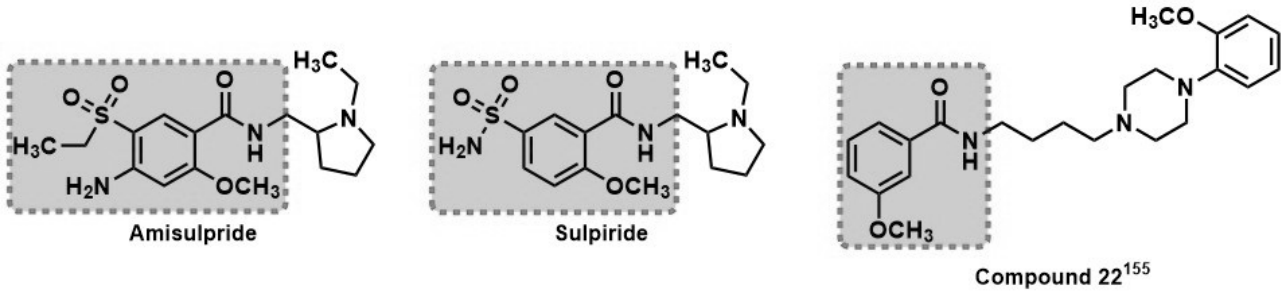

Figure 21. Lead structures that inspired the synthesis of derivatives **89-100**. The substituted benzamides applied to the 4-anilino-ethyl linker are highlighted in grey.

Table 7. General overview of the benzamide derivatives with various substitutions **89-102**.

Compound	R	Compound	R
89	*2*-OCH_3	**96**	*3,5*-OCH_3
90	*3*-OCH_3	**97**	*4,5*-OCH_3
91	*4*-OCH_3	**98**	*3,4,5*-OCH_3
92	*2,3*-OCH_3	**99**	*2*-OCH_3 *5*-SO_2NH_2[a]
93	*2,4*-OCH_3	**100**	*2*-OCH_3 *4*-NH_2 *5*-SO_2Et[b]
94	*2,5*-OCH_3	**101**	*3*-CN[c]
95	*2,6*-OCH_3	**102**	*4*-CN[c]

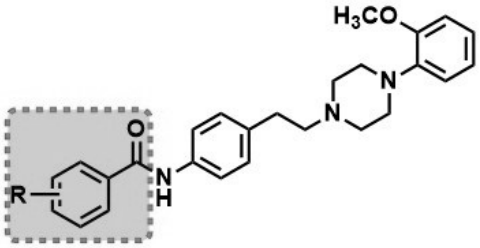

[a] Ligand based on the benzamide displayed by sulpiride; [b] ligand based on the benzamide displayed by amisulpride; [c] ligands based on the benzamide displayed by the studied derivative of Gadhyia *et Al.*[366]

Furthermore, monosubstituted *3*- and *4*-cyano benzamide derivatives (**101-102**) were prepared with the purpose of having a general comparison among electron withdrawing group (EWG) and electron donating group (EDG), -CN and -OCH_3 respectively. Particularly, recent studies have been proved that the unit *4*-cyanobenzamide might play a crucial role in fine-tuning a ligand within the binding pockets of D_3 receptor,[366] thus this variation was included in the study described herein.

However, the comparison in terms of electron density manipulation within methoxy and cyano groups remained incomplete for two reasons:

1) Only monosubstituted -CN derivatives were synthetized because the di- or tri-substituted substrates were neither commercially available nor synthetically affordable.
2) The *2*-CN benzamide derivative was attempted to be synthetized but the *ortho* position, which is near to the amidic -NH, created some chemical issues that rendered the achievement of this compound impossible.

In the conditions of HATU amidation, the amidic -NH exerted a nucleophilic attack on the electrophile carbon of the cyano group in *ortho* position, generating two by-products: 3-imino-isonindolin-1-one and isoindoline-1,3-dione, respectively **A** and **B** in figure 22. Although the major product was the wanted *2*-CN benzamide ligand, all three compounds had same or very similar retention time as it is shown from the HPLC/HRAM-MS report attached. Thereby, isolation of desired product was not possible either in normal phase or in reversed phase chromatography.

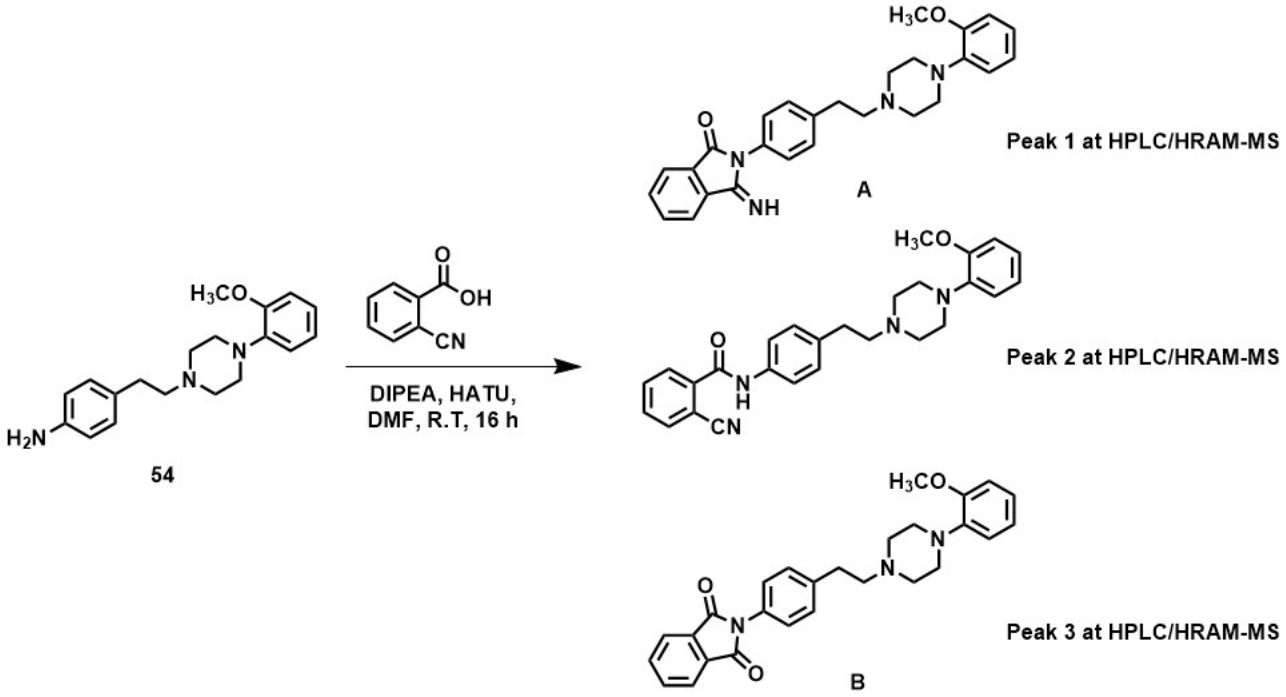

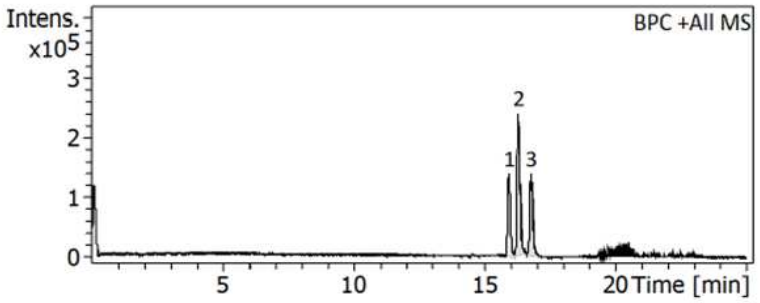

#	RT [min]	Area	S/N	Max. m/z	FWHM [min]	Area Frac. %
1	15.9	1069675	122.4	221.1255	0.1	25.91
2	16.3	1954958	211.6	441.2292	0.1	47.36
3	16.8	1103206	122.6	442.2127	0.1	26.73

Figure 22. Outlook of the chemical problem observed in the HATU coupling with *2*-CN benzamide derivative. The structures of the desired product with the related by-products **A** and **B** are represented above. The peaks of the corresponding compounds are shown in the HPLC/HRAM-MS report below.

As a consequence, different conditions of amide synthesis were attempted, by changing equivalents of HATU and DIPEA, using different reactants such as 1-Ethyl-3-(3-dimethylaminopropyl)carbodiimide and hydroxybenzotriazole, or dicyclohexyl carbodiimide and 4-dimethylaminopyridine, or even the corresponding symmetric anhydride (*2*-CN benzoic anhydride), but the mixture of the three compounds was always obtained. All the attempted conditions are listed in table 8. The equivalents of reactants were calculated in relation to amount of aniline **54** (1 eq.). The solvent used was DMF for all the attempts due to solubility reasons, and time of reaction was always 6 hours. No heating was executed.

Table 8. Summary of amidation conditions attempted to obtain the desired *2*-CN benzamide product. The mixture of desired compound and relative side products was obtained in all attempts listed in this table.

Attempts	2-CN benzoic Acid (eq.)	HATU (eq.)	DIPEA (eq.)	EDC (eq.)	HOBt (eq.)	DCC (eq.)	DMAP (eq.)	2-CN benzoic anhydride (eq.)
1)	1.5	1.5	3	-	-	-	-	-
2)	2	2.5	4	-	-	-	-	-
3)	1.2	1.2	3	-	-	-	-	-
4)	0.8	0.8	2	-	-	-	-	-
5)	0.5	0.5	2	-	-	-	-	-
6)	1.1	-	-	1.1	1	-	-	-
7)	0.8	-	-	1	1	-	-	-
8)	1.1	-	-	-	-	1.2	Catalytic Amount	-
9)	-	-	1.5	-	-	-	-	1.5
10)	-	-	-	-	-	-	-	1.1

Reactants: EDC, 1-Ethyl-3-(3-dimethylaminopropyl)carbodiimide; HOBt, hydroxybenzotriazole; DCC, dicyclohexyl carbodiimide; DMAP, 4-dimethylaminopyridine.

Moreover, monitoring the reactions at HPLC/HRAM-MS demonstrated that the mixture of desired derivative and the two side products was formed after 15 minutes from the beginning of every reaction showed in table 8. That is the reason why, SANDMEYER reaction[367] was chosen as final synthetical approach to afford the desired product. The reaction was performed on substrate 2-amino-N-(4-(2-hydroxyethyl)phenyl)benzamide (**A** in scheme 30) adapting the conditions from the related literature,[368] because the aromatic ring of 1-(2-methoxyphenyl)piperazine **3** might have interfered with the regioselectivity of reaction. Nevertheless, the reaction did not go as expected, the *2*-NH_2 was favoured to react with amidic -NH generating a benzotriazin-4-one ring derivative (**B** in scheme 30). Indeed, recent studies confirmed this type of application of SANDMEYER reaction[369–372] and no traces of *2*-CN benzamide derivative were obtained.

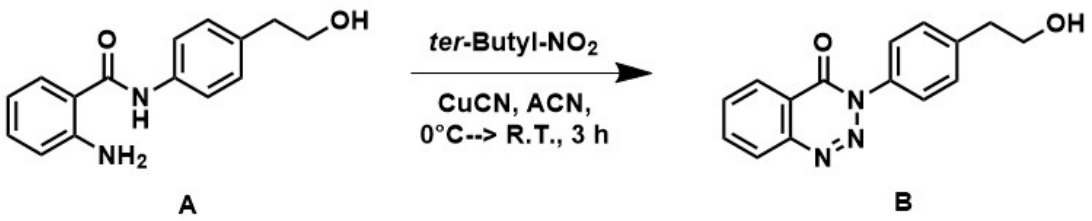

Scheme 30. Representation of SANDMEYER attempted in order to obtain the *2*-CN benzamide derivative. The unexpected benzotriazin-4-one structure **B** was produced.

Based on these results, the *2*-CN benzamide derivative was not achieved. Anyway, the study on amides with aromatic modifications was expanded by applying first a simple phenyl ring and then several modifications to the aromatic terminal (See table 9, compounds **103-126**). For instance, the first change was the bioisosteric replacement with a pyridine ring (**104-106**), which is known to be the classical bioisostere of an aromatic ring. Usually, the replacement with pyridine units may improve parameters such as polarity, hydrophilicity or interaction with cytochrome P and human serum albumin.[373] In addition, the different positions of nitrogen were tested within the heteroaryl ring.

Afterwards, a second ring was added to generate compound **107** that started an analysis on different moieties such as benzo fused or not fused aliphatic (**108-112**) and heteroaromatic rings (**113-126**). Specifically, coumarin-4-aniline ethyl linker derivatives were produced within this library (**110-112**). In the last years, coumarin-piperazines have gained a lot of interest, because both natural and synthetic coumarins have effects on the CNS, in particular on the serotoninergic and dopaminergic systems, and thus they can be used in the treatment of Parkinson´s disease, Alzheimer´s syndrome and psychiatric disorders.[374] Due to this, many interesting and effective coumarin-piperazine based dopamine D_2/D_3 ligands have been recently developed[375–378] and coumarin core was included in the library of acylated-4-aniline ethyl linker compounds presented here.

Subsequently, the coumarin unit was replaced by heteroaromatic 5-membered rings; the modification was exerted by changing the attachment position and the heteroatom within the di-aromatic structures (**113-119**). Ultimately, the last variation was the insertion of a non-fused heterocycle, following the same criteria: switching the attachment position (*2*- or *3*-) and the heteroatom within the aryl ring (sulphur, nitrogen or oxygen, **121-126**). However, compound **120** features the sulphonamide of tosyl group as bioisosteric replacement of amide function, based on literature.[379]

Table 9. Outlook of dopamine D_2/D_3 ligands **103-126** that bear an aromatic acylated motif linked to the scaffold 4-anilino ethyl linker.

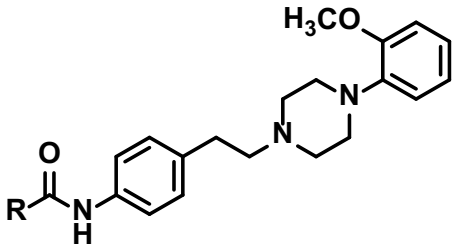

Compound	R	Compound	R	Compound	R
103	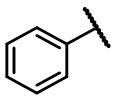	**111**	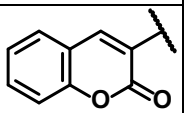	**119**	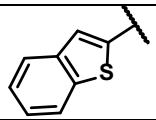
104	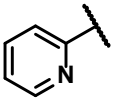	**112**	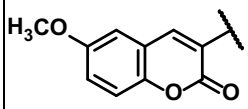	**120**	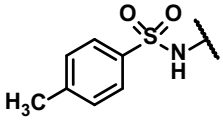
105	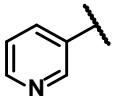	**113**	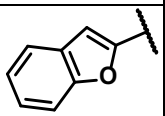	**121**	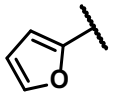
106	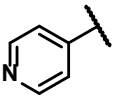	**114**	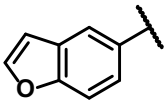	**122**	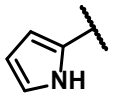
107	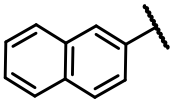	**115**	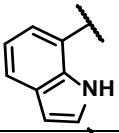	**123**	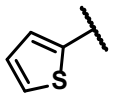
108	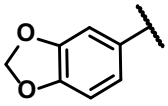	**116**	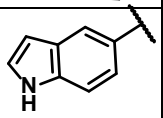	**124**	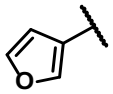
109	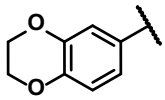	**117**	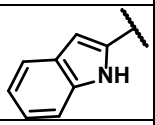	**125**	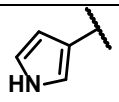
110	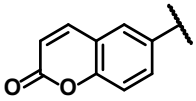	**118**	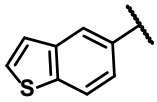	**126**	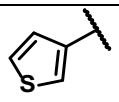

4 Pharmacology and SAR

The synthesized dopamine D_2/D_3 receptor ligands were assessed for their *in vitro* binding properties to determine their affinities at the target receptors. Only ligands with high affinity might represent potent drug-like candidates and may be considered for further development, including *in vivo* and clinical studies. All *in vitro* studies were conducted in Professor Holger Stark's research group, as previously reported with slight modifications. [239,241,380] In this section, the biological evaluation of the synthetized compounds is discussed and structure-activity relationships are analysed for every set of ligands. In addition, drug-likeness properties of selected ligands are described in this chapter as well.

4.1 Pharmacological Evaluation

In vitro binding studies can be conducted to determine receptor localization and distribution, to characterize receptors of interest and their regulation, to examine ligand kinetics, and to assess affinity and selectivity for off-targets. These studies aid in the development of new, potent drug-like candidates. Typically, the ligands, that are used in binding studies, are radio- or fluorescence-labelled and they must exhibit high affinity and selectivity for the receptors of interest. High receptor affinity is associated with slow dissociation, which provides favourable conditions for performing assays. Additionally, the selection of the model system is crucial; using receptor-overexpressing recombinant cell lines allows to have a detailed examination of interactions with the receptor.[381]

Despite being complex, assays conducted in presence of an antagonist can be simplified into a two-part system consisting of ligand (L) and receptor (R). The cell homogenate and the desired biological target are mixed for a determined incubation time, allowing for collision and equilibration of binding. The binding to the receptor of interest follows the Law of Mass Action. During this process, a complex between the free, unbound ligand (L^*) and R is formed until equilibrium is reached, resulting in the bound ligand (L-R), see equation 1. This reaction is reversible. In the binding assay, free ligands are separated from the bound ligand by rapid filtration through a glass fibre filter, after which the bound ligand is measured. Quantification of the bound ligand is performed using scintillation counting.[381]

$$L^* + R \underset{k_{off}}{\overset{k_{on}}{\rightleftharpoons}} [L\text{-}R] \qquad K_d = \frac{k_{off}}{k_{on}}$$

Equation 1. K_d: equilibrium binding constant; k_{off}: dissociation rate constant; k_{on}: dissociation rate constant; L: ligand; R: receptor.

The concentration of the unbound ligand (L^*) determines the first reaction rate, while the concentration of the formed complex (L-R) defines the second reaction rate. At equilibrium, established by the dissociation constant (K_d), the concentrations of bound and unbound ligand remain the same. K_d is calculated as the ratio of the association rate constant (k_{on}) to the dissociation rate constant (k_{off}) and it is expressed in molar units (e.g., nanomolar nM or micromolar μM). A low K_d value indicates that the ligand occupies the target receptor at low concentrations, demonstrating high affinity.

Radioligand binding studies have few disadvantages, when compared with newly introduced techniques such as environmental concerns and radioactive waste disposal; but they remain the most prevalent technique for the robust determination of ligand affinity. The radioligand binding assays continue to be a widely used approach in this field. There are three major types of radioligand binding assays: saturation, kinetic, and competition binding assays. In these tests, the separation of bound from unbound ligands takes place at different times, depending on their specific applications. In a saturation analysis, separation occurs after the equilibrium state is reached, when the quantification of the formed complex is used to examine affinity. In contrast, in a kinetic assay, separation happens at various times during complex formation, thus the rate of reaching equilibrium becomes crucial. This allows the observation of association and dissociation constants (k_{on} and k_{off}), and thus the kinetics of the bimolecular reaction.[382]

In a saturation binding assay, the receptor is incubated with increasing concentrations of the ligand until all available membrane receptors are occupied, leaving no free binding sites. This point, known as saturation, is indicated by a plateau on the binding curve (See figure 23). The maximum number of receptors, that can be occupied by a specific ligand in the assay, is referred as B_{max}. Beyond this saturation point, further increases in ligand concentration do not result in more receptor-ligand complexes. Specific binding refers to the ligand bound to the biological target of interest. The assay is considered reliable if it achieves at least 70% specific binding over non-specific binding and excellent if it reaches 90% (signal/noise ratio).[382] Assays with less than 50% specific binding are not considered reliable.

However, the radiolabelled ligand might also interact non-specifically with other cell membrane structures and glass-fibre filters, which can interfere with the results. Although it was initially believed that non-specific binding is not saturable, this has been proven otherwise.[383] Non-specific binding is measured in presence of a high concentration of unlabelled ligand that occupies all receptors. In this scenario, the radioligand can only bind non-specifically to other cellular membrane components. The non-specific binding must be subtracted from the total binding to obtain the specific

binding. Fractional occupancy of receptors refers to the fraction of receptors that are occupied (bound to the ligand) out of the total number of receptors present, as it is depicted by the equation below.[384]

$$Fractional\ Occupancy = \frac{[L]}{[L] + K_d}$$

Equation 2. L: ligand; K_d: binding constant.

Traditionally, K_d and B_{max} values are obtained from the Scatchard plot[385] using linear regression. Nonetheless, this method is not longer used, due to its lack of accuracy and unreliable results. Linear regression assumes that the data are normally distributed and that the standard deviation is the same for every measurement, which is not the case. Nowadays, a more economical approach for obtaining K_d and B_{max} values is through competition binding assays. In these assays, also known as displacement assays, a constant concentration of labelled ligand is used, and increasing concentrations of unlabelled ligand are introduced to compete for the biological target. The IC_{50} value is calculated, which represents the concentration of unlabelled ligand that displaces 50% of the labelled radioligand (Figure 23). The inhibition constant (K_i) values are extracted from the IC_{50} value using the CHENG-PRUSOFF equation[386,387] (Equation 3). Data analysis is performed using non-linear regression with specific mathematical software (e.g., GraphPad).

$$K_i = \frac{IC_{50}}{1 + \frac{[L]}{K_d}}$$

Equation 3. Cheng-Prusoff equation. K_i: inhibition constant; IC_{50}: concentration of unlabelled ligand that displaces 50% of the labelled radioligand; L: Ligand; K_d: binding constant.

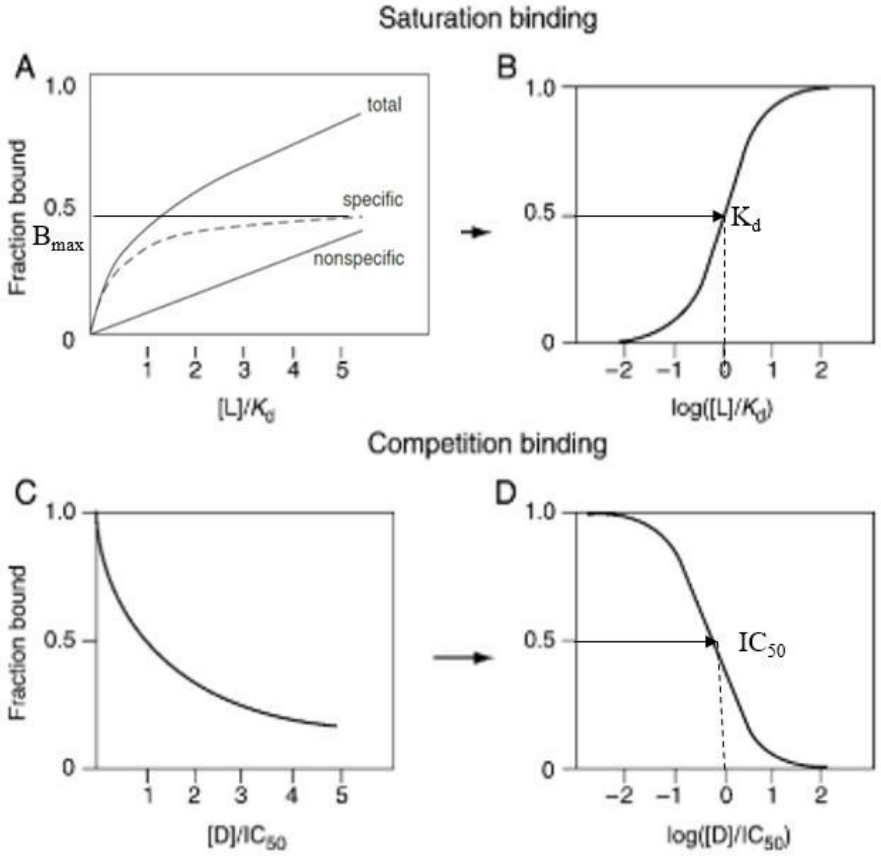

Figure 23. Saturation binding (**A** and **B**, above) and competition binding data (**C** and **D,** below), using different plotting methods. For **A** and **C,** the methods are not transformed, while for **B** and **D** semilogarithmic methods are evaluated. L: labeled ligand; D: unlabeled ligand, K_d: equilibrium binding constant of labeled ligand, B_{max}: maximal specific binding, IC_{50}: half-maximal binding concentration of test (unlabeled) ligand. Adapted from McKinney *et al.*[381]

Based on this theoretical background, all compounds synthetized in this project were tested at dopamine D_{2short} and D_3 receptors for their affinities. The affinity at human recombinant dopamine receptors was determined by incubation of test compounds, membrane preparations from CHO-K1 cells stably expressing D_{2S}, D_3 receptors and radioligand for 120 min. [^{3}H]spiperone was used as radioligand for D_{2S}/D_3 receptors and **haloperidol** was used as reference compound.[241,380] Bound radioligand was harvested through GF/B filters by washing three times with distilled water and measured using liquid scintillation counting. Nonspecific binding was determined using 10 μM Haloperidol. Obtained data from at least three independent experiments in triplicates were analysed with GraphPad Prism 7 using nonlinear regression (one site competition on logarithmic scale). Cheng‑Prusoff equation was used to transform IC_{50} to K_i values. Statistical analysis was performed on pK_i values and transformed into mean K_i values and corresponding 95% confidence intervals (CIs).

4.2 Drug-likeness analysis

Drug-likeness properties of selected final compounds was assessed by Data Warrior.[388] Drug-likeness refers to the desirable properties that a compound should have for being considered as potential drug candidate. These properties include good water solubility, no expression of potential toxic or mutagenic characteristics, optimal lipophilicity for BBB penetration (especially for CNS drugs). Having these favourable properties, it helps researchers to screen quickly large libraries of compounds in order to identify promising "hit" structures that have optimal properties for further drug development. In summary, drug-likeness analysis encompasses the ideal characteristics that enhance the chances of a molecule becoming a successful drug candidate.[389]

In the early 2000s, researchers at Pfizer Research Centre made a significant discovery. They noticed a correlation between a compound's physicochemical properties and its potential to become a viable drug candidate. Specifically, they found associations between parameters like permeability, solubility, and the likelihood of a molecule exhibiting drug-like characteristics. These observations led to the "Rule of 5" by Lipinski and colleagues. These rules proposed that a compound is more likely to become a promising drug candidate if it respects the following thresholds for specific molecular properties:

- Molecular weight lower than 500 or equal
- Maximum of five H-bond donors
- Maximum of ten H-bond acceptors
- Calculated logP (*c*LogP) lower than 5 or equal

The key idea behind the Rule of 5 is that compounds are less likely to be successfully developed into drugs if they do not follow these established guidelines. Therefore, the Rule of 5 provides a simple and effective tool to filter potential drug candidates early in the drug discovery process.[390,391]

While Lipinski's Rule of Five (Ro5) remains a widely accepted guideline in the pharmaceutical industry and academia for estimating oral bioavailability, it is crucial to assess its limitations. This rule serves as a valuable tool for understanding pharmacokinetic and pharmacodynamic profiles, simplifying the drug development pipeline by prioritizing promising drug-like candidates. However, it is important to acknowledge that Ro5 is not an absolute determinant. There are numerous marketed drugs that do not respect completely this rule, exhibiting higher molecular weights or increased lipophilicity, such as **bromocriptine**, **imatinib**, and **fosinopril**.[392–396] Theoretically, Ro5 applies to compounds that are not actively transported into cells, and it does not distinguish definitevely between

drug and non-drug candidates. Instead, it represents a statistical analysis-based guideline for identifying potential drug-like candidates.[397] The significance of Ro5 lies in its ability to inspire further exploration and refinement of the concept. Researchers have tailored the rule to specific drug subclasses, such as CNS drugs, by defining customized cut-off values. These efforts have led to the identification of additional parameters closely associated with CNS penetration and oral availability, expanding the understanding of drug-likeness beyond the original Rule of 5 framework. For example, further parameters that might be considered are the Polar Surface Area, the optimal *c*LogP that should be between 2 and 5,[389] the molecular weight should not be greater than 450,[398] or the aqueous solubility that should be 60 μg/ml for CNS drugs. The aqueous solubility is estimated as *c*LogS, a logarithm value of concentration measured in mol/L. Around 80% of marketed drugs have *c*LogS > -4.[352] Regarding polar surface area (PSA), this value represents the sum of all surfaces over polar atoms in the molecule, it needs to be under 140 Å for a drug to cross the intestinal membrane and to be absorbed.[399] Drugs with < 60 Å are entirely absorbed,[352] while compounds that exert their action in CNS should have PSA < 90 Å.[398]

In addition to evaluating various parameters that influence drug-likeness, Data Warrior assesses drug-likeness as a distinct parameter. This software compares the structures or fragments of compounds with those of commercially available drugs. By comparing these drugs with Fluka chemicals, which are considered non-drug-like, Data Warrior determines that approximately 80% of commercially available drugs have positive drug-like values. This indicates that these molecules contain fragments found in marketed drugs, while negative values suggest the opposite (Figure 24).[388] Although the Ro5 provides insights into the solubility and permeability of compounds, it does not address their potential toxic effects. To fill this gap, various programs have incorporated parameters to estimate the genotoxic, tumorigenic, or mutagenic potential of screened ligands. Specifically, Data Warrior compares the structures and fragments of compounds against a database of highly or potentially toxic substances to estimate any additional risk associated with the compound.[388]

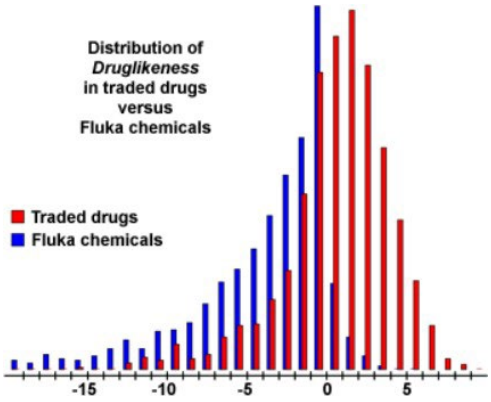

Figure 24. Distribution of commercially available drugs versus Fluka chemicals (non-drugs). Adapted by Sander et al.[388]

4.3 Sulphur-based dopamine D_2/D_3 receptor ligands

The development of highly potent ligands targeting the dopamine D_2/D_3 receptor subtypes holds significant importance for advancing our understanding of their role in various neurological disorders, such as Parkinson's disease, schizophrenia, and addiction. In this context, dopamine D_3 receptor has gained much more interest in the recent years, because its major location in limbic areas gives the opportunity to have possible antipsychotics devoid of side effects. However, the main obstacle lies in the high structural similarity among dopamine receptor subtypes, which has made the synthesis of highly selective D_3 receptor ligands a difficult task. Furthermore, even promising candidates have often failed in clinical trials due to unfavourable characteristics, including poor solubility, bioavailability, and drug-likeness. Indeed, designing and obtaining dopamine D_2/D_3 receptor ligands with potential selectivity on D_3 receptor requires a delicate balance of properties, such as appropriate lipophilicity for BBB penetration, adequate solubility to ensure disintegration, absorption, or bioavailability of orally administered drugs. Despite these challenges, no selective dopamine D_2/D_3 receptor ligand has yet reached the market, although several candidates are currently undergoing clinical trials for conditions like schizophrenia and addictive behaviours.

In this context, the development of **BP 897**, a high-affinity D_3 receptor partial agonist,[400] has provided encouragement and served as a catalyst for additional research efforts aimed at designing and developing novel D_2/D_3 receptor ligands with improved pharmacological properties. These medicinal chemistry efforts led to the achievement of crystal structures of the two receptors and even to a marketed drug that is **cariprazine**. It was approved for the treatment of schizophrenia and bipolar I disorder in adults by FDA in 2015, it acts as a partial agonist at dopamine D_2 and D_3 receptors, with a higher binding affinity for D_3 receptors reaching sub-nanomolar values. This latter characteristic is thought to contribute to the efficacy of **cariprazine,** in treating negative and cognitive symptoms of schizophrenia.[401]

Although **BP897** and **cariprazine** are distant in terms of development, they represent the most important milestones, together with **aripiprazole**, achieved in the treatment of psychotic disorders and development of dopamine D_2/D_3 ligands as antipsychotics. Therefore, **BP897** and **cariprazine** have been used as lead compounds for design, development and evaluation of the compounds synthetized in this project, especially the framework displayed by **BP897**, 1-(2-Methoxyphenyl)piperazine (**3)** served as PP for the entire library of compounds described here. In particular, sulphur-based ligands were obtained by introducing sulphur containing moieties as structural modifications at the western side of the scaffold. So, following the lead compounds and the

guidelines of *N*-phenylpiperazines-based pharmacophore model (Section 1.1.2), sulphide, sulfoxide and sulphone groups were examined at the place of arylamide moiety, linked to the 1-(2-Methoxyphenyl)piperazine by a butyl linker and cyclohexyl ring (e.g. **BP897** and **cariprazine**, see figure 25). Subsequently, the sulphur was evaluated in more rigid structure like heteroaromatic ring (thiazole moiety) and in special configuration such as sulfoximine, considered possible bioisostere of amides and sulphonamides, attached to a phenyl ring used as linker modification.

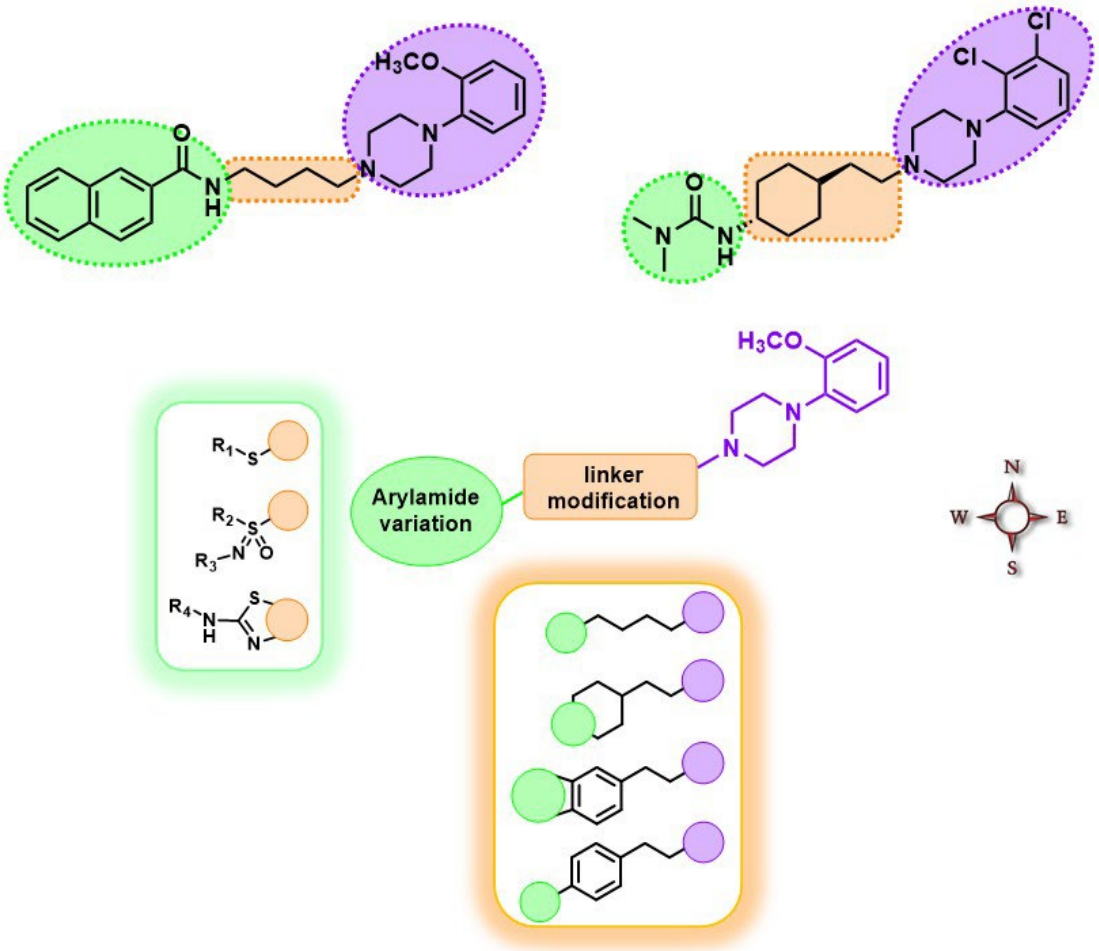

Figure 25. Design of sulphur-based dopamine D_2/D_3 ligands described in the project. The two lead compounds, **BP897** and c**ariprazine** are depicted above, while the blueprint with corresponding structural modifications is drawn below. The areas required by the pharmacophore model are marked in green for arylamide moiety (secondary pharmacophore), orange for apolar linker and lilla for *N*-phenylpiperazine (primary pharmacophore).

Sulphur-based dopamine D_2/D_3 ligands **4-6**, **12-16**, **22-26**, **30-31**, **34**, **36-37**, and **42** were in vitro examined in radioligand binding assay to determine affinities at receptors of interest (Tables 10 and 11). The ratio of receptor affinities K_i (D_2R) / K_i (D_3R) determines the selectivity index between the

two subtypes. Binding constants are given as mean values with a corresponding confidence interval (CI).

Table 10. Biological data of sulphur-based ligands **4-6** and **12-16**.

Compound	Structure	K_i D_2R(nM) (CI 95%)	K_i D_3R(nM) (CI 95%)	Ratio (D_2R/D_3R)[a]
Haloperidol	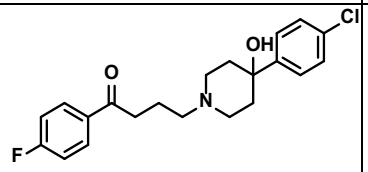	2.61 (2.02; 3.39)	13.5 (10.4; 17.4)	0.2
4	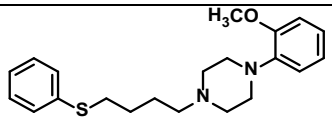	45.6 (31.4; 66.2)	73.6 (38.5; 141.0)	0.6
5	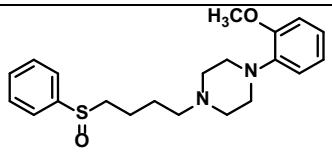	574 (165; 1999)	782 (307; 1994)	0.7
6	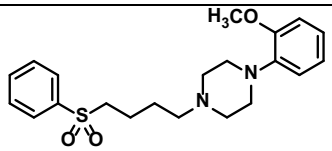	1571 (316; 7811)	4122 (1095; 15513)	0.4
12	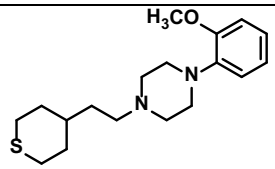	155 (51.0; 468)	340 (117; 983)	0.5
14	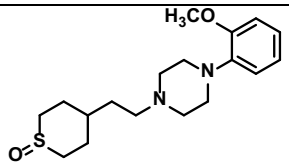	870 (625; 1211)	484 (254; 920)	2
16	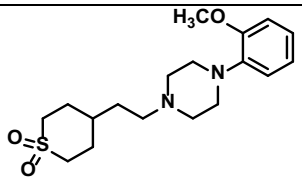	1614 (560; 4579)	2257 (691; 7372)	0.7

[a] Ratio K_i (D_2R)/ K_i (D_3R).

Table 11. Biological data of sulphur-based ligands **22-26**, **30-31**, **34**, **36-37** and **42**.

Compound	Structure	K_i D_2R(nM) (CI 95%)	K_i D_3R(nM) (CI 95%)	Ratio (D_2R/D_3R)[a]
Haloperidol	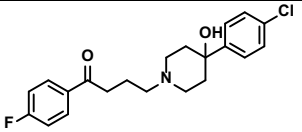	2.61 (2.02; 3.39)	13.5 (10.4; 17.4)	0.2
22	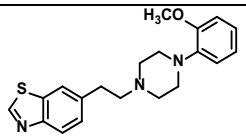	24.6 (23.9; 25.4)	31.4 (19.3; 51.1)	0.8
23	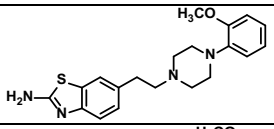	8.3 (5.9; 11.6)	45.4 (22.3; 92.7)	0.2
24	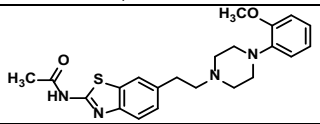	26.3 (14.8; 46.7)	14.4 (10.1; 20.6)	2
25	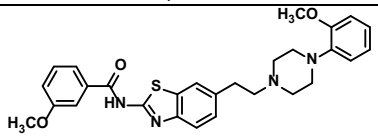	79.3 (38.5; 163.0)	10.7 (5.02; 22.9)	7
26	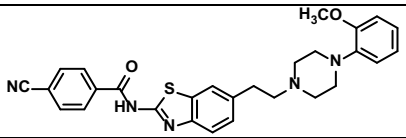	66.3 (61.5; 71.6)	22.8 (7.5; 69.4)	3
30	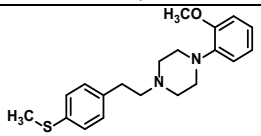	89.0 (48.7; 163.0)	86.9 (55.8; 135.0)	1
31	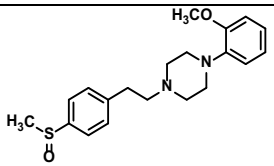	1215 (255; 5784)	1401 (895; 2192)	1
34	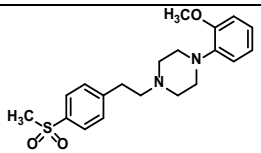	425 (149; 1211)	283 (123; 648)	2
36	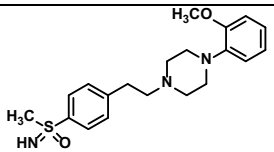	233 (81; 674)	321 (124; 833)	0.7
37	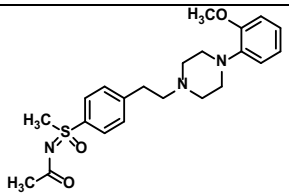	359 (252; 512)	82 (51; 131)	4
42	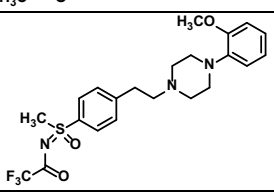	296 (163; 536)	323 (140; 749)	1

[a] Ratio K_i (D_2R)/ K_i (D_3R).

All the compounds belonging to the first set of ligands show affinity at both target receptors in nanomolar ranges. In this study, the driving force is the analysis of sulphur alongside the pharmacophore model, which means that different sulphur-based moieties and oxidations states of sulphur atom are evaluated here. The ligands **4-6** and **12,14,16, c**haracterized by classical cores such as butyl or cyclohexyl linkers, demonstrate that the more oxidized sulphur is, the worse affinity values are. Looking through table 10, it is observable that biological profiles are quite similar along these derivatives, **4** is the best compound and butyl linker is more suitable for carrying a sulphur atom within D_2 and D_3 receptors. However, it must be considered that butyl linker derivatives feature an aromatic ring that influences the receptor-ligand interaction positively. A high electron density is very beneficial in the western area that is supposed to bind the second binding pocket, based on the pharmacophore model, represented in figure 25.

Comparing derivatives **22-26, 30-31, 34, 36-37** and **42** , it appears clearly that *2*-aminothiazole is working better than sulfoximine as potential bioisostere of arylamide function. This trend is confirmed also when these sulphur-based moieties are considered as prolongation of the aromatic spacer, because *N*-substituted derivatives **24-26** show more interesting values than **37,42** either in terms of affinity or in terms of ratio towards D_3 receptor. It is reasonable thinking that *2*-aminothiazole is improving the ability of aromatic spacer to have an extended and linear conformation that is optimal for binding D_2 and D_3 receptors, as well as the greater lipophilicity of an heteroaromatic ring might enhance the affinity towards both target receptors.

Among the sulphur-based ligands described, benzo-aminothiazole derivatives **22-26** have the most interesting pharmacological profiles; their innovative structure gives a further option to develop a new category of dopamine D_2/D_3 ligands. Within this small set of compounds, derivative **23** bears the highest affinity value on D_2 receptor while **25** is the best ligand for D_3, proving once more that the presence of amide as *N*-substituting group is a perfect fit to binding D_3 receptor rather than D_2. Indeed, product **25** shows the highest ratio between the two receptor subtypes. The presence of a second aromatic ring seems not to be a problem in terms of binding properties: **25** and **26** have slightly better values at D_3R than **23**, meaning that an aryl amide works well with heteroaromatic linker such as aminothiazole fused with benzene. Additionally, EDG such as -OCH_3 may be a better function than EWG like -CN (**25**, **26**). However, it would have been interesting to perform position alterations but they were not conducted within this small series.

Looking at the results obtained by sulphur-based ligands bearing a phenylethyl spacer (**30-31**, **34**, **36-37**, **42**), derivative **30** has the best pharmacological profile, meaning that an electron rich and highly lipophilic sulphur-based function on western side of molecule might be the most effective within the binding pockets. Indeed, replacement of sulphide with sulfoxide and sulphone has worsened the

binding affinities of the oxidized derivatives **31** and **34**. Interestingly, the introduction of a H-bond donor/acceptor like NH does not bring any advantages to affinity values, because **36** has similar nanomolar range of its isoelectronic analogous **34**. Free *NH*-sulfoximine (**36**) seems to be more suitable for D_2 rather than D_3, whereas *N*-substituted one (**37**) shows increased affinity at D_3 receptor with one-digit number of difference and improved ratio towards D_3 over D_2. On the other hand, the latter characteristics disappear completely due to the substitution of CH_3 function with CF_3 (**42**), thus going back to a D_2-preference behaviour like **36**. To conclude, the study on sulphur-based dopamine D_2/D_3 ligands shed light on the possibility of using moieties with sulphur as heteroatom at the place of the arylamide function. According to the results, the sulphur centre should be within in a rigid and planar structure (derivatives **22-26**) or attached to a phenyl ring like in the sulphur/sulfoximine ligands (**30-31**, **34**, **36-37**, **42**). Additionally, the results show that sulphur can be part of the apolar linker, only if it is in the configuration of sulphide (see derivatives **4-6**).

However, the most interesting results have been achieved with sulphur-based units combined with heteroaromatic and aromatic linker, which cover for the lipophilicity expected in the arylamide area. In this configuration, the secondary pharmacophore has a broader number of substitution and thus the opportunity of obtaining potential novel dopamine D_2/D_3 ligands increases. Indeed, compounds **22-26**, **30-31**,**34**,**36-37** and **42** were chosen as lead structures for additional investigations on the developed aromatic linker with opportune variations. Therefore, these derivatives were further examined to estimate their drug-likeness properties and the ones of the phenyl spacer. The data and results of the assessment performed by using Data Warrior are listed in table 12.

Table 12. Drug-likeness properties of compounds **22-26**, **30-31**, **34**, **36-37**, **42**.

Cpd[a]	MW	*c*LogP	*c*LogS	H-bond Acceptor	H-bond donor	PSA[b]	Ro5 violations	Drug-likeness	Mut.[c]	Tum.[d]
22	353.49	3.170	-2.901	4	0	56.84	0	7.270	No	Yes
23	368.50	3.341	-3.717	5	1	82.86	0	7.164	No	No
24	410.54	3.722	-3.983	6	1	85.94	0	7.740	No	No
25	502.64	5.096	-5.171	7	1	95.17	1	7.970	No	No
26	497.62	5.002	-5.926	7	1	109.73	0	3.690	No	No
30	342.51	3.693	-3.522	3	0	41.01	0	7.107	No	No
31	358.50	2.722	-2.265	4	0	51.99	0	7.021	No	No
34	374.50	2.220	-3.091	5	0	58.23	0	9.025	No	No
36	373.52	2.744	-3.287	5	1	65.01	0	8.773	No	No
37	415.56	2.520	-3.322	6	0	70.59	0	8.908	No	No
42	469.53	3.004	-4.062	6	0	70.59	0	-18.220	No	No

[a]: Compound; [b] Polar Surface Area; [c] Mutagenic properties; [d] Tumorigenic properties.

All compounds, except **22**, do not show any potential of mutagenic and tumorigenic properties. Comparing the structures, the deaminated thiazole ring (**22**) might be the trigger of some tumorigenic biochemical cascades, this can be seen as reason to investigate for more variations in that position. All compounds show values of polar surface area below 140 square Å, which means that they have a high grade of cell permeability. Nevertheless, to have an optimal BBB permeability, the PSA value should be lower than 60 square Å,[402] which is observable only for derivatives **22**,**30**,**31** and **34**. Therefore, molecules **23-26**, **36-37** and **42** might have problems to act on dopamine D_2 and D_3 receptors in CNS, but these compounds show positive drug-likeness score, except molecules **26** and **42** that present a low and negative scores respectively. In this set of ligands, only **25** is violating one Lipinski rule (MW > 500) and the *c*LogP can be considered equal to 5, which is not a real violation as well as for compound **26**. However, as already mentioned in section 4.2, the Lipinski rule of 5 is more a guideline for rational design rather than an exclusive determinant. Ultimately, from a general viewpoint the sulphur-based ligands **26** and **42** might not be seen as potential candidates for further biological evaluation due to very high PSA and low drug-likeness score for **26**, or negative score for **42**.

In conclusion, all 17 sulphur-based ligands proved to have promising affinity values at both D_2 and D_3 receptors, demonstrating that a not oxidized sulphur containing function is well tolerated. The replacement of the classical linkers (e.g., butyl chain and cyclohexyl ring) with aromatic spacers optimize the pharmacological profiles of the ligands in terms of affinity at both target receptors, showing even preference behaviours. Therefore, the sulphur-based ligands bearing the aromatic linker were taken as lead compounds to expand the study on this type of spacer, as demonstrated in the next set of molecules synthetized in this PhD project.

4.4 Dopamine D_2/D_3 receptor ligands with aromatic linker variations

The results obtained by the sulphur ligands with an aromatic linker prompted a further investigation performed with the second set of ligands. It has been achieved that a benzyl ring can be an innovative alternative to the classic spacers in the last decades. Therefore, a deeper study was necessary. In addition, a previous replacement of butyl chain proved to be beneficial, resulting in the development of clinical candidates such as **SB277011A** or **SB26952** or a marketed drug like **cariprazine.** The 1,4-

disubstituted cyclohexyl unit, used as a linker, is a conformation restriction that was applied as hit-to-lead optimization (Figure 26).

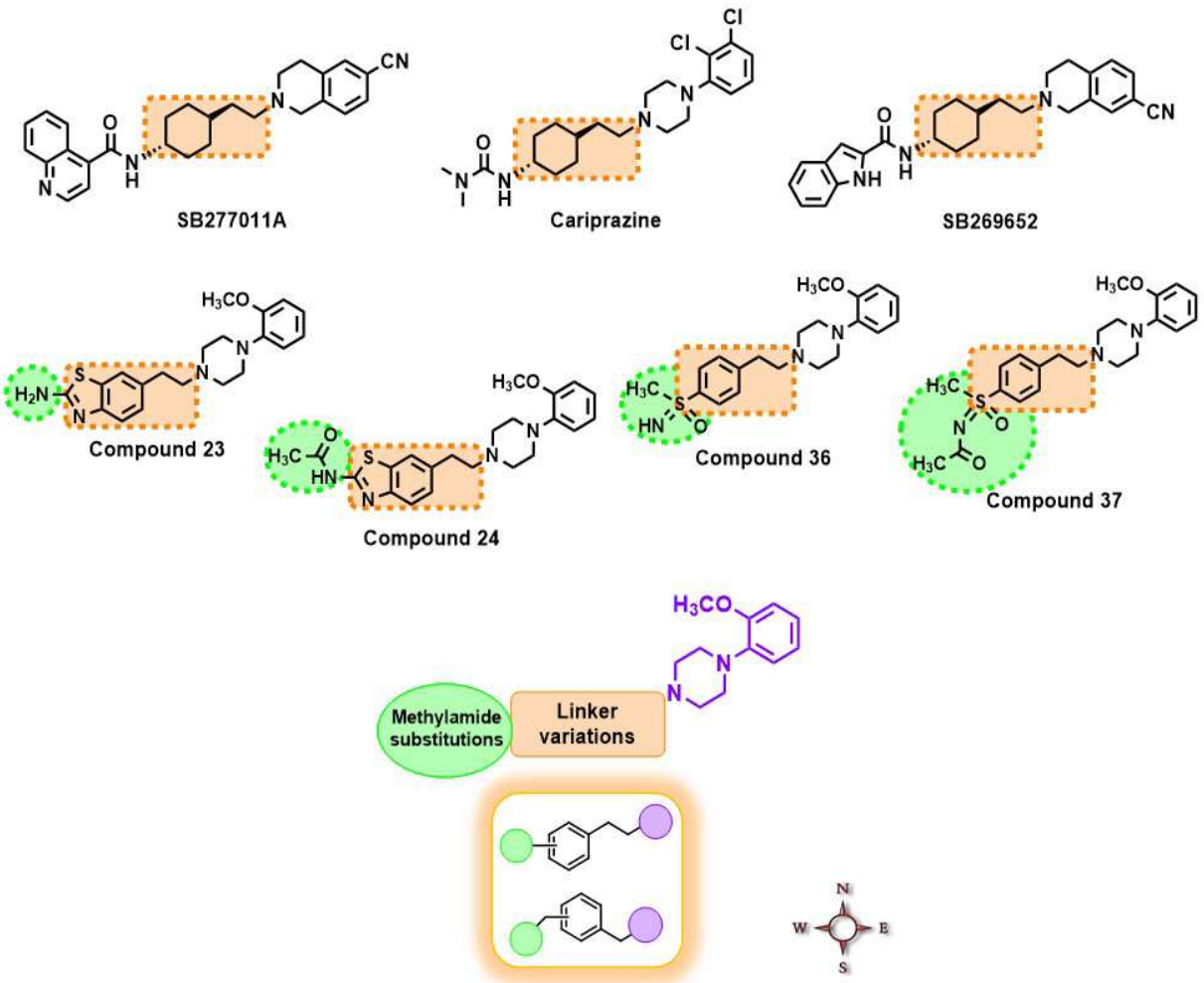

Figure 26. Reference compounds that served as inspiration for the evaluation of aromatic linker. The blueprint with the related linker variations is shown below. The compounds shown above are the clinical candidates and marketed drug **SB277011A**, **SB269652**, **cariprazine**. In the second row the sulphur-based ligands (**22-23** and **36-37**) are depicted, whose results were the driving force of the study described here.

Inspired by this type of optimization and driven by the previous results of sulphur-based ligands, the evaluation on the developed aromatic linker was performed with a set of conformationally restricted 1-(2-methoxyphenyl) piperazine derivatives, whereby piperazine **3** is used as PP, methylamide is used as H-bond donor/acceptor function (SP) connected by the aromatic linker used for derivatives **30-31**, **34**, **36-37** and **42**. To have a better overview on this alternative spacer, a second variation of the benzyl ring was added: phenylmethyl (Figure 26). For each variation (phenylethyl and phenylmethyl), the substitution patterns in *ortho*, *meta* and *para* positions are considered in order to analyse which conformation is respecting the linearity concept of butyl chain and the cyclohexyl ring. Moreover,

further variations of the methylamide group are added by using nitro or cyano as EWG, aniline, methanamine and acetanilide as EDG in different positions, thanks to the changeable western end position of developed aromatic linkers.

Dopamine D_2/D_3 ligands with aromatic linker variations **45-50, 53-55** and **59-67** were in vitro examined in radioligand binding assay to determine affinities at receptors of interest. The results of phenylethyl linker derivatives are listed in table 13, while the binding data of phenylmethyl linker derivatives are grouped in table 14. The ratio of receptor affinities K_i (D_2R) / K_i (D_3R) determines the selectivity index between the two subtypes. Binding constants are given as mean values with a corresponding confidence interval (CI).

Table 13. Binding affinity values of dopamine D2/D3 receptor ligands with phenylethyl linker **45-50** and **53-55**.

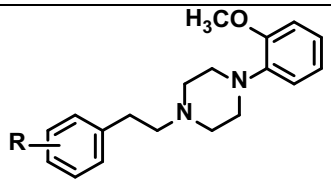

Compound	R	K_i D_2R(nM) (CI 95%)	K_i D_3R(nM) (CI 95%)	Ratio (D_2R/D_3R)[a]
Haloperidol	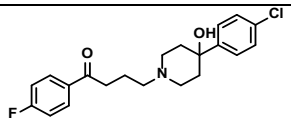	2.61 (2.02; 3.39)	13.5 (10.4; 17.4)	0.2
45	*2*-NO_2	221 (24; 2044)	294 (142; 609)	1
46	*3*-NO_2	365 (67; 2000)	239 (83; 693)	2
53	*4*-NO_2	206 (55; 768)	160 (79; 325)	1
47	*2*-NH_2	236 (95; 588)	434 (106; 1781)	0.5
48	*3*-NH_2	219 (53; 913)	195 (65; 584)	1
54	*4*-NH_2	75.6 (34.3; 167.0)	106 (51.5; 219)	0.7
49	*2*-(H_3CCONH-)	498 (330; 750)	1179 (621; 2237)	0.4
50	*3*-(H_3CCONH-)	193 (88; 424)	201 (153; 263)	1
55	*4*-(H_3CCONH-)	14.9 (5.9; 37.4)	9.2 (4.1; 20.7)	2

[a] Ratio K_i (D_2R)/ K_i (D_3R).

Table 14. Binding affinity values of dopamine D_2/D_3 receptor ligands with phenylmethyl linker **59-67**

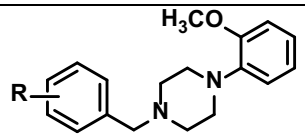

Compound	R	K_i D_2R (nM) (CI 95%)	K_i D_3R (nM) (CI 95%)	Ratio (D_2R/D_3R)[a]
Haloperidol	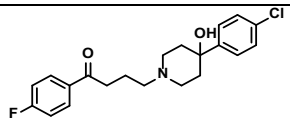	2.61 (2.02; 3.39)	13.5 (10.4; 17.4)	0.2
59	*2*-CN	1453 (542; 3898)	9498 (3968; 22732)	0.2
60	*3*-CN	498 (165; 1499)	2030 (1241; 3322)	0.2
61	*4*-CN	580 (143; 2353)	1711 (119; 2459)	0.2
62	*2*-(H_2N-CH_2-)	7003 (3558; 13782)	35795 (24359; 52600)	0.3
63	*3*-(H_2N-CH_2-)	1135 (465; 2771)	2402 (1674; 3445)	0.2
64	*4*-(H_2N-CH_2-)	774 (347; 1725)	627 (321; 1223)	0.5
65	*2*-(H_3CCONH-CH_2-)	126 (62.1; 254)	415 (179; 965)	1
66	*3*-(H_3CCONH-CH_2-)	413 (246; 695)	889 (315; 2511)	0.3
67	*4*-(H_3CCONH-CH_2-)	324 (101; 1042)	205 (66; 638)	0.5

[a] Ratio K_i (D_2R)/ K_i (D_3R).

All compounds (**45-50**, **53-55** and **59-67**) show modest to low nanomolar affinity values on both receptors. Comparing the two linkers evaluated in this study, it is clear that phenylethyl spacer is providing higher binding properties than the phenylmethyl one. The amide derivatives **50**,**55** and **59-67** demonstrate to have better binding properties than the corresponding precursors and intermediates. It is not the case for the final product **49,** because **45** and **47** showed better affinity values than the amide analogous. If the positions of the amide group are considered (*ortho*, *meta*, *para*), a progressive increase of the affinity values towards both receptors is observed. Notably, the *para* derivatives **55**

and **67** show a slight preference for D_3 over D_2, thus the phenylethyl linker with *4*-substituent on the aromatic ring is fully respecting the key points of the pharmacophore model: linearity and extension (See section 1.1.2). In contrast, a bent conformation represented by *ortho* and *meta* substitutions provides a slight preference towards dopamine D_2 over D_3 and, as a consequence, the derivatives **49-50** and **62-63** feature a different pharmacological profile when compared with the one of *para* isomers.

Concerning electron density, it is tenable assessing that:

1) the presence of EWG as nitro or cyano at the place of EDG as amide, aniline or methanamine decreases the affinity at both target receptors.
2) the amide unit is working better than aniline or methanamine function as electron-donating group in terms of binding properties.

The difference of affinity values between the synthetized ligands depends on structural conformation and H-bond/acceptor properties of the amide group, but manipulation of electron density is a further factor that may play an important role in binding the secondary pocket of D_2 and D_3 receptors. For instance, compound **55** presents a pharmacological profile 100-fold better than **53**, this optimization rate is not found in **54** even though it has an electron-donating group like **55**. The latter aspect is also evident for the phenylmethyl linker derivatives (Table 14), whereby intermediates **62-64** have worse K_i values than corresponding precursors **59-61** and methylamide ligands (**65-67**) have the best profiles. Regarding the phenylethyl ligands, a different situation is observed for **45**, **47** and **49**, in which the precursor shows better binding properties. Particularly for **49**, the reasons could be the bent conformation and the steric hindrance, because the values between **45** and **47** are comparable. However, the pharmacological behavior with positive trend through the replacement of EWG with EDG is found again for **46**, **48** and **50** albeit with little intensity.

Compound **55** is the most promising of this set of compounds with low nanomolar affinity at both receptors (D_2R K_i = 14.9 nM, D_3R K_i = 9.2 nM). The structure of **55** proves that *para*-substitution with phenylethyl linker is a suitable orientation for binding the target receptors. The innovation of aromatic spacers is the inclusion of a phenyl ring in the linker itself and not in the carbonyl function, as it is represented in the pharmacophore model. In this sense, the area of the ligand, where the acyl function is supposed to be, becomes a possibility of infinite modifications that allow to investigate deeply the second binding pocket of D_2 and D_3 receptors. Therefore, derivative **55** has been used as a reference structure for further SAR studies in the final part of the PhD project. Due to this, compound **55** was examined to estimate drug-likeness properties together with its precursors (**53-55**)

and their phenylmethyl analogues (**61**, **64**, **67**) to have a proper overview. The data obtained by using Data Warrior are listed in table 15.

Table 15. Drug-likeness analysis of phenylethyl linker derivatives **53-55** and phenylmethyl linker derivatives **61**, **64**, **67**.

Cpd[a]	MW	*c*LogP	*c*LogS	H-bond Acceptor	H-bond donor	PSA[b]	Ro5 violations	Drug-likeness	Mut.[c]	Tum.[d]
53	341.41	2.295	-3.134	5	0	61.53	0	1.930	No	No
54	311.43	2.540	-2.750	4	1	41.73	0	7.093	No	No
55	353.46	2.920	-3.016	5	1	44.81	0	7.524	No	No
61	307.40	2.622	-3.335	4	0	39.50	0	1.299	No	No
64	311.43	1.791	-2.522	4	1	41.73	0	5.241	No	No
67	353.46	2.199	-2.720	5	1	44.81	0	6.601	No	No

[a]: Compound; [b] Polar Surface Area; [c] Mutagenic properties; [d] Tumorigenic properties.

All the analysed compounds (**53-55**, **61**, **64**, **67**) do not show any potential of mutagenic and tumorigenic properties. The *p*-nitro-phenylethyl linker derivative (**53**) and p-cyano-phenylmethyl linker derivative (**61**) show low drug-likeness scores. Considering that the other parameters are within the acceptable values, the reason could be connected to the presence of EWG like nitro and cyano. Particularly for compound **53**, the polar surface area value is slightly above the optimal value of 60 square Å, therefore the difficulty of going through BBB induces an inefficient drug-likeness profile. None of compounds violate the Lipinski´s rule of 5.

Among the dopamine D_2/D_3 ligands **54-55**, **64** and **67**, the obtained data are quite similar to each other compound. For example, the PSA parameters are exactly the same (**54** and **64**, **55** and **67**) as well as the values of *c*LogP and *c*LogS are comparable. Nevertheless, **54** shows higher lipophilicity than the phenylmethyl analogous (**64**) and thus a better drug-likeness profile, indicating that aromatic amine is more promising than aliphatic one. Molecule **55** demonstrated to be the best ligand in the drug-likeness estimation, having the highest score. Based on these data combined with the binding affinities at D_2 and D_3 receptors, derivative **55** represents a highly promising drug candidate, therefore it was further analysed with marketed drugs such as **haloperidol** and **cariprazine** to predict ADMET properties, which are grouped in table 16.

The ADMET properties of **55**, **haloperidol** and **cariprazine** have been evaluated through the pkCSM online tool.[403] Concerning the ADMET *in silico* prediction, some key features have been estimated and compared with the ones showed by the marketed drugs. It is possible to see that *para*-acetamide derivative features a very similar profile to reference compounds. Indeed, **55** shows slightly better

intestinal absorption and comparable distribution values, confirming that compound **55** has an elevate grade of absorption by passive diffusion. The satisfactory value of BBB permeability indicates that the most promising anilide can be a suitable tool for mental disorders, which requires physicochemical parameters that are in line with marketed drugs **haloperidol** and **cariprazine**. The target derivative is supposed to be a substrate of CYP2D6 and CYP3A4 that are the two main isoforms of cytochrome P450 responsible for drug metabolism. Nevertheless, *in silico* predictions assess that **55** is likely going to be cytochrome P450 inhibitor (CYP1A2, CYP2D6 and CYP3A4), which is observable also in the drugs with the difference that **haloperidol** is inhibiting CYP2D6 and CYP3A4 while **cariprazine** only CYP2D6. One main difference is related to toxicity data, showing that **55** may have mutagenic characteristics due to the positiveness of AMES toxicity test, which is in contrast to the data obtained from Data Warrior assessment, so further evaluations might be necessary to clarify this point. In addition, according to the pkCSM online evaluation, *p*-acetamide phenylethyl linker derivative could lead to long QT syndrome-fatal ventricular arrhythmia. Ultimately, lead derivative **55** has promising ADMET profile that can be easily compared with the ones of **haloperidol** and **cariprazine**, but inconvenient parameters relatively to toxicity have to be evaluated in order to improve it with structural modifications.

Table 16. In silico ADMET prediction for compound **55** and reference compounds.

Cpd	Absorption		Distribution		Metabolism							Excretion	Toxicity
	Intestinal absorption in humans (% absorbed) [a]	Caco2 permeability (log Papp in 10^{-6} cm/s)	VDss (human) (log L/Kg) [b]	BBB permeability (logBB) [c]	Cyp substrate		Cyp inhibitor					Total clearance (log ml/min/kg)	AMES toxicity
					2D6	3A4	1A2	2C19	2C9	2D6	3A4		
Haloperidol	89.6	0.9	1.4	0.1	Yes	Yes	No	No	No	Yes	Yes	1.1	No
Cariprazine	87.2	1.0	0.9	0.2	Yes	Yes	No	No	No	Yes	No	0.6	No
55	90.2	0.9	1.1	0.2	Yes	Yes	Yes	No	No	Yes	Yes	0.9	Yes

[a] Intestinal absorbance value < 30%: poor soluble; [b] Volume of Distribution (VDss): log VDss < -0.15 is low and log VDss > 0.45 is high. [c] log BB < -1: poorly distributed in the brain. Results obtained by using the pkCSM online tool available at https://biosig.lab.uq.edu.au/pkcsm/

To summarize, all 18 ligands with aromatic linker variations showed interesting affinity values on both D_2 and D_3 receptors. Most of the compounds revealed a slight preference towards D_2 over D_3 (**45**, **47**, **49-50**, **54**, **59-63**, **65-66**), whereas **46, 48, 53, 55, 64** and **67** showed major tendency at D_3 over D_2. Compound **55** resulted to be the best pharmacological profile with the highest biding properties at both receptors. SAR evaluation demonstrated that linear and extended conformation of dopamine D_2 and D_3 ligands can be successfully represented by the linkers proposed: phenylmethyl and phenylethyl. In particular, the second spacer can be considered a promising alternative to the

widely used chain of four carbon atoms and the cyclohexyl-ethyl linker.[19,404] Furthermore, EDG in combination with phenylethyl linker leads to higher affinity than EWG, especially if EDG is represented by an amide unit.

Considering the results obtained by this set of ligands, compound **55** was believed to represent a starting point for further development of selective dopamine D_2 and D_3 ligands. That was the reason why, it has been chosen as lead compound for additional investigations of different residues to search for dopamine D_2/D_3 ligands with optimized pharmacological profiles.

4.5 Substituted-anilino-ethyl linker-based dopamine D_2/D_3 ligands

The conclusive phase of the PhD project focused on the application of several structural motifs to the developed scaffold, represented by 4-aniline-ethyl linker combined with 1-(2-methoxyphenyl)piperazine. Compounds **54** and **55**, that feature this scaffold, achieved interesting binding profiles at D_2 and D_3 receptors as well as promising physicochemical properties. Thereby, **55** was taken as lead structure while **54** was used as substrate for the entire library.On the basis of the pharmacophore model of substituted *N*-phenylpiperazine based ligands (Section 1.1.2), amides and ureas were added to the substrate, following the requirement of a H-bond donor/acceptor group, necessary for the interaction with the second binding site (See figure below).

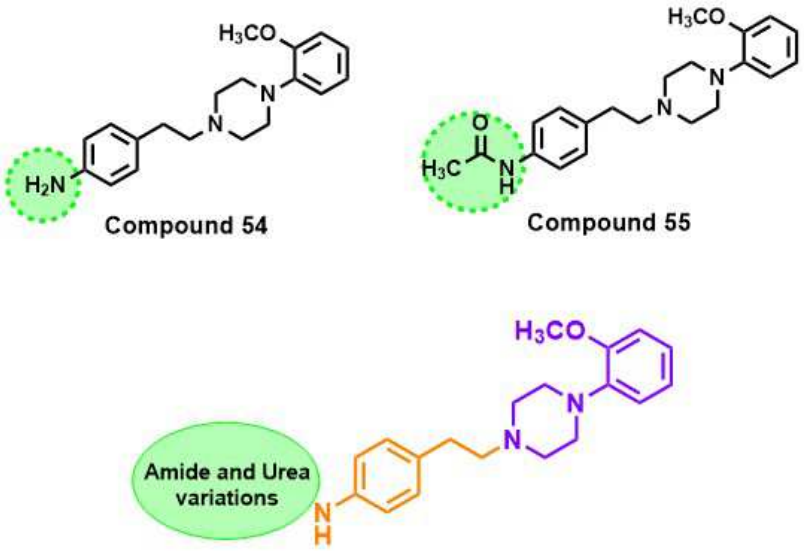

Figure 27. General blueprint of amide- and urea-containing ligands with the corresponding reference structures shown above.

The amide and urea derivatives show different modifications, attached to the acyl function, such as alkyl, cycloalkyl, aryl, heteroaryl or biphenyl moieties. The purpose was testing and evaluating whether manipulation of size, molecular weight, electron density, hydrophilicity in combination with the developed scaffold might influence the binding profile at D_2 and D_3 receptors´ sites. In the same time, the versatility and utility of the core 4-aniline-ethyl linker was examined as well, thanks to the free NH_2 which gave a wide range of structural opportunities.

A large library of 58 acylated-anilino-ethyl derivatives was examined *in vitro* with radioligand binding assays to determine affinities at receptors of interest. The ratio of receptor affinities K_i (D_2) / K_i (D_3) determines the selectivity index between the two subtypes. Binding constants are given as mean values with a corresponding confidence interval (CI). The results of these dopamine D_2/D_3 ligands are listed in different tables, depending on the type of modification that was inserted to the privileged scaffold. The pharmacological results of amide derivatives with aliphatic modification are presented in table 17. The aliphatic modification consists of acyl-like function elongation by inserting one, two or three more carbon atoms and the application of cyclic substitution patterns.

Table 17. Pharmacological data of ligands **69-79**, that bear an aliphatic modification.

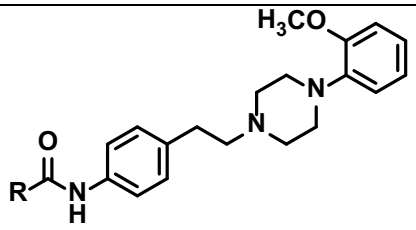

Cpd [a]	R	K_i D_2R (nM) (CI 95%)	K_i D_3R(nM) (CI 95%)	Ratio (D_2R/D_3R)[b]	Cpd [a]	R	K_i D_2R(nM) (CI 95%)	K_i D_3R(nM) (CI 95%)	Ratio (D_2R/D_3R)[b]
69	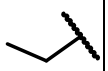	47.7 (19.3; 118.0)	22.3 (12.3; 40.3)	2	**75**	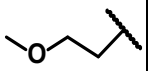	52 (16; 168)	20.6 (9.0; 46.9)	3
70	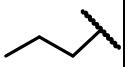	34.4 (14.2; 83.6)	19.2 (7.8; 47.5)	2	**76**	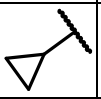	17.4 (16.2; 18.8)	27.6 (7.9; 96.6)	0.6
71	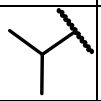	49.1 (15.5; 155.0)	25.1 (14.3; 44.1)	2	**77**	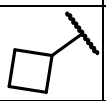	34.8 (17.8; 68.1)	23.3 (14.9; 36.4)	2
72	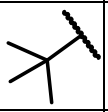	65.7 (30.8; 140.0)	69.1 (38.8; 123.0)	1	**78**	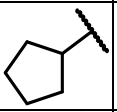	26 (6; 106)	11.3 (2.9; 43.8)	2
73	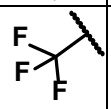	33.8 (18.1; 63.2)	69.3 (48.8; 98.3)	0.5	**79**	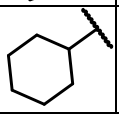	24.0 (12.4; 46.6)	15.5 (14.8; 16.2)	2
74	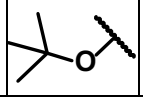	17.8 (13.2; 24.2)	39.8 (17.8; 89.0)	0.5	-	-	-	-	-

[a] Cpd, Compound; [b] Ratio K_i (D_2R)/ K_i (D_3R).

All the amides with aliphatic substitution present values in the nanomolar range at both dopamine D_2 and D_3 receptors, indicating that amide function with aliphatic moieties is working well with the scaffold 4-aniline-ethyl linker. The ligands **69-79** show comparable pharmacological profiles and very similar ratio within the two receptor subtypes.

However, elongating the acyl function by inserting more carbon atoms or even heteroatoms seems to be beneficial for the D_3 binding site, because compounds **69-72** and **75** feature a slight preference towards D_3 over D_2; indeed, **75** shows the highest ratio among the ligands described here. On the other hand, increasing the size of carbonyl group with bulkier substituents is optimal for D_2 binding site, because derivatives **73** and **74** have a major tendency at D_2 receptor albeit with little intensity. This is not true for the amides that have an aliphatic cyclic substitution pattern; within **76-79**, a rise in the size of the ring leads to higher affinities at D_3 receptor rather than D_2.

Table 18. Pharmacological data of urea-containing ligands **80-88** with aliphatic and aromatic variations.

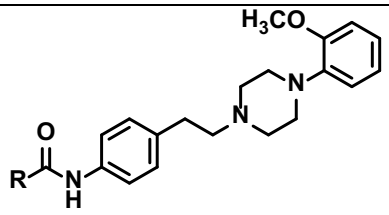

Cpd [a]	R	K_i D_2R(nM) (CI 95%)	K_i D_3R(nM) (CI 95%)	Ratio (D_2R/D_3R)[b]	Cpd [a]	R	K_i D_2R(nM) (CI 95%)	K_i D_3R(nM) (CI 95%)	Ratio (D_2R/D_3R)[b]
80	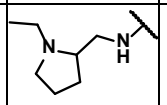	4.86 (3.35; 7.06)	24.1 (12.9; 44.7)	0.2	**85**	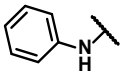	5.7 (1.4; 23.6)	5.6 (3.9; 8.0)	1
81		18.7 (4.6; 76.2)	31.8 (8.4; 120.0)	0.6	**86**	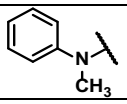	256 (136; 482)	340 (303; 381)	0.8
82		22.8 (7.9; 66.2)	72.5 (24.8-212.0)	0.3	**87**	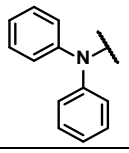	454 (214; 854)	560 (230; 1461)	0.8
83	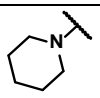	22.6 (11.1; 46.1)	67.4 (22.2; 204.5)	0.3	**88**	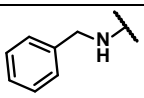	18.2 (8.2; 40.7)	7.7 (4.8; 12.6)	2
84	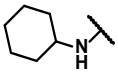	6.95 (6.05; 7.99)	12.6 (10.4; 15.3)	0.6	-	-	-	-	-

[a] Cpd, Compound; [b] Ratio K_i (D_2R)/ K_i (D_3R).

Alongside these compounds and corresponding results, aliphatic moieties with cyclic substitution patterns were applied to urea bond, that is more hydrophilic than amide. Additionally, aromatic rings were added to check whether a further phenyl ring might have an impact on a binding mode of the

entire molecule. The results of *in vitro* evaluation of urea-containing derivatives are listed in table below.

The urea-containing ligands with aliphatic modification (**80-84**) present similar binding affinity values to the amide analogues (**69-79**); same situation has been found for the ureas with aromatic variation, except ligands **86** and **87** that have pharmacological values up to three-digit numbers. Overall, all the urea derivatives demonstrate to have nanomolar range values.

The ligand **80**, that supports the ethyl-pyrrolidine fragment of **sulpiride** and **amisulpride**, presents low nanomolar affinity values preferentially at D_2 receptor. As already mentioned in section 3.3, the structures of these two drugs inspired some structural modifications. Notably, the chosen drugs have a selectivity towards D_3 receptor, but ethyl-pyrrolidine fragment in combination with 4-aniline-ethyl linker is more affine at D_2. The two marketed drugs have been chosen because they are important antipsychotics, widely used in treatment of schizophrenia due to their antagonist activity at the receptors of interest.

Along the lines of derivative **80**, compounds **81-84** show binding properties preferentially at D_2 receptor rather than D_3 as well. However, products **84** and **80** have better pharmacological profiles than the other ones (**81-83**), indicating that a double substitution or a structural rigidity on the second nitrogen atom of urea is less beneficial than the free NH for D_2 binding site. Thereby, a second H-bond donor group seems to be optimal in that side of the molecule. This is a detail that can be found across the ureas with aromatic modification too. Indeed, compounds **85** and **88**, having a second NH, are more affine than **86** and **87**, that have a double substituted nitrogen atom. Conversely, **85** does not show any preference of receptor, while **88** presents a major tendency towards D_3 receptor over D_2.

Considering the results obtained by ligands **85** and **88**, an additional aromatic ring in the general scaffold of 4-aniline-ethyl linker does not create any problems, but instead it could be optimal for binding the D_3 receptor. On the other hand, the insertion of a fourth phenyl ring, as it is shown by **87**, leads to a worsening of affinity values at the target receptors. Since an aromatic modification with urea bond worked very well from a pharmacological viewpoint, a further phenyl ring with several and different substitution pathways was applied to an amide bond, as it is depicted by the following synthetized dopamine D_2/D_3 ligands **89-126**.

To conclude, the amides with aliphatic variations (**69-79**) and the ureas with aliphatic or aromatic modifications (**80-88**) have nanomolar affinity values at D_2 and D_3 receptors, whereby the amide-containing derivatives have a major tendency towards D_3, whilst the urea-containing ligands towards D_2. The pharmacological examination of these ligands proves once more the versatility and utility of the privileged scaffold developed in this project. Therefore, all compounds were further examined to

estimate the physicochemical properties and the drug-likeness scores by using the assessment program Data Warrior, as performed for the other ligands. The results are listed in table 19.

Table 19. Drug-likeness and physicochemical parameters of substituted-anilino-ethyl linker derivatives with aliphatic amide and urea variations **69-88**.

Cpd[a]	MW	*c*LogP	*c*LogS	H-bond Acceptor	H-bond donor	PSA[b]	Ro5 violations	Drug-likeness	Mut.[c]	Tum.[d]
69	367.49	3.374	-3.286	5	1	44.81	0	8.273	No	No
70	381.52	3.829	-3.556	5	1	44.81	0	5.467	No	No
71	381.52	3.593	-3.446	5	1	44.81	0	7.376	No	No
72	395.56	4.158	-3.623	5	1	44.81	0	3.460	No	No
73	407.44	3.404	-3.756	5	1	44.81	0	-19.59	No	No
74	411.54	4.269	-4.118	6	1	54.04	0	-36.83	No	No
75	397.52	2.876	-2.907	6	1	54.04	0	7.413	No	No
76	379.50	3.238	-3.532	5	1	44.81	0	9.158	No	No
77	393.53	3.580	-3.802	5	1	44.81	0	7.914	No	No
78	407.56	3.922	-4.072	5	1	44.81	0	6.099	No	No
79	421.58	4.264	-4.342	5	1	44.81	0	3.650	No	No
80	465.64	3.464	-3.682	7	2	60.08	0	10.357	No	No
81	408.54	3.706	-3.519	6	1	48.05	0	7.250	No	No
82	424.54	2.884	-2.900	7	1	57.28	0	6.788	No	No
83	422.57	4.048	-3.789	6	1	48.05	0	5.736	No	No
84	436.59	4.205	-4.769	6	2	56.84	0	3.265	No	No
85	430.55	4.358	-4.702	6	2	56.84	0	7.342	No	No
86	444.58	4.607	-4.678	6	1	48.05	0	6.324	Yes	Yes
87	506.65	5.266	-6.698	6	1	48.05	2	7.586	No	No
88	444.58	4.067	-4.518	6	2	56.84	0	7.522	No	No

[a]: Compound; [b] Polar Surface Area; [c] Mutagenic properties; [d] Tumorigenic properties

Among aliphatic amide- and urea-containing dopamine D_2/D_3 ligands, only compound **86** might have possible mutagenic and tumorigenic characteristics. The reason may be the methyl group attached to the second NH, because derivative **87** has a similar chemical structure with a phenyl ring at the place of $-CH_3$ and it does not show any putative toxic properties. The diphenylurea substituted ligand (**87**) is the only molecule that violates two Ro5, due to its greater molecular weight and *c*LogP. However, these data do not exclude this molecule from further evaluations (see section 4.2), because **87** has got a promising drug-likeness score and the highest aqueous solubility value, which is crucial for absorption and distribution characteristics.

All the compounds have values within the optimal parameters in terms of lipophilicity, water solubility and polar surface area, showing that these structures might be considered as good drug

candidates, but further examinations are necessary. Notably, all the compounds have PSA values below 60 square Å, indicating that the represented structures can pass throughout the BBB, which is crucial for potential CNS drugs. Nevertheless, derivatives **73** and **74** have negative drug-likeness scores, which can be related to the presence of -CF_3 and -Boc moieties for **73** and **74**, respectively. Based on these results, it seems that heteroatoms like fluorine or oxygen in those configurations are not well tolerated, as it has been obtained for sulfoximine derivative **42** as well (see above). Indeed, derivative **72**, characterized by a pivalic amide, that has three methyl groups attached to the carbonyl function, presents a good drug-likeness profile, albeit with one of the lowest scores. Whereas, the highest drug-likeness score is hold by compound **80** that has the ethyl-pyrrolidine fragment of **sulpiride** and **amilsulpride**, demonstrating that the combination of privileged scaffold with some fragments of marketed drugs could be beneficial.

In conclusion, all the dopamine D_2/D_3 ligands with 4-aniline-ethyl linker substituted with amide and urea variations (**69-88**) present interesting pharmacological behaviours as well as promising drug-likeness properties. Within the structures of the described compounds, the chemical diversity is minimal and thus the pharmacological and physicochemical profiles are comparable. Nevertheless, this aspect is a consequence of the high similarity grade of target receptors, but on the other side it proves the great versatility of 4-aniline-ethyl linker, as potential scaffold for future dopamine D_2/D_3 ligands. The evaluation has highlighted that some moieties are better tolerated than others in the binding sites, or some functions bind preferentially D_2 receptor rather than D_3 and vice versa, providing important tools to perform additional structure-activity relationship studies.

Based on SAR executed on derivatives **69-88** and on the results obtained by urea-containing derivatives with aromatic substitutions (**85-88**), the following work has been performed on ligands with 4-aniline-ethyl linker substituted with aromatic amide groups. The additional phenyl ring has been undergone several and diverse variations with the purposing of analysing the new scaffold in combination with aromatic moieties as SPs. Following the corresponding literature,[155,366,405] 3-methoxy benzamide combined with the classical butyl linker has resulted to produce very affine dopamine D_2/D_3 ligands with high selectivity ratio towards D_3 receptor. According to the results, 3-methoxy benzamide, thanks to its binding mode with the second binding pocket, may fine-tune the pharmacological behaviour of the entire ligand in term of selectivity between the receptor subtypes. Consequently, 3-methoxybenzamide has been added to the aniline scaffold, obtaining intriguing results (derivative **90**, table 20). So, to have a complete overview of this type of substitution, the OCH_3 has been evaluated in different positions on the aromatic ring, or di- and tri-substituted. In addition to that, the benzamide fragments of **sulpiride** and **amilsulpride** have been considered as well as the replacement of OCH_3 group with an electron withdrawing one such as -CN. However, the

comparison among -CN and -OCH3 remained incomplete for synthetical problems explained in section 3.3.

The pharmacological data of anilides with an aromatic variation **(89-102**) are given in table 20. The ratio of receptor affinities K_i (D_2) / K_i (D_3) determines the selectivity index between the two subtypes. Binding constants are given as mean values with a corresponding confidence interval (CI).

Table 20. Binding affinity values of ligands **89-102**.

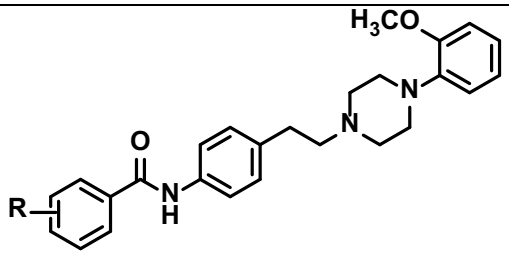

Cpd [a]	R	K_i D_2R(nM) (CI 95%)	K_i D_3R(nM) (CI 95%)	Ratio (D_2R/D_3R)[b]	Cpd [a]	R	K_i D_2R(nM) (CI 95%)	K_i D_3R(nM) (CI 95%)	Ratio (D_2R/D_3R)[b]
89	*2*-OCH_3	92.3 (35.4; 241.0)	29.4 (8.5; 102.0)	3	**96**	*3,5*-OCH_3	107 (81; 142)	80 (59; 110)	1
90	*3*-OCH_3	38.9 (23.4; 65.0)	3.98 (2.31; 6.86)	10	**97**	*4,5*-OCH_3	20.2 (7.3; 56.0)	12.4 (9.8; 15.7)	2
91	*4*-OCH_3	11.1 (4.1; 30.0)	4.5 (1.6; 12.9)	3	**98**	*3,4,5*-OCH_3	216 (146; 320)	121 (58; 252)	2
92	*2,3*-OCH_3	120 (60; 240)	8.3 (6.3; 10.8)	15	**99**	*2*-OCH_3 *5*-SO_2NH_2	138 (62; 310)	221 (53; 923)	0.6
93	*2,4*-OCH_3	135 (51; 359)	79 (22; 286)	2	**100**	*2*-OCH_3 *4*-NH_2 *5*-SO_2Et	143 (118; 173)	139 (58; 333)	1
94	*2,5*-OCH_3	267 (83; 855)	399 (322; 495)	0.7	**101**	*3*-CN	129 (44; 378)	39.6 (34.7; 45.2)	3
95	*2,6*-OCH_3	291 (188; 451)	594 (107; 3294)	0.5	**102**	*4*-CN	9.6 (8.4; 11.0)	5.30 (3.23; 8.68)	2

[a] Compound; [b] Ratio K_i (D_2R)/ K_i (D_3R).

In general, all the benzamides show binding affinities in the nanomolar range; particularly, derivatives **89-92,97** and **102** have nanomolar affinity values. However, going throughout the structures evaluated here, it is possible to observe a worsening trend in terms of affinities, starting from the mono-substituted ligands (**89-92**). It seems that a more complicated modification is not completely an advantage and it leads to a decrease of affinity values.

Among the mono -OCH_3 benzamides, the *para* derivative **91** turned out to have the best pharmacological profile towards both receptors with slight preference at D_3, which is found similarly in the *ortho*-derivative **89** with worsened values. Regarding the *meta* derivative **90**, the first

compound of this series, a greater selectivity towards D_3 receptor is observed, which proves that methoxy function is working well in those positions of the phenyl ring. In fact, this assumption is confirmed by another molecule, the *2,3*-disubstituted aromatic amide **92** that resulted to be the dopamine D_2/D_3 ligand with the highest selectivity index within the two receptor subtypes.

Regarding the di- and tri-substituted methoxy benzamide products (**92-100**), they present interesting binding properties, but only compounds **92** and **97** show low nanomolar values, demonstrating that two OCH_3 are well tolerated only if they are next to each other. The positions *4,5* seem to work for both receptors, while *2,3* only for D_3.

Surprisingly, a decrease of affinity at target receptors is obtained for derivatives **98-100**, as the trimethoxy phenyl ring, presented by **98**, is the structural core of mescaline.[406] The natural psychoactive alkaloid acts as agonist on serotoninergic receptors with high influence on the dopamine release as well.[407,408] The compounds **99** and **100** bear the benzamide fragments that are found in **sulpiride** and **amisulpride**, respectively. These drugs have been chosen due to the highly selectivity towards D_3 receptor, but the corresponding derivatives have been shown slightly affine at both receptors without any type of subtype preference.

The mono -CN benzamide ligands **101** and **102** have been tested to have a better overview and precise comparison between electron withdrawing and donating functions (-CN and $-OCH_3$), but it is incomplete because of chemistry problems related to the obtaining of the *ortho* derivative. However, compounds **101** and **102** show interesting results, because they feature similar pharmacological behaviours to mono $-OCH_3$ analogues. The cyano group attached to the phenyl ring is more beneficial in *para* position, showing low nanomolar affinities at both D_2 and D_3 receptors, while **102** features worse affinities values with slightly higher preference towards D_3 rather than D_2. Despite having an incomplete comparison, these last two compounds prove again that a simple modification pattern is better accepted within the binding pockets and that a substitution in the position *3*- and *4*- or together might be more suitable for D_3 than for D_2.

Consequently, more simple aromatic variations have been tested with an amide function in radioligand binding assays. First a phenyl ring without substitutions has been attached to the scaffold of **54**, then it was replaced with a pyridine ring. Then, a second phenyl ring has been added, it has been modified with heterocycles, analysing diverse heteroatoms and different positions of linkage to the acyl function. Ultimately, the benzene ring has been replaced by a non-fused heterocycle with distinct heteroatoms and switching the attachment position to the amide. All the ligands with the corresponding pharmacological data are grouped in table 21. Binding constants are given as mean values with a corresponding confidence interval (CI).

Table 21. Pharmacological data of substituted-aniline-ethyl linker-based ligands with aromatic amide variations **103-126**.

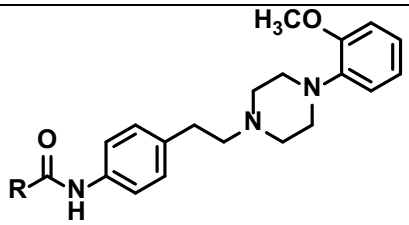

Cpd [a]	R	K_i D_2R(nM) (CI 95%)	K_i D_3R(nM) (CI 95%)	Ratio (D_2R/D_3R)[b]	Cpd [a]	R	K_i D_2R(nM) (CI 95%)	K_i D_3R(nM) (CI 95%)	Ratio (D_2R/D_3R)[b]
103	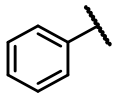	15.4 (9.7; 24.6)	1.8 (1.05; 3.2)	9	**115**	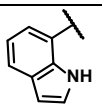	233 (87; 625)	38.9 (11.3; 134.0)	6
104	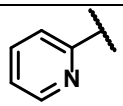	89 (47; 167)	117 (52; 263)	0.8	**116**	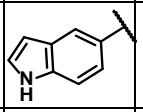	37.7 (10.4; 137.0)	4.99 (3.16; 7.89)	8
105	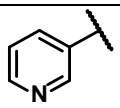	61.3 (34.8; 108.0)	46.1 (17.1; 124.0)	1	**117**	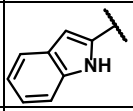	43.5 (18.9; 100.0)	40.3 (11.7; 139.0)	1
106	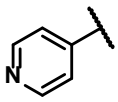	14.4 (8.8, 23.6)	11.9 (3.7; 38.3)	1	**118**	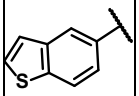	142 (112; 180)	21.6 (5.9; 78.7)	7
107	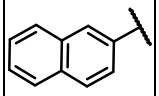	74.9 (39.6; 142.0)	6.1 (2.8; 13.2)	12	**119**	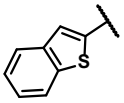	19.3 (8.7; 42.8)	15.7 (5.8; 42.7)	1
108	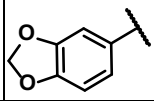	14.2 (8.7; 23.3)	9.6 (4.0; 23.0)	2	**120**	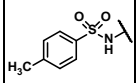	18.4 (6.3; 53.6)	14.4 (5.9; 35.1)	1
109	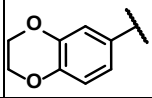	29.8 (18.8; 47.4)	4.7 (1.7; 12.7)	6	**121**		10.7 (5.7; 19.9)	7.9 (3.8; 16.5)	1
110	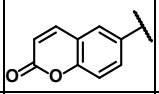	11.1 (3.3; 36.9)	7.1 (2.9; 16.7)	2	**122**	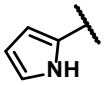	10.2 (5.6; 18.3)	12.5 (4.7; 33.8)	0.8
111	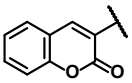	116 (53; 258)	177 (72; 431)	0.7	**123**	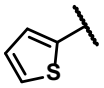	9.5 (3.6; 24.5)	9.3 (3.9; 21.0)	1
112	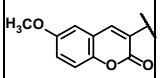	112 (25; 501)	128 (64; 255)	1	**124**	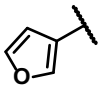	5.7 (2.9; 11.1)	10.4 (2.8; 38.0)	0.5
113	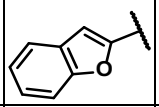	83.9 (43.8; 161.0)	45 (21; 97)	2	**125**	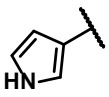	13.2 (10.0; 17.5)	13.1 (8.5; 19.8)	1
114	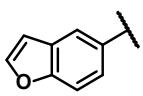	32.4 (22.2; 47.2)	19.9 (12.6; 31.5)	2	**126**	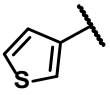	5.8 (2.7; 12.6)	6.9 (2.2; 21.7)	0.8

[a] Compound; [b] Ratio K_i (D_2R)/ K_i (D_3R).

The anilides with aromatic motifs present nanomolar affinity values at both receptors of interest in table 21. The first compound of this series (**103**) shows even a preferential binding at D_3 receptor over D_2, confirming that an additional phenyl ring could improve the pharmacological profile albeit with little influence. The replacement of benzene with a pyridine ring, that is more hydrophilic, leads to a decrease of binding properties towards both receptors for picolinamide and nicotinamide derivatives (**104** and **105**, respectively). Whereas, the isonicotinamide ligand (**106**) , that has pyridinic nitrogen in *para* position, has similar binding profile to compound **103**, indicating that a hydrophilic pyridine is suitable for both receptors only with that nitrogen configuration.

In line with the results obtained by ligands **103-106**, the naphthyl moiety, supported by lead compound **BP897**, has been added to the scaffold producing compound **107** with a modest tendency towards D_3 receptor. Thereby, the second aromatic ring was replaced by a 1,3 dioxolane and 1,4 dioxane rings; compounds **108** and **109** present similar pharmacological profile with little preferential tendency at D_3 receptor, when compared with the data of **107**. Then, the second ring substitution continued with the insertion of a coumarin structure.

Coumarins are natural organic compounds found in various plants and they are widely distributed in the environment. These compounds, derived from secondary plant metabolism, possess antioxidant properties and they have been shown to exhibit neuroprotective effects.[374] As a result, coumarins and their derivatives have gained significant interest within the scientific community, leading to numerous research publications that explore their potential as drug candidates. Researchers have incorporated coumarin moieties into dopaminergic and serotonergic pharmacophores, aiming to develop novel therapeutic agents. Notably, a study by Teran *et al.* demonstrated that coupling of the coumarin moiety with 4-phenylpiperazine resulted in increased affinity for both the $5HT_{1A}$ and D_3 receptors, highlighting the potential of these compounds in targeting specific neurological pathways.[409] Due to this, coumarin moiety was incorporated in the western part of the molecule.

Surprisingly, replacement of the blueprint's naphthyl moiety with coumarin scaffold enhances affinity at both D_2 and D_3 receptors only for compound **110**, while the ligands **111** and **112** feature a worsened binding profile, due to the exchanged position of chromen ring. In this way, it seems that the aromatic ring, directly linked to amide group, has stronger interactions with second binding pocket. Consequently, the tetrahydropyran-2-one ring was substituted with an aromatic structure, generating compounds with fused-ring heterocycles (**113-119**).

Among **113-119**, the position exchange of the aromatic ring was tested as well, it is possible to notice slightly higher affinity values when the aromatic ring is attached to the amide bond for benzofurane (**113-114**) and benzopyrrole ligands (**116-117**). Whereas, the derivative **115** presents a comparable

pharmacological profile with little tendency towards D_3 receptor. On the other hand, for benzothiophene ligands **118** and **119**, the product, that has the aromatic ring linked to the amide (**118**), has worse affinity values than **119**, that has the thiophene ring attached to carbonyl function. However, the binding profile at D_3 receptor remaines the same, the great difference is observed in the affinity at D_2 receptor, demonstrating that thiophene attached to the amide bond is more effective. In addition, as another sulphur-based modification, sulphonamide with toluene (tosyl group) was evaluated as bioiosteric replacement of arylamide. The product **120** has resulted to have similar binding properties, when compared with the ones of the unsubstituted arylamide compound **103**, thus giving inspiration for further studies on sulphonamide modifications combined with 4-aniline ethyl linker.

Finally, a non-fused heterocycle has been evaluated as well, by changing the type of heteroatom and the attachment position to the amide (*2*- or *3*-). In spite of these variations, the compounds **121-126** exhibit very similar pharmacological behaviours with nanomolar affinity values at both D_2 and D_3 receptors. In fact, no preferential binding properties has been observed. Nevertheless, these heteroaromatic anilides suggest that heteroatom variation is highly suitable in the binding pocket of both receptors; thereby, modifications on heteroaromatic structures might lead to optimization of related binding properties.

In conclusion, a set of 38 substituted-aniline ethyl linker-based ligands with aromatic amide variations (**89-126**) have been characterized, showing high affinity at both dopamine D_2 and D_3 receptors. Comparing the results with the ones obtained by aliphatic amide modifications (**69-84**), it can be affirmed that both substitution patterns are suitable for both target receptors. Indeed, an aliphatic amide or urea function might drive the binding preferentially towards D_2 receptor, while an aromatic amide or urea may be more suitable for D_3 receptor, albeit no great receptor subtype selectivity has been described here.

Within this set of aromatic amides with aniline ethyl linker, some ligands (**90, 92, 97, 102-103, 106-110** and **113-126**) have been selected for further analysis in order to estimate the drug-likeness properties of these structures. As it happened for the previous ligands, the software Data Warrior has been used to run this investigation. The other ligands have been discarded from this evaluation to avoid structure redundancy that generates identical data and because of irrelevant affinity values (e.g. three digits value). The results of the selected ligands are listed in table below.

Table 22. Drug-likeness and physicochemical parameters of selected substituted-anilino-ethyl linker derivatives with aromatic amide modifications.

Cpd[a]	MW	*c*LogP	*c*LogS	H-bond Acceptor	H-bond donor	PSA[b]	Ro5 violations	Drug-likeness	Mut.[c]	Tum.[d]
90	445.56	4.294	-4.204	6	1	54.04	0	7.799	No	No
92	475.59	4.224	-4.222	7	1	63.27	0	7.799	No	No
97	475.59	4.224	-4.222	7	1	63.27	0	7.799	No	No
102	440.55	4.199	-4.959	6	1	68.60	0	3.520	Yes	No
103	415.54	4.364	-4.186	5	1	44.81	0	7.799	No	No
106	416.52	3.363	-3.391	6	1	57.70	0	7.799	No	No
107	465.59	5.558	-5.792	5	1	44.81	1	7.800	No	No
108	459.54	4.475	-4.897	7	1	63.27	0	7.648	No	No
109	473.57	4.343	-4.368	7	1	63.27	0	0.568	No	No
110	483.57	4.202	-4.940	7	1	71.11	0	5.105	No	No
113	455.56	4.869	-5.369	6	1	57.95	0	7.907	No	No
114	455.56	4.815	-5.345	6	1	57.95	0	7.263	No	No
115	454.57	4.403	-4.711	6	2	60.60	0	7.778	No	No
116	454.57	4.403	-4.711	6	2	60.60	0	7.778	No	No
117	454.57	4.457	-4.735	6	2	60.60	0	8.568	No	No
118	471.62	5.203	-5.425	5	1	73.05	1	7.929	No	No
119	471.62	5.285	-5.535	5	1	73.05	1	8.775	No	No
120	465.62	3.859	-4.351	6	1	70.26	0	3.141	No	No
121	405.50	3.552	-3.868	6	1	57.95	0	7.579	No	No
122	404.51	3.140	-3.234	6	2	60.60	0	8.590	No	No
123	421.56	4.230	-4.196	5	1	73.05	0	9.140	No	No
124	405.45	3.498	-3.844	6	1	57.95	0	8.270	No	No
125	404.51	3.086	-3.21	6	2	60.60	0	8.728	No	No
126	421.56	4.148	-4.086	5	1	73.05	0	8.885	Yes	No

[a]: Compound; [b] Polar Surface Area; [c] Mutagenic properties; [d] Tumorigenic properties.

According to the results presented in table 22, all the compounds do not show potential toxic characteristics except compounds **102** and **126**. The first derivative bears a -CN group in *para* position that may cause mutagenic reactions, while ligand **126** has thiophene ring substituted in position *3*-, which could trigger mutagenic mechanisms. The assessment of **126** has been interesting because the analogous derivative (**123**), that has thiophene ring substituted in position *2*-, does not show any potential risk factors.

The evaluated compounds resulted to have only positive drug-likeness scores, indicating that all the structures might lead to possible drug candidates. However, some ligands have low drug-likeness points, when compared with the average values observed in this list. For example, compounds **102**

and **120** have a score of 3 circa and **109** scores 0.568. Surely, the reasons might be connected to the high values of polar surface area, which are slightly above the threshold of 60 square Å, meaning that these three compounds (**102**, **109** and **120**) could have difficulty to pass through BBB. On the other hand, the rest of structures show high drug-likeness properties; particularly, ligands **117**, **119**, **122** and **123** feature the best drug-likeness scores. The common point of these compounds is that they bear fused-ring heterocycles (**117** and **119**) or non-fused heterocycles (**122** and **123**) connected to the amide through position *2*-, which suggests that this configuration with 4-aniline ethyl linker might be highly druggable.

Regarding Ro5, only three compounds violate one rule (**107, 118, 119**), because they have *c*LogP higher than 5, due to the presence of highly lipophilic moieties like naphthyl or benzothiophene. Nonetheless, being Lipinski´s rules only guidelines, this violation does not hamper the drug-candidacy of these structures. Indeed, **107, 118, 119** have the other parameters within optimal values as well as high drug-likeness score.

Most of the molecules have PSA value lower than 60 square Å, indicating that they would reach the central nervous system without any problems. Few compounds (**92, 97, 108, 109, 115-117, 122** and **125**) have values slightly above the threshold, but the excess is so small that it can be omitted. Whereas, benzothiophene (**118, 119**) and thiophene (**123,126**) amides have a PSA value of 73.05 Å, compounds **110** and **120** have 71.11 Å and 70.26 Å respectively, and ligand **102** has 68.60 Å. Clearly, these parameters are higher enough to perform further investigations on BBB permeability. Overall, all the listed ligands show good aqueous solubility and promising profile in terms of drug-likeness, confirming once again that the 4-aniline ethyl linker combined with 1-(2-methoxyphenyl)piperazine represents a valuable scaffold.

To conclude, a large set of 58 substituted anilino-ethyl linker-based dopamine D_2/D_3 ligands have been characterized, demonstrating optimal binding properties at receptors of interest and highly promising drug-likeness profiles. In line with the pharmacophore model (Section 1.1.2), the compounds, that have an amide with aliphatic and aromatic modifications, proved to be more suitable for D_3 receptor, particularly the ones with aromatic moiety. Whereas, the urea-containing ligands resulted to be more suitable for D_2 receptor. However, no compounds feature receptor subtype selectivity greater than 15. This is a consequence of the high structural similarity between the target receptors as well as of the large suitability of 4-aniline ethyl linker within the binding pockets of both D_2 and D_3 receptor. Indeed, the main achievement is that the aromatic linker, developed in the PhD project, represent a real opportunity of expanding the knowledge on dopamine D_2/D_3 receptor ligands with the purpose of providing tools for novel antipsychotic agents.

5. Summary

Dopamine D_2 and D_3 receptors are considered the main targets for treating dopamine related disorders such as drug addiction, schizophrenia, psychiatric disorders and Parkinson's disease. However, majority of medications cause extrapyramidal side effects as a result of binding to other monoamine receptors or to off-target receptors. Consequently, it has been necessary to have preferring dopamine D_2 and D_3 receptor ligands in order to reduce the onset of side effects and to enhance the patient adherence.

In this matter, substituted *N*-phenylpiperazines have been highly useful, because their structure provided clinical candidates like **BP897** or marketed drugs like **cariprazine.** Additionally, the pharmacophore model of substituted *N*-phenylpiperazines presented insightful tools to develop novel dopamine D_2/D_3 ligands. Therefore, this pharmacophore model (Section 1.1.2) together with **BP897** and **cariprazine** were taken as lead structures to design and synthetize the dopamine D_2/D_3 ligands presented in the PhD project.

The main goal was to examine combination between various linkers and different motifs as SPs alongside the 1-(2-methoxyphenyl)piperazine used always as PP. Thereby, the first modification was the insertion of a sulphur-based moiety in the classical linkers, supported by the lead compounds (butyl chain and 1,4-disubstituted cyclohexyl unit**)**, connected to the chosen piperazine. Sulphur-based ligands **4-6**, **12,14,16** were synthetized and characterized at receptors of interest. This preliminary study prompted the second analysis, in which sulphur-based motifs were evaluated with an original aromatic linker, producing derivatives **22-26**, **30-31**, **34**, **36-37** and **42**. In this set of ligands, interesting results have been achieved with compounds **23-25**, displaying nanomolar affinity values with different subtype tendency: for **23** K_i (D_2) = 8.3 nM, K_i (D_3) = 45.4 nM; for **24** K_i (D_2) = 26.3 nM, K_i (D_3) = 14.4 nM; for **25** K_i (D_2) = 79.3 nM, K_i (D_3) = 10.7 nM. These results highlighted that most effective sulphur moiety within binding pockets is the aminothiazole ring combined with an aromatic spacer. On the other hand, innovative functions such as sulfoximines did not have comparable affinity values, but an efficient synthetical protocol was achieved. In details, the synthesis has shed light on the critical issues of sulfoximine and its reactions, which were analysed and successfully resolved (Section 3.1).

The second set of ligands (**45-50**, **53-55** and **59-67**) was drawn up with the purpose of expanding the evaluation of the aromatic linker supported by the previous sulphur compounds (**30-31**, **34**, **36-37** and **42**). Thereby, a second modification of the phenyl spacer was introduced (phenylmethyl) and structural variations were applied such as exchange of position (*ortho*, *meta*, *para*) and replacements

of methylamide. Among these compounds, the best binding profile was obtained by derivative **55** (K_i (D_2) = 14.9 nM and K_i (D_3) = 9.2 nM). The chemistry, described in section 3.2, was immediate but noteworthy, because it held solutions for issues concerning competition between S_N2 and E2 mechanisms or applications of microwave reactor. Accordingly, the scaffold, represented by compound **55**, was used as reference structure to perform the last part of the PhD project.

The 58 substituted anilino-ethyl linker-based ligands were produced and examined. Therefore, numerous structural variations were applied focusing on optimization of binding profiles. So, aliphatic/aromatic amides and ureas (**69-126**) were synthetized and characterized at dopamine D_2 and D_3 receptors. Within this group of compounds, an aromatic amide associated to phenylethyl spacer resulted to be the most suitable configuration for target receptors. The chemistry, used for these molecules, was simple and highly efficient, thanks to the versatility of free aniline group supported by the privileged scaffold (see section 3.3).

To conclude, a library of 93 novel dopamine D_2/D_3 ligands has been designed, synthetized and characterized at receptors of interest, showing an original linker that has been demonstrated to be functional, due to variations like aminothiazole moieties (e.g. compounds **23-25**). Indeed, a second alternative linker is provided, bearing an aromatic aminothiazole-ethyl unit (Figure 28). The established linkers may be used for developing novel dopamine D_2/D_3 ligands, but further studies are necessary to assess their functionality *in vivo* analyses and their stability in metabolic evaluations (e.g. compound **55**). Unfortunately, no receptor subtype selectivity has been achieved in this project, but promising tendency values towards D_3 receptor have been obtained with the structures of **90**, **92**, **107**, depicted in figure 28 with their affinity values. These ligands can be used to develop additional molecules in order to afford better selectivity indices. Moreover, 1-(2-methoxyphenyl) piperazine has been used as unique PP, so the application of the established linkers combined with privileged SP moieties can be the background of a future project, focusing on primary pharmacophore variations.

The entire PhD Project, including the chemical and pharmacological experimental work, was executed in the laboratories of Professor Holger Stark, located in the institute of Pharmacy of Heinrich Heine University.

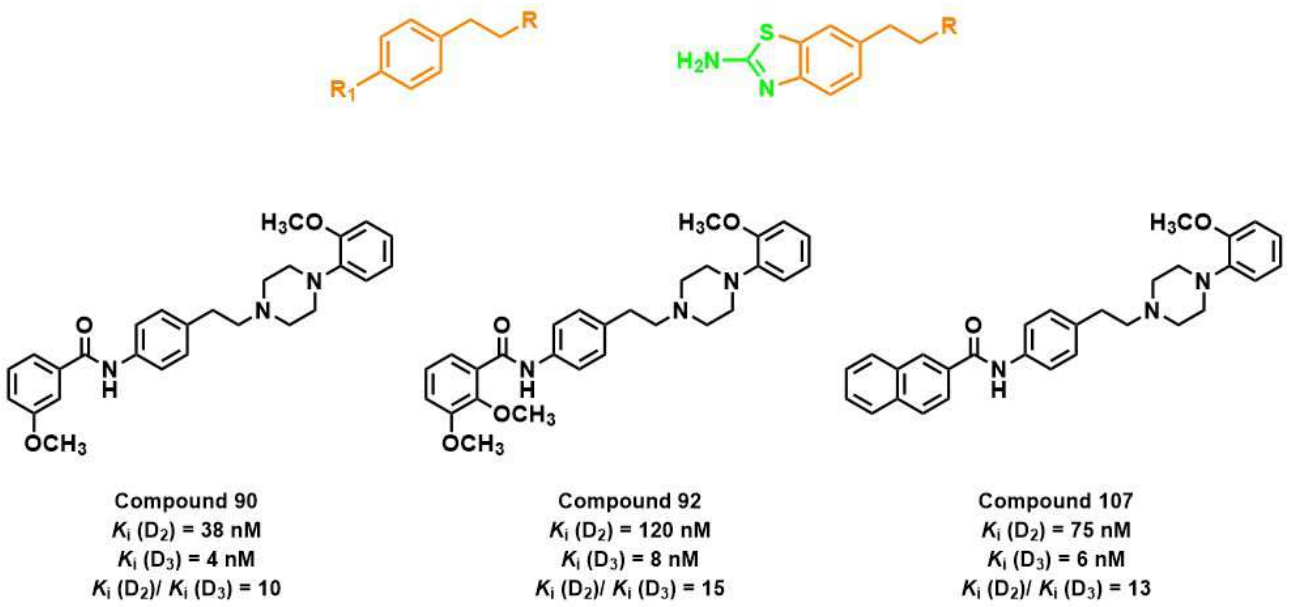

Figure 28. Outlook of the phenylethyl linker provided in this PhD project, which is highlighted in orange. Next to this, a second alternative linker with aminothiazole variation is represented. The area, coloured in green, is the moiety usable as spacer and secondary pharmacophore. The structures drawn in black are the compounds that feature the highest tendencies towards D_3 receptor obtained in this project. The molecules represent an interesting outcome that might serve as background for further evaluations.

6 Experimental Section

6.1 Chemistry

All the chemical experiments, the analytical characterizations and the purity evaluations of the entire library of ligands were executed in the laboratories of Professor Stark, located in the institute of pharmacy of Heinrich Heine University. All starting materials were obtained from Merck KGaA. Analytical thin-layer chromatography was performed on ALUGRAM® silica gel 60-UV_{254} plates and visualized by UV light (Macherey-Nagel, Düren, Germany) and preparative column chromatography was performed on a silica gel 60 M, 0.04-0.063 mm (Macherey-Nagel, Düren, Germany).

^{1}H-NMR spectra were recorded on a Bruker Advance III spectrometer (Bruker, Rheinstetten, Germany) at 300/600 MHz and ^{13}C-NMR spectra at 75 and 150 MHz. The chemical shifts for ^{1}H-NMR and ^{13}C-NMR were referenced to TMS via residual solvent signals (^{1}H, CDCl3 at δ = 7.26 ppm; ^{13}C, CDCl3 at δ = 77.36 ppm; ^{1}H, DMSO-d6 at δ = 2.50 ppm; ^{13}C, DMSO-d6 at δ = 39.43 ppm). To identify the signals of protons bonded to aromatic rings, these abbreviations are used: Ar = aryl-moiety; Ar-Pip = aryl-piperazine moiety Ar-Bmd = benzamide and benzenesulfonamide moieties Ar-Ur = aromatic urea moieties; NH_2 = aniline; SO_2NH/CONH = sulphonamide or amide. Chemical shifts are given as parts per million (ppm) and reported as follows: s (singlet), d (doublet), dd (double of doublets), t (triplet), q (quartet), p (pentet), or m (multiplet). The coupling constant (*J*) is given in Hertz (Hz).

Melting points were determined on a M-564 Büchi melting point apparatus (Büchi, Essen, Germany). Microwave reactions were performed with sealed microwave vials designed for 0.5-2 mL reaction volumes in a Biotage Initiator 2.0 oven (Biotage, Uppsala, Sweden). Accurate mass values for identification of target compounds were determined on Advion APCI mass spectrometer express CMS in negative and positive mode (Advion, Ithaca, NY, USA) and data are shown as $[M+H^+]^+$. Solvents have been evaporated using a Rotavapor R II (Büchi) with a PC 3001 VARIO Chemie-Vacuum pump (Vacuubrand) and CVC 3000 Vacuum controlling system (Vacuubrand). The compounds have been dried with the high-vacuum pump (Hybrid-Pumpe RC 6; Vacuubrand). Compounds purity of molecules **12** and **88** was determined by elemental analysis Vario MICRO cube Elemental Analyzer (Elementar Analysensysteme, Hanau, Germany). Measured valued were within ± 0.4% of the theoretical and calculated values for the final compounds.

Purity determination of described ligands was performed with high performance liquid chromatography connected to low resolution mass spectrometer for compounds **4-6, 14, 16, 22-26, 30-31, 34, 36-37, 42, 45-46, 53, 48-49,55, 59-61, 65-67, 74, 90, 96-98, 102-103, 107**, to diode array

detector for compounds **80-81, 83, 86-87, 89, 91-95, 99-101, 104-106, 108-109, 113, 115-117** and to high resolution mass spectrometer for compounds **47-48, 54, 62-64, 69-73, 75-79, 82, 84-85, 110-112, 114, 118-126**. HPLC-MS, HPLC-DAD and HPLC/HRAM-MS data are shown as $[M+H^+]^+$ with purity grade in brackets (%). The stock solutions for HPLC-MS/DAD/HRAMS-MS measurements (approximately 1 mg/mL) were diluted with methanol hyper grade for HPLC and concentrations of approximately 0.1-0.2 mg/mL were obtained (injection: 2 µl). Relative purity of the compounds was determined.

Ion-trap LC/MS analysis were made with this HPLC system: Elute SP LC System (Bruker Daltonics, Bremen, Germany) with vacuum degasser, binary pump, autosampler, column oven. Column: Intensity Solo 2 C18 (100 mm * 2.1 mm); Temperature: 40°C; Mobile phase: A. water hypergrade for LC-MS with 0.1 % formic acid (v/v) (Merck); B. Acetonitrile hypergrade for LC-MS (for LC-MS); Flow Rate: 0.2 ml/min; MS-System: amaZon speed ETD ion Trap LC/MS System (Bruker Daltonics, Bremen, Germany); Ionization: electron spray; Polarity: positive; Alternating ion-Polarity :on; Scan Range: m/z: 80-1200; Nebulizer: Nitrogen, 15 Psi; Dry Gas: Nitrogen, 8 l/min, 200 °C; Mass range Mode: Ultra Scan.

Methods of LC-MS measurements: (Method 1 for **45-46, 49-50, 55 59-61, 65-67**): Analysis: 0- 4 min 98 % A, 4-5 min gradient 98-95 % A, 5-9 min 95 % A, 9-16 min gradient 95 to 5 % A, 16-17 min. gradient 5 to 0% A, reconditioning: 17-18 min. gradient to 0 to 98 % A, 18-21 min 98 % A. (Method 2 for **53**): Analysis: 0- 4 min 95 % A, 4-14 min gradient 95 to 20 % A, 14-16 min gradient 20 to 5 % A, 16-17 min. gradient 5 to 0% A, reconditioning: 17-18 min. gradient to 95 % A, 18-21 min 95 % A. (Method 3 **4-6, 12, 14, 16, 22-26, 30-31, 34, 36-37, 42, 47-48, 54, 62-64, 69-126**): MS-System: compact (Bruker Daltonics, Bremen, Germany); Ionization: electron spray; Polarity: positive; Scan range: m/z: 50-1300; Nebulizer: Nitrogen, 1.8 Bar; Dry Gas: Nitrogen, 9 L/min, 220 °C; Mass range mode: Ultra Scan. Quantification was done using Extracted Ion Chromatograms.

6.1.1 General Methods

N-Alkylation (A)

1-(2-Methoxyphenyl) piperazine (1.5 eq.) and Na_3PO_4 (1.5 eq.) were added into a solution of the corresponding alkylating agent (1. eq) in acetonitrile at room temperature. The reaction mixture was left to stir 20 hours at reflux. After that, the inorganic salts were filtered off and acetonitrile was removed under reduced pressure. The crude oil was solubilized in EtOAc and washed with HCl 1M. The acidic aqueous solution was neutralized with NaOH 6 M and extracted with dichloromethane

three times. Organic layers were combined, dried over Mg_2SO_4 and then concentrated under reduced pressure. The crude oil was purified by column chromatography in SiO_2 or flash chromatography using dichloromethane/methanol or ethyl acetate/hexane as eluents.[410,411]

Oxidation of sulphur (B)

The corresponding sulphide or sulfoxide (1 eq.) was dissolved in dichloromethane. Then, a solution of *m*-CPBA (1.1 eq.) in dichloromethane was added dropwise at room temperature. The addition lasted 1 or 2 hours, depending on the amount used.The mixture was stirred at room temperature for one more hour. Afterwards, the reaction solution was washed with $NaHCO_3$ three times in order to remove the *meta*-chlorobenzoic acid which was formed as a side product. The organic layer was dried with Mg_2SO_4 and concentrated under reduced pressure.[412]

Mesylation of alcohol (C)

Triethylamine (1.5 eq.) and mesyl chloride (1.5 eq.) were added to a stirring solution of the corresponding alcohol (1 eq.) in dichloromethane with ice bath. The reaction was stirred for 15 minutes in ice bath. After that, the mixture of reaction was treated with Iced water, a solution of HCl 1 M and $NaHCO_3$, it was dried over Mg_2SO_4 and concentrated under reduced pressure.[413]

Reduction of nitro group (D)

A round bottom flask with two necks was charged by the corresponding nitro precursor (1 eq.) and Pd/C 10% (1 eq.) in methanol. Subsequently, the flask was purged first with N_2 atmosphere to make dry conditions and then with H_2. The reaction was stirred at room temperature for 18 hours. The mixture was filtered off with Buchner filter on Celyte, the solution was concentrated under reduced pressure.[414]

N-Acylation (E)

Diisopropylethylamine or triethylamine (1.5 eq.) and the corresponding acylating chemical (1.5 eq.) were added at room temperature into a solution of free NH_2 compound or free NH-sulfoximine derivative (1 eq.) in dichloromethane or tetrahydrofuran. The mixture of reaction was left to stir at room temperature up to reflux between 3-6 h, depending on the acylating agent used. Afterwards, the solution of reaction was washed with deionized water two times and with brine one time, dried with Mg_2SO_4 and evaporated with Rotavapor R II. The crude reaction mixture was further purified with column chromatography or flash chromatography using dichloromethane/methanol or ethyl acetate/hexane as eluents.[415,416]

Imination of sulfoxide (F)

The corresponding sulfoxide (1 eq.) was solubilized in dichloromethane, then trifluoroacetamide (CF_3CONH_2, 4 eq.), magnesium oxide (MgO, 4 eq.) and the catalyst rhodium acetate ($Rh_2(OAc)_4$, 2.5% eq.) were added. To this stirring suspension iodobenzene-diacetate (PhI(OAc)2, 1.5 eq.) was added and the reaction was stirred at room temperature for 16 hours. The suspension reaction was filtered with Buchner filter on Celyte, the obtained solution was concentrated under reduced pressure.[302]

Reduction of nitrile (G)

The catalyst Raney-Ni 50%-50% (1.5 eq.) was added into a solution of NaOH (20 ml), it was stirred for 1 hour at 90 °C in order to be activated. Afterwards, the mixture was washed first with water and then with methanol three times each. Finally, the methanolic solution of activated catalyst was added to a solution of respective benzonitrile derivative (1 eq.) in ammonia/methanol (10 mL). The reaction mixture was stirred at 40 °C under H_2 atmosphere into autoclave for 16 hours. Subsequently, the reaction was filtered off with Celyte through Buchner filter and it was concentrated under reduced pressure.[417]

N-Acylation with HATU (H)

To a stirring solution of corresponding carboxylic acid (1 eq.) and diisopropylethylamine (3 eq.) in dimethylformamide, hexafluorophosphate azabenzotriazole tetramethyl uronium (HATU, 1.2 eq.) was added. After 15 minutes, aniline **54** (1 eq.) was added and the mixture of reaction was left to stir at room temperature for 16 hours. Subsequently, dimethylformamide was removed and crude of reaction was solubilized in dichloromethane. The organic layer was washed with deionized water 2 times and with brine one time, dried with Mg_2SO_4 and evaporated with Rotavapor R II. The crude reaction mixture was further purified with column chromatography or flash chromatography using dichloromethane/methanol or ethyl acetate/hexane as eluents.[418]

Urea synthesis (I)

Obtained aniline **54** (1 eq.) was solubilized in 20 ml of dioxane circa, diphosgene (2 eq.) was added to the stirring solution and reaction was stirred at reflux for 2 hours to form the isocyanate **68**. Due to high reactivity properties of intermediate, dioxane was removed and crude of reaction was solubilized in acetonitrile to perform directly the following synthetical step. Therefore, corresponding amine (1 eq.) was added to the stirring solution of isocyanate in ACN; the mixture of reaction was left to stir at reflux for 10 hours. Acetonitrile was removed and crude oil was solubilized in dichloromethane.

The organic phase was washed with brine two times, dried with Mg_2SO_4 and evaporated with Rotavapor R II. The crude reaction mixture was further purified with column chromatography or flash chromatography using dichloromethane/methanol or ethyl acetate/hexane as eluents.[419,420]

6.1.2 Synthesis Procedures

1-(2-Methoxyphenyl)-4-(4-(phenylthio)butyl)piperazine (4)

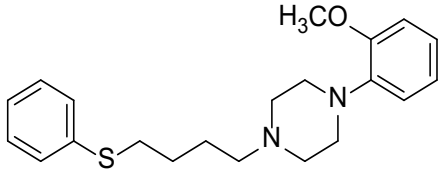

1-Bromo-4-chlorobutane (**1**) was used as alkylating agent and was coupled with thiophenol **2** (1 eq.), after 1.30 hour 1-(2-methoxyphenyl)piperazine **3** was added according to the conditions of procedure **A**. The crude product was purified by flash chromatography using Biotage Sfär SiO_2 10 gr as cartridge in ethyl acetate/hexane from 20 % up to 80% of ethyl acetate. White solid. Yield = 48%. ^{1}H NMR (300 MHz, $CDCl_3$) δ = 7.36 – 7.25 (m, 4H Ar), 7.21 – 7.13 (m, 1H Ar), 7.04 – 6.83 (m, 4H Ar-Pip), 3.86 (s, 3H), 3.19 – 2.90 (m, 6H), 2.66 (s, 4H), 2.50 – 2.37 (m, 2H), 1.78 – 1.61 (m, 4H). ^{13}C NMR (75 MHz, $CDCl_3$) δ = 152.39, 141.40, 136.85, 129.13, 128.99, 125.89, 123.06, 121.12, 118.35, 111.28, 58.15, 55.48, 53.53, 50.66, 33.61, 27.25, 26.01. HPLC-MS (ESI [+]) m/z $[M+H^+]^+$ = 357.17 (95.26 %); MS (APCI [+]) m/z $[M+H^+]^+$ calculated for $[C_{21}H_{29}N_2OS]^+$ = 357.2, found 357.0. mp = 71.3°C M = 356,53 g/mol.

1-(2-Methoxyphenyl)-4-(4-(phenylsulfinyl)butyl)piperazine (5)

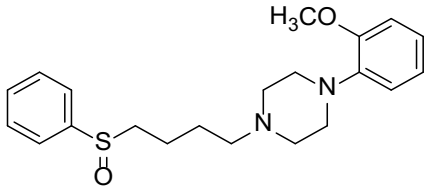

Procedure **B** was used to obtain this product starting from previous sulphide **4**. The crude mixture of reaction was purified by flash chromatography using Biotage Sfär SiO_2 25 gr as a cartridge in dichloromethane/methanol from 1% to 10% of methanol. Light yellow solid. Yield = 48%. ^{1}H NMR (300 MHz, $CDCl_3$) δ = 7.31 – 7.08 (m, 5H Ar), 7.03 – 6.78 (m, 4H Ar-Pip), 3.80 (s, 3H), 3.59 (td, 2H), 3.50 – 3.14 (m, 8H), 2.92 (t, 2H), 2.16 – 1.99 (m, 2H), 1.67 (p, 2H). ^{13}C NMR (75 MHz, $CDCl_3$) δ = 152.15, 139.79, 136.10, 129.55, 129.10, 126.29, 124.00, 121.30, 118.84, 111.30, 71.07, 64.49, 55.52, 45.11, 33.50, 26.55, 21.42. HPLC-MS (ESI [+]) m/z $[M+H^+]^+$ = 373.23 (100 %); MS (APCI

[+]) m/z $[M+H^+]^+$ calculated for $[C_{21}H_{29}N_2O_2S]^+$ = 373.2, found 373.2. mp = 84.2°C. M = 372,53 g/mol.

1-(2-Methoxyphenyl)-4-(4-(phenylsulfonyl)butyl)piperazine (6)

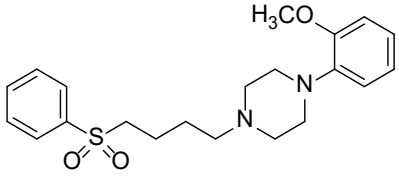

Procedure **B** was used to obtain this product using the previous sulfoxide **5**. The crude mixture of reaction was purified by flash chromatography using Biotage Sfär SiO_2 25 gr as a cartridge in dichloromethane/methanol from 1% to 10% of methanol. Yellowish solid. Yield = 32%. ^{1}H NMR (300 MHz, $CDCl_3$) δ = 7.64 – 7.42 (m, 5H Ar), 7.07 – 6.82 (m, 4H Ar-Pip), 3.83 (s, 3H), 3.63 – 3.22 (m, 10H), 2.98 – 2.74 (m, 2H), 2.13 (t, 2H), 1.91 (dt, *J* = 14.9, 7.5 Hz, 1H), 1.70 (dt, *J* = 14.9, 7.5 Hz, 1H). ^{13}C NMR (75 MHz, $CDCl_3$) δ = 152.08, 143.37, 139.38, 131.11, 129.36, 124.12, 123.94, 121.22, 118.76, 111.28, 64.50, 64.00, 56.12, 55.44, 44.91, 21.20, 19.50. HPLC-MS (ESI [+]) m/z $[M+H^+]^+$ = 389.15 (95.5 %); MS (APCI [+]) m/z $[M+H^+]^+$ calculated for $[C_{21}H_{29}N_2O_3S]^+$ = 389.2, found 389.1. mp = 98.2°C. M = 388,53 g/mol.

Ethyl 2-(tetrahydro-4H-thiopyran-4-ylidene)acetate (8)[421]

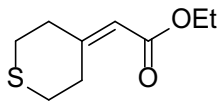

A round bottom flask with two necks was charged with a solution of sodium hydride (NaH, 1.2 eq.) in tetrahydrofuran. The reagent ethyl 2-(diethoxy phosphoryl)acetate (1.1 eq.) was added dropwise at 0°C under N_2 atmosphere. The mixture was stirred at room temperature for one hour. Afterwards, a solution of tetrahydro-4*H*-thiopyran-4-one **7** (1 eq.) in tetrahydrofuran was added dropwise at 0°C into the solution. Once the addition was completed, the HORNER-WADSWORTH-EMMONS reaction was left to stir at room temperature under N_2 atmosphere for three hours.[422] Deionized water was added to the mixture to quench the reaction and the mixture was extracted with dichloromethane for three times. The organic layers were combined, dried over Mg_2SO_4 and concentrated under reduced pressure. The intermediate was used for the next step of synthesis without performing any further purification. Yellow liquid. Yield = 88 %. ^{1}H NMR (300 MHz, DMSO-d6) δ = 5.71 – 5.61 (m, 1H), 4.07 – 3.94 (m, 2H), 3.07 – 2.97 (m, 2H), 2.73 – 2.57 (m, 4H), 2.43 (ddd, 2H), 1.13 (q, 3H). MS (APCI [+]) m/z $[M+H^+]^+$ calculated for $[C_9H_{15}O_2S]^+$ = 187.0, found 187.0. M = 186,27 g/mol.

Ethyl 2-(tetrahydro-2H-thiopyran-4-yl)acetate (9)[421]

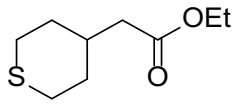

Triethylamine (1.3 eq.) was added into a solution of unsaturated ethyl ester **8** (1 eq.) and platinum dioxide (PtO_2, 0.6 eq.) in ethanol under N_2 atmosphere. Afterwards, H_2 was added and the reaction was stirred at room temperature for three hours. Then, the suspension was filtrated through a pad of Celyte and solvent was evaporated.[423] The crude product was used for the next step of synthesis without any further purification. Yellow liquid. Yield = 50 %. ^{1}H NMR (300 MHz, $CDCl_3$) δ = 4.11 (q, *J* = 7.1 Hz, 2H), 2.76 – 2.52 (m, 4H), 2.19 (d, 2H), 2.00 (dq, *J* = 3.4 Hz, 2H), 1.83 (tdq, 1H), 1.39 (dtd, *J* = 3.4 Hz, 2H), 1.25 (d, *J* = 7.1 Hz, 3H). MS (APCI [+]) m/z $[M+H^+]^+$ calculated for $[C_9H_{17}O_2S]^+$ = 189.0, found 189.0. M = 188,29 g/mol.

2-(Tetrahydro-2*H*-thiopyran-4-yl)ethan-1-ol (10)[421]

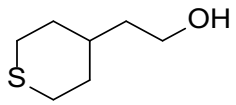

A solution of lithium-aluminium hydride 2M ($LiAlH_4$, 2.5 eq.) in tetrahydrofuran was added under N_2 atmosphere into a stirring solution of ethyl ester **9** in tetrahydrofuran at 0°C. The reaction was stirred at room temperature under inert atmosphere. Subsequently, the reaction mixture was cooled down to 0°C, diluted with diethyl ether, quenched with aqueous solution of Rochelle Salt and left to stir vigorously for 1.30 hours more. The organic phase was separated from the aqueous one, dried over Mg_2SO_4 and concentrated under reduced pressure.[424] The pure intermediate was used for the following reaction without performing any further purification. Yellow oil. Quantitative yield. ^{1}H NMR (300 MHz, $CDCl_3$) δ = 3.67 (t, 2H), 2.73 – 2.51 (m, 4H), 2.07 – 1.94 (m, 2H), 1.71 – 1.60 (m, 1H), 1.48 (ddd, 3H), 1.41 (s, 2H). MS (APCI [+]) m/z $[M+H^+]^+$ calculated for $[C_7H_{15}OS]^+$ = 147.0, found 146.9. M = 146,25 g/mol.

2-(Tetrahydro-2H-thiopyran-4-yl)ethyl methanesulfonate (11)[425]

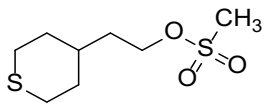

The corresponding alcohol **10** was converted in mesylated following the procedure **C**. The pure intermediated was obtained and used for the alkylation step without any further purification. Yellowish oil. Quantitative yield. ^{1}H NMR (300 MHz, $CDCl_3$) δ = 4.26 (t, 2H), 3.00 (s, 3H), 2.74 –

2.53 (m, 4H), 2.02 (dtt, 2H), 1.71 – 1.62 (m, 2H), 1.59 – 1.47 (m, 1H), 1.45 – 1.32 (m, 2H). MS (APCI [+]) m/z $[M+H^+]^+$ calculated for $[C_8H_{17}O_3S_2]^+$ = 225.0, found 225.0. M = 224,33 g/mol.

1-(2-Methoxyphenyl)-4-(2-(tetrahydro-2*H*-thiopyran-4-yl)ethyl)piperazine (12)

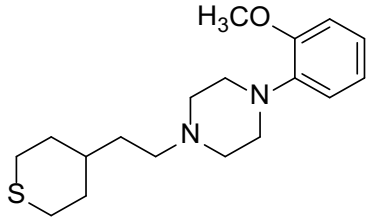

The mesylate **11** and 1-(2-methoxyphenyl) piperazine **3** were mixed in order to perform the alkylation with procedure **A**. The pure product was obtained through column chromatography in dichloromethane/methanol 98:2. Light yellow solid. Yield = 48 %. ^{1}H NMR (300 MHz, $CDCl_3$) δ = 7.03 – 6.82 (m, 4H Ar-Pip), 3.85 (s, 3H), 3.12 (d, 4H), 2.76 – 2.53 (m, 8H), 2.50 – 2.40 (m, 2H), 2.02 (ddd, 2H), 1.52 – 1.22 (m, 5H). ^{13}C NMR (75 MHz, $CDCl_3$) δ = 152.35, 141.31, 123.09, 121.10, 118.33, 111.25, 56.16, 55.45, 53.62, 50.59, 35.92, 34.37, 34.31, 28.79. Elemental analysis (calculated/found): %C 67.46/67.16, %H 8.81/8.82, %N 8.74/8.33 and %S 10/9.75; MS (APCI [+]) m/z $[M+H^+]^+$ calculated for $[C_{18}H_{29}N_2OS]^+$ = 321.2, found 319.9. mp = 57.1°C. M = 320.50 g/mol.

2-(1-Oxidotetrahydro-2*H*-thiopyran-4-yl)ethyl methanesulfonate (13)

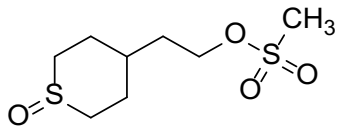

The mesylate intermediate with sulphide was oxidized according to procedure **C**. The intermediate was obtained without further purification and used for the next step of synthesis. Lilla oil. Yield = 63%. ^{1}H NMR (300 MHz, $CDCl_3$) δ = 4.36 – 4.21 (m, 2H), 3.32 (dq, 1H), 3.06 – 2.98 (m, 4H), 2.65 (td, 1H), 2.46 (td, 1H), 2.20 – 2.05 (m, 2H), 1.90 (dt, 1H), 1.85 – 1.64 (m, 4H). MS (APCI [+]) m/z $[M+H^+]^+$ calculated for $[C_8H_{17}O_4S_2]^+$ = 241.0, found 241.0. M = 240,33 g/mol.

4-(2-(4-(2-Methoxyphenyl)piperazin-1-yl)ethyl)tetrahydro-2*H*-thiopyran-1-oxide (14)

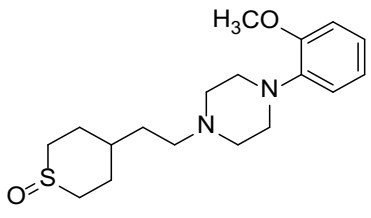

The alkylation was carried out between **13** and 1-(2-methoxyphenyl) piperazine **3** under the conditions of procedure **A**. The crude product was purified by column chromatography in dichloromethane/methanol 95:5. Yellow solid. Yield = 40 %. ^{1}H NMR (300 MHz, $CDCl_3$) δ = 7.06 – 6.80 (m, 4H Ar-Pip), 3.91 – 3.82 (m, 3H), 3.30 (ddd, 1H), 3.17 – 2.96 (m, 5H), 2.71 – 2.61 (m, 4H), 2.54 – 2.38 (m, 3H), 2.31 – 2.05 (m, 3H), 1.81 – 1.68 (m, 1H), 1.62 – 1.33 (m, 4H). ^{13}C NMR (75 MHz, $CDCl_3$) δ = 152.26, 141.20, 123.01, 120.99, 118.20, 111.17, 56.37, 55.85, 55.36, 53.56, 50.59, 45.90, 34.65, 34.09, 33.62, 32.25, 28.29, 22.11. HPLC-MS (ESI [+]) m/z $[M+H^+]^+$ = 337.20 (96.9 %); MS (APCI [+]) m/z $[M+H^+]^+$ calculated for $[C_{18}H_{29}N_2O_2S]^+$ = 337.20, found 337.2. mp = 113.8°C. M = 336.49 g/mol.

2-(1,1-Dioxidotetrahydro-2*H*-thiopyran-4-yl)ethyl methanesulfonate (15)[421]

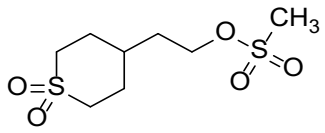

The mesylate bearing sulfoxide (**13**) was oxidized once more according to procedure **C**. There was no need to perform further purification and the crude intermediate was used directly for the following alkylation step. Light pink oil. Yield = 67 %. ^{1}H NMR (300 MHz, $CDCl_3$) δ = 4.04 (t, 2H), 3.12 – 3.02 (m, 3H), 3.02 (d, 3H), 3.00 – 2.97 (m, 1H), 1.94 (dddd, 2H), 1.74 – 1.63 (m, 4H), 1.60 – 1.53 (m, 1H). MS (APCI [+]) m/z $[M+H^+]^+$ calculated for $[C_8H_{17}O_5S_2]^+$ = 257.0, found 257.0. M = 256,33 g/mol.

4-(2-(4-(2-Methoxyphenyl)piperazin-1-yl)ethyl)tetrahydro-2*H*-thiopyran1,1-dioxide (16)

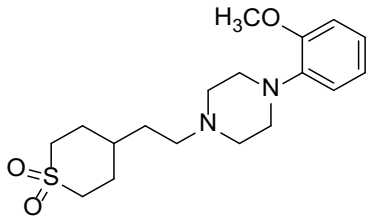

Piperazine was alkylated by the mesylate with sulfone **15** using procedure **A**. The crude product was purified by column chromatography in dichloromethane/methanol 95:5. Light red solid. Yield = 44%. ^{1}H NMR (300 MHz, $CDCl_3$) δ = 7.04 – 6.83 (m, 4H Ar-Pip), 3.86 (s, 3H), 3.15 – 2.90 (m, 8H), 2.65 (t, 4H), 2.49 – 2.41 (m, 2H), 2.17 – 2.07 (m, 2H), 1.89 (qd, 2H), 1.62 – 1.53 (m, 2H), 1.25 (s, 1H). ^{13}C NMR (75 MHz, $CDCl_3$) δ = 152.37, 141.26, 123.17, 121.12, 118.32, 111.30, 56.23, 55.49, 53.64, 51.06, 50.65, 33.83, 32.12, 30.15. HPLC-MS (ESI [+]) m/z $[M+H^+]^+$ = 353.11 (100 %); MS (APCI

[+]) m/z $[M+H^+]^+$ calculated for $[C_{18}H_{29}N_2O_3S]^+$ = 353.2, found 353.1. mp = 129.5°C. M = 352.49 g/mol.

2-(4-Aminophenyl)ethan-1-ol (18)

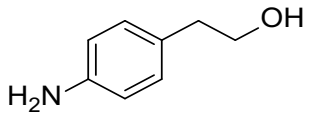

The starting material 2-(4-nitrophenyl)ethan-1-ol **17** was reduced following the procedure **D**. The crude product was used for the following step of synthesis with no further purification. Orange oil. Yield = 92%. ^{1}H NMR (300 MHz, DMSO-d6) δ = 6.92 – 6.80 (m, 2H Ar), 6.53 – 6.44 (m, 2H Ar), 5.06 – 4.75 (m, 2H NH_2), 4.51 (t, 1H OH), 3.48 (td, *J* = 7.4 2H), 2.54 (d, *J* = 7.4 Hz, 2H). MS (APCI [+]) m/z $[M+H^+]^+$ calculated for $[C_8H_{12}NO]^+$ = 138.0, found 137.9. M = 137,18 g/mol.

2-(2-Aminobenzo[d]thiazol-6-yl)ethan-1-ol (19)[426]

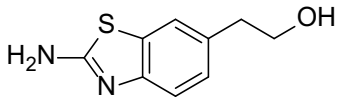

A solution of 2-(4-aminophenyl)ethan-1-ol **18** (1 eq.) and ammonium thiocyanate (NH_4SCN, 3 eq.) in ethanol was stirred for one hour at room temperature. After that, a bromine solution (Br_2, 1 eq.) was added dropwise at 0°C. After completion, the mixture was stirred for another three hours at room temperature.[427] The reaction mixture was quenched in aqueous solution of NaOH 6 M, adjusted to pH = 7, diluted with water and extracted with dichloromethane three times. The organic layers were combined, dried with Mg_2SO_4, filtered off and the solvent was evaporated under vacuum. The crude intermediate was purified by column chromatography in dichloromethane/ethyl acetate 1:1 Yellowish oil. Yield = 57 %. ^{1}H NMR (300 MHz, DMSO-d6) δ = 7.47 (d, 1H Ar), 7.33 (s, 2H NH_2), 7.22 (d, *J* = 8.1 Hz, 1H Ar), 7.04 (dd, *J* = 8.1, 1H Ar), 4.61 (t, 1H OH), 3.58 (td, *J* = 7.1, 2H), 2.71 (t, *J* = 7.1 Hz, 2H). MS (APCI [+]) m/z $[M+H^+]^+$ calculated for $[C_9H_{12}N_2OS]^+$ = 195.0, found 195.1. M = 194,25 g/mol.

6-(2-Chloroethyl)benzo[d]thiazol-2-amine (20)

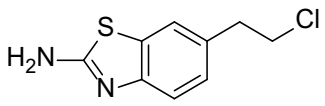

Aminothiazole ethyl alcohol **19** (1 eq.), triphenylphosphine (Ph_3P, 1.2 eq.), tetrabutylammonium iodide (1.2 eq.) were mixed in dichloroethane under N_2 atmosphere. The reaction mixture was stirred at 80°C for 12 hours. Afterwards, the solvent was evaporated, the crude intermediate was solubilized

in dichloromethane and washed with water and brine. The organic phase was dried over Mg_2SO_4, filtered and concentrated under vacuum.[276] The pure intermediate was obtained by column chromatography in hexane/ethyl acetate 1:1. Brown oil. Yield = 91 %. ^{1}H NMR (300 MHz, $CDCl_3$) δ = 7.53 – 7.42 (m, 2H Ar), 7.16 (dd, 1H Ar), 5.32 (s, 2H NH_2), 3.72 (t, *J* = 7.4 Hz, 2H), 3.11 (t, *J* = 7.4 Hz, 2H). MS (APCI [+]) m/z $[M+H^+]^+$ calculated for $[C_9H_{10}ClN_2S]^+$ = 213.0, found 213.1. M = 212,70 g/mol.

6-(2-Chloroethyl)benzo[d]thiazole (21)[426]

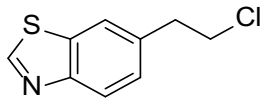

Isopentyl nitrite (2 eq.) was added dropwise to a stirring solution of aminothiazole ethyl chloride (**20**) in tetrahydrofuran at room temperature. The reaction was left to stir at reflux for 4 hours. Then, the mixture was poured into iced water and extracted with ethyl acetate. The organic phase was washed with Brine, dried over Mg_2SO_4 and concentrated under reduced pressure.[428] The crude residue was purified by flash chromatography with Biotage Sfär SiO_2 in dichloromethane/methanol from 1 % to 10 % of methanol. Brown oil. Yield = 45 %. ^{1}H NMR (300 MHz, $CDCl_3$) δ = 8.96 (s, 1H Ar-thiaz), 8.08 (d, *J* = 8.4 Hz, 1H Ar), 7.82 (d, *J* = 1.7 Hz, 1H Ar), 7.37 (dd, *J* = 8.4, 1.7 Hz, 1H Ar), 3.78 (t, *J* = 7.2 Hz, 2H), 3.21 (t, *J* = 7.2 Hz, 2H). MS (APCI [+]) m/z $[M+H^+]^+$ calculated for $[C_9H_8ClNS]^+$ = 198.0, found 198.1. M = 197,68 g/mol.

6-(2-(4-(2-Methoxyphenyl)piperazin-1-yl)ethyl)benzo[d]thiazole (22)

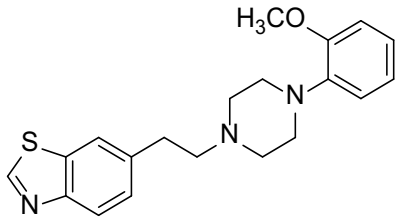

Adapted from procedure **A**, thiazole ethyl chloride **21** (1 eq.) and 1-(2-methoxyphenyl) piperazine **3** (1.5 eq.) were mixed with KI (4 eq.) and K_2CO_3 (10 eq.) in ACN. The crude material was purified by flash chromatography with Biotage Sfär SiO_2 in dichloromethane/methanol from 0 % to 10 % of methanol. Yellow oil. Yield = 43%. ^{1}H NMR (300 MHz, $CDCl_3$) δ = 8.37 (s, 1H), 7.50 (d, 1H Ar), 7.26 (s, 1H Ar), 6.84 (dd, 1H Ar), 6.51 – 6.26 (m, 4H Ar-Pip), 3.31 (s, 3H), 2.59 (t, 4H), 2.45 (dd, 2H), 2.19 (dt, 6H). ^{13}C NMR (75 MHz, $CDCl_3$) δ = 153.28, 152.28, 151.86, 141.27, 138.25, 133.99, 127.46, 123.33, 123.00, 121.44, 121.02, 118.24, 111.19, 60.62, 55.37, 53.48, 50.67, 33.59. HPLC-

MS (ESI [+]) m/z $[M+H^+]^+$ = 354.18 (100 %); MS (APCI [+]) m/z $[M+H^+]^+$ calculated for $[C_{20}H_{24}N_3OS]^+$ = 354.2, found 354.0. M = 353,48 g/mol.

6-(2-(4-(2-Methoxyphenyl)piperazin-1-yl)ethyl)benzo[d]thiazol-2-amine (23)

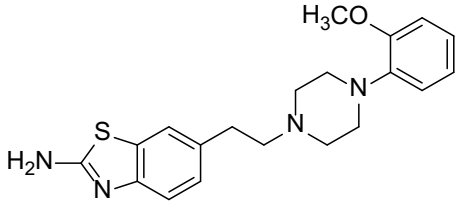

Adapted from procedure **A**, aminothiazole ethyl chloride **21** (1 eq.) and piperazine **3** (1.5 eq.) were mixed with KI (4 eq.) and K_2CO_3 (10 eq.) in ACN. The crude mixture was purified by flash chromatography with Biotage Sfär SiO2 10 gr in dichloromethane/methanol from 0 % to 10 % of methanol. Yellow solid. Yield = 30%. ^{1}H NMR (300 MHz, $CDCl_3$) δ = 7.48 – 7.44 (m, 2H Ar), 7.17 (dd,1H Ar), 7.04 – 6.84 (m, 4H Ar-Pip), 5.31 (d, 2H NH_2), 3.87 (s, 3H), 3.15 (s, 4H), 2.95 – 2.88 (m, 2H), 2.80 – 2.66 (m, 6H). ^{13}C NMR (75 MHz, $CDCl_3$) δ = 165.48, 152.39, 150.60, 141.34, 134.65, 131.99, 126.97, 123.14, 121.14, 120.90, 119.20, 118.38, 111.29, 60.95, 55.48, 53.57, 50.69, 44.50, 33.43. HPLC-MS (ESI [+]) m/z $[M+H^+]^+$ = 369.58 (97.4 %); MS (APCI [+]) m/z $[M+H^+]^+$ calculated for $[C_{20}H_{25}N_4OS]^+$ = 369.2, found 369.1. mp = 210.1°C. M = 368,50 g/mol.

N-(6-(2-(4-(2-Methoxyphenyl)piperazin-1-yl)ethyl)benzo[d]thiazol-2-yl)acetamide (24)

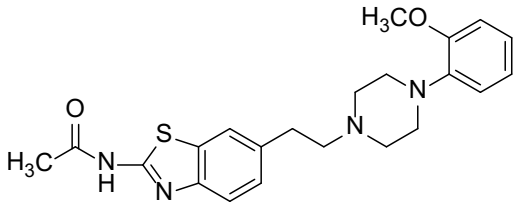

Aminothiazole derivative with free NH_2 (**23**) was acylated by acetic anhydride according to procedure **E**. The product was obtained without any further purification. Brown solid. Quantitative yield. ^{1}H NMR (300 MHz, $CDCl_3$) δ = 10.64 (s, 1H CONH), 7.67 (d, 2H Ar), 7.31 (dd, 1H Ar), 7.05 – 6.85 (m, 4H Ar-Pip), 3.87 (s, 3H), 3.15 (s, 4H), 2.98 (dd, 2H), 2.86 – 2.70 (m, 6H), 2.30 (s, 3H). ^{13}C NMR (75 MHz, $CDCl_3$) δ = 167.78, 158.43, 151.24, 144.82, 140.14, 135.40, 130.86, 126.48, 122.03, 120.25, 120.00, 118.99, 117.23, 110.16, 59.52, 54.34, 52.33, 49.45, 32.29, 22.42. HPLC-MS (ESI [+]) m/z $[M+H^+]^+$ = 411.08 (100 %); MS (APCI [+]) m/z $[M+H^+]^+$ calculated for $[C_{22}H_{27}N_4O_2S]^+$ = 411.2, found 411.2. mp = 182.5°C. M = 410,54 g/mol.

3-Methoxy-*N*-(6-(2-(4-(2-methoxyphenyl)piperazin-1-yl)ethyl)benzo[d]thiazol-2-yl)benzamide (25)

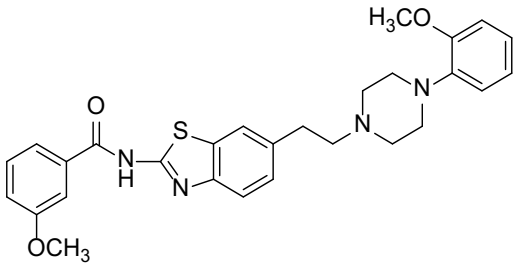

The acylation of free NH_2-compound (**23**) with 3-methoxy benzoyl chloride was performed using procedure **E**. The crude material was purified by column chromatography in dichloromethane/ammonia in methanol 98:2. White solid. Yield = 45 %. ^{1}H NMR (300 MHz, $CDCl_3$) δ = 11.48 (s, 1H CONH), 7.62 (d, 1H Ar), 7.52 – 7.42 (m, 2H Ar), 7.31 – 6.72 (m, 8H Ar-Bmd/Ar-Pip), 3.80 (s, 3H), 3.67 (s, 3H), 3.07 (s, 4H), 2.88 (dd, 2H), 2.77 – 2.57 (m, 6H). ^{13}C NMR (75 MHz, $CDCl_3$) δ = 165.76, 160.03, 159.08, 152.28, 146.28, 141.28, 136.58, 133.41, 132.17, 130.03, 127.24, 122.98, 121.02, 120.48, 119.88, 119.71, 118.24, 112.65, 111.18, 60.69, 55.38, 53.48, 50.67, 33.55. HPLC-MS (ESI [+]) m/z $[M+H^+]^+$ = 503.20 (100 %); MS (APCI [+]) m/z $[M+H^+]^+$ calculated for $[C_{28}H_{31}N_4O_3S]^+$ = 503.2, found 502.9. mp = 91.1°C. M = 502.63 g/mol.

4-Cyano-*N*-(6-(2-(4-(2-methoxyphenyl)piperazin-1-yl)ethyl)benzo[d]thiazol-2-yl)benzamide (26)

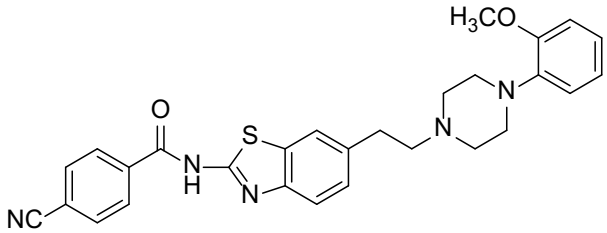

Aminothiazole derivative **23** was obtained by acylating the free amino derivative with 4-cyano benzoyl chloride following the conditions of procedure **E**. The crude product was purified by column chromatography in dichloromethane/ammonia in methanol 98:2. Yellow solid. Yield = 55 %. ^{1}H NMR (300 MHz, $CDCl_3$) δ = 8.08 – 7.99 (m, 2H Ar-Bmd), 7.72 – 7.62 (m, 3H Ar-Bmd/CONH), 7.26 (d, *J* = 8.3 Hz, 1H Ar), 7.16 (dd, *J* = 8.3, 2H Ar), 6.98 – 6.77 (m, 4H Ar-Pip), 3.81 (s, 3H), 3.09 (s, 4H), 2.93 (t, 2H), 2.86 – 2.59 (m, 6H). ^{13}C NMR (151 MHz, $CDCl_3$) δ = 164.74, 159.55, 152.28, 145.30, 141.22, 136.14, 132.69, 131.86, 128.63, 127.55, 123.04, 121.34, 121.03, 119.93, 118.26, 117.63, 116.38, 111.20, 103.27, 60.53, 55.39, 53.45, 50.60, 33.47. HPLC-MS (ESI [+]) m/z $[M+H^+]^+$

= 498.19 (100 %); MS (APCI [+]) m/z $[M+H^+]^+$ calculated for $[C_{28}H_{28}N_5O_2S]^+$ = 498.1, found 497.8. mp = 229°C. M = 497,62 g/mol.

2-(4-(Methylthio)phenyl)ethan-1-ol (28)[429]

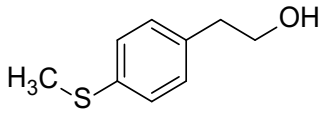

The starting material 2-(4-(methylthio)phenyl)acetic acid **27** (1eq.) was solubilized in tetrahydrofuran, in which a solution of borane-dimethylsulfide complex (1.5 eq.) in tetrahydrofuran 2.0 M was added dropwise under nitrogen atmosphere. The mixture of reaction was stirred for 4 hours at room temperature. Then, the mixture was cooled down in ice bath and a saturated solution of ammonium chloride was added, the solution was left to stir for additional 30 minutes at room temperature.[430] After that, the reaction solution was extracted with dichloromethane two times, the organic layers were combined, dried over Mg_2SO_4 and concentrated under reduced pressure. The obtained intermediate was used for the next step of synthesis without further purification. Colourless oil. Quantitative yield. ^{1}H NMR (300 MHz, $CDCl_3$) δ = 7.28 – 7.12 (m, 4H Ar), 3.84 (t, *J* = 6.5 Hz, 2H), 2.83 (t, *J* = 6.5 Hz, 2H), 2.47 (s, 3H). MS (APCI [+]) m/z $[M+H^+]^+$ calculated for $[C_9H_{13}OS]^+$ = 169.1, found 169.0. M = 168,25 g/mol.

4-(Methylthio)phenethyl methanesulfonate (29)[429]

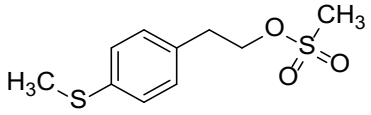

2-(4-(Methylthio)phenyl)ethan-1-ol **28** was treated following the procedure **C**. The obtained intermediate was used for the next step of synthesis without further purification. Light yellow oil. Quantitative yield. ^{1}H NMR (300 MHz, $CDCl_3$) δ = 7.25 – 7.13 (m, 4H Ar), 4.39 (t, *J* = 6.9 Hz, 2H), 3.02 (t, *J* = 6.9 Hz, 2H), 2.87 (s, 3H), 2.47 (s, 3H). MS (APCI [+]) m/z $[M+H^+]^+$ calculated for $[C_{10}H_{15}O_3S_2]^+$ = 169.1, found 169.0. M = 246,34 g/mol.

1-(2-Methoxyphenyl)-4-(4-(methylthio)phenethyl)piperazine (30)

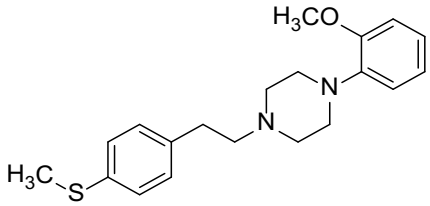

The product was synthetized from the corresponding mesylate **29** with procedure **A**. The crude material was purified with flash chromatography using the cartridge Biotage Sfär SiO_2 25gr in ethyl acetate/hexane from 30%to 60% of ethyl acetate. Light red solid. Yield = 51 %. ^{1}H NMR (300 MHz, $CDCl_3$) δ = 7.24 – 7.13 (m, 4H Ar), 7.05 – 6.84 (m, 4H Ar-Pip), 3.87 (s, 3H), 3.19 (s, 4H), 2.88 (6H), 2.77 – 2.69 (m, 2H), 2.47 (s, 3H). ^{13}C NMR (75 MHz, $CDCl_3$) δ = 152.37, 149.46, 141.38, 141.10, 129.39, 127.30, 123.32, 121.18, 118.48, 111.32, 60.39, 55.51, 53.44, 50.31, 42.67, 16.37. HPLC-MS (ESI [+]) m/z $[M+H^+]^+$ = 343.15 (98.7 %); MS (APCI [+]) m/z $[M+H^+]^+$ calculated for $[C_{20}H_{27}N_2OS]^+$ = 343.2, found 343.0. mp = 79°C. M = 342.50 g/mol.

1-(2-Methoxyphenyl)-4-(4-(methylsulfinyl)phenethyl)piperazine (31)

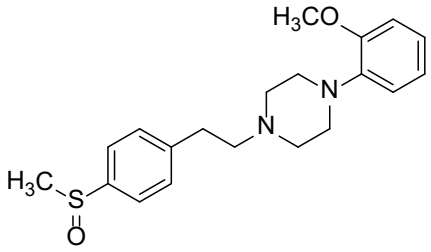

This derivative was obtained oxidizing sulphide **30** according to procedure **B**. The pure product was obtained by flash chromatography with the cartridge Biotage Sfär SiO_2 25gr and dichloromethane/methanol from 0% until 12% of methanol as eluent. White solid. Yield = 19%. ^{1}H NMR (300 MHz, $CDCl_3$) δ = 7.23 (s, 4H Ar), 7.10 – 6.87 (m, 4H Ar-Pip), 3.87 (s, 3H), 3.75 – 3.47 (m, 8H), 3.41 – 3.27 (m, 4H), 2.47 (s, 3H). ^{13}C NMR (75 MHz, $CDCl_3$) δ = 152.18, 139.78, 137.08, 134.24, 129.60, 127.34, 124.08, 121.34, 118.88, 111.33, 72.61, 64.86, 55.55, 45.19, 28.30, 16.13. HPLC-MS (ESI [+]) m/z $[M+H^+]^+$ = 359.07 (100 %); MS (APCI [+]) m/z $[M+H^+]^+$ calculated for $[C_{20}H_{27}N_2O_2S]^+$ = 359.2, found 359.1. mp = 118°C. M = 358.50 g/mol.

4-(Methylsulfinyl)phenethyl methanesulfonate (32)

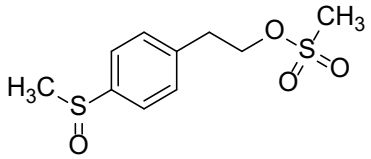

Methanesulfonate with sulphide **29** was oxidized with the conditions of procedure **B** in order to have number. The obtained intermediate was used for the following step of synthesis with no further purification. Colourless oil. Yield = 81 %. ^{1}H NMR (300 MHz, $CDCl_3$) δ = 7.65 – 7.59 (m, 2H Ar), 7.46 – 7.38 (m, 2H Ar), 4.44 (t, *J* = 6.7 Hz, 2H), 3.13 (t, *J* = 6.7 Hz, 2H), 2.92 (s, 3H), 2.73 (s, 3H). MS (APCI [+]) m/z $[M+H^+]^+$ calculated for $[C_{10}H_{15}O_4S_2]^+$ = 263.0, found 263,1. M = 262,34 g/mol.

4-(Methylsulfonyl)phenethyl methanesulfonate (33)

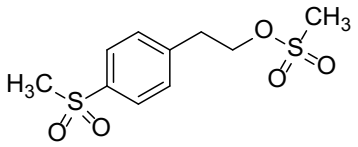

This intermediate was obtained by the oxidation of the sulfoxide with the mesylate **32** following procedure **B**. The obtained compound was used for the following step of synthesis with no further purification. Yellowish oil. Yield = 86 %. ^{1}H NMR (300 MHz, $CDCl_3$) δ = 7.91 (dd, 2H Ar), 7.43 (t, 2H Ar), 4.62 (td, 2H), 3.45 (t, 2H), 2.90 (d, 3H), 2.74 (s, 3H). MS (APCI [+]) m/z $[M+H^+]^+$ calculated for $[C_{10}H_{15}O_5S_2]^+$ = 279.0, found 279,0. M = 278,34 g/mol.

1-(2-Methoxyphenyl)-4-(4-(methylsulfonyl)phenethyl)piperazine (34)

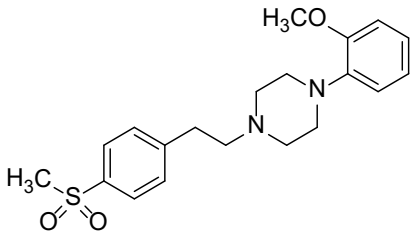

1-(2-Methoxyphenyl) piperazine **3** was alkylated by the mesylate **33** according to procedure **A**. The crude product was purified by flash chromatography in dichloromethane/methanol from 0 % to 10 % with cartridge Biotage Sfär SiO_2 25gr. White solid. Yield = 29%. ^{1}H NMR (300 MHz, $CDCl_3$) δ = 7.92 – 7.80 (m, 2H Ar), 7.43 (d, 2H Ar), 7.05 – 6.82 (m, 4H Ar-Pip), 3.86 (s, 3H), 3.13 (t, 4H), 3.04 (s, 3H), 2.95 (dd, 2H), 2.72 (dt, 6H). ^{13}C NMR (75 MHz, $CDCl_3$) δ = 152.34, 147.12, 141.22, 138.45, 129.81, 127.61, 123.16, 121.10, 118.32, 111.28, 59.77, 55.47, 53.46, 50.65, 44.67, 33.52. HPLC-MS (ESI [+]) m/z $[M+H^+]^+$ = 375.18 (95.2 %); MS (APCI [+]) m/z $[M+H^+]^+$ calculated for $[C_{20}H_{27}N_2O_3S]^+$ = 375.2, found 375.2. mp = 120.8°C. M = 374.50 g/mol.

4-(S-Methyl-*N*-(2,2,2-trifluoroacetyl)sulfonimidoyl)phenethyl methanesulfonate (35)

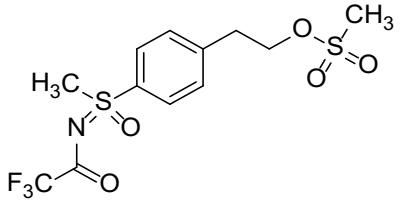

The BOLM synthesis of sulfoximine was performed on the corresponding sulfoxide with mesylate **32** following procedure **F**. The pure intermediate was obtained by flash chromatography with Biotage

Sfär SiO_2 25 gr in dichloromethane/methanol from 0 % to 10 %. Colourless oil. Yield = 75 %. ^{1}H NMR (300 MHz, $CDCl_3$) δ = 7.98 – 7.92 (m, 2H Ar), 7.56 – 7.51 (m, 2H Ar), 4.47 (t, *J* = 6.5 Hz, 2H), 3.45 (s, 3H), 3.19 (t, *J* = 6.5 Hz, 2H), 2.95 (s, 3H). ^{19}F NMR (282 MHz, $CDCl_3$) δ = -75.98 (s, 3F). MS (APCI [+]) m/z $[M+H^+]^+$ calculated for $[C_{12}H_{15}F_3NO_5S_2]^+$ = 374.0, found 373.9. M = 373,36 g/mol.

Imino(4-(2-(4-(2-methoxyphenyl)piperazin-1-yl)ethyl)phenyl)(methyl)-λ^6-sulfanone (36)

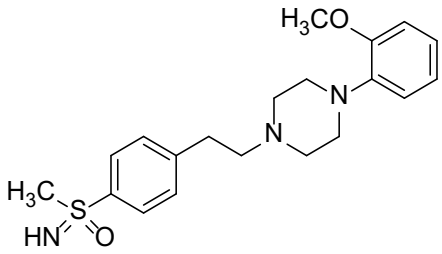

The derivative was obtained by the alkylation between piperazine **3** and mesylate with sulfoximine **35** using procedure **A**. The crude mixture was purified by flash chromatography with Biotage Sfär SiO_2 25 gr in dichloromethane/methanol from 0 to 15 %. Brown solid. Yield = 32%. ^{1}H NMR (300 MHz, $CDCl_3$) δ = 8.00 – 7.89 (m, 2H Ar), 7.48 – 7.38 (m, 2H Ar), 7.06 – 6.84 (m, 4H Ar-Pip), 3.87 (s, 3H), 3.12 (d, 7H), 2.95 (dd, 2H), 2.88 – 2.66 (m, 7H). ^{13}C NMR (75 MHz, $CDCl_3$) δ = 152.36, 146.09, 141.50, 141.07, 129.76, 128.06, 123.32, 121.16, 118.42, 111.32, 59.78, 55.50, 53.43, 50.45, 46.41, 33.22. HPLC-MS (ESI [+]) m/z $[M+H^+]^+$ = 374.19 (95.2 %); MS (APCI [+]) m/z $[M+H^+]^+$ calculated for $[C_{20}H_{28}N_3O_2S]^+$ = 374.2, found 374.0. mp = 124°C. M = 373.52 g/mol.

N-((4-(2-(4-(2-Methoxyphenyl)piperazin-1-yl)ethyl)phenyl)(methyl)(oxo)-λ^6-sulfaneylidene)acetamide (37)

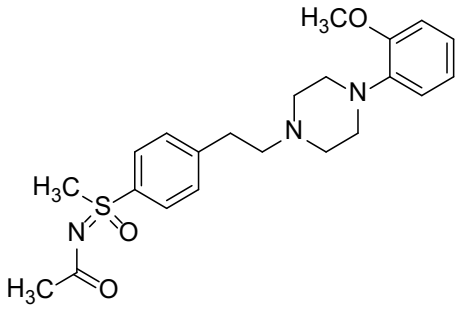

Free *NH*-sulfoximine compound **36** and acetic anhydride were used to obtain this derivative following the procedure **E**. The pure product was obtained by column chromatography with dichloromethane/ammonia in methanol 98:2. White sticky oil. Yield = 47 %. ^{1}H NMR (300 MHz, $CDCl_3$) δ = 7.95 – 7.84 (m, 2H Ar), 7.49 – 7.41 (m, 2H Ar), 7.05 – 6.83 (m, 4H Ar-Pip), 3.86 (s, 3H),

3.32 (s, 3H), 3.12 (s, 4H), 2.93 (dd, 2H), 2.71 (dt, 6H), 2.14 (s, 3H). ^{13}C NMR (75 MHz, $CDCl_3$) δ = 180.36, 152.35, 147.36, 141.27, 136.39, 130.11, 127.31, 123.14, 121.10, 118.31, 111.29, 59.74, 55.47, 53.47, 50.70, 44.30, 33.52, 26.92. HPLC-MS (ESI [+]) m/z $[M+H^+]^+$ = 416.20 (96.9 %); MS (APCI [+]) m/z $[M+H^+]^+$ calculated for $[C_{22}H_{30}N_3O_3S]^+$ = 416.2, found 415.8. M = 415,55 g/mol.

Methyl 2-(4-(methylthio)phenyl)acetate (38)[431]

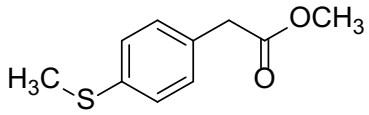

To a stirring solution of 2-(4-(methylthio)phenyl)acetic acid **27** (1eq.) in methanol, thionyl chloride was added dropwise ($SOCl_2$, 1.5 eq.). The reaction was stirred at room temperature for one hour. Then, triethylamine (1.5 eq.) was added and a saturated solution of $NaHCO_3$ was added to reach pH values of 7-8. The mixture solution was extracted with dichloromethane three times, dried with Mg_2SO_4 and concentrated under reduced pressure.[432] The methyl-ester intermediate was used for the next step of synthesis without further purification. Colourless oil. Quantitative yield. ^1H NMR (600 MHz, $CDCl_3$) δ = 7.23 – 7.18 (m, 4H Ar), 3.69 (s, 3H), 3.59 (s, 2H), 2.47 (s, 3H). MS (APCI [+]) m/z $[M+H^+]^+$ calculated for $[C_{10}H_{13}O_2S]^+$ = 197.0, found 196.9. M = 196,26 g/mol.

Methyl 2-(4-(methylsulfinyl)phenyl)acetate (39)

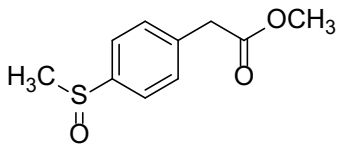

The sulphide intermediate **38** was oxidized following the conditions of procedure **B**. Light white oil. Yield = 75 %. ^1H NMR (300 MHz, $CDCl_3$) δ = 7.58 – 7.52 (m, 2H Ar), 7.41 – 7.35 (m, 2H Ar), 3.64 (s, 3H), 3.63 (s, 2H), 2.65 (s, 3H). MS (APCI [+]) m/z $[M+H^+]^+$ calculated for $[C_{10}H_{13}O_3S]^+$ = 213.0, found 213.1. M = 212,26 g/mol.

2-(4-(Methylsulfinyl)phenyl)acetaldehyde (40)

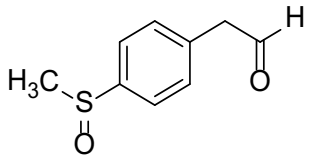

Two necks round bottom flaks was charged with a solution of ester **39** (1 eq.) in toluene. To this, a solution of diisobutylaluminiumhydride 1 M in toluene (2 eq.) was added under N_2 atmosphere at -78°C. The reaction was left to stir at -78°C for 14 hours under N_2 atmosphere. A Rochelle salt solution

was used to quench the reaction and the mixture was left to stir vigorously at room temperature for one more hour. After that, the reaction solution was extracted with ethyl acetate 4 times. The organic layers were combined, dried over Mg_2SO_4 and concentrated under reduced pressure.[433] The crude mixture was purified by flash chromatography using Biotage Sfär SiO_2 25 gr as a cartridge and dichloromethane/methanol from 1 % to 15 % of methanol as eluent. Yellow liquid. Yield = 30 %. ^{1}H NMR (300 MHz, $CDCl_3$) δ = 9.79 (t, *J* = 2.0 Hz, 1H), 7.69 – 7.62 (m, 2H Ar), 7.43 – 7.36 (m, 2H Ar), 3.80 (d, *J* = 2.0 Hz, 2H), 2.73 (s, 3H). MS (APCI [+]) m/z $[M+H^+]^+$ calculated for $[C_9H_{11}O_2S]^+$ = 183.0, found 183.1. M = 182,24 g/mol.

2,2,2-Trifluoro-*N*-(methyl(oxo)(4-(2-oxoethyl)phenyl)-λ^6-sulfaneylidene)acetamide (41)

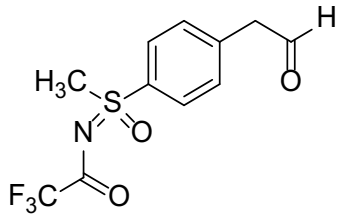

The BOLM reaction for sulfoximines was performed on the corresponding sulfoxide **40** under conditions of procedure **F**. The pure intermediate was obtained by flash chromatography with Biotage Sfär SiO_2 5 gr in dichloromethane/methanol from 0 % to 10 % of methanol. Yellowish liquid. Yield = 16 %. ^{1}H NMR (300 MHz, $CDCl_3$) δ 9.74 (t, *J* = 6.0 Hz, 1H), 7.76 – 7.71 (m, 2H Ar), 7.45 (dt, 2H Ar), 3.83 (dt, *J* = 6.0 Hz, 2H), 3.21 (s, 3H). ^{19}F NMR (282 MHz, $CDCl_3$) δ = -71.09. (s, 3F). MS (APCI [+]) m/z $[M+H^+]^+$ calculated for $[C_{11}H_{11}F_3NO_3S]^+$ = 294.0, found 294.0. M = 293,26 g/mol.

2,2,2-Trifluoro-*N*-((4-(2-(4-(2-methoxyphenyl)piperazin-1-yl)ethyl)phenyl)(methyl)(oxo)-l6-sulfaneylidene)acetamide (42)

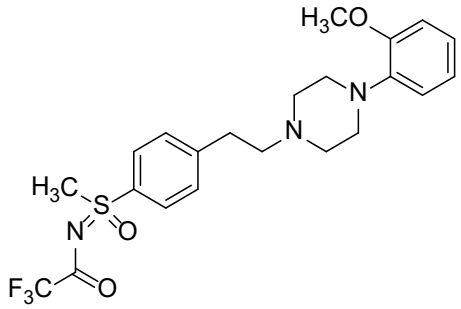

The sulfoximine with aldehyde function **41** and 1-(2-methoxyphenyl) piperazine were mixed in dichloroethane and treated with $NaBH(OAc)_3$ and acetic acid. The reaction was left to stir under N_2 atmosphere for 16 hours.[328] The solvent was evaporated and the crude material was directly purified

by flash chromatography with Biotage Sfär SiO_2 5 gr in ethyl acetate/dichloromethane from 60 % to 40 % of ethyl acetate. Yellow sticky oil. Yield = 38 %. ^{1}H NMR (600 MHz, $CDCl_3$) δ = 7.93 – 7.88 (m, 2H Ar), 7.55 – 7.48 (m, 2H Ar), 7.01 (ddd, 1H Ar-Pip), 6.97 – 6.91 (m, 2H Ar-Pip), 6.87 (dd, 1H Ar-Pip), 3.87 (s, 3H), 3.44 (s, 3H), 3.13 (s, 4H), 2.97 (dd, 2H), 2.82 – 2.68 (m, 6H). ^{19}F NMR (565 MHz, $CDCl_3$) δ = -75.96 (s, 3F). ^{13}C NMR (151 MHz, $CDCl_3$) δ = 152.39, 148.73, 141.23, 134.33, 130.55, 127.38, 123.24, 121.15, 118.37, 117.02, 115.11, 111.33, 59.57, 55.51, 53.48, 50.69, 44.51, 33.54. HPLC-MS (ESI [+]) m/z $[M+H^+]^+$ = 470.06 (95.8 %); MS (APCI [+]) m/z $[M+H^+]^+$ calculated for $[C_{22}H_{27}F_3N_3O_3S]^+$ = 470.2, found 470.0. M = 469,52 g/mol.

1-(2-Methoxyphenyl)-4-(2-nitrophenethyl)piperazine hydrochloride (45)

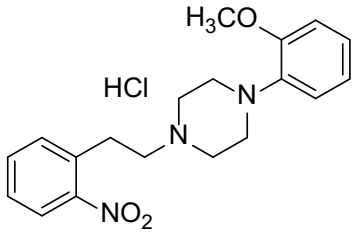

1-(2-Bromoethyl)-2-nitrobenzene (**43**) and 1-(2-methoxyphenyl) piperazine were mixed together in order to obtain this derivative adapting procedure **A** by using microwave reactor and dimethylformamide as solvent. The microwave reaction was stirred for 5 minutes at 130°C. The crude oil was purified by column chromatography in SiO_2 with dichloromethane/methanol 98:2. Light yellow oil. Yield = 50%. The product was solubilized in Et_2O and a solution of HCl in dioxane (2 M) was added drop by drop. A white precipitate of HCl salt was obtained. ^{1}H-NMR (300 MHz, $CDCl_3$) δ = 12.98 (s, 1H), 7.91 (dd, 1H Ar), 7.53 (td, 1H Ar), 7.44 – 7.32 (m, 2H Ar), 7.04 – 6.83 (m, 4H Ar-Pip), 3.87 (s, 3H), 3.75 – 3.46 (m, 8H), 3.38 (s, 2H), 3.24 (s, 2H). ^{13}C-NMR (75 MHz, $CDCl_3$) δ = 159.56, 149.63, 134.58, 133.93, 129.04, 126.03, 125.45, 124.75, 121.48, 119.32, 118.21, 111.70, 57.60, 55.70, 52.54, 47.69, 28.59. HPLC-MS (ESI [+]) m/z $[M+H^+]^+$ = 342.17 (100 %); MS (APCI [+]) m/z $[M+H^+]^+$ calculated for $[C_{19}H_{24}N_3O_3]^+$: 342.1, found 342.2. M = 377.41 g/mol (HCl salt) mp = 203-205 °C (Et_2O).

1-(2-Methoxyphenyl)-4-(3-nitrophenethyl)piperazine hydrochloride (46)

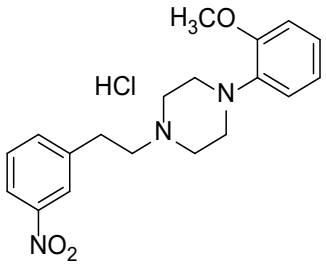

1-(2-Bromoethyl)-3-nitrobenzene (**44**) and 1-(2-methoxyphenyl) piperazine were mixed together in order to obtain this derivative adapting procedure **A** by using microwave reactor and dimethylformamide as solvent. The microwave reaction was stirred for 5 minutes at 130°C. The pure product was obtained by purification through column chromatography in SiO_2 with dichloromethane/methanol 98:2. Yellow oil. Yield = 60%. The product was solubilized in Et_2O and a solution of HCl in dioxane (2 M) was added drop by drop. A white precipitate of HCl salt was obtained. ^{1}H-NMR (300 MHz, $CDCl_3$) δ = 12.98 (s, 1H), 8.15 – 8.04 (m, 2H Ar), 7.57 (dt, 1H Ar), 7.46 (t, 1H Ar), 7.06 – 6.83 (m, 4H Ar-Pip), 3.87 (s, 3H), 3.18 – 3.09 (m, 4H), 2.96 (dd, 2H), 2.78 – 2.70 (m, 6H). ^{13}C-NMR (75 MHz, $CDCl_3$) δ = 155.04, 152.50, 150.97, 135.47, 130.43, 126.64, 123.83, 123.57, 122.85, 121.68, 114.94, 112.20, 55.88, 51.88, 51.83, 48.00, 29.97. HPLC-MS (ESI [+]) m/z $[M+H^+]^+$ = 342.17 (100 %); MS (APCI [+]) m/z $[M+H^+]^+$ calculated for $[C_{19}H_{24}N_3O_3]^+$: 342.1, found 341.9. M = 377.41 g/mol (HCl salt). mp = 194-196 °C (Et_2O).

1-(2-Methoxyphenyl)-4-(4-nitrophenethyl)piperazine hydrochloride (53)

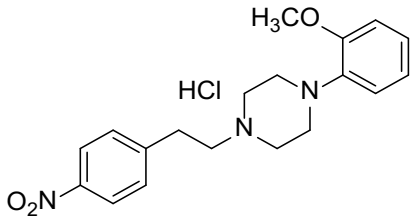

2-(4-Nitrophenyl) ethan1-ol **51** was first activated as mesylated **52** following the procedure **C** and then was alkylated to 1-(2-methoxyphenyl) piperazine based on **A**. Crude product was purified with column chromatography in SiO_2 with dichloromethane/methanol 98:2. Yellow oil. Yield = 71 %. The free base product was solubilized in Et_2O and a solution of HCl in dioxane (2 M) was added drop by drop. A white pp of HCl salt was obtained. ^{1}H-NMR (300 MHz, DMSO-d6) δ = 10.61 (s, 1H), 8.19 – 8.12 (m, 2H Ar), 7.59 – 7.52 (m, 2H Ar), 6.98 – 6.82 (m, 4H Ar-Pip), 3.77 (s, 3H), 3.66 – 3.54 (m, 6H), 3.25 (dd, 4H), 3.03 (t, 2H). ^{13}C-NMR (75 MHz, DMSO-d6) δ = 151.83, 146.51, 145.46, 139.02, 130.13, 123.78, 120.87, 118.41, 112.02, 55.44, 55.28, 51.03, 46.93, 39.25, 29.05. HPLC-MS (ESI [+]) m/z $[M+H^+]^+$ = 342.13 (100 %); MS (APCI [+]) m/z $[M+H^+]^+$ calculated for $[C_{19}H_{24}N_3O_3]^+$: 342.1, found 342.0. M = 377.41 g/mol (HCl salt). mp = 222 °C (Et_2O).

2-(2-(4-(2-Methoxyphenyl)piperazin-1-yl)ethyl)aniline (47)

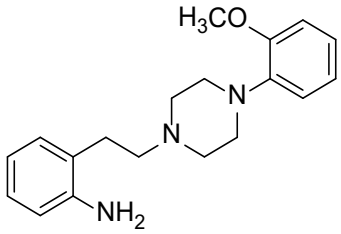

The *ortho* nitro derivative (**45**) was reduced following the procedure **D**. The crude product was characterized and used for the following step of synthesis with no further purification. White solid. Yield = 79%. ^{1}H-NMR (300 MHz, $CDCl_3$) δ = 7.08 – 6.98 (m, 3H Ar), 6.97 – 6.91 (m, 2H Ar/ Ar-pip), 6.91 – 6.84 (m, 1H Ar-pip), 6.76 – 6.64 (m, 2H Ar-pip), 4.03 (s, 2H NH_2), 3.87 (s, 3H), 3.13 (s, 4H), 2.87 – 2.63 (m, 8H). ^{13}C-NMR (75 MHz, $CDCl_3$) δ = 152.28, 145.22, 141.18, 130.27, 127.38, 125.81, 123.03, 121.01, 118.53, 118.20, 115.83, 111.22, 58.82, 55.37, 53.68, 50.71, 29.95. HPLC/HRAM-MS (ESI [+]) m/z $[M+H^+]^+$ = 312.2088 (100 %); MS (APCI [+]) m/z $[M+H^+]^+$ calculated for $[C_{19}H_{26}N_3O]^+$: 311.2, found 312.0. M = 311,43 (free base). mp = 97.8 °C (Et_2O).

3-(2-(4-(2-Methoxyphenyl)piperazin-1-yl)ethyl)aniline (48)

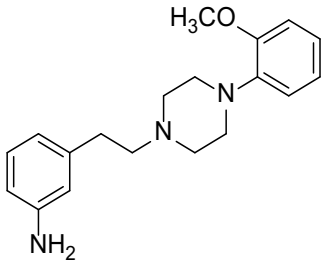

The *meta* NO_2-derivative (**46**) was reduced following the procedure **D**. The crude product was characterized and used for the following step of synthesis with no further purification. Yellow solid. Yield = 92%. ^{1}H-NMR (300 MHz, $CDCl_3$) δ = 7.12 – 6.84 (m, 5H Ar/Ar-pip), 6.67 – 6.50 (m, 3H Ar-pip), 3.87 (s, 3H), 3.76 – 3.49 (m, 2H NH_2), 3.14 (t, 4H), 2.83 – 2.58 (m, 8H). ^{13}C-NMR (75 MHz, $CDCl_3$) δ = 152.29, 146.48, 141.61, 141.36, 129.34, 122.93, 121.01, 119.06, 118.23, 115.51, 112.95, 111.17, 60.60, 55.39, 53.46, 50.69, 33.64. HPLC/HRAM-MS (ESI [+]) m/z $[M+H^+]^+$ = 312.2128 (100 %); MS (APCI [+]) m/z $[M+H^+]^+$ calculated for $[C_{19}H_{26}N_3O]^+$: 311.2, found 312.0. M = 311,43 (free base). mp = 109.6 °C (Et_2O).

4-(2-(4-(2-Methoxyphenyl) piperazin-1-yl)ethyl)aniline (54)

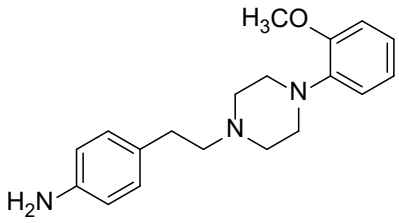

Based on procedure **D** the product was obtained by reducing the *para* nitro compound (**53**). Crude product was used without further purification in the next step of synthesis. Light orange solid. Yield = 96%. ^{1}H-NMR (300 MHz, DMSO-d6) δ = 7.02 – 6.83 (m, 6H Ar/Ar-pip), 6.53 – 6.46 (m, 2H Ar-pip), 4.83 (s, 2H NH_2), 3.77 (s, 3H), 2.97 (t, 4H), 2.64 – 2.52 (m, 6H), 2.50 – 2.42 (m, 2H). ^{13}C-NMR (75 MHz, DMSO-d6) δ = 151.93, 146.50, 141.27, 128.94, 127.23, 122.27, 120.80, 117.83, 113.94, 111.86, 60.54, 55.26, 53.00, 50.04, 32.03. HPLC/HRAM-MS (ESI [+]) m/z $[M+H^+]^+$ = 312.2120 (100 %); MS (APCI [+]) m/z $[M+H^+]^+$ calculated for $[C_{19}H_{26}N_3O]^+$: 312.2, found 311.9. M = 311,43 (free base). mp = 87.4 °C (Et_2O).

N-(2-(2-(4-(2-Methoxyphenyl)piperazin-1-yl)ethyl)phenyl)acetamide (49)

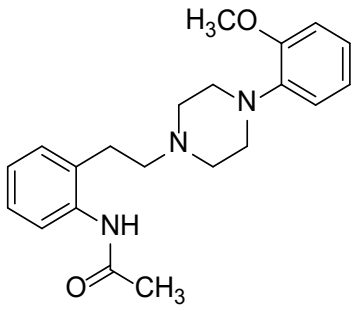

Aniline with *ortho* NH_2 **47** was acylated by acetic anhydride according to procedure **E**. The pure product was obtained by column chromatography in SIO_2 with dichloromethane/ammonia in methanol 95:5. Pink solid. Yield = 74%. ^{1}H-NMR (300 MHz, DMSO-d6) δ = 9.53 (s, 1H CONH), 7.42 – 7.34 (m, 1H Ar), 7.28 – 7.06 (m, 3H Ar), 6.99 – 6.83 (m, 4H Ar-Pip), 3.77 (s, 3H), 2.98 (t, *J* = 4.6 Hz, 4H), 2.76 (dd, 4H), 2.59 (t, *J* = 4.6 Hz, 4H), 2.07 (s, 3H). ^{13}C-NMR (75 MHz, DMSO-d6) δ = 168.25, 151.97, 141.23, 136.22, 134.60, 129.69, 126.06, 125.75, 125.13, 122.26, 120.81, 117.87, 112.04, 58.58, 55.30, 53.00, 49.97, 28.57, 23.36. HPLC-MS (ESI [+]) m/z $[M+H^+]^+$ = 354.19 (99.97 %); MS (APCI [+]) m/z $[M+H^+]^+$ calculated for $[C_{21}H_{28}N_3O_2]^+$: 354.2, found 354.1. M = 353.47 g/mol (free base). mp = 115 °C (Et_2O).

N-(3-(2-(4-(2-Methoxyphenyl) piperazin-1-yl)ethyl)phenyl)acetamide (50)

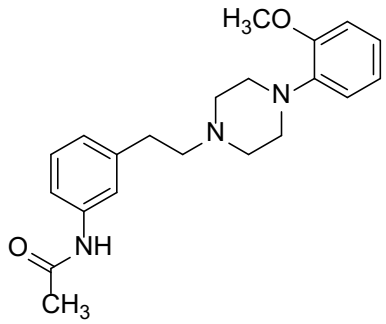

The derivative having NH_2 **48** in *meta* position was acylated by acetic anhydride according to procedure **E**. The pure product was obtained by column chromatography in SIO_2 with dichloromethane/ammonia in methanol 95:5. White solid. Yield = 74%. ^{1}H-NMR (300 MHz, DMSO-d6) δ = 9.85 (s, 1H), 7.47 – 7.36 (m, 2H Ar), 7.19 (t, 1H Ar), 6.96 – 6.85 (m, 5H Ar/Ar-Pip), 3.77 (s, 3H), 2.95 (d, 4H), 2.72 (dd, 2H), 2.56 (t, 6H), 2.02 (s, 3H). ^{13}C-NMR (75 MHz, DMSO-d6) δ = 168.08, 151.95, 141.28, 140.85, 139.18, 128.37, 123.31, 122.20, 120.80, 119.18, 117.84, 116.68, 112.03, 59.68, 55.29, 52.91, 49.98, 32.84, 23.88. HPLC-MS (ESI [+]) m/z $[M+H^+]^+$ = 354.18 (99.45 %); MS (APCI [+]) m/z $[M+H^+]^+$ calculated for $[C_{21}H_{28}N_3O_2]^+$: 354.2, found 354.2. M = 353.47 g/mol (free base). mp = 124 °C (Et_2O).

N-(4-{2-[4-(2-Methoxyphenyl)piperazin-1-yl]ethyl}phenyl)acetamide hydrochloride (55)

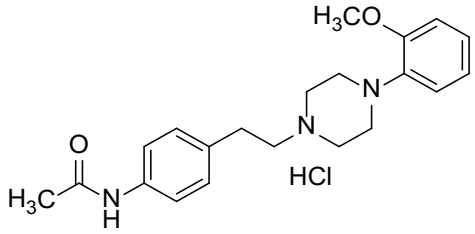

Based on procedure **E** the product was obtained by acylating para NH_2 compound (**54**). The pure product was obtained by column chromatography in SIO_2 with dichloromethane/ammonia in methanol 95:5. Free base derivative was solubilized in iPrOH and a solution of HCl in dioxane (2 N) was added drop by drop. A white precipitate of HCl salt was obtained. ^{1}H-NMR (300 MHz, DMSO-d6) δ = 10.59 (s, 1H), 9.84 (s, 1H), 7.50 – 7.44 (m, 2H Ar), 7.18 – 7.12 (m, 2H Ar), 6.95 – 6.85 (m, 4H Ar-Pip), 3.77 (s, 3H), 2.96 (t, 5H), 2.70 (dd, 2H), 2.55 (q, 5H), 2.02 (s, 3H). ^{13}C-NMR (75 MHz, DMSO-d6) δ = 168.25, 151.82, 139.40, 138.12, 131.35, 128.90, 123.48, 120.85, 119.24, 118.26, 111.92, 56.30, 55.37, 51.20, 46.94, 28.76, 23.98. HPLC-MS (ESI [+]) m/z $[M+H^+]^+$ = 354.19 (96.77

%); MS (APCI [+]) m/z $[M+H^+]^+$ calculated for $[C_{21}H_{28}N_3O_2]^+$: 354.2, found 354.0. M = 389.47 g/mol (HCl salt). mp = 296 °C (iPrOH).

2-((4-(2-Methoxyphenyl)piperazin-1-yl)methyl)benzonitrile hydrochloride (59)

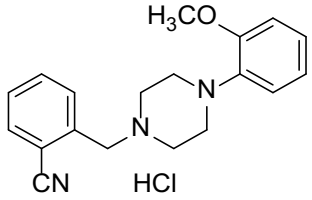

1-(2-Methoxyphenyl)piperazine was alkylated by 2-(bromomethyl)benzonitrile **56** following the conditions of **A**. The crude product was purified by column chromatography in SiO_2 with dichloromethane/methanol 98:2. Yellow oil. Yield = 95 %. The pure compound was solubilized in Et_2O and a solution of HCl in dioxane (2 M) was added drop by drop. A white precipitate of HCl salt was obtained. ^{1}H-NMR (300 MHz, $CDCl_3$) δ = 13.31 (s, 1H), 7.82 (ddd, *J* = 7.6, 1.4 Hz, 1H Ar), 7.69 (td, *J* = 7.6, 1.4 Hz, 1H Ar), 7.60 (dt, *J* = 7.5 Hz, 1H Ar), 7.48 (td, *J* = 7.5, 1.4 Hz, 1H Ar), 6.97 – 6.82 (m, 4H Ar-Pip), 3.76 (s, 3H), 3.70 (s, 2H), 2.95 (s, 4H), 2.56 (t, 4H). ^{13}C-NMR (75 MHz, DMSO-d6) δ = 151.82, 139.26, 139.17, 133.43, 133.12, 132.36, 130.37, 123.49, 120.78, 118.29, 117.22, 113.92, 112.05, 56.59, 55.37, 51.28, 46.66. HPLC-MS (ESI [+]) m/z $[M+H^+]^+$ = 308.12 (98.22 %); MS (APCI [+]) m/z $[M+H^+]^+$ calculated for $[C_{19}H_{22}N_3O]^+$: 308.1, found 308.2. M = 343.40 g/mol (HCl salt). mp = 243-245 °C (Et_2O).

3-((4-(2-Methoxyphenyl)piperazin-1-yl)methyl)benzonitrile hydrochloride (60)

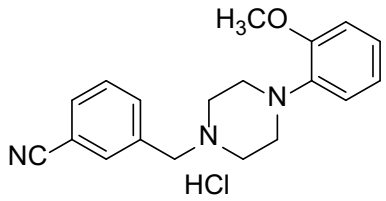

3-(Bromomethyl)benzonitrile **57** and the piperazine were mixed to obtain the desired product following procedure **A**. Pure compound was obtained through column chromatography in SiO_2 with dichloromethane/methanol 98:2. Light-yellow oil. Yield = 76 %. The obtained derivative was solubilized in Et_2O and a solution of HCl in dioxane (2 M) was added drop by drop. A white precipitate of HCl salt was obtained. ^{1}H-NMR (300 MHz, DMSO-d6) δ = 11.38 (s, 1H), 8.17 (t, 1H Ar), 7.99 (ddt, *J* = 7.8 Hz, 2H Ar), 7.70 (t, *J* = 7.8 Hz, 1H Ar), 7.06 – 6.86 (m, 4H Ar-Pip), 4.45 (d, 2H), 3.78 (s, 3H), 3.51 – 3.00 (m, 8H). ^{13}C-NMR (75 MHz, DMSO-d6) δ = 151.80, 139.20, 136.40, 135.18, 133.00, 131.11, 129.81, 123.44, 120.76, 118.24, 112.01, 111.64, 57.39, 55.32, 50.78, 46.60.

HPLC-MS (ESI [+]) m/z $[M+H^+]^+$ = 308.16 (97.53 %); MS (APCI [+]) m/z $[M+H^+]^+$ calculated for $[C_{19}H_{22}N_3O]^+$: 308.1, found 308.3. M = 343.40 g/mol (HCl salt). mp = 232 °C (Et_2O).

4-((4-(2-Methoxyphenyl)piperazin-1-yl)methyl)benzonitrile (61)

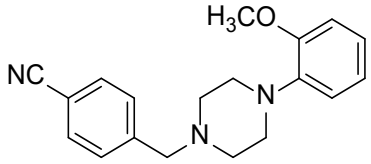

To obtain this derivative, 4-(chloromethyl)benzonitrile **58** was used for the alkylation with piperazine and procedure **A**. The obtained crude was purified by column chromatography in SiO_2 with dichloromethane/methanol 98:2. Yellow oil. Yield = 88 %. ^{1}H-NMR (300 MHz, $CDCl_3$) δ = 7.68 – 7.58 (m, 2H Ar), 7.53 – 7.45 (m, 2H Ar), 7.04 – 6.83 (m, 4H Ar-Pip), 3.86 (s, 3H), 3.62 (s, 2H), 3.10 (d, 4H), 2.65 (t, 4H). ^{13}C-NMR = (75 MHz, $CDCl_3$) δ 152.56, 144.45, 141.57, 132.26, 129.73, 123.10, 121.25, 119.07, 118.43, 111.65, 111.16, 62.75, 55.58, 53.66, 50.84. HPLC-MS (ESI [+]) m/z $[M+H^+]^+$ = 308.15 (99.38 %); MS (APCI [+]) m/z $[M+H^+]^+$ calculated for $[C_{19}H_{22}N_3O]^+$: 308.1, found 307.9. M = 307.40 g/mol (free base). mp = 116-118 °C (Et_2O).

(2-{[4-(2-Methoxyphenyl)piperazin-1-yl]methyl}phenyl)methanamine (62)

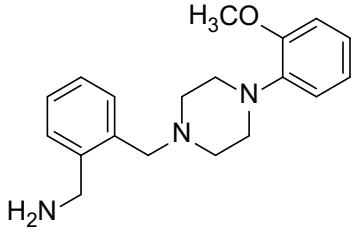

Compound bearing *ortho* CN function (**59**) was reduced following procedure **G**. The obtained crude mixture was purified by column chromatography in SiO_2 with dichloromethane/methanol 95:5. White solid. Yield = 96%. ^{1}H-NMR (300 MHz, $CDCl_3$) δ = 7.36 – 7.18 (m, 4H Ar), 6.98 (ddt, 1H Ar-Pip), 6.91 – 6.81 (m, 3H Ar-Pip), 3.91 (s, 2H NH_2), 3.85 (s, 3H), 3.60 (s, 2H), 3.35 (s, 2H), 3.04 (s, 4H), 2.68 (t, 4H). ^{13}C-NMR (75 MHz, $CDCl_3$) δ =152.22, 142.22, 141.14, 136.02, 131.34, 129.58, 128.36, 127.00, 122.98, 120.98, 118.25, 111.16, 61.66, 55.36, 53.17, 50.73, 44.78. HPLC/HRAM-MS (ESI [+]) m/z $[M+H^+]^+$ = 312.2068 (99.05 %); MS (APCI [+]) m/z $[M+H^+]^+$ calculated for $[C_{19}H_{26}N_3O]^+$: 312.2, found 312.2. M = 311,43 g/mol (free base). mp = 189.5 °C (Et_2O).

(3-((4-(2-Methoxyphenyl)piperazin-1-yl)methyl)phenyl)methanamine (63)

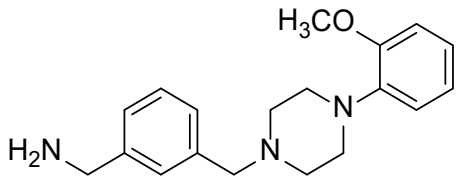

Compound bearing *meta* CN function (**60**) was reduced following procedure **G**. The obtained crude mixture was purified by column chromatography in SiO_2 with dichloromethane/methanol 95:5. White solid. Yield = 92%. ^{1}H-NMR (300 MHz, $CDCl_3$) δ = 7.25 – 7.11 (m, 4H Ar), 6.94 – 6.81 (m, 3H Ar-Pip), 6.77 (dd, 1H Ar-Pip), 3.79 (s, 2H NH_2), 3.77 (s, 3H), 3.50 (s, 2H), 3.01 (t, *J* = 4.8 Hz, 4H), 2.58 (t, *J* = 4.8 Hz, 4H), 1.85 (s, 2H). ^{13}C-NMR (75 MHz, $CDCl_3$) δ = 152.28, 143.07, 141.41, 138.38, 128.46, 128.08, 127.93, 125.91, 122.87, 120.98, 118.23, 111.15, 63.19, 55.36, 55.32, 53.39, 50.65, 46.39. HPLC/HRAM-MS (ESI [+]) m/z $[M+H^+]^+$ = 312.2005 (100 %); MS (APCI [+]) m/z $[M+H^+]^+$ calculated for $[C_{19}H_{26}N_3O]^+$: 312.2, found 312.3. M = 311,43 g/mol (free base). mp = 167-170 °C (Et_2O).

(4-((4-(2-Methoxyphenyl)piperazin-1-yl)methyl)phenyl)methanamine (64)

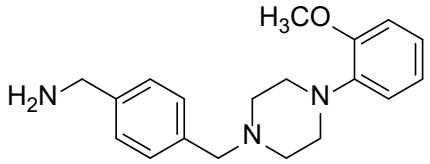

The corresponding *para* CN precursor (**61**) was reduced following procedure **G**. The crude product was purified b column chromatography in SiO2 with dichloromethane/methanol 95:5. White solid. Yield = 86%. ^{1}H-NMR (300 MHz, $CDCl_3$) δ 7.25 (d, 2H Ar), 7.22 – 7.17 (m, 2H Ar), 6.95 – 6.76 (m, 4H Ar-pip), 3.78 (s, 2H NH_2), 3.77 (s, 3H), 3.50 (s, 2H), 3.01 (t, *J* = 4.8 Hz, 4H), 2.58 (t, *J* = 4.8 Hz, 4H), 1.80 (s, 2H). ^{13}C-NMR (75 MHz, $CDCl_3$) δ = 152.28, 141.91, 141.40, 136.61, 129.60, 127.05, 122.86, 120.98, 118.23, 111.15, 62.88, 55.32, 53.31, 50.65, 46.19. HPLC/HRAM-MS (ESI [+]) m/z $[M+H^+]^+$ = 312.2068 (96.24 %); MS (APCI [+]) m/z $[M+H^+]^+$ calculated for $[C_{19}H_{26}N_3O]^+$: 312.2, found 312.0. M = 311,43 g/mol (free base). mp = 97-99 °C (Et_2O).

N-(2-((4-(2-Methoxyphenyl)piperazin-1-yl)methyl)benzyl)acetamide hydrochloride (65)

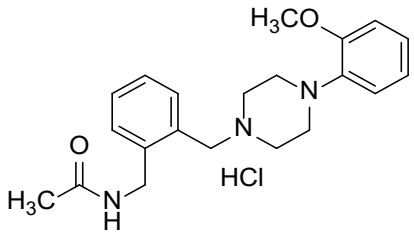

The *ortho* methanamine intermediate **62** was acylated using acetic anhydride and procedure **E**. The crude material was purified by column chromatography in SiO_2 with dichloromethane/ammonia in methanol 95:5. Light brown oil. Yield = 88%. The pure compound was solubilized in Et_2O and a solution of HCl in dioxane (2 M) was added drop by drop into it. A white precipitate of HCl salt was obtained. ^{1}H-NMR (300 MHz, DMSO-d6) δ = 10.93 (s, 1H CONH), 9.05 (t, *J* = 5.9 Hz, 1H), 7.67 (dd, 1H Ar), 7.53 – 7.31 (m, 3H Ar), 7.07 – 6.85 (m, 4H Ar-Pip), 4.53 (d, 2H), 4.41 (d, *J* = 5.9 Hz, 2H), 3.79 (s, 3H), 3.57 – 2.99 (m, 8H), 1.89 (s, 3H). ^{13}C-NMR (150 MHz, DMSO-d6) δ = 170.12, 151.85, 139.80, 139.08, 132.63, 129.98, 129.93, 127.47, 127.37, 123.71, 120.85, 118.38, 112.04, 55.73, 55.43, 51.06, 46.81, 40.06, 22.48. HPLC-MS (ESI [+]) m/z $[M+H^+]^+$ = 354.18 (96.27 %); MS (APCI [+]) m/z $[M+H^+]^+$ calculated for $[C_{21}H_{28}N_3O_2]^+$: 354.2, found 354.0. M = 389.47 g/mol (HCl salt). mp = 204 °C (Et_2O).

N-(3-((4-(2-Methoxyphenyl)piperazin-1-yl)methyl)benzyl)acetamide hydrogenoxalate (66)

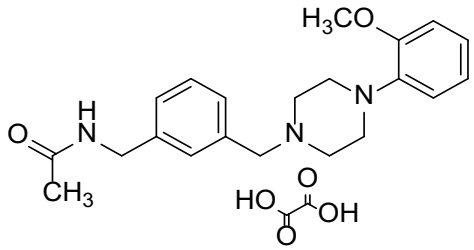

The derivative having NH_2 in *meta* position (**63**) was acylated by acetic anhydride according to procedure **E.** Brown oil. Yield = 67%. The obtained pure product was solubilized in EtOAc and stirred at room temperature during the dropwise addition of oxalic acid (1.1 eq.) solution in EtOAc. A white precipitate of oxalic salt was obtained. ^{1}H-NMR (300 MHz, DMSO-d6) δ = 8.37 (t, *J* = 5.9 Hz, 1H CONH), 7.40 – 7.23 (m, 4H Ar), 7.02 – 6.84 (m, 4H Ar-Pip), 4.27 (d, *J* = 5.9 Hz, 2H), 3.97 (s, 2H), 3.77 (s, 3H), 3.08 (s, 4H), 2.93 (s, 4H), 1.88 (s, 3H). ^{13}C-NMR (75 MHz, DMSO-d6) δ = 168.99, 162.76, 162.39, 157.87, 151.90, 139.83, 128.83, 128.37, 127.03, 126.99, 122.76, 120.76,

118.06, 112.00, 60.56, 55.29, 51.93, 48.56, 41.96, 22.47. HPLC-MS (ESI [+]) m/z $[M+H^+]^+$ = 354.20 (99.91 %); MS (APCI [+]) m/z $[M+H^+]^+$ calculated for $[C_{21}H_{28}N_3O_2]^+$: 354.2, found 354.2. M = 443.50 g/mol (Hydrogenoxalic salt). mp = 84 °C (EtOAc).

N-(4-((4-(2-Methoxyphenyl)piperazin-1-yl)methyl)benzyl)acetamide hydrochloride (67)

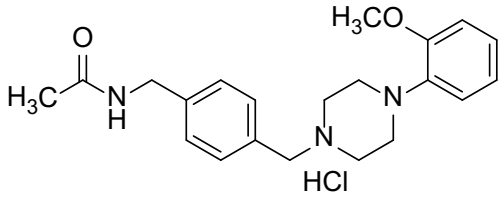

Based on procedure **E** the product was obtained by acylating para NH_2 compound **64**. The pure derivative was obtained by column chromatography in SiO_2 with dichloromethane/ammonia in methanol 95:5. Yellowish oil. Yield = 89%. The obtained compound was solubilized in EtOH and a solution of HCl in dioxane (2 M) was added dropwise. A white precipitate of HCl salt was obtained. ^{1}H-NMR (300 MHz, DMSO-d6) δ = 11.12 (s, 1H CONH), 8.43 (t, *J* = 5.9 Hz, 1H), 7.61 – 7.55 (m, 2H Ar), 7.33 (d, 2H Ar), 7.06 – 6.83 (m, 4H Ar-Pip), 4.34 (d, 2H), 4.28 (d, *J* = 5.9 Hz, 2H), 3.56 (s, 3H), 3.50 – 3.29 (m, 4H), 3.22 – 2.99 (m, 4H), 1.88 (s, 3H). ^{13}C-NMR (150 MHz, DMSO-d6) δ = 169.25, 151.83, 141.12, 139.12, 131.61, 127.91, 127.46, 123.67, 120.81, 118.35, 111.96, 58.24, 55.38, 50.55, 46.71, 41.78, 22.57. HPLC-MS (ESI [+]) m/z $[M+H^+]^+$ = 354.18 (100 %); MS (APCI [+]) m/z $[M+H^+]^+$ calculated for $[C_{21}H_{28}N_3O_2]^+$: 354.2, found 354.1. M = 389.47 g/mol (HCl salt). mp = 222 °C (EtOH).

N-(4-(2-(4-(2-Methoxyphenyl)piperazin-1-yl)ethyl)phenyl)propionamide (69)

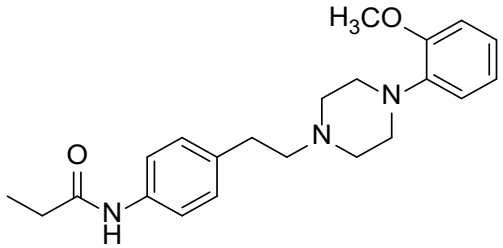

Obtained aniline **54** (1 eq.), diisopropylethylamine (1.5 eq.) and propionic anhydride (1.5 eq.) were mixed together in order to obtain the desired product following procedure **E**. Pure compound was obtained by flash chromatography with Biotage Sfär Silica 25 gr in dichloromethane/methanol from 0 to 10% of methanol. Brown solid. Yield = 91%. ^{1}H NMR (300 MHz, $CDCl_3$) δ = 7.44 (d, 2H Ar), 7.31 (s, 1H CONH), 7.16 (d, 2H Ar), 7.05 – 6.83 (m, 4H Ar-Pip), 3.86 (s, 3H), 3.15 (t, 4H), 2.91 – 2.64 (m, 8H), 2.37 (q, *J* = 7.5 Hz, 2H), 1.23 (t, *J* = 7.5 Hz, 3H). ^{13}C NMR (75 MHz, $CDCl_3$) δ =

172.00, 152.25, 141.09, 136.17, 135.80, 129.20, 123.08, 121.02, 120.02, 118.28, 111.19, 60.30, 55.36, 53.24, 50.31, 32.59, 30.70, 9.73. HPLC/HRAM-MS (ESI [+]) m/z $[M+H^+]^+$ = 368.2454 (100 %); MS (APCI [+]) m/z $[M+H^+]^+$ calculated for $[C_{22}H_{29}N_3O_2]^+$: 368.2, found 368.2. M = 367.49 g/mol (free base). mp = 131-135°C (MeOH).

N-(4-(2-(4-(2-Methoxyphenyl)piperazin-1-yl)ethyl)phenyl)butyramide (70)

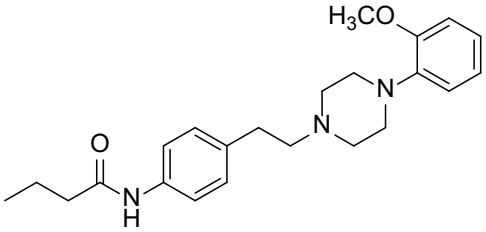

Butyryl chloride (1.5 eq.) was added to a solution of aniline **54** (1 eq) and DIPEA (1.5 eq.), the mixture of reaction was executed according to procedure **E**. Pure compound was obtained by flash chromatography with Biotage Sfär Silica 25 gr in dichloromethane/methanol from 0 to 10% of methanol. White solid. Yield = 62%. ^{1}H NMR (300 MHz, $CDCl_3$) δ = 7.43 (d, 2H Ar), 7.24 (s, 1H CONH), 7.19 – 7.14 (m, 2H Ar), 7.04 – 6.91 (m, 3H Ar-Pip), 6.90 – 6.83 (m, 1H Ar-Pip), 3.86 (s, 3H), 3.13 (t, 4H), 2.86 – 2.72 (m, 6H), 2.70 – 2.61 (m, 2H), 2.38 – 2.25 (m, 2H), 1.82 – 1.67 (m, 2H), 0.98 (dt, 4H). ^{13}C NMR (75 MHz, $CDCl_3$) δ = 171.21, 152.28, 141.26, 136.14, 136.06, 129.19, 122.98, 121.02, 120.03, 118.24, 111.20, 60.45, 55.35, 53.34, 50.53, 39.65, 32.84, 19.10, 13.77. HPLC/HRAM-MS (ESI [+]) m/z $[M+H^+]^+$ = 382.2642 (97.99 %). MS (APCI [+]) m/z $[M+H^+]^+$ calculated for $[C_{23}H_{31}N_3O_2]^+$: 382.2, found 382.1. M = 381.52 g/mol (free base). mp = 145.2°C (MeOH).

N-(4-(2-(4-(2-Methoxyphenyl)piperazin-1-yl)ethyl)phenyl)isobutyramide hydrochloride (71)

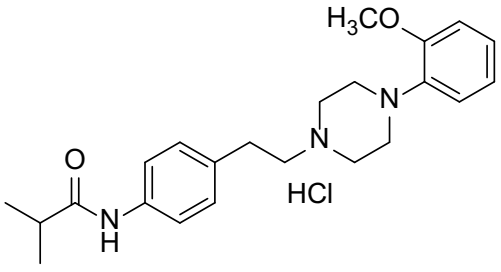

Isobutyryl chloride (1.5 eq.) was added to a solution of aniline **54** (1 eq.) and DIPEA (1.5 eq.), the mixture of reaction was performed according to procedure **E**. Pure compound was obtained by crystallization of hydrochloride salt directly from reaction solution. White solid. Yield = 75%. ^{1}H NMR (300 MHz, DMSO-d6) δ = 11.18 (s, 1H), 9.94 (s, 1H CONH), 7.64 – 7.56 (m, 2H Ar), 7.23 –

7.16 (m, 2H Ar), 7.06 – 6.98 (m, 2H Ar-Pip), 6.96 – 6.88 (m, 2H Ar-Pip), 3.79 (s, 3H), 3.67 – 3.44 (m, 5H), 3.26 – 2.99 (m, 7H), 2.61 (p, 1H), 1.10 (s, 3H), 1.07 (s, 3H). ^{13}C NMR (75 MHz, DMSO-d6) δ = 175.17, 151.78, 139.41, 138.21, 131.34, 128.79, 123.40, 120.82, 119.36, 118.19, 111.89, 56.28, 55.35, 51.13, 34.79, 28.70, 19.49. HPLC/HRAM-MS (ESI [+]) m/z $[M+H^+]^+$ = 382.2621 (97.59 %). MS (APCI [+]) m/z $[M+H^+]^+$ calculated for $[C_{23}H_{31}N_3O_2]^+$: 382.2, found 382.2. M = 417.52 g/mol (HCl salt). mp = 271-275°C (THF).

N-(4-(2-(4-(2-Methoxyphenyl)piperazin-1-yl)ethyl)phenyl)pivalamide (72)

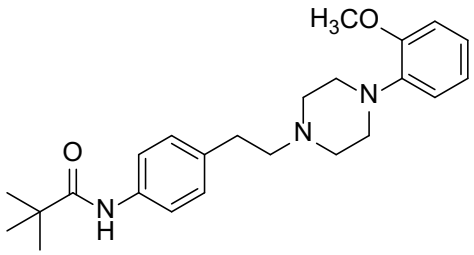

Pivaloyl chloride (1.5 eq.) was added to a solution of aniline (1 eq.) and DIPEA (1.5 eq.), the mixture of reaction was stirred following procedure **E**. Pure compound was obtained by flash chromatography with Biotage Sfär Silica 25 gr in dichloromethane/methanol from 0 to 10% of methanol. Yellow sticky solid. Yield = 71%. ^{1}H NMR (300 MHz, $CDCl_3$) δ = 7.48 – 7.40 (m, 2H Ar), 7.29 (s, 1H CONH), 7.20 – 7.14 (m, 2H Ar), 7.04 – 6.84 (m, 4H Ar-Pip), 3.86 (s, 3H), 3.13 (s, 4H), 2.86 – 2.63 (m, 8H), 1.31 (s, 9H). ^{13}C NMR (75 MHz, $CDCl_3$) δ = 176.50, 152.27, 141.23, 136.13, 129.17, 122.99, 121.01, 120.16, 118.23, 111.19, 60.38, 55.37, 53.44, 53.26, 50.45, 39.55, 32.72, 27.65, 27.41. HPLC/HRAM-MS (ESI [+]) m/z $[M+H^+]^+$ = 396.2776 (100 %). MS (APCI [+]) m/z $[M+H^+]^+$ calculated for $[C_{24}H_{33}N_3O_2]^+$: 396.2, found 396.0. M = 395.55 g/mol (free base). mp = 134.7°C (MeOH).

2,2,2-Trifluoro-*N*-(4-(2-(4-(2-methoxyphenyl)piperazin-1-yl)ethyl)phenyl)acetamide (73)

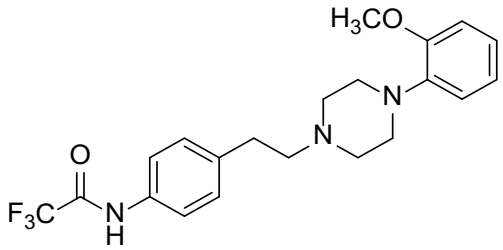

Trifluoroacetic anhydride (1.5 eq.) and triethylamine (1.5 eq.) were added to a stirring solution of aniline (1 eq.) in THF (~ 20 ml). The reaction was left to stir basing on procedure **E**. Pure compound was obtained by flash chromatography with Biotage Sfär Silica HC 25 gr in

dichloromethane/methanol from 0 to 10% of methanol. Light orange solid. Yield = 55%. ^{1}H NMR (300 MHz, DMSO-d6) δ = 11.32 (s, 1H CONH), 7.70 – 7.62 (m, 2H Ar), 7.38 – 7.30 (m, 2H Ar), 7.08 – 6.87 (m, 4H Ar-Pip), 3.81 (s, 3H), 3.55 – 2.97 (m, 12H). ^{19}F NMR (282 MHz, DMSO-d6) δ = -73.58 (s, 1F), -73.87 (s, 2F). ^{13}C NMR (75 MHz, DMSO-d6) δ 154.69, 154.19, 151.82, 139.48, 134.96, 129.23, 123.39, 121.34, 120.82, 118.23, 111.89, 56.34, 55.32, 51.38, 47.22, 29.12. HPLC/HRAM-MS (ESI [+]) m/z $[M+H^+]^+$ = 408.1920 (100 %). MS (APCI [+]) m/z $[M+H^+]^+$ calculated for $[C_{21}H_{24}F_3N_3O_2]^+$: 408.2, found 408.1. M = 407.44 g/mol (free base). mp = 207.3°C (MeOH).

tert-Butyl(4-(2-(4-(2-methoxyphenyl)piperazin-1-yl)ethyl)phenyl)carbamate (74)

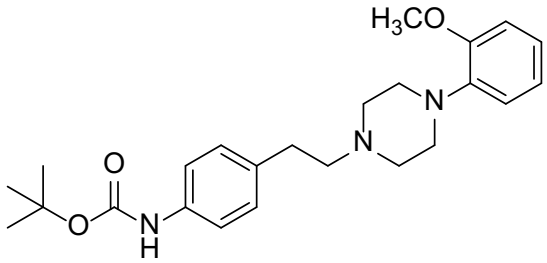

BOC-anhydride (1.5 eq.) and DIPEA (1.5 eq.) were added to a stirring solution of aniline **54** (1 eq.) in tetrahydrofuran (~20 ml). The reaction was left to stir basing on procedure **E**. Pure compound was obtained by flash chromatography with Biotage Sfär Silica 25 gr in dichloromethane/methanol from 0 to 10% of methanol. Yellow sticky oil. Yield = 78%. ^{1}H NMR (600 MHz, DMSO-d6) δ = 7.30 – 7.26 (m, 2H Ar), 7.16 – 7.12 (m, 2H Ar), 7.03 – 6.99 (m, 1H Ar-Pip), 6.97 – 6.90 (m, 2H Ar-Pip), 6.86 (dd, 1H Ar-Pip), 6.47 (s, 1H CONH), 3.86 (s, 3H), 3.14 (s, 4H), 2.85 – 2.61 (m, 8H), 1.51 (s, 9H). ^{13}C NMR (151 MHz, DMSO-d6) δ = 152.96, 152.38, 141.33, 136.56, 134.93, 129.61, 129.30, 123.10, 121.12, 118.90, 118.37, 115.42, 111.29, 80.51, 60.67, 55.47, 53.54, 53.51, 50.61, 32.86, 29.82, 28.47. HPLC-MS (ESI [+]) m/z $[M+H^+]^+$ = 412.33 (100 %). MS (APCI [+]) m/z $[M+H^+]^+$ calculated for $[C_{24}H_{33}N_3O_3]^+$: 412.2, found 411.9. M = 411.55 g/mol (free base).

3-Methoxy-*N*-(4-(2-(4-(2-methoxyphenyl)piperazin-1-yl)ethyl)phenyl)propenamide (75)

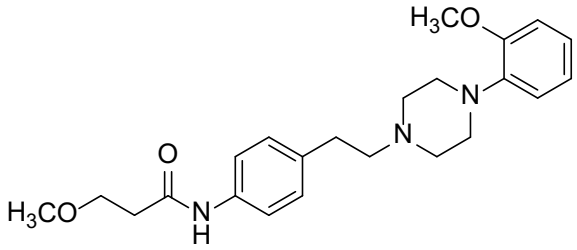

3-Methoxypropanoic acid and obtained aniline were mixed together to obtain this derivative following conditions of procedure **H**. Pure product was obtained by flash chromatography with Biotage Sfär Silica 25 gr in dichloromethane/methanol from 0% to 10% of methanol. Brown oil. Yield = 38%. ^{1}H NMR (300 MHz, $CDCl_3$) δ = 8.17 (s, 1H CONH), 7.47 – 7.38 (m, 2H Ar), 7.21 – 7.13 (m, 2H Ar), 7.04 – 6.91 (m, 3H Ar-Pip), 6.90 – 6.83 (m, 1H Ar-Pip), 3.86 (s, 3H), 3.72 (t, 2H), 3.44 (s, 3H), 3.13 (s, 4H), 2.88 – 2.72 (m, 6H), 2.64 (ddd, 4H). ^{13}C NMR (75 MHz, $CDCl_3$) δ = 169.71, 152.28, 141.28, 136.12, 129.16, 122.96, 121.01, 120.09, 118.24, 111.18, 68.65, 60.56, 58.94, 55.38, 53.43, 50.60, 37.97, 32.95. HPLC/HRAM-MS (ESI [+]) m/z $[M+H^+]^+$ = 398.2645 (99.14 %). MS (APCI [+]) m/z $[M+H^+]^+$ calculated for $[C_{23}H_{31}N_3O_3]^+$: 398.2, found 398.1. M = 397.52 g/mol (free base).

N-(4-(2-(4-(2-Methoxyphenyl)piperazin-1-yl)ethyl)phenyl)cyclopropanecarboxamide hydrochloride (76)

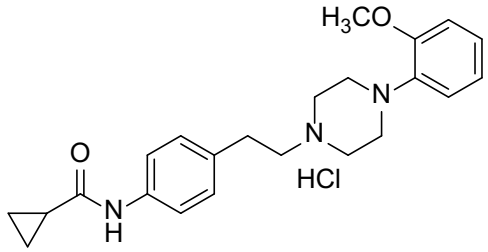

Cyclopropane carbonyl chloride (1.5 eq.) was added to a solution of aniline (1 eq.) and DIPEA (1.5 eq.) in THF (~20 ml), the reaction was performed according to procedure **E**. Pure product was collected as hydrochloride salt precipitated in reaction solution. White solid. Yield = 75%. ^{1}H NMR (300 MHz, DMSO-d6) δ = 11.19 (s, 1H), 10.34 (s, 1H CONH), 7.66 – 7.53 (m, 2H Ar), 7.26 – 7.16 (m, 2H Ar), 7.08 – 6.87 (m, 4H Ar-Pip), 3.79 (s, 3H), 3.60 (d, 2H), 3.50 (d, 2H), 3.31 (d, 2H), 3.25 – 3.00 (m, 6H), 1.83 (tt, 1H), 0.78 (dq, 4H). ^{13}C NMR (75 MHz, DMSO-d6) δ = 171.55, 151.78, 139.40, 138.15, 131.28, 128.85, 123.41, 120.81, 119.18, 118.19, 111.88, 56.26, 55.34, 51.11, 46.86, 28.68, 14.44, 7.08. HPLC/HRAM-MS (ESI [+]) m/z $[M+H^+]^+$ = 380.2461 (97.62 %). MS (APCI [+]) m/z $[M+H^+]^+$ calculated for $[C_{23}H_{29}N_3O_2]^+$: 380.2, found 380.1. M = 415.5 g/mol (HCl salt). mp = 277°C (THF).

N-(4-(2-(4-(2-Methoxyphenyl)piperazin-1-yl)ethyl)phenyl)cyclobutanecarboxamide (77)

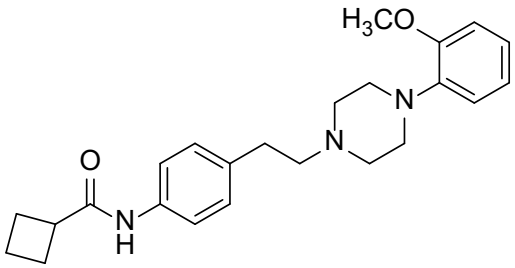

Cyclobutane carbonyl chloride (1.5 eq.) was added to a solution of aniline (1 eq.) and DIPEA (1.5 eq.), the reaction was performed according to procedure **E**. Pure compound was obtained through flash chromatography with Biotage Sfär Silica 25 gr in dichloromethane/methanol from 0% to 10% of methanol. Brown solid. Yield = 34%. ^{1}H NMR (300 MHz, DMSO-d6) δ = 9.78 (s, 1H CONH), 7.57 (d, 2H Ar), 7.18 (d, 2H Ar), 7.06 – 6.85 (m, 4H Ar-Pip), 3.79 (s, 3H), 3.23 (p, 13H), 2.29 – 2.17 (m, 2H), 2.10 (ddt, 2H), 1.94 (ddd, 1H), 1.80 (tq, 1H). ^{13}C NMR (75 MHz, DMSO-d6) δ = 172.76, 166.26, 151.82, 137.90, 128.78, 123.11, 120.80, 119.27, 118.11, 111.87, 57.14, 55.32, 51.62, 47.79, 33.72, 24.56, 17.70, 5.49. HPLC/HRAM-MS (ESI [+]) m/z $[M+H^+]^+$ = 394.2621 (99.55 %). MS (APCI [+]) m/z $[M+H^+]^+$ calculated for $[C_{24}H_{31}N_3O_2]^+$: 394.2, found 394.2. M = 393.53 g/mol (free base). mp = 131°C (MeOH).

N-(4-(2-(4-(2-Methoxyphenyl)piperazin-1-yl)ethyl)phenyl)cyclopentanecarboxamide (78)

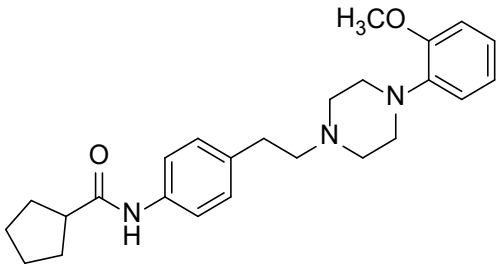

Cyclopentane carboxylic acid (1 eq.) and obtained aniline **54** (1 eq.) were mixed together to obtain this derivative following conditions of procedure **H**. Pure product was collected by flash chromatography with Biotage Sfär Silica 25 gr in dichloromethane/methanol from 0% to 10% of methanol. White solid. Yield = 64%. ^{1}H NMR (300 MHz, $CDCl_3$) δ = 7.44 (d, 2H Ar), 7.25 – 7.12 (m, 3H Ar/CONH), 7.04 – 6.83 (m, 4H Ar-Pip), 3.86 (s, 3H), 3.69 (p, 1H), 3.19 – 3.12 (m, 4H), 2.82 (dd, 6H), 2.73 – 2.67 (m, 2H), 1.99 – 1.84 (m, 4H), 1.78 (td, 2H), 1.68 – 1.56 (m, 2H). ^{13}C NMR (75 MHz, $CDCl_3$) δ = 174.60, 152.27, 141.04, 136.34, 129.18, 123.11, 121.02, 119.99, 118.29, 111.21, 60.37, 55.49, 53.39, 50.32, 46.82, 38.62, 32.62, 30.54, 26.02. HPLC/HRAM-MS (ESI [+]) m/z

$[M+H^+]^+$ = 408.2677 (98.39 %). MS (APCI [+]) m/z $[M+H^+]^+$ calculated for $[C_{25}H_{33}N_3O_2]^+$: 408.2, found 408.1. M = 407.56 g/mol (free base). mp = 172.5°C (MeOH).

N-(4-(2-(4-(2-Methoxyphenyl)piperazin-1-yl)ethyl)phenyl)cyclohexanecarboxamide hydrochloride (79)

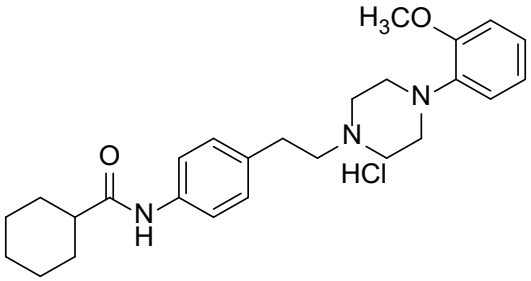

Cyclobutane carbonyl chloride (1.5 eq.) was added to a solution of aniline **54** (1 eq.) and DIPEA (1.5 eq.), the reaction was performed according to procedure **E**. Pure product was collected as hydrochloride salt precipitated in reaction solution. Light yellow solid. Yield = 67%. ^{1}H NMR (300 MHz, DMSO-d6) δ = 11.16 (s, 1H), 9.88 (s, 1H CONH), 7.59 (d, 2H Ar), 7.19 (d, 2H Ar), 7.06 – 6.86 (m, 4H Ar-Pip), 3.79 (s, 3H), 3.60 (td, 6H), 3.50 (d, 2H), 3.07 (q, 4H), 2.39 – 2.27 (m, 1H), 1.78 – 1.73 (m, 6H), 1.42 (t, 2H), 1.29 – 1.19 (m, 2H). ^{13}C NMR (75 MHz, DMSO-d6) δ = 174.25, 151.78, 139.40, 138.26, 131.25, 128.79, 123.40, 120.81, 119.28, 118.19, 111.88, 66.99, 56.28, 55.33, 51.12, 46.87, 44.75, 29.11, 28.69, 25.20, 25.09. HPLC/HRAM-MS (ESI [+]) m/z $[M+H^+]^+$ = 422.2942 (100 %). MS (APCI [+]) m/z $[M+H^+]^+$ calculated for $[C_{26}H_{35}N_3O_2]^+$: 422.2, found 422.1. M = 457.59 g/mol (HCl salt). mp = 275.3°C (THF).

1-((1-Ethylpyrrolidin-2-yl)methyl)-3-(4-(2-(4-(2-methoxyphenyl)piperazin-1-yl)ethyl)phenyl)urea (80)

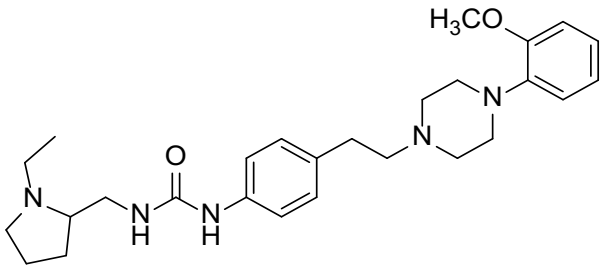

(1-Ethylpyrrolidin-2-yl) methanamine (1 eq.) was added to a stirring solution of related isocyanate **68** previously prepared. The reaction was carried out following procedure **I**. Pure product was collected through flash chromatography in Biotage Sfär Silica 25gr with dichloromethane/methanol from 0 up to 15 % of methanol. Orange sticky solid. Yield = 37%. ^{1}H NMR (300 MHz, $CDCl_3$) δ = 8.52 (s, 1H CONH), 7.38 (d, J = 8.3 Hz, 3H CONH/Ar), 7.11 (d, *J* = 8.3 Hz, 2H Ar), 7.05 – 6.82 (m,

4H Ar-Pip), 3.85 (s, 3H), 3.78 – 3.63 (m, 4H), 3.41 (dd, *J* = 12.9, Hz, 1H), 3.22 (s, 4H), 3.02 (dd, *J* = 12.9, 1H), 2.89 (d, 6H), 2.80 (q, 2H), 2.26 – 1.92 (m, 5H), 1.43 (t, 3H). ^{13}C NMR (75 MHz, $CDCl_3$) δ = 157.24, 152.19, 140.65, 137.54, 133.22, 129.05, 123.33, 121.05, 119.43, 118.41, 111.20, 68.29, 60.14, 55.43, 53.73, 53.18, 51.03, 49.74, 31.95, 29.74, 27.61, 23.21, 10.90. HPLC-DAD (ESI [+]) λ_{max} = 244 nm (99.36 %). MS (APCI [+]) m/z $[M+H^+]^+$ calculated for $[C_{27}H_{39}N_5O_2]^+$: 466.3, found 466.4. M = 465.64 g/mol (free base). mp = 54.1°C (MeOH).

N-(4-(2-(4-(2-Methoxyphenyl)piperazin-1-yl)ethyl)phenyl)pyrrolidine-1-carboxamide (81)

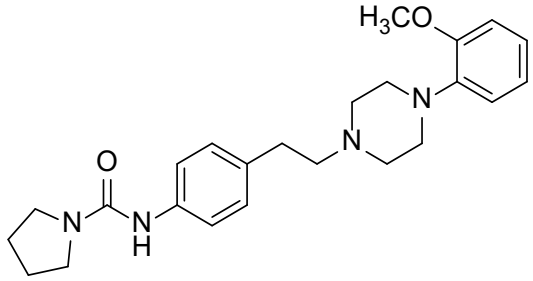

Pyrrolidine-1-carbonyl chloride (1.5 eq.) was added to a solution of aniline **54** (1 eq.) and DIPEA (1.5 eq.) in tetrahydrofuran, the reaction was performed according to procedure **E**. Pure compound was obtained through flash chromatography with Biotage Sfär Silica 25 gr in dichloromethane/methanol from 0% to 10% of methanol. Yellow solid. Yield = 25%. ^{1}H NMR (600 MHz, $CDCl_3$) δ = 7.35 – 7.31 (m, 2H Ar), 7.15 – 7.11 (m, 2H Ar), 7.02 – 6.98 (m, 1H Ar-Pip), 6.97 – 6.91 (m, 2H Ar-Pip), 6.86 (dd, 1H Ar-Pip), 6.14 (s, 1H CONH), 3.86 (s, 3H), 3.47 – 3.43 (m, 4H), 3.15 (s, 4H), 2.84 – 2.80 (m, 2H), 2.77 (s, 4H), 2.69 – 2.64 (m, 2H), 1.98 – 1.91 (m, 4H). ^{13}C NMR (151 MHz, $CDCl_3$) δ = 154.04, 152.28, 141.23, 137.33, 134.48, 129.08, 122.99, 121.02, 119.79, 118.27, 111.19, 60.59, 55.37, 53.40, 50.50, 45.81, 32.75, 25.63. HPLC-DAD (ESI [+]) λ_{max} = 244, 276 nm (100 %). MS (APCI [+]) m/z $[M+H^+]^+$ calculated for $[C_{24}H_{32}N_4O_2]^+$: 409.6, found 409.6. M = 408.55 g/mol (free base). mp = 94°C (MeOH).

N-(4-(2-(4-(2-Methoxyphenyl)piperazin-1-yl)ethyl)phenyl)morpholine-4-carboxamide (82)

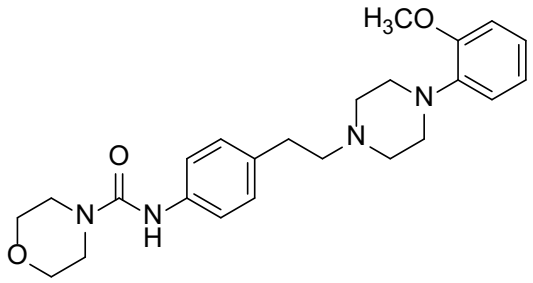

Morpholine-4-carbonyl chloride (1.5 eq.) was added to a solution of aniline **54** (1 eq.) and DIPEA (1.5 eq.), the mixture of reaction was stirred following procedure **E**. Pure compound was obtained by column chromatography in dichloromethane/ammonia in methanol 98:2. White solid. Yield 67%. ^{1}H NMR (300 MHz, $CDCl_3$) δ = 7.22 – 7.17 (m, 2H Ar), 7.11 – 7.05 (m, 2H Ar), 6.96 – 6.83 (m, 3H Ar-Pip), 6.83 – 6.76 (m, 1H Ar-Pip), 6.31 (s, 1H CONH), 3.79 (s, 3H), 3.64 (dd, 4H), 3.41 – 3.36 (m, 4H), 3.06 (t, 4H), 2.76 – 2.62 (m, 6H), 2.61 – 2.54 (m, 2H). ^{13}C NMR (75 MHz, $CDCl_3$) δ = 155.30, 152.30, 141.34, 136.74, 135.45, 129.16, 122.92, 121.02, 120.42, 118.23, 111.22, 66.50, 60.59, 55.36, 53.44, 50.65, 44.28, 32.91. HPLC/HRAM-MS (ESI [+]) m/z $[M+H^+]^+$ = 425.2723 (97.89 %). MS (APCI [+]) m/z $[M+H^+]^+$ calculated for $[C_{24}H_{32}N_4O_3]^+$: 425.2, found 425.1. M = 424.55 g/mol (free base). mp = 146.9°C (MeOH).

N-(4-(2-(4-(2-Methoxyphenyl)piperazin-1-yl)ethyl)phenyl)piperidine-1-carboxamide (83)

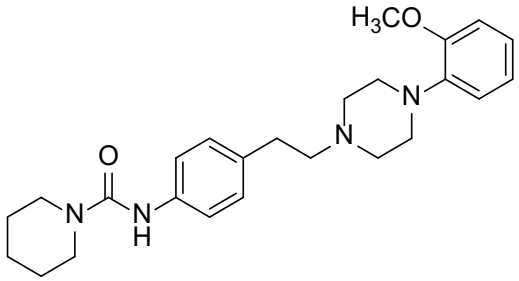

Piperidine-1-carbonyl chloride (1.5 eq.) was added to a solution of aniline (1 eq.) and DIPEA (1.5 eq.), the mixture of reaction was stirred following procedure **E**. Pure compound was obtained by column chromatography in dichloromethane/ammonia in methanol 98:2. Yellowish liquid. Yield = 21%. ^{1}H NMR (600 MHz, $CDCl_3$) δ = 7.29 – 7.26 (m, 2H Ar), 7.13 (d, 2H Ar), 7.01 (td, 1H Ar-Pip), 6.94 (dtd, 2H Ar-Pip), 6.86 (dd, 1H Ar-Pip), 6.31 (s, 1H CONH), 3.87 (s, 3H), 3.68 (t, 1H), 3.44 (t, 4H), 3.16 (s, 4H), 2.83 (dd, 5H), 2.74 – 2.68 (m, 2H), 2.58 (t, 1H), 1.66 – 1.59 (m, 5H). ^{13}C NMR (151 MHz, $CDCl_3$) δ = 155.12, 152.39, 141.33, 137.45, 134.56, 129.05, 122.93, 121.09, 120.11, 118.33, 111.50, 60.24, 55.39, 53.21, 50.27, 45.31, 32.43, 25.68, 24.38. HPLC-DAD (ESI [+]) λ_{max} = 245 nm (95.58 %). MS (APCI [+]) m/z $[M+H^+]^+$ calculated for $[C_{25}H_{34}N_4O_2]^+$: 423.2, found 422.9. M = 422.57 g/mol (free base).

1-Cyclohexyl-3-(4-(2-(4-(2-methoxyphenyl)piperazin-1-yl)ethyl)phenyl)urea hydrochloride (84)

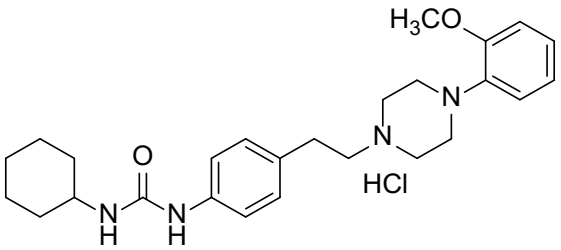

After the preparation of isocyanate **68** (1eq.), cyclohexanamine (1 eq.) was added to a solution of intermediate in acetonitrile. The reaction was executed according to procedure **I**. A white precipitate of hydrochloride salt of product was collected from mixture of reaction and purified through recrystallization in isopropanol. White solid. Yield = 89%. ^{1}H NMR (600 MHz, DMSO-d6) δ = 10.73 (s, 1H), 8.58 (s, 1H CONH), 7.35 (d, *J* = 8.1 Hz, 2H Ar), 7.12 (d, *J* = 8.1 Hz, 2H Ar), 7.02 (td, 1H Ar-Pip), 6.98 (dd, 1H Ar-Pip), 6.96 – 6.89 (m, 2H Ar-Pip), 6.26 (d, 1H CONH), 3.79 (s, 3H), 3.61 (d, 2H), 3.54 – 3.41 (m, 4H), 3.20 (2H), 3.06 – 2.96 (m, 4H), 1.78 (dt, *J* = 12.9, 2H), 1.66 (dp, *J* = 12.9, 2H), 1.52 (tt, 1H), 1.29 (tdd, 2H), 1.21 – 1.09 (m, 4H). ^{13}C NMR (151 MHz, DMSO-d6) δ = 155.03, 152.42, 139.99, 129.30, 123.92, 121.38, 118.82, 118.23, 112.63, 57.01, 55.93, 51.76, 48.00, 47.43, 33.44, 29.17, 25.76, 24.75. HPLC/HRAM-MS (ESI [+]) m/z $[M+H^+]^+$ = 437.3323 (97.12 %). MS (APCI [+]) m/z $[M+H^+]^+$ calculated for $[C_{26}H_{36}N_4O_2]^+$: 437.2, found 437.1. M = 473.06 g/mol (HCl salt). mp = 272.2°C (iPrOH).

1-(4-(2-(4-(2-Methoxyphenyl)piperazin-1-yl)ethyl)phenyl)-3-phenylurea hydrochloride (85)

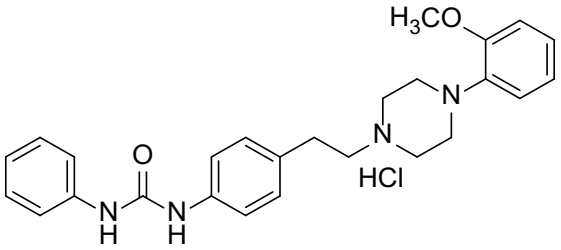

After the preparation of isocyanate **68** (1 eq.), unsubstituted aniline (1 eq.) was added to a solution of intermediate in acetonitrile. The reaction was executed according to procedure **I**. A white precipitate of hydrochloride salt of product was collected from mixture of reaction and purified through recrystallization in isopropanol. White solid. 72%. ^{1}H NMR (600 MHz, DMSO-d6) δ = 10.36 (s, 1H), 9.02 (d, 2H CONH), 7.53 – 7.39 (m, 4H Ar), 7.27 (t, 2H Ar), 7.20 (d, 2H Ar), 7.03 (t, 1H Ar), 7.00 – 6.88 (m, 4H Ar-Pip), 3.79 (s, 3H), 3.62 (d, 2H), 3.52 (d, 2H), 3.34 (q, 2H), 3.22 (q, 2H), 3.05 – 2.95

(m, 4H). ^{13}C NMR (75 MHz, DMSO-d6) δ = 152.66, 151.80, 139.78, 139.33, 138.59, 129.88, 129.03, 128.74, 123.49, 121.67, 120.83, 118.25, 117.97, 111.89, 56.41, 55.36, 51.23, 46.95, 28.71. HPLC/HRAM-MS (ESI [+]) m/z $[M+H^+]^+$ = 431.2849 (99.50 %). MS (APCI [+]) m/z $[M+H^+]^+$ calculated for $[C_{26}H_{30}N_4O_2]^+$: 431.2, found 431.2. M = 467.01 (HCl salt). mp = 235.9°C (iPrOH).

3-(4-(2-(4-(2-Methoxyphenyl)piperazin-1-yl)ethyl)phenyl)-1-methyl-1-phenylurea (86)

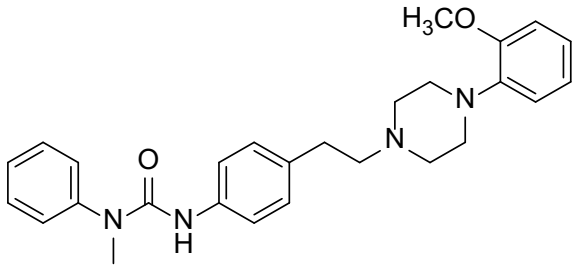

Methyl(phenyl)carbamic chloride (1.5 eq.) was added to a solution of aniline **54** (1 eq.) and DIPEA (1.5 eq.), the mixture of reaction was stirred following procedure **E**. Pure compound was obtained by column chromatography in dichloromethane/ methanol 98:2. Brown sticky oil. Yield = 54%. ^{1}H NMR (300 MHz, $CDCl_3$) δ = 7.41 (tt, 2H Ar), 7.33 – 7.24 (m, 3H Ar), 7.16 – 7.10 (m, 2H Ar), 7.05 – 6.99 (m, 2H Ar), 6.96 – 6.84 (m, 3H Ar-Pip), 6.83 – 6.76 (m, 1H Ar-Pip), 6.12 (s, 1H CONH), 3.79 (s, 3H), 3.27 (s, 3H), 3.05 (s, 4H), 2.74 – 2.61 (m, 6H), 2.59 – 2.50 (m, 2H). ^{13}C NMR (75 MHz, $CDCl_3$) δ = 154.53, 152.28, 142.99, 141.32, 136.90, 134.91, 130.32, 129.03, 127.82, 127.46, 122.92, 121.00, 119.53, 118.23, 111.17, 60.63, 55.35, 53.42, 50.63, 37.27, 32.86. HPLC-DAD (ESI [+]) λ_{max} = 244 nm (100 %). MS (APCI [+]) m/z $[M+H^+]^+$ calculated for $[C_{27}H_{32}N_4O_2]^+$: 445.2, found 445.2. M = 444.58 g/mol (free base).

3-(4-(2-(4-(2-Methoxyphenyl)piperazin-1-yl)ethyl)phenyl)-1,1-diphenylurea (87)

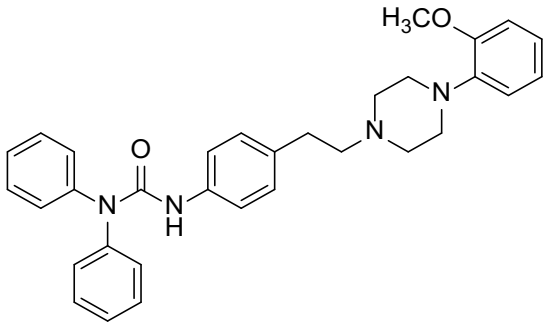

Diphenyl carbamic chloride (1.5 eq.) was added to a solution of aniline (1 eq.) and DIPEA (1.5 eq.) in tetrahydrofuran, the reaction was performed according to procedure **E**. Pure compound was obtained through flash chromatography with Biotage Sfär Silica 25 gr in dichloromethane/methanol

from 0% to 10% of methanol. Yellowish sticky oil. Yield = 26%. ^{1}H NMR (300 MHz, $CDCl_3$) δ = 7.37 – 7.15 (m, 12H Ar-Ur/Ar), 7.08 – 7.02 (m, 2H Ar), 6.97 – 6.75 (m, 4H Ar-Pip), 6.33 (s, 1H CONH), 3.78 (s, 3H), 3.05 (t, 4H), 2.77 – 2.51 (m, 8H). ^{13}C NMR (75 MHz, $CDCl_3$) δ = 153.60, 152.29, 142.42, 141.32, 136.54, 135.33, 129.59, 129.13, 127.50, 126.63, 122.94, 121.01, 119.57, 118.24, 111.18, 60.61, 55.38, 53.43, 50.63, 32.88. HPLC-DAD (ESI [+]) λ_{max} = 248 nm (100 %). MS (APCI [+]) m/z $[M+H^+]^+$ calculated for $[C_{32}H_{34}N_4O_2]^+$: 507.2, found 507.4. M = 506.65 (free base).

1-Benzyl-3-(4-(2-(4-(2-methoxyphenyl)piperazin-1-yl)ethyl)phenyl)urea (88)

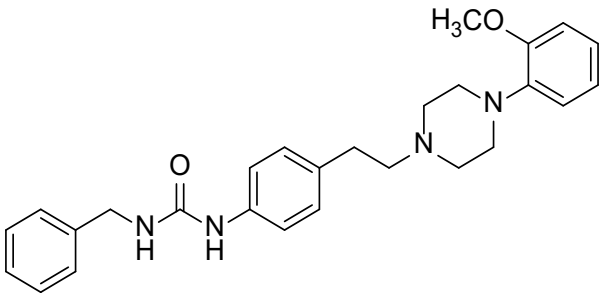

Unsubstituted benzylamine (1 eq.) was added to a stirring solution of related isocyanate (1 eq.) previously prepared. The reaction was carried out following procedure **I**. Pure product was obtained by column chromatography in dichloromethane/ammonia in methanol 98:2. White solid. Yield = 30%. ^{1}H NMR (600 MHz, DMSO-d6) δ = 8.45 (s, 1H CONH), 7.35 – 7.28 (m, 6H Ar-Ur/Ar), 7.28 – 7.22 (m, 1H Ar-Ur), 7.11 – 7.07 (m, 2H Ar), 6.96 – 6.90 (m, 2H Ar-Pip), 6.89 – 6.85 (m, 2H Ar-Pip), 6.56 (t, 1H CONH), 4.29 (d, 2H), 3.77 (s, 3H), 2.96 (s, 4H), 2.67 (dd, 2H), 2.60 – 2.50 (m, 6H). ^{13}C NMR (151 MHz, DMSO-d6) δ = 155.78, 152.51, 141.85, 140.88, 138.79, 133.59, 129.22, 128.75, 127.60, 127.15, 122.75, 121.35, 118.39, 118.35, 112.54, 60.49, 55.83, 53.48, 50.56, 43.27, 32.58. Elemental analysis (calculated/found): %C 72.94/72.93, %H 7.26/7.40, %N 12.60/12.27. MS (APCI [+]) m/z $[M+H^+]^+$ calculated for $[C_{27}H_{32}N_4O_2]^+$: 445.2, found 445.2. M = 444.58 g/mol (free base). mp = 171.8°C (MeOH).

2-Methoxy-*N*-(4-(2-(4-(2-methoxyphenyl)piperazin-1-yl)ethyl)phenyl)benzamide (89)

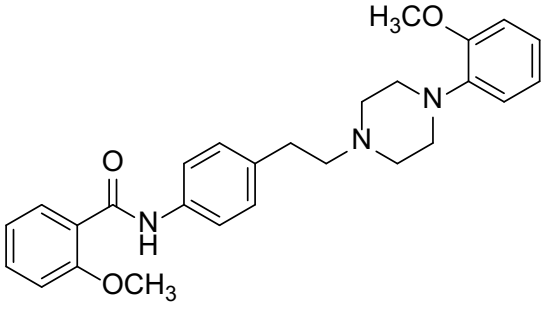

2-Methoxybenzoic acid (1 eq.) and obtained aniline (1 eq.) were mixed together to obtain this derivative following conditions of procedure **H**. Pure product was collected by flash chromatography with Biotage Sfär Silica 25 gr in dichloromethane/methanol from 0% to 10% of methanol. Brown sticky oil. Yield 35%. ^{1}H NMR (600 MHz, $CDCl_3$) δ = 9.78 (s, 1H CONH), 8.23 (dd, *J* =1.9 Hz, 1H Ar-Bmd), 7.61 – 7.55 (m, 2H Ar-Bmd), 7.47 (ddd, *J* = 1.9 Hz, 1H Ar-Bmd), 7.23 – 7.18 (m, 2H Ar), 7.10 (td, 1H Ar-Pip), 7.03 – 6.98 (m, 2H Ar), 6.92 – 6.89 (m, 2H Ar-Pip), 6.87 – 6.84 (m, 1H Ar-Pip), 4.02 (s, 3H), 3.84 (s, 3H), 3.19 (s, 4H), 3.02 – 2.88 (m, 6H), 2.88 – 2.83 (m, 2H). ^{13}C NMR (151 MHz, $CDCl_3$) δ = 163.37, 157.28, 152.26, 140.49, 136.73, 134.70, 133.34, 132.37, 129.28, 123.42, 121.63, 121.61, 121.05, 120.93, 118.38, 111.61, 111.34, 59.80, 56.30, 56.21, 53.24, 49.56. HPLC-DAD (ESI [+]) λ_{max} = 243 nm (99.09 %). MS (APCI [+]) m/z $[M+H^+]^+$ calculated for $[C_{27}H_{31}N_3O_3]^+$: 446.2, found 446.2. M = 445.24 g/mol (free base).

3-Methoxy-*N*-(4-(2-(4-(2-methoxyphenyl)piperazin-1-yl)ethyl)phenyl)benzamide (90)

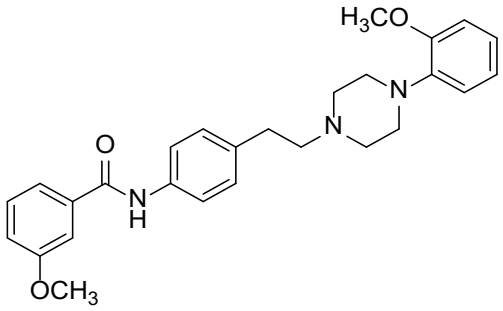

3-Methoxybenzoyl chloride (1.5 eq.) was added to a solution of aniline (1 eq.) and DIPEA (1.5 eq.), the mixture of reaction was stirred following procedure **E**. Pure compound was obtained by column chromatography in dichloromethane/ ammonia in methanol 98:2. Light yellow solid. Yield = 65%. ^{1}H NMR (300 MHz, $CDCl_3$) δ = 7.87 (s, 1H CONH), 7.53 – 7.45 (m, 2H Ar), 7.38 – 7.21 (m, 3H Ar-Bmd), 7.20 – 7.10 (m, 2H Ar), 7.02 – 6.75 (m, 5H Ar-Bmd/Ar-Pip), 3.77 (d, 6H), 3.15 – 2.95 (m, 4H), 2.82 – 2.51 (m, 8H). ^{13}C NMR (75 MHz, $CDCl_3$) δ = 165.59, 159.96, 152.29, 141.32, 136.72, 136.51, 136.00, 129.73, 129.30, 122.95, 121.02, 120.43, 119.21, 118.72, 118.24, 117.97, 112.60, 112.49, 111.20, 60.54, 55.47, 55.37, 53.45, 50.66, 33.05. HPLC-MS (ESI [+]) m/z $[M+H^+]^+$ = 446.25 (96 %). MS (APCI [+]) m/z $[M+H^+]^+$ calculated for $[C_{27}H_{31}N_3O_3]^+$: 446.2, found 446.2. M = 445.24 g/mol (free base). mp = 143.7°C (MeOH).

4-Methoxy-*N*-(4-(2-(4-(2-methoxyphenyl)piperazin-1-yl)ethyl)phenyl)benzamide hydrochloride (91)

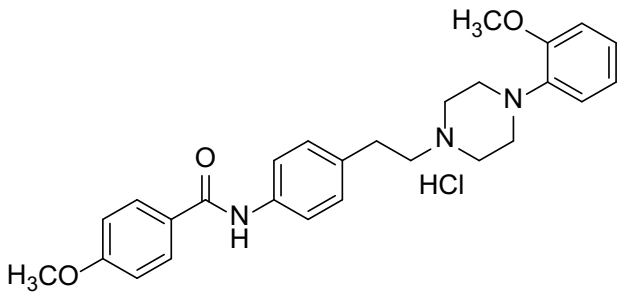

4-Methoxybenzoyl chloride (1.5 eq.) was added to a solution of aniline **54** (1 eq.) and DIPEA (1.5 eq.), the reaction was performed according to procedure **E**. The desired product was collected as hydrochloride salt precipitated in reaction solution and purified by recrystallization in ethanol. White solid. Yield = 57%. ^{1}H NMR (300 MHz, DMSO-d6) δ = 10.97 (s, 1H), 10.13 (s, 1H CONH), 8.04 – 7.94 (m, 2H Ar-Bmd), 7.76 (d, *J* = 8.4 Hz, 2H Ar), 7.26 (d, *J* = 8.4 Hz, 2H Ar), 7.09 – 7.04 (m, 2H Ar-Bmd), 7.03 – 6.87 (m, 4H Ar-Pip), 3.82 (d, 6H), 3.67 – 3.44 (m, 4H), 3.33 – 2.95 (m, 8H). ^{13}C NMR (75 MHz, DMSO-d6) δ = 164.78, 161.86, 151.80, 139.41, 138.07, 129.57, 128.76, 126.84, 123.42, 120.82, 120.56, 118.22, 113.56, 111.90, 56.29, 55.34, 51.18, 46.91, 28.75. HPLC-DAD (ESI [+]) λ_{max} = 279 nm (100 %). MS (APCI [+]) m/z $[M+H^+]^+$ calculated for $[C_{27}H_{31}N_3O_3]^+$: 446.2, found 446.6. M = 482.02 (HCl salt). mp = 283.4°C (EtOH).

2,3-Dimethoxy-*N*-(4-(2-(4-(2-methoxyphenyl)piperazin-1-yl)ethyl)phenyl)benzamide (92)

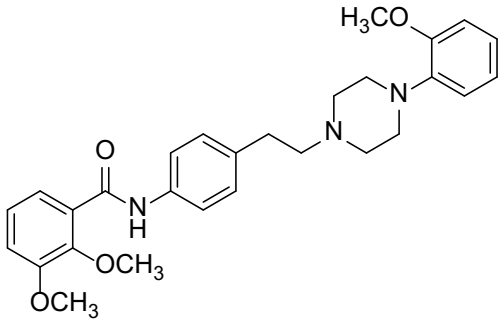

2,3-Dimethoxybenzoyl chloride (1.5 eq.) was added to a solution of aniline (1 eq.) and DIPEA (1.5 eq.), the reaction was performed according to procedure **E**. Pure derivative was obtained by flash chromatography with Biotage Sfär Silica 25gr in dichloromethane/methanol from 0 to 10% of methanol. White solid. Yield = 42%. ^{1}H NMR (600 MHz, $CDCl_3$) δ = 9.96 (s, 1H CONH), 7.78 (dd, *J* = 8.0, 1.6 Hz, 1H Ar-Bmd), 7.63 – 7.60 (m, 2H Ar), 7.25 – 7.22 (m, 2H Ar), 7.20 (t, *J* = 8.0 Hz, 1H Ar-Bmd), 7.09 (dd, *J* = 1.6 Hz, 1H Ar-Bmd), 7.00 (ddd, *J* = 7.9, 1.8 Hz, 1H Ar-Pip), 6.97 (dd, *J* =

7.9, 1.8 Hz, 1H Ar-Pip), 6.92 (td, + = 1.4 Hz, 1H Ar-Pip), 6.86 (dd, *J* = 1.4 Hz, 1H Ar-Pip), 3.98 (s, 3H), 3.92 (s, 3H), 3.87 (s, 3H), 3.15 (s, 4H), 2.88 – 2.83 (m, 2H), 2.76 (s, 4H), 2.71 – 2.66 (m, 2H). ^{13}C NMR (151 MHz, $CDCl_3$) δ = 162.91, 152.62, 152.30, 147.21, 141.32, 136.50, 136.29, 129.30, 126.97, 124.77, 123.00, 122.95, 121.02, 120.29, 118.25, 115.68, 111.20, 61.68, 60.60, 56.17, 55.38, 53.45, 50.63, 33.03. HPLC-DAD (ESI [+]) λ_{max} = 277 nm (100 %). MS (APCI [+]) m/z $[M+H^+]^+$ calculated for $[C_{28}H_{33}N_3O_4]^+$: 476.2, found 476.6. M = 475.59 g/mol (free base). mp = 118.3°C (MeOH).

2,4-Dimethoxy-*N*-(4-(2-(4-(2-methoxyphenyl)piperazin-1-yl)ethyl)phenyl)benzamide (93)

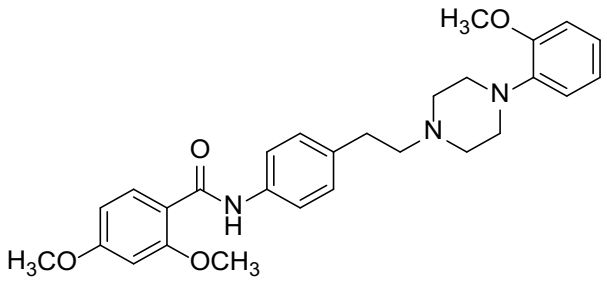

2,4-Dimethoxybenzoic acid (1 eq.) and obtained aniline (1 eq.) were mixed together to obtain this derivative following conditions of procedure **H**. Pure product was obtained by flash chromatography with Biotage Sfär Silica 25 gr in dichloromethane/methanol from 0% to 10% of methanol. Light yellow solid. Yield = 61%. ^{1}H NMR (600 MHz, $CDCl_3$) δ = 9.65 (s, 1H CONH), 8.22 (d, *J* = 8.8 Hz, 1H AR-Bmd), 7.59 – 7.53 (m, 2H Ar), 7.23 – 7.13 (m, 2H Ar), 7.00 – 6.83 (m, 4H Ar-Pip), 6.62 (dd, *J* = 8.8, 1H Ar-Bmd), 6.50 (d, 1H Ar-Bmd), 3.99 (s, 3H), 3.84 (d, 6H), 3.14 (s, 4H), 2.86 – 2.78 (m, 6H), 2.74 – 2.70 (m, 2H). ^{13}C NMR (151 MHz, $CDCl_3$) δ = 163.76, 163.13, 158.59, 152.28, 141.07, 136.75, 135.46, 134.12, 129.19, 123.08, 121.02, 120.66, 118.27, 114.65, 111.25, 98.75, 98.69, 60.35, 56.26, 55.63, 55.43, 55.35, 53.37, 50.29. HPLC-DAD (ESI [+]) λ_{max} = 254 nm (98.37 %). MS (APCI [+]) m/z $[M+H^+]^+$ calculated for $[C_{28}H_{33}N_3O_4]^+$: 476.2, found 476.3. M = 475.59 g/mol (free base). mp = 154.7°C (MeOH).

2,5-Dimethoxy-*N*-(4-(2-(4-(2-methoxyphenyl)piperazin-1-yl)ethyl)phenyl)benzamide (94)

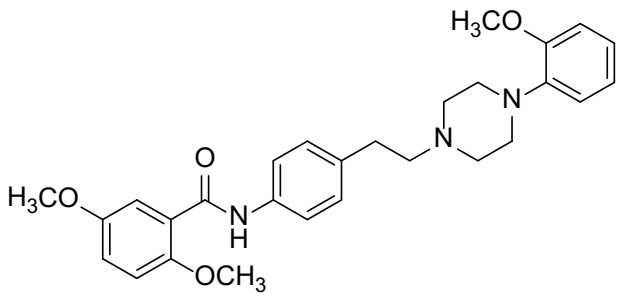

2,5-Dimethoxybenzoic acid (1 eq.) and obtained aniline (1 eq.) were mixed together to obtain this derivative following conditions of procedure **H**. Pure product was obtained by flash chromatography with Biotage Sfär Silica 25 gr in dichloromethane/methanol from 0% to 10% of methanol. Brownish solid. Yield = 82%. ^{1}H NMR (300 MHz, $CDCl_3$) δ = 9.93 (s, 1H CONH), 7.82 (d, 1H Ar-Bmd), 7.63 – 7.57 (m, 2H Ar), 7.25 – 7.18 (m, 2H Ar), 7.07 – 6.91 (m, 5H Ar-Pip/Ar-Bmd), 6.90 – 6.84 (m, 1H Ar-Bmd), 4.01 (s, 3H), 3.85 (d, 6H), 3.20 (s, 4H), 2.97 – 2.78 (m, 8H). ^{13}C NMR (75 MHz, $CDCl_3$) δ = 163.04, 154.15, 152.28, 151.55, 140.61, 136.68, 135.00, 129.29, 123.39, 122.24, 121.06, 120.81, 119.87, 118.44, 115.66, 113.32, 111.27, 60.21, 56.89, 55.86, 53.49, 49.88, 32.22. HPLC-DAD (ESI [+]) λ_{max} = 240 nm (96.99 %). MS (APCI [+]) m/z $[M+H^+]^+$ calculated for $[C_{28}H_{33}N_3O_4]^+$: 476.2, found 476.1. M = 475.59 g/mol (free base). mp = 73.6°C (MeOH).

2,6-Dimethoxy-*N*-(4-(2-(4-(2-methoxyphenyl)piperazin-1-yl)ethyl)phenyl)benzamide (95)

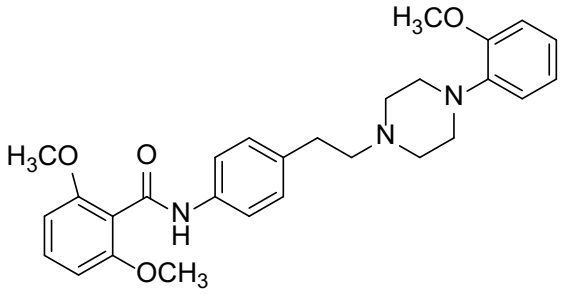

2,6-Dimethoxybenzoic acid (1 eq.) and obtained aniline (1 eq.) were mixed together to obtain this derivative following conditions of procedure **H**. Pure product was collected by flash chromatography with Biotage Sfär Silica 25 gr in dichloromethane/methanol from 0% to 10% of methanol. Brown solid. Yield = 33%. ^{1}H NMR (600 MHz, $CDCl_3$) δ = 7.60 – 7.56 (m, 2H Ar), 7.51 (s, 1H CONH), 7.30 (t, *J* = 8.4 Hz, 1H Ar-Bmd), 7.20 (d, 2H Ar), 7.01 (ddd, 1H Ar-Pip), 6.93 (dtd, 2H Ar-Pip), 6.86 (dd, 1H Ar-Pip), 6.58 (d, *J* = 8.4 Hz, 2H Ar-Bmd), 3.86 (s, 3H), 3.81 (s, 6H), 3.23 (s, 4H), 3.00 – 2.86 (m, 6H), 2.81 (d, 2H). ^{13}C NMR (75 MHz, $CDCl_3$) δ = 163.72, 157.57, 152.20, 140.63, 136.80,

134.87, 131.11, 129.18, 123.35, 121.06, 119.94, 118.43, 115.89, 111.21, 104.10, 60.07, 56.05, 55.40, 53.16, 49.71, 32.02. HPLC-DAD (ESI [+]) λ_{max} = 248 nm (100 %). MS (APCI [+]) m/z $[M+H^+]^+$ calculated for $[C_{28}H_{33}N_3O_4]^+$: 476.2, found 475.9. M = 475.59 g/mol (free base). mp = 173.4°C (MeOH).

3,5-Dimethoxy-*N*-(4-(2-(4-(2-methoxyphenyl)piperazin-1-yl)ethyl)phenyl)benzamide (96)

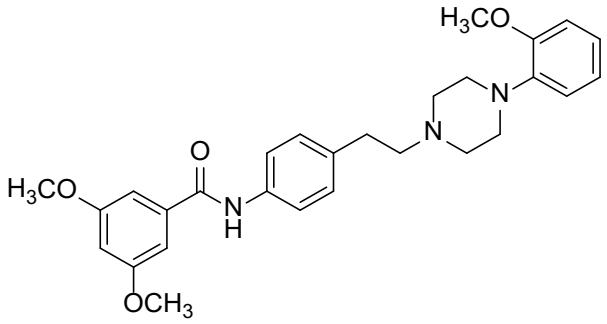

Obtained aniline **54** (1 eq.) was solubilized in tetrahydrofuran (~20 ml), then 3,5-dimethoxybenzoyl chloride (1.5 eq.) and DIPEA (1.5 eq.) were added in the solution of reaction that was performed following conditions of procedure **E**. Pure derivative was obtained by flash chromatography with Biotage Sfär Silica 25gr in dichloromethane/methanol from 0% up to 10% of methanol. White solid. Yield = 69%. ^{1}H NMR (300 MHz, $CDCl_3$) δ = 7.87 (s, 1H CONH), 7.59 – 7.51 (m, 2H Ar), 7.25 – 7.18 (m, 2H Ar), 7.04 – 6.91 (m, 5H Ar-Pip/Ar-Bmd), 6.86 (dd,1H Ar-Bmd), 6.59 (t,1H Ar-Bmd), 3.84 (d, 9H), 3.14 (s, 4H), 2.90 – 2.63 (m, 8H). ^{13}C NMR (75 MHz, $CDCl_3$) δ = 165.61, 161.10, 152.37, 141.42, 137.37, 136.83, 136.03, 129.39, 123.02, 121.09, 120.44, 118.32, 111.27, 105.06, 103.81, 60.63, 55.69, 55.45, 53.55, 50.76, 33.15. HPLC-MS (ESI [+]) m/z $[M+H^+]^+$ = 476.30 (95.1 %). MS (APCI [+]) m/z $[M+H^+]^+$ calculated for $[C_{28}H_{33}N_3O_4]^+$: 476.2, found 476.3. M = 475.59 g/mol (free base). mp = 151.4°C (MeOH).

4,5-Dimethoxy-*N*-(4-(2-(4-(2-methoxyphenyl)piperazin-1-yl)ethyl)phenyl)benzamide hydrochloride (97)

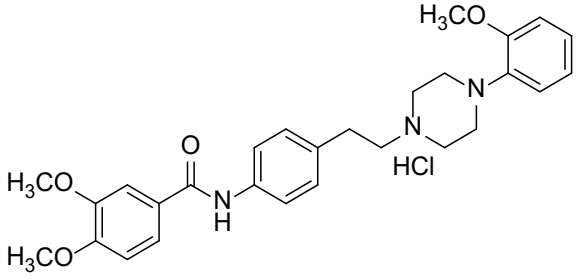

4,5-Dimethoxybenzoyl chloride (1.5 eq.) was added to a solution of aniline **54** (1 eq.) and DIPEA (1.5 eq.), the reaction was performed according to procedure **E**. The desired product was collected as hydrochloride salt precipitated in reaction solution and purified by recrystallization in isopropanol. Brown solid. ^{1}H NMR (300 MHz, DMSO-d6) δ = 10.85 (s, 1H), 10.13 (s, 1H CONH), 7.81 – 7.72 (m, 2H Ar), 7.64 (dd, *J* = 8.4, 2.1 Hz, 1H Ar-Bmd), 7.56 (d, *J* = 2.1 Hz, 1H Ar-Bmd), 7.28 (d, 2H Ar), 7.09 (d, *J* = 8.4 Hz, 1H Ar-Bmd), 6.97 (tdd, 4H Ar-Pip), 3.98 – 3.75 (m, 9H), 3.71 – 3.45 (m, 5H), 3.30 – 2.95 (m, 7H). ^{13}C NMR (75 MHz, DMSO-d6) δ = 173.24, 164.80, 160.97, 151.60, 148.26, 138.02, 131.92, 128.76, 123.90, 121.02, 120.72, 118.23, 111.90, 111.02, 110.86, 69.86, 62.59, 55.62, 53.96, 51.20, 46.94. HPLC-MS (ESI [+]) m/z $[M+H^+]^+$ = 476.29 (100 %). MS (APCI [+]) m/z $[M+H^+]^+$ calculated for $[C_{28}H_{33}N_3O_4]^+$: 476.2, found 476.3. M = 512.05 g/mol (HCl salt). mp = 245-249°C (iPrOH).

3,4,5-Trimethoxy-*N*-(4-(2-(4-(2-methoxyphenyl)piperazin-1-yl)ethyl)phenyl)benzamide (98)

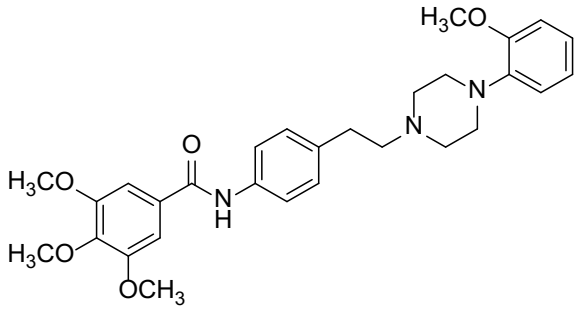

Obtained aniline (1 eq.) was solubilized in tetrahydrofuran (~20 ml), then 3,4,5-trimethoxybenzoyl chloride (1.5 eq.) and DIPEA (1.5 eq.) were added in the solution of reaction that was performed following conditions of procedure **E**. Pure derivative was obtained by flash chromatography with Biotage Sfär Silica 25gr in dichloromethane/methanol from 0% up to 10% of methanol. White solid. Yield = 68%. ^{1}H NMR (600 MHz, $CDCl_3$) δ = 8.28 (s, 1H CONH), 7.61 (d, *J* = 8.1 Hz, 2H Ar), 7.18 (d, *J* = 8.1 Hz, 2H Ar), 7.13 (s, 2H Ar-Bmd), 7.04 – 6.98 (m, 1H Ar-Pip), 6.92 (d, 2H Ar-Pip), 6.86 (d, 1H Ar-Pip), 3.88 (s, 6H), 3.87 (s, 3H), 3.85 (s, 3H), 3.17 (s, 4H), 2.92 – 2.79 (m, 6H), 2.73 (dd, 2H). ^{13}C NMR (151 MHz, $CDCl_3$) δ 165.67, 153.31, 152.29, 141.17, 140.86, 136.48, 130.41, 129.29, 123.35, 121.15, 120.82, 118.41, 111.30, 104.77, 61.01, 60.18, 56.46, 55.47, 53.32, 50.06, 32.38. HPLC-MS (ESI [+]) m/z $[M+H^+]^+$ = 506.32 (100 %). MS (APCI [+]) m/z $[M+H^+]^+$ calculated for $[C_{29}H_{35}N_3O_5]^+$: 506.2, found 506.3. M = 505.62 g/mol (free base). mp = 169.8°C (MeOH).

2-Methoxy-*N*-(4-(2-(4-(2-methoxyphenyl)piperazin-1-yl)ethyl)phenyl)-5-sulfamoylbenzamide (99)

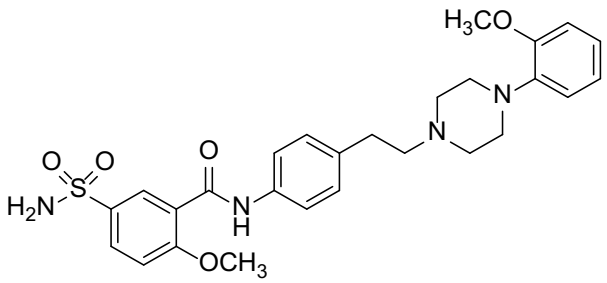

2-Methoxy-5-sulfamoylbenzoic acid (1 eq.) and obtained aniline (1 eq.) were mixed together to obtain this derivative following conditions of procedure **H.** The derivative was collected as a solid precipitate in the mixture of reaction, it was purified through recrystallization in ethanol. Light pink solid. Yield = 30%. ^{1}H NMR (300 MHz, DMSO-d6) δ = 10.25 (s, 1H CONH), 8.03 (d, 1H Ar-Bmd), 7.92 (dd, 1H Ar-Bmd), 7.71 (d, 2H NH_2), 7.41 – 7.25 (m, 5H Ar-Bmd/Ar), 7.09 – 6.88 (m, 4H Ar-Pip), 3.96 (s, 3H), 3.80 (s, 3H), 3.44 (q, 10H), 3.00 (t, 2H). ^{13}C NMR (75 MHz, DMSO-d6) δ = 179.76, 163.35, 158.62, 151.84, 139.29, 137.56, 136.18, 129.06, 127.34, 125.19, 123.54, 122.14, 120.84, 120.06, 118.35, 112.30, 111.93, 56.49, 55.99, 55.35, 51.45, 47.18, 47.17. HPLC-DAD (ESI [+]) λ_{max} = 242 nm (97.28 %). MS (APCI [+]) m/z $[M+H^+]^+$ calculated for $[C_{27}H_{32}N_4O_5S]^+$: 525.2, found 525.2. M = 524.64 g/mol (free base). mp = 143.4°C (EtOH).

4-Amino-5-(ethylsulfonyl)-2-methoxy-*N*-(4-(2-(4-(2-methoxyphenyl)piperazin-1-yl)ethyl)phenyl)benzamide (100)

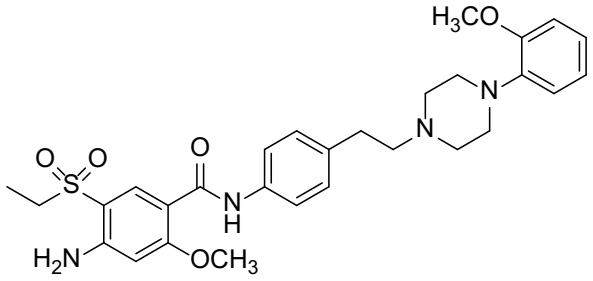

4-Amino-5-(ethylsulfonyl)-2-methoxybenzoic acid (1 eq.) and obtained aniline **54** (1 eq.) were mixed together to obtain this derivative following conditions of procedure **H.** Pure product was obtained by flash chromatography with Biotage Sfär Silica 25gr in dichloromethane/methanol from 0% up to 10%. Yellowish solid. Yield = 37%. ^{1}H NMR (300 MHz, $CDCl_3$) δ = 9.36 (s, 1H CONH), 8.55 (s, 1H Ar-Bmd), 7.57 – 7.49 (m, 2H Ar), 7.22 – 7.14 (m, 2H Ar), 7.03 – 6.84 (m, 4H Ar-Pip), 6.23 (s, 1H Ar-Bmd), 5.61 (s, 2H NH_2), 3.99 (s, 3H), 3.86 (s, 3H), 3.10 (q, 6H), 2.87 – 2.62 (m, 8H), 1.26 (d, 3H). ^{13}C NMR (75 MHz, $CDCl_3$) δ = 161.96, 161.87, 152.28, 151.08, 141.31, 136.73, 136.36,

136.18, 129.18, 122.95, 121.00, 120.57, 118.22, 112.68, 112.31, 111.19, 98.70, 60.57, 56.58, 55.37, 53.45, 50.66, 49.70, 33.03, 29.71. HPLC-DAD (ESI [+]) λ_{max} = 234 nm (100 %). MS (APCI [+]) m/z $[M+H^+]^+$ calculated for $[C_{29}H_{36}N_4O_5S]^+$: 553.2, found 553.1. M = 552.69 g/mol (free base). mp = 93.3°C (MeOH).

3-Cyano-*N*-(4-(2-(4-(2-methoxyphenyl)piperazin-1-yl)ethyl)phenyl)benzamide (101)

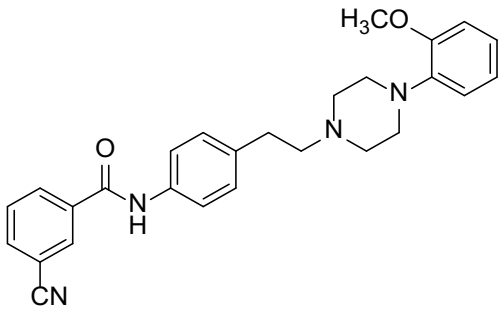

3-Cyanobenzoic acid (1 eq.) and obtained aniline **54** (1 eq.) were mixed together to obtain this derivative following conditions of procedure **H.** Pure product was obtained by flash chromatography with Biotage Sfär Silica 25gr in dichloromethane/methanol from 0% up to 10%. Brown solid. Yield = 93%. ^{1}H NMR (300 MHz, DMSO-d6) δ = 10.42 (s, 1H CONH), 8.40 (t,1H Ar), 8.25 (dt, 1H Ar), 8.07 (dt, 1H Ar), 7.80 – 7.71 (m, 3H Ar-Bmd/Ar), 7.33 – 7.27 (m, 2H Ar), 7.03 – 6.89 (m, 4H Ar-Pip), 3.80 (s, 3H), 3.62 (p, 2H), 3.13 (t, 8H), 2.95 (t, 2H). ^{13}C NMR (75 MHz, DMSO-d6) δ = 163.53, 151.86, 146.51, 137.32, 135.84, 134.97, 132.46, 131.21, 129.84, 128.96, 123.25, 120.83, 120.59, 118.30, 118.23, 111.90, 111.50, 55.32, 53.55, 51.80, 47.83,12.46. HPLC-DAD (ESI [+]) λ_{max} = 228 nm (98.97 %). MS (APCI [+]) m/z $[M+H^+]^+$ calculated for $[C_{27}H_{28}N_4O_2]^+$: 441.2, found 441.5. M = 440.55 g/mol (free base). mp = 230-235°C (MeOH).

4-Cyano-*N*-(4-(2-(4-(2-methoxyphenyl)piperazin-1-yl)ethyl)phenyl)benzamide (102)

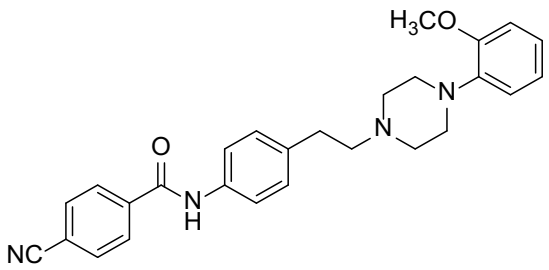

4-Cyanobenzoyl chloride (1.5 eq.) was added to a solution of obtained aniline (1 eq.) and DIPEA (1.5 eq.), the mixture of reaction was stirred following procedure **E**. Pure compound was obtained by

column chromatography in dichloromethane/ammonia in methanol 98:2. White solid. Yield = 65%. ^{1}H NMR (300 MHz, $CDCl_3$) δ = 7.93 – 7.81 (m, 3H CONH/Ar-Bmd), 7.73 – 7.66 (m, 2H Ar-Bmd), 7.48 (d, 2H Ar), 7.17 (d, 2H Ar), 6.99 – 6.75 (m, 4H Ar-Pip), 3.80 (s, 3H), 3.06 (s, 4H), 2.85 – 2.52 (m, 8H). ^{13}C NMR (75 MHz, $CDCl_3$) δ = 164.00, 152.39, 141.38, 139.03, 137.60, 135.46, 132.72, 129.62, 129.57, 127.90, 123.12, 121.14, 120.73, 118.35, 118.04, 115.45, 111.30, 60.55, 55.49, 53.55, 50.75, 33.14. HPLC-MS (ESI [+]) m/z $[M+H^+]^+$ = 441.22 (98.4 %). MS (APCI [+]) m/z $[M+H^+]^+$ calculated for $[C_{27}H_{28}N_4O_2]^+$: 441.2, found 441.2. M = 440.55 g/mol (free base). mp = 206.1°C (MeOH).

N-(4-(2-(4-(2-Methoxyphenyl)piperazin-1-yl)ethyl)phenyl)benzamide (103)

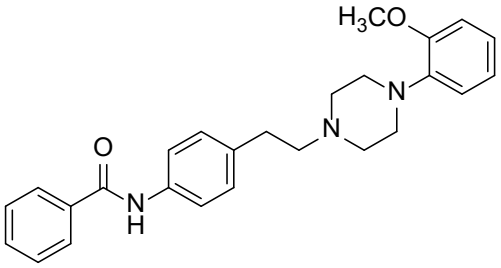

Obtained aniline **54** (1 eq.) was solubilized in tetrahydrofuran (~20 ml), then benzoyl chloride (1.5 eq.) and DIPEA (1.5 eq.) were added in the solution of reaction that was performed following conditions of procedure **E**. Pure derivative was obtained by flash chromatography with Biotage Sfär Silica 25gr in dichloromethane/methanol from 0% up to 10% of methanol. White solid. Yield = 70%. ^{1}H NMR (300 MHz, DMSO-d6) δ = 10.26 (s, 1H CONH), 8.01 – 7.92 (m, 2H Ar-Bmd), 7.74 (d, *J* = 8.4 Hz, 2H Ar), 7.63 – 7.49 (m, 3H Ar-Bmd), 7.26 (d, *J* = 8.4 Hz, 2H Ar), 7.05 – 6.86 (m, 4H Ar-Pip), 3.79 (s, 3H), 3.27 – 2.80 (m, 12H). ^{13}C NMR (75 MHz, DMSO-d6) δ = 165.40, 151.83, 140.04, 137.61, 134.88, 131.50, 128.76, 128.33, 127.63, 123.02, 120.81, 120.55, 118.07, 111.87, 57.52, 55.31, 51.75, 47.95, 29.91. HPLC-MS (ESI [+]) m/z $[M+H^+]^+$ = 416.29 (100 %). MS (APCI [+]) m/z $[M+H^+]^+$ calculated for $[C_{26}H_{29}N_3O_2]^+$: 416.2, found 416.3. M = 415.54 g/mol (free base). mp=223°C (MeOH).

N-(4-(2-(4-(2-Methoxyphenyl)piperazin-1-yl)ethyl)phenyl)picolinamide (104)

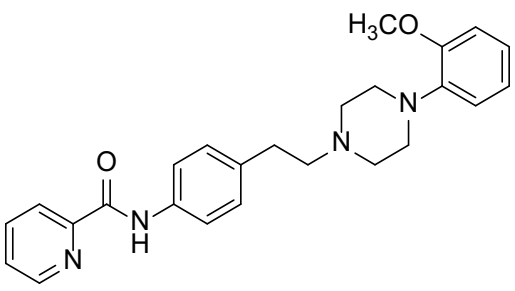

Picolinic acid (1 eq.) and obtained aniline (1 eq.) were mixed together to obtain this derivative following conditions of procedure **H**. Pure product was obtained by flash chromatography with Biotage Sfär Silica 25gr in dichloromethane/methanol from 0% up to 10%. Brownish solid. Yield = 65%. ^{1}H NMR (600 MHz, DMSO-d6) δ = 10.60 (s, 1H CONH), 8.77 – 8.67 (m, 1H Ar-Bmd), 8.16 (dt, 1H Ar-Bmd), 8.07 (td, 1H Ar-Bmd), 7.85 (d, 2H Ar), 7.68 (ddd, 1H Ar-Bmd), 7.26 (d, 2H Ar), 7.02 – 6.85 (m, 4H Ar-Pip), 3.78 (s, 3H), 3.34 (s, 6H), 3.09 (q, 6H). ^{13}C NMR (75 MHz, DMSO-d6) δ = 168.09, 162.32, 151.89, 149.88, 148.40, 138.12, 128.88, 126.88, 122.31, 120.81, 120.34, 118.06, 111.88, 107.86, 66.84, 55.31, 52.25, 48.40, 31.71. HPLC-DAD (ESI [+]) λ_{max} = 235 nm (100 %). MS (APCI [+]) m/z $[M+H^+]^+$ calculated for $[C_{25}H_{28}N_4O_2]^+$: 417.2, found 417.7. M = 416.53 g/mol (free base). mp = 175°C (MeOH).

N-(4-(2-(4-(2-Methoxyphenyl)piperazin-1-yl)ethyl)phenyl)nicotinamide (105)

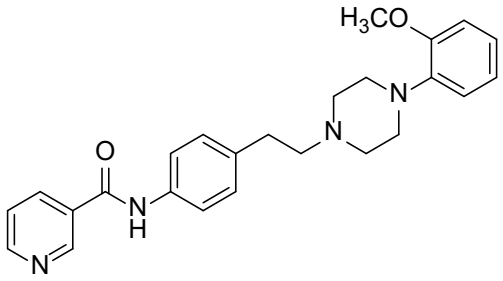

Nicotinic acid (1 eq.) and obtained aniline (1 eq.) were mixed together to obtain this derivative following conditions of procedure **H**. Pure product was obtained by flash chromatography with Biotage Sfär Silica 25gr in dichloromethane/methanol from 0% up to 10%. Brown solid. Yield = 78%. ^{1}H NMR (300 MHz, DMSO-d6) δ = 10.46 (s, 1H CONH), 9.12 (d, 1H Ar-Bmd), 8.78 (d,1H Ar-Bmd), 8.31 (d, 1H Ar-Bmd), 7.77 (d, *J* = 8.2 Hz, 2H Ar), 7.63 – 7.49 (m, 1H Ar-Bmd), 7.31 (d, *J* = 8.2 Hz, 2H Ar), 7.06 – 6.89 (m, 4H Ar-Pip), 3.81 (s, 3H), 3.35 (d,10H), 3.01 (dd, 2H). ^{13}C NMR (75 MHz, DMSO-d6) δ = 169.14, 157.65, 157.15, 153.87, 145.73, 140.63, 135.80, 134.13, 128.73, 126.07, 125.72, 123.29, 117.14, 60.55, 57.60, 54.09, 36.19, 28.70. HPLC-DAD (ESI [+]) λ_{max} = 274 nm (98.43 %). MS (APCI [+]) m/z $[M+H^+]^+$ calculated for $[C_{25}H_{28}N_4O_2]^+$: 417.2, found 417.7. M = 416.53 g/mol (free base). mp = 164.7°C (MeOH).

N-(4-(2-(4-(2-Methoxyphenyl)piperazin-1-yl)ethyl)phenyl)isonicotinamide (106)

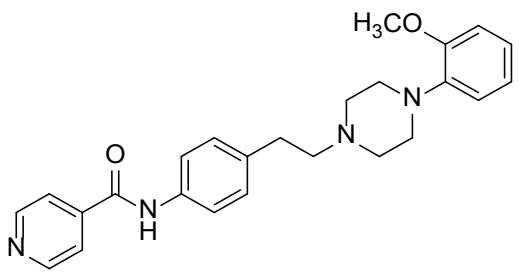

Isonicotinic acid (1 eq.) and obtained aniline (1 eq.) were mixed together to obtain this derivative following conditions of procedure **H**. Pure product was obtained by flash chromatography with Biotage Sfär Silica 25gr in dichloromethane/methanol from 0% up to 10%. Yellowish solid. Yield = 50%. ^{1}H NMR (300 MHz, $CDCl_3$) δ = 8.81 – 8.73 (m, 2H Ar-Bmd), 7.99 (s, 1H CONH), 7.74 – 7.65 (m, 2H Ar), 7.56 (d, 2H Ar-Bmd), 7.26 – 7.21 (m, 2H Ar), 7.06 – 6.83 (m, 4H Ar-Pip), 3.87 (s, 3H), 3.13 (s, 4H), 2.91 – 2.63 (m, 8H). ^{13}C NMR (75 MHz, $CDCl_3$) δ = 163.69, 152.28, 150.74, 142.11, 141.29, 137.55, 135.26, 129.46, 122.98, 121.01, 120.89, 120.60, 118.23, 111.18, 60.45, 55.37, 53.45, 50.66, 33.07. HPLC-DAD (ESI [+]) λ_{max} = 238 nm (100 %). MS (APCI [+]) m/z $[M+H^+]^+$ calculated for $[C_{25}H_{28}N_4O_2]^+$: 417.2, found 417.7. M = 416.53 g/mol (free base). mp = 176.5°C (MeOH).

N-(4-(2-(4-(2-Methoxyphenyl)piperazin-1-yl)ethyl)phenyl)-2-naphthamide (107)

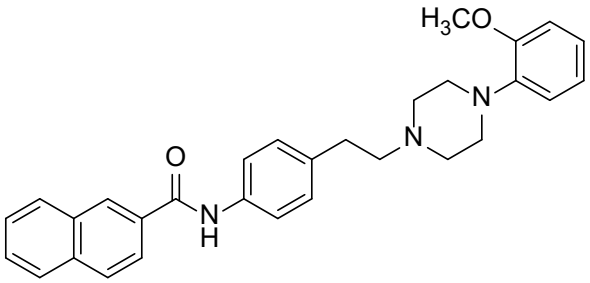

Obtained aniline (1 eq.) was solubilized in tetrahydrofuran (~20 ml), then 2-naphthoyl chloride (1.5 eq.) and DIPEA (1.5eq.) were added in the solution of reaction that was performed following conditions of procedure **E**. Pure derivative was obtained by flash chromatography with Biotage Sfär Silica 25gr in dichloromethane/methanol from 0% up to 10% of methanol. White solid. Yield = 41%. ^{1}H NMR (600 MHz, $CDCl_3$) δ = 8.11 – 7.89 (m, 1H CONH), 7.68 (s, 1H Ar-Bmd), 7.62 – 7.47 (m, 4H Ar-Bmd), 7.37 – 7.14 (m, 4H Ar-Bmd/ Ar), 6.98 – 6.82 (m, 2H Ar), 6.69 – 6.47 (m, 4H Ar-Pip), 3.52 (s, 3H), 2.79 (s, 3H), 2.60 – 2.11 (m, 9H). ^{13}C NMR (151 MHz, DMSO-d6) δ = 165.87, 152.40, 141.43, 136.82, 136.20, 134.95, 132.74, 132.34, 129.46, 129.08, 128.83, 127.99, 127.93, 127.63, 127.04, 123.69, 123.07, 121.13, 120.58, 118.36, 111.30, 60.64, 55.49, 53.55, 50.75, 33.15, 29.83. HPLC-MS (ESI [+]) m/z $[M+H^+]^+$ = 466.29 (100 %). MS (APCI [+]) m/z $[M+H^+]^+$ calculated for $[C_{30}H_{31}N_3O_2]^+$: 466.2, found 466.3. M = 465.60 g/mol (free base). mp = 195°C (MeOH).

N-(4-(2-(4-(2-Methoxyphenyl)piperazin-1-yl)ethyl)phenyl)benzo[d][1,3]dioxole-5-carboxamide hydrochloride (108)

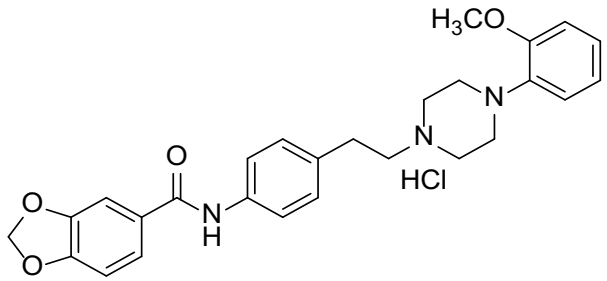

Benzo[d][1,3]dioxole-5-carbonyl chloride (1.5 eq.) was added to a solution of aniline (1 eq.) and DIPEA (1.5 eq.), the reaction was performed according to procedure **E**. The desired product was collected as hydrochloride salt precipitated in reaction solution and purified by recrystallization in isopropanol. White solid. Yield = 78%. ^{1}H NMR (600 MHz, DMSO-d6) δ = 11.08 (s, 1H), 10.12 (s, 1H CONH), 7.77 – 7.73 (m, 2H Ar), 7.59 (dd, *J* = 8.2, 1.8 Hz, 1H Ar-Bmd), 7.53 (d, *J* = 1.8 Hz, 1H Ar-Bmd), 7.28 – 7.23 (m, 2H Ar), 7.07 – 7.01 (m, 2H Ar-Pip), 6.98 (dd, *J* = 8.2, 1H Ar-Bmd), 6.96 – 6.89 (m, 2H Ar-Bmd), 6.13 (s, 2H), 3.80 (s, 3H), 3.67 – 3.47 (m, 4H), 3.32 – 3.00 (m, 8H). ^{13}C NMR (151 MHz, DMSO-d6) δ = 164.90, 152.30, 150.51, 147.84, 139.92, 138.44, 132.54, 129.28, 129.10, 123.92, 123.35, 121.33, 121.11, 118.71, 112.39, 108.40, 108.20, 102.29, 56.81, 55.85, 51.68, 47.44, 29.29. HPLC-DAD (ESI [+]) λ_{max} = 224 nm (97.79 %). MS (APCI [+]) m/z $[M+H^+]^+$ calculated for $[C_{27}H_{29}N_3O_4]^+$: 460.2, found 460.6. M = 496.00 g/mol (HCl salt). mp = 277.7°C (iPrOH).

N-(4-(2-(4-(2-Methoxyphenyl)piperazin-1-yl)ethyl)phenyl)-2,3-dihydrobenzo[b][1,4]dioxine-6-carboxamide (109)

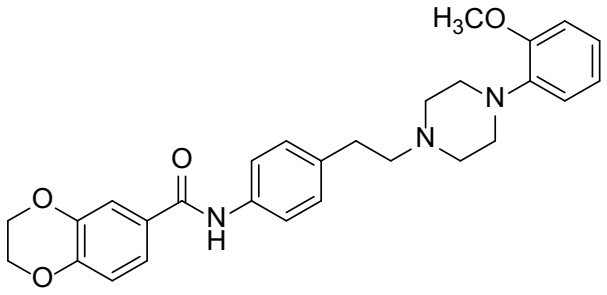

Obtained aniline (1 eq.) was solubilized in tetrahydrofuran (~20 ml), then 2,3-dihydrobenzo[b][1,4]dioxine-6-carbonyl chloride (1.5 eq.) and DIPEA (1.5 eq.) were added in the solution of reaction that was performed following conditions of procedure **E**. Pure derivative was obtained by flash chromatography with Biotage Sfär Silica 25gr in dichloromethane/methanol from 0% up to 10% of methanol. White solid. Yield = 63%. ^{1}H NMR (600 MHz, $CDCl_3$) δ 7.76 (s, 1H

CONH), 7.56 – 7.50 (m, 2H Ar), 7.41 (d, *J* = 2.2 Hz, 1H Ar-Bmd), 7.36 (dd, *J* = 2.2 Hz, 1H Ar-Bmd), 7.24 – 7.17 (m, 2H Ar), 7.00 (ddd, *J* = 8.0, 1H Ar-Pip), 6.96 (dd, 1H Ar-Bmd), 6.94 – 6.90 (m, 2H Ar-Pip), 6.86 (dd, *J* = 8.0, 1H Ar-Pip), 4.32 – 4.26 (m, 4H), 3.87 (s, 3H), 3.15 (s, 4H), 2.87 – 2.67 (m, 8H). ^{13}C NMR (151 MHz, $CDCl_3$) δ 164.90, 152.28, 146.75, 143.54, 141.23, 136.28, 136.19, 129.29, 128.24, 123.00, 121.02, 120.46, 120.33, 118.27, 117.44, 116.64, 111.19, 64.58, 64.23, 60.40, 55.38, 53.32, 50.47, 32.81. HPLC-DAD (ESI [+]) λ_{max} = 277 nm (100 %). MS (APCI [+]) m/z $[M+H^+]^+$ calculated for $[C_{28}H_{31}N_3O_4]^+$: 474.2, found 474.6. M = 473.57 g/mol (free base). mp = 202.1°C (MeOH).

N-(4-(2-(4-(2-Methoxyphenyl)piperazin-1-yl)ethyl)phenyl)-2-oxo-2*H*-chromene-6-carboxamide (110)

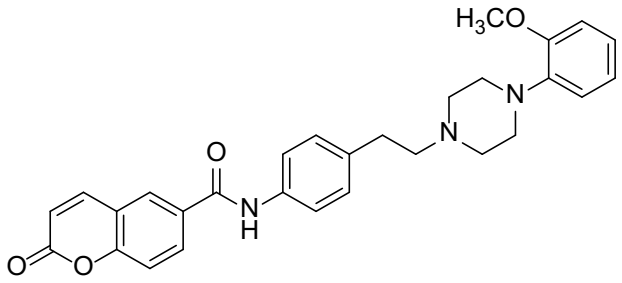

2-Oxo-2*H*-chromene-6-carboxylic acid (1 eq.) and obtained aniline (1 eq.) were mixed together to obtain this derivative following conditions of procedure **H**. Pure product was obtained by flash chromatography with Biotage Sfär Silica 25gr in dichloromethane/methanol from 0% up to 10%. White solid. Yield = 57%. ^{1}H NMR (300 MHz, DMSO-d6) δ = 10.37 (s, 1H CONH), 8.33 (d, 1H Ar-Bmd), 8.21 – 8.13 (m, 2H Ar-Bmd), 7.72 (d, *J* = 8.3 Hz, 2H Ar), 7.54 (d, 1H Ar-Bmd), 7.28 (d, *J* = 8.3 Hz, 2H Ar), 7.04 – 6.86 (m, 4H Ar-Pip), 6.59 (d, 1H Ar-Bmd), 3.79 (s, 3H), 3.12 (s, 10H), 2.91 (dd, 2H). ^{13}C NMR (75 MHz, DMSO-d6) δ = 164.09, 159.59, 155.31, 151.87, 144.08, 140.00, 137.39, 131.05, 131.02, 128.90, 128.35, 123.08, 120.82, 120.55, 118.44, 118.15, 116.97, 116.42, 111.89, 55.30, 52.03, 48.26, 32.55, 30.26. HPLC/HRAM-MS (ESI [+]) m/z $[M+H^+]^+$ = 484.2451 (100 %). MS (APCI [+]) m/z $[M+H^+]^+$ calculated for $[C_{29}H_{29}N_3O_4]^+$: 484.2, found 484.2. M = 483.57 g/mol (free base). mp = 206°C (MeOH).

N-(4-(2-(4-(2-Methoxyphenyl)piperazin-1-yl)ethyl)phenyl)-2-oxo-2H-chromene-3-carboxamide (111)

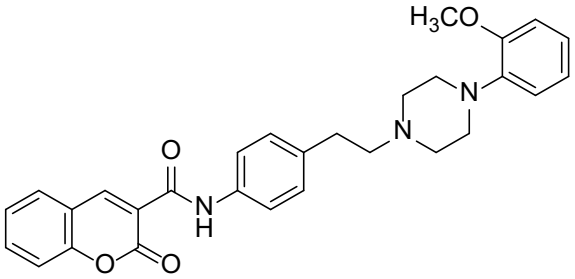

2-Oxo-2H-chromene-3-carboxylic acid (1 eq.) and obtained aniline (1 eq.) were mixed together to obtain this derivative following conditions of procedure **H**. Pure product was obtained by flash chromatography with Biotage Sfär Silica 25gr in dichloromethane/methanol from 0% up to 10%. Yellowish solid. Yield = 70%. ^{1}H NMR (300 MHz, DMSO-d6) δ = 10.68 (s, 1H CONH), 8.92 (s, 1H Ar-Bmd), 8.02 (dd, 1H Ar-Bmd), 7.83 – 7.70 (m, 3H Ar-Bmd), 7.59 – 7.45 (m, 2H Ar), 7.36 – 7.30 (m, 2H Ar), 7.10 – 6.87 (m, 4H Ar-Pip), 3.80 (s, 3H), 3.46 – 3.29 (m, 9H), 3.02 (dd, 3H). ^{13}C NMR (75 MHz, DMSO-d6) δ = 160.47, 159.81, 153.87, 151.84, 147.46, 139.29, 136.73, 134.33, 132.68, 130.29, 129.32, 125.30, 123.53, 120.83, 120.18, 119.83, 118.46, 118.34, 116.24, 111.91, 56.29, 55.34, 51.47, 47.18, 29.05. HPLC/HRAM-MS (ESI [+]) m/z $[M+H^+]^+$ = 484.2304 (100 %). MS (APCI [+]) m/z $[M+H^+]^+$ calculated for $[C_{29}H_{29}N_3O_4]^+$: 484.2, found 484.2. M = 483.57 g/mol (free base). mp = 248.6°C (MeOH).

6-Methoxy-*N*-(4-(2-(4-(2-methoxyphenyl)piperazin-1-yl)ethyl)phenyl)-2-oxo-2H-chromene-3-carboxamide (112)

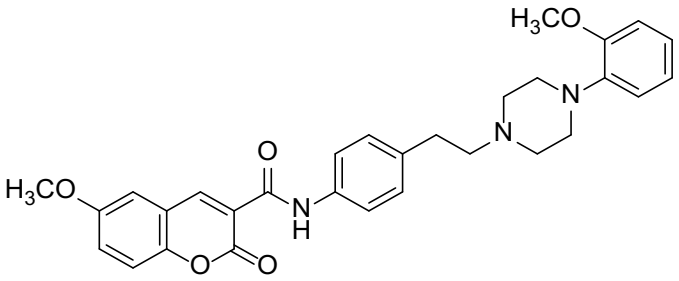

6-Methoxy-2-oxo-2H-chromene-3-carboxylic acid (1 eq.) and obtained aniline (1 eq.) were mixed together to obtain this derivative following conditions of procedure **H.** The desired product was collected as precipitate from the solution of reaction and was purified by recrystallization with ethanol. Yellow solid. Yield = 78%. ^{1}H NMR (300 MHz, DMSO-d6) δ = 10.73 (s, 1H CONH), 8.88 (s, 1H Ar-Bmd), 7.73 (d, 2H Ar), 7.58 (d, 1H Ar-Bmd), 7.51 (d, 1H Ar-Bmd), 7.41 – 7.29 (m, 3H Ar-Bmd/Ar), 7.07 – 6.88 (m, 4H Ar-Pip), 3.84 (s, 3H), 3.80 (s, 3H), 3.42 (d, 10H), 3.05 – 2.98 (m, 2H).

^{13}C NMR (75 MHz, DMSO-d6) δ = 160.67, 159.77, 156.05, 151.84, 148.39, 147.40, 139.31, 136.69, 132.72, 129.32, 123.52, 122.23, 120.83, 120.17, 119.77, 118.94, 118.33, 117.39, 111.91, 111.83, 56.34, 55.83, 55.34, 51.47, 47.21, 29.08. HPLC/HRAM-MS (ESI [+]) m/z $[M+H^+]^+$ = 514.2046 (96.82 %). MS (APCI [+]) m/z $[M+H^+]^+$ calculated for $[C_{30}H_{31}N_3O_5]^+$: 514.2, found 514.2. M = 513.59 g/mol (free base). mp = 252.5°C (MeOH).

N-(4-(2-(4-(2-Methoxyphenyl)piperazin-1-yl)ethyl)phenyl)benzofuran-2-carboxamide (113)

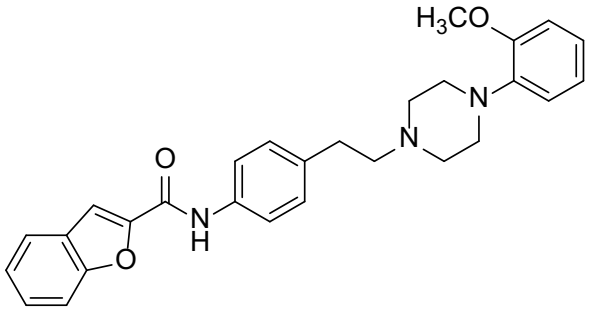

Benzofuran-2-carboxylic acid (1 eq.) and obtained aniline (1 eq.) were mixed together to obtain this derivative following conditions of procedure **H**. Pure product was obtained by flash chromatography with Biotage Sfär Silica 25gr in dichloromethane/methanol from 0% up to 10%. Brown solid. Yield = 49%. ^{1}H NMR (300 MHz, $CDCl_3$) δ = 8.36 (s, 1H CONH), 7.73 – 7.62 (m, 3H Ar-Bmd), 7.60 – 7.52 (m, 2H Ar), 7.45 (ddd, 1H Ar-Bmd), 7.32 (ddd, 1H Ar-Bmd), 7.28 – 7.22 (m, 2H Ar), 7.04 – 6.83 (m, 4H Ar-Pip), 3.87 (s, 3H), 3.14 (s, 4H), 2.90 – 2.83 (m, 2H), 2.79 – 2.64 (m, 6H). ^{13}C NMR (75 MHz, $CDCl_3$) δ = 156.53, 154.80, 152.29, 148.56, 141.30, 136.96, 135.31, 129.40, 127.73, 127.21, 123.92, 122.96, 122.86, 121.01, 120.20, 118.24, 111.82, 111.35, 111.19, 60.51, 55.38, 55.36, 53.46, 50.65, 33.06. HPLC-DAD (ESI [+]) λ_{max} = 285 nm (100 %). MS (APCI [+]) m/z $[M+H^+]^+$ calculated for $[C_{28}H_{29}N_3O_3]^+$: 456.2, found 456.7. M = 455.56 g/mol (free base). mp = 166.6°C (MeOH).

N-(4-(2-(4-(2-Methoxyphenyl)piperazin-1-yl)ethyl)phenyl)benzofuran-5-carboxamide (114)

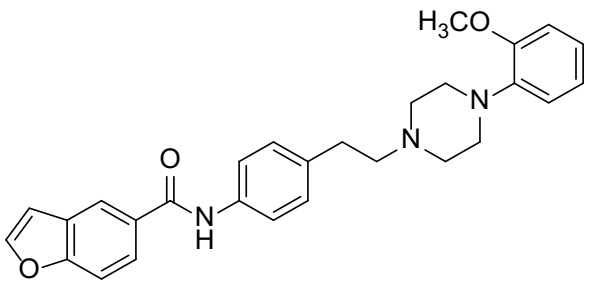

Benzofuran-5-carboxylic acid (1 eq.) and obtained aniline (1 eq.) were mixed together to obtain this derivative following conditions of procedure **H**. Pure product was obtained by flash chromatography with Biotage Sfär Silica 25gr in dichloromethane/methanol from 0% up to 10%. White solid. Yield = 53%. ^{1}H NMR (300 MHz, $CDCl_3$) δ 8.07 (d, 1H CONH), 7.85 (s, 1H Ar-Bmd), 7.74 (dd, 1H Ar-Bmd), 7.63 (d, 1H Ar-Bmd), 7.49 (dd, 3H Ar-Bmd/Ar), 7.19 – 7.13 (m, 2H Ar), 6.97 – 6.84 (m, 3H Ar-Bmd/Ar-Pip), 6.83 – 6.74 (m, 2H Ar-Pip), 3.80 (s, 3H), 3.07 (s, 4H), 2.82 – 2.54 (m, 8H). ^{13}C NMR (75 MHz, $CDCl_3$) δ = 165.95, 156.69, 152.29, 146.47, 141.33, 136.64, 136.15, 130.19, 129.32, 127.73, 123.48, 122.95, 121.02, 120.80, 120.44, 118.24, 111.64, 111.19, 107.04, 60.57, 55.37, 53.46, 50.68, 33.07. HPLC/HRAM-MS (ESI [+]) m/z $[M+H^+]^+$ = 456.2331 (96.31 %). MS (APCI [+]) m/z $[M+H^+]^+$ calculated for $[C_{28}H_{29}N_3O_3]^+$: 456.2, found 456.2. M = 455.56 g/mol (free base). mp = 189.3°C (MeOH).

N-(4-(2-(4-(2-Methoxyphenyl)piperazin-1-yl)ethyl)phenyl)-1*H*-indole-7-carboxamide (115)

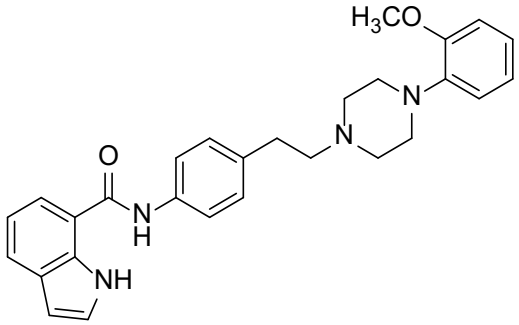

1*H*-Indole-7-carboxylic acid (1 eq.) and obtained aniline (1 eq.) were mixed together to obtain this derivative following conditions of procedure **H**. Pure product was obtained by flash chromatography with Biotage Sfär Silica 25gr in dichloromethane/methanol from 0% up to 10%. Yellow solid. Yield = 93%. ^{1}H NMR (300 MHz, DMSO-d6) δ = 11.20 (s, 1H NH), 10.28 (s, 1H CONH), 7.95 (s, 1H Ar-Bmd), 7.85 – 7.79 (m, 3H Ar-Bmd/Ar), 7.38 (t, 1H Ar-Bmd), 7.30 (d, 2H Ar), 7.15 (t, 1H Ar-Bmd), 7.06 – 6.87 (m, 4H Ar-Pip), 6.54 (dd,1H Ar-Bmd), 3.80 (s, 3H), 3.60 (q, 2H), 3.13 (q, 3H), 2.99 (dd, 2H), 2.89 (s, 2H), 2.73 (s, 2H), 2.69 (s, 1H). ^{13}C NMR (75 MHz, DMSO-d6) δ = 165.91, 162.29, 151.85, 139.50, 137.89, 134.09, 129.24, 128.84, 126.76, 124.30, 123.40, 120.83, 120.65, 120.56, 118.28, 118.07, 117.24, 111.91, 101.19, 55.34, 53.55, 51.61, 47.46, 35.75. HPLC-DAD (ESI [+]) λ_{max} = 241 nm (98.79 %). MS (APCI [+]) m/z $[M+H^+]^+$ calculated for $[C_{28}H_{30}N_4O_2]^+$: 455.2, found 455.7. M = 454.57 g/mol (free base). mp = 85.5°C (MeOH).

N-(4-(2-(4-(2-Methoxyphenyl)piperazin-1-yl)ethyl)phenyl)-1*H*-indole-5-carboxamide (116)

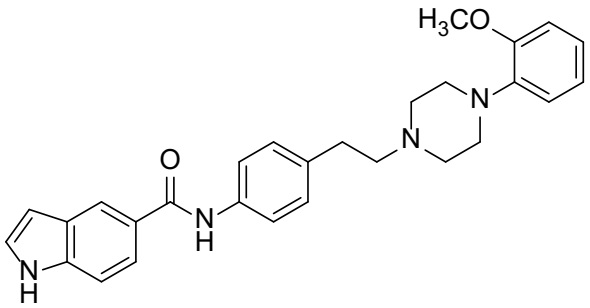

1*H*-indole-5-carboxylic acid (1 eq.) and obtained aniline **54** (1 eq.) were mixed together to obtain this derivative following conditions of procedure **H**. Pure product was obtained by flash chromatography with Biotage Sfär Silica 25gr in dichloromethane/methanol from 0% up to 10%. White solid. Yield = 33%. ^{1}H NMR (300 MHz, DMSO-d6) δ = 11.38 (s, 1H NH), 10.07 (s, 1H CONH), 8.26 (d,1H Ar-Bmd), 7.74 (d, 3H Ar-Bmd), 7.52 – 7.44 (m, 2H Ar), 7.22 (d, 2H Ar), 6.97 – 6.87 (m, 4H Ar-Pip), 6.58 (t,1H Ar-Bmd), 3.78 (s, 3H), 3.04 (s, 4H), 2.88 – 2.69 (m, 8H). ^{13}C NMR (75 MHz, $CDCl_3$) δ = 166.45, 151.96, 140.85, 137.85, 137.60, 128.72, 127.01, 126.90, 125.82, 122.64, 120.94, 120.86, 120.40, 120.33, 118.02, 111.93, 111.07, 102.25, 92.96, 59.14, 55.34, 52.64, 49.37, 27.94. HPLC-DAD (ESI [+]) λ_{max} = 244 nm (97.28 %). MS (APCI [+]) m/z $[M+H^+]^+$ calculated for $[C_{28}H_{30}N_4O_2]^+$: 455.2, found 455.4. M = 454.57 g/mol (free base). mp = 155.9°C (MeOH).

N-(4-(2-(4-(2-Methoxyphenyl)piperazin-1-yl)ethyl)phenyl)-1*H*-indole-2-carboxamide (117)

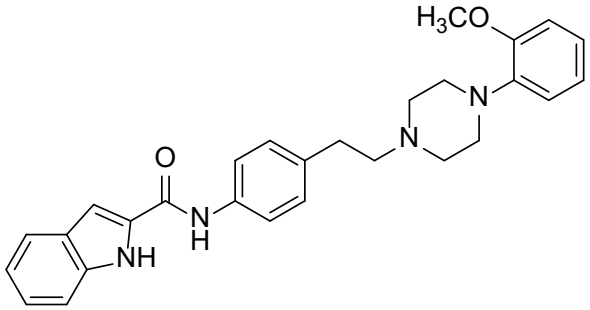

1*H*-Indole-5-carboxylic acid (1 eq.) and obtained aniline (1 eq.) were mixed together to obtain this derivative following conditions of procedure **H**. Pure product was obtained by flash chromatography with Biotage Sfär Silica 25gr in dichloromethane/methanol from 0% up to 10%. Light brown solid. Yield = 76%. ^{1}H NMR (300 MHz, DMSO-d6) δ = 11.72 (d, 1H NH), 10.19 (s, 1H CONH), 7.76 (d, 2H Ar), 7.68 (d, 1H Ar-Bmd), 7.52 – 7.45 (m, 1H Ar-Bmd), 7.42 (d, 1H Ar-Bmd), 7.31 – 7.25 (m,

2H Ar), 7.24 – 7.18 (m, 1H Ar-Bmd), 7.07 (ddd, 1H Ar-Bmd), 7.02 – 6.86 (m, 4H Ar-Pip), 3.79 (s, 3H), 3.22 – 2.80 (m, 12H). ^{13}C NMR (75 MHz, DMSO-d6) δ = 159.63, 151.89, 140.21, 137.28, 136.78, 131.46, 128.91, 127.00, 123.74, 122.97, 121.70, 120.82, 120.27, 119.90, 118.12, 112.36, 111.89, 103.76, 55.31, 54.89, 52.16, 48.61, 45.74. HPLC-DAD (ESI [+]) λ_{max} = 308 nm (100 %). MS (APCI [+]) m/z $[M+H^+]^+$ calculated for $[C_{28}H_{30}N_4O_2]^+$: 455.2, found 455.1. M = 454.57 g/mol (free base). mp = 208.2°C (MeOH).

N-(4-(2-(4-(2-Methoxyphenyl)piperazin-1-yl)ethyl)phenyl)benzo[b]thiophene-5-carboxamide hydrochloride (118)

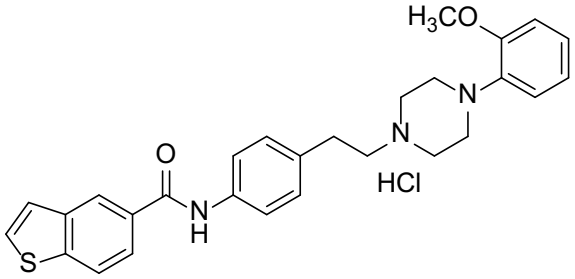

Benzo[b]thiophene-5-carboxylic acid (1 eq.) and obtained aniline **54** (1 eq.) were mixed together to obtain this derivative following conditions of procedure **H**. Pure product was obtained by column chromatography in dichloromethane/ammonia in methanol 99:1. Brown oil. Yield = 62%. Free base derivative was solubilized in ethyl acetate and a solution of HCl in dioxane (2 N) was added drop by drop. A white precipitate of HCl salt was obtained. ^{1}H NMR (600 MHz, DMSO-d6) δ = 10.60 (s, 1H), 10.38 (s, 1H CONH), 8.52 (s, 1H Ar-Bmd), 8.16 (d, 1H Ar-Bmd), 7.97 – 7.87 (m, 2H Ar), 7.84 – 7.76 (m, 2H Ar), 7.61 (d, 1H Ar-Bmd), 7.29 (d, 2H Ar-Bmd), 7.06 – 6.90 (m, 4H Ar-Pip), 3.80 (s, 3H), 3.66 – 3.44 (m, 6H), 3.06 (d, 6H). ^{13}C NMR (151 MHz, DMSO-d6) δ = 166.09, 152.32, 142.56, 139.90, 139.63, 138.51, 131.70, 129.49, 129.37, 124.94, 123.96, 123.78, 123.68, 123.06, 121.33, 121.14, 121.10, 121.00, 118.76, 112.41, 56.87, 55.86, 51.79, 47.53, 29.40. HPLC/HRAM-MS (ESI [+]) m/z $[M+H^+]^+$ = 472.2057 (100 %). MS (APCI [+]) m/z $[M+H^+]^+$ calculated for $[C_{28}H_{29}N_3O_2S]^+$: 472.2, found 472.2. M = 508.08 g/mol (HCl salt). mp = 242°C (EtOAc).

N-(4-(2-(4-(2-Methoxyphenyl)piperazin-1-yl)ethyl)phenyl)benzo[b]thiophene-2-carboxamide (119)

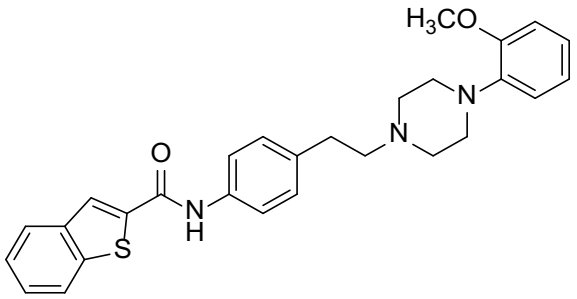

Benzo[b]thiophene-2-carboxylic acid (1 eq.) and obtained aniline (1 eq.) were mixed together to obtain this derivative following conditions of procedure **H**. Pure product was obtained by column chromatography in dichloromethane/ammonia in methanol 99:1. White solid. Yield = 53%. ^{1}H NMR (300 MHz, DMSO-d6) δ = 10.46 (s, 1H CONH), 8.35 (s, 1H Ar-Bmd), 8.10 – 7.98 (m, 2H Ar-Bmd), 7.68 (d, *J* = 8.2 Hz, 2H Ar), 7.49 (qd, 2H Ar-Bmd), 7.25 (d, *J* = 8.2 Hz, 2H Ar), 6.96 – 6.82 (m, 4H Ar-Pip), 3.77 (s, 3H), 2.97 (s, 4H), 2.75 (t, *J* = 7.6 Hz, 2H), 2.58 (d, *J* = 8.4 Hz, 6H). ^{13}C NMR (75 MHz, DMSO-d6) δ = 160.11, 151.94, 141.24, 140.42, 140.17, 139.13, 136.45, 136.10, 128.87, 126.43, 125.59, 125.35, 125.02, 122.82, 122.30, 120.80, 120.30, 117.86, 111.87, 59.80, 55.28, 52.95, 50.02, 32.17. HPLC/HRAM-MS (ESI [+]) m/z $[M+H^+]^+$ = 472.2128 (100 %). MS (APCI [+]) m/z $[M+H^+]^+$ calculated for $[C_{28}H_{29}N_3O_2S]^+$: 472.2, found 472.2. M = 471.62 g/mol (free base). mp = 194.8°C (MeOH).

N-(4-(2-(4-(2-Methoxyphenyl)piperazin-1-yl)ethyl)phenyl)-4-methylbenzenesulfonamide (120)

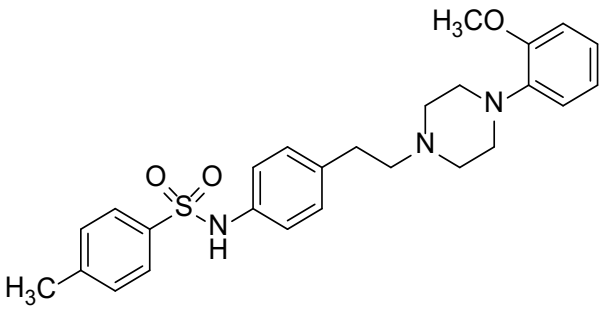

Tosyl chloride (1.5 eq.) was added to a solution of obtained aniline (1 eq.) and DIPEA (1.5 eq.) in THF (~20 ml), the mixture of reaction was stirred following procedure **E**. Pure compound was obtained by column chromatography in dichloromethane/ammonia in methanol 98:2. Brown orange solid. Yield = 50%.^{1}H NMR (300 MHz, DMSO-d_6) δ = 10.09 (s, 1H SO_2NH), 7.63 (d, *J* = 8.0 Hz, 2H Ar-Bmd), 7.34 (d, *J* = 8.0 Hz, 2H Ar-Bmd), 7.10 (d, 2H Ar), 7.04 – 6.81 (m, 6H Ar/Ar-pip), 3.77

(s, 3H), 2.94 (s, 4H), 2.71 – 2.52 (m, 6H), 2.51 – 2.45 (m, 2H), 2.33 (s, 3H). ^{13}C NMR (75 MHz, $CDCl_3$) δ = 152.25, 143.70, 141.15, 137.37, 136.32, 134.63, 129.61, 129.54, 127.26, 123.05, 122.12, 121.02, 118.24, 111.20, 60.22, 55.37, 53.32, 50.47, 32.72, 21.55; HPLC/HRAM-MS (ESI [+]) m/z $[M+H^+]^+$ = 466.2245 (100 %). MS (APCI [+]) m/z $[M+H^+]^+$ calculated for $[C_{26}H_{32}N_3O_3S]^+$ = 466.2, found 466.1. M = 465.61 g/mol (free base). mp = 154.3°C (MeOH).

N-(4-(2-(4-(2-Methoxyphenyl)piperazin-1-yl)ethyl)phenyl)furan-2-carboxamide hydrochloride (121)

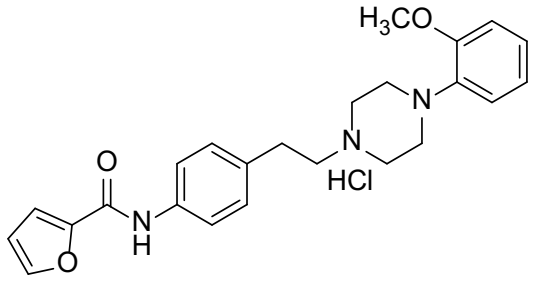

Furan-2-carbonyl chloride (1.5 eq.) was added to a solution of aniline (1 eq.) and DIPEA (1.5 eq.), the reaction was performed according to procedure **E**. The desired product was collected as hydrochloride salt precipitated in reaction solution and purified by recrystallization in isopropanol. White solid. Yield = 61%. ^{1}H NMR (300 MHz, DMSO-d6) δ = 10.74 (s, 1H), 10.24 (s, 1H CONH), 7.94 (d, 1H Ar-Bmd), 7.80 – 7.70 (m, 2H Ar), 7.37 (d, *J* = 3.5 Hz, 1H Ar-Bmd), 7.27 (d, 2H Ar), 7.07 – 6.89 (m, 4H Ar-Pip), 6.71 (dd, *J* = 3.5, 1H Ar-Bmd), 3.81 (s, 3H), 3.64 (d, 4H), 3.23 (q, 4H), 3.06 (s, 4H). ^{13}C NMR (75 MHz, DMSO-d6) δ = 156.17, 151.80, 147.42, 145.70, 139.31, 137.25, 132.17, 128.88, 123.50, 120.83, 120.61, 118.26, 114.73, 112.12, 111.90, 56.25, 55.34, 51.20, 46.93, 28.78. HPLC/HRAM-MS (ESI [+]) m/z $[M+H^+]^+$ = 406.2317 (100 %). MS (APCI [+]) m/z $[M+H^+]^+$ calculated for $[C_{24}H_{27}N_3O_3]^+$ = 406.2, found 406.1. M = 441.96 g/mol (HCl salt). mp = 254.4°C (iPrOH).

N-(4-(2-(4-(2-Methoxyphenyl)piperazin-1-yl)ethyl)phenyl)-1*H*-pyrrole-2-carboxamide (122)

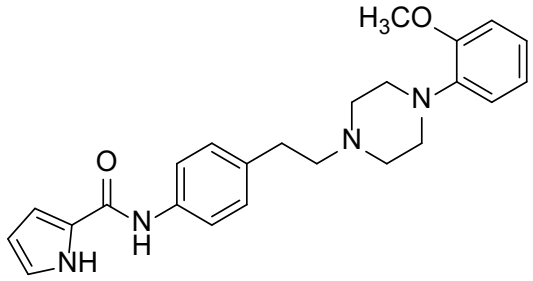

1*H*-pyrrole-2-carboxylic acid (1 eq.) and obtained aniline **54** (1 eq.) were mixed together to obtain this derivative following conditions of procedure **H**. Pure product was obtained by column chromatography in dichloromethane/ammonia in methanol 99:1. Orange solid. Yield = 34%. ^{1}H NMR (300 MHz, MeOD) δ = 7.65 – 7.56 (m, 2H Ar), 7.25 (d, 2H Ar), 7.08 – 6.88 (m, 6H Ar-Pip/Ar-Bmd), 6.22 (dd, 1H Ar-Bmd), 3.86 (s, 3H), 3.25 – 3.04 (m, 8H), 3.04 – 2.90 (m, 4H). ^{13}C NMR (75 MHz, MeOD) δ = 153.97, 141.42, 138.65, 134.98, 130.09, 127.08, 125.14, 123.71, 122.30, 122.23, 119.68, 112.92, 112.58, 60.43, 55.98, 54.04, 50.42, 32.24. HPLC/HRAMS-MS (ESI [+]) m/z $[M+H^+]^+$ = 405.2337 (100 %). MS (APCI [+]) m/z $[M+H^+]^+$ calculated for $[C_{24}H_{28}N_4O_2]^+$ = 405.2, found 405.2. M = 404.51 g/mol (free base). mp = 99.2°C (MeOH).

N-(4-(2-(4-(2-Methoxyphenyl)piperazin-1-yl)ethyl)phenyl)thiophene-2-carboxamide hydrochloride (123)

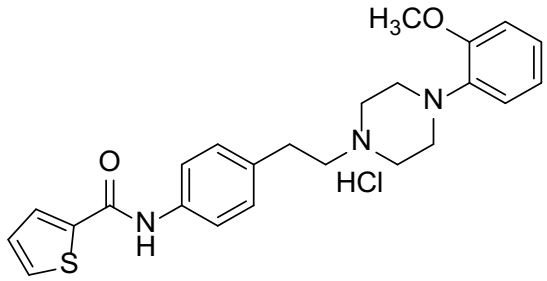

Thiophene-2-carbonyl chloride (1.5 eq.) was added to a solution of aniline (1 eq.) and DIPEA (1.5 eq.), the reaction was performed according to procedure **E**. The desired product was collected as hydrochloride salt precipitated in reaction solution and purified by recrystallization in isopropanol. Brown solid. Yield = 47%. ^{1}H NMR (300 MHz, MeOD) δ = 7.81 (dd, 1H Ar-Bmd), 7.66 – 7.56 (m, 3H Ar-Bmd/Ar), 7.25 (d, 2H Ar), 7.12 – 7.04 (m, 3H Ar-Bmd/Ar-Pip), 6.97 (d, 1H Ar-Pip), 6.93 – 6.85 (m, 1H Ar-Pip), 3.81 (s, 3H), 3.69 – 3.30 (m, 10H), 3.10 – 3.01 (m, 2H). ^{13}C NMR (151 MHz, MeOD) δ = 161.41, 152.51, 139.34, 137.46, 132.05, 131.19, 128.93, 128.79, 127.59, 125.49, 121.34, 120.97, 119.11, 111.95, 57.59, 54.90, 51.85, 29.39. HPLC/HRAM-MS (ESI [+]) m/z $[M+H^+]^+$ = 422.2221 (98.58 %). MS (APCI [+]) m/z $[M+H^+]^+$ calculated for $[C_{24}H_{27}N_3O_2S]^+$ = 422.2, found 422.1. M = 458.02 g/mol (HCl salt). mp = 210.4°C (iPrOH).

N-(4-(2-(4-(2-Methoxyphenyl)piperazin-1-yl)ethyl)phenyl)furan-3-carboxamide (124)

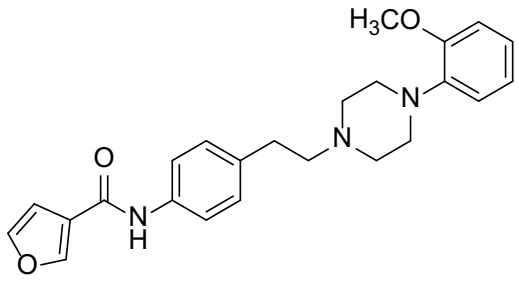

Furan-3-carbonyl acid (1 eq.) and obtained aniline (1 eq.) were mixed together to obtain this derivative following conditions of procedure **H**. Pure product was obtained by column chromatography in dichloromethane/ammonia in methanol 99:1. White solid. Yield = 76%. ^{1}H NMR (600 MHz, MeOD) δ = 8.21 (dd, *J* = 1.6 Hz, 1H Ar-Bmd), 7.68 – 7.64 (m, 2H Ar), 7.62 (t, 1H Ar-Bmd), 7.34 – 7.31 (m, 2H Ar), 7.07 (ddd, *J* = 1.6 Hz, 1H Ar-Bmd), 6.99 (ddd, 2H Ar-Pip), 6.96 – 6.91 (m, 2H Ar-Pip), 3.87 (s, 3H), 3.77 – 3.50 (m, 4H), 3.46 – 3.33 (m, 4H), 3.16 – 2.90 (m, 4H). ^{13}C NMR (151 MHz, MeOD) δ = 163.57, 154.01, 147.02, 145.40, 140.49, 138.78, 133.40, 130.27, 125.61, 124.15, 122.66, 122.24, 119.94, 113.05, 109.83, 58.92, 56.05, 53.74, 30.74. HPLC/HRAM-MS (ESI [+]) m/z $[M+H^+]^+$ = 406.2267 (100 %). MS (APCI [+]) m/z $[M+H^+]^+$ calculated for $[C_{24}H_{27}N_3O_3]^+$ = 406.2, found 406.2. M = 405.5 g/mol (free base). mp = 157.8°C (MeOH).

N-(4-(2-(4-(2-Methoxyphenyl)piperazin-1-yl)ethyl)phenyl)-1*H*-pyrrole-3-carboxamide hydrochloride (125)

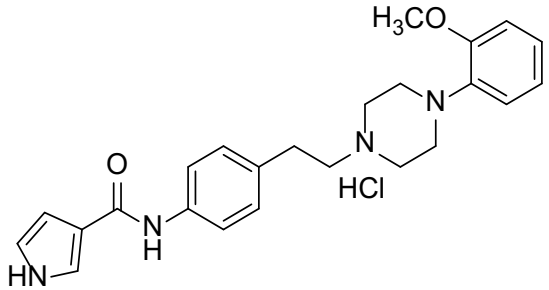

1*H*-pyrrole-3-carboxylic acid (1 eq.) and obtained aniline (1 eq.) were mixed together to obtain this derivative following conditions of procedure **H**. Pure product was obtained by column chromatography in dichloromethane/methanol 98:2. Red oil. Yield = 37%. Free base derivative was solubilized in ethyl acetate and a solution of HCl in dioxane (2 N) was added drop by drop. A white precipitate of HCl salt was obtained. ^{1}H NMR (300 MHz, MeOD) δ = 7.66 – 7.59 (m, 2H Ar), 7.50 (t, 1H Ar-Bmd), 7.30 – 7.22 (m, 2H Ar), 7.08 – 6.88 (m, 4H Ar-Pip), 6.80 (dd, 1H Ar-Bmd), 6.70 (dd, 1H Ar-Bmd), 3.86 (s, 3H), 3.28 – 3.04 (m, 10H), 2.97 (dt, 2H). ^{13}C NMR (75 MHz, MeOD) δ =

166.64, 153.98, 141.25, 138.96, 130.05, 125.22, 122.94, 122.54, 122.23, 120.45, 119.73, 112.94, 108.54, 60.18, 56.03, 53.99, 50.16, 31.97. HPLC/HRAM-MS (ESI [+]) m/z $[M+H^+]^+$ = 405.2333 (97.47 %). MS (APCI [+]) m/z $[M+H^+]^+$ calculated for $[C_{24}H_{28}N_4O_2]^+$ = 405.2, found 405.2. M = 440.97 (HCl salt). mp = 177.3°C (EtOAc).

N-(4-(2-(4-(2-Methoxyphenyl)piperazin-1-yl)ethyl)phenyl)thiophene-3-carboxamide hydrochloride (126)

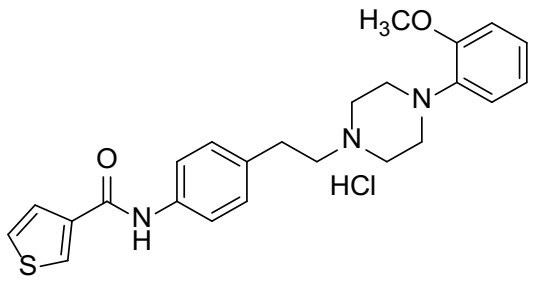

Thiophene-3-carbonyl acid (1 eq.) and obtained aniline **54** (1 eq.) were mixed together to obtain this derivative following conditions of procedure **H**. Pure product was obtained by column chromatography in dichloromethane/methanol 98:2. Orange oil. Yield = 57%. Free base derivative was solubilized in ethyl acetate and a solution of HCl in dioxane (2 N) was added drop by drop. A white precipitate of HCl salt was obtained. ^{1}H NMR (600 MHz, MeOD) δ = 8.22 (dd, *J* = 1.3 Hz, 1H Ar-Bmd), 7.71 – 7.67 (m, 2H Ar), 7.62 (dd, *J* = 5.1, 1.3 Hz, 1H Ar-Bmd), 7.52 (dd, *J* = 5.1 Hz, 1H Ar-Bmd), 7.35 – 7.32 (m, 2H Ar), 7.08 (ddd, *J* = 8.2 Hz, 1H Ar-Pip), 7.00 (ddd, *J* = 8.2 Hz, 2H Ar-Pip), 6.94 (td, 1H Ar-Pip), 3.87 (s, 3H), 3.77 – 3.34 (m, 8H), 3.16 – 2.92 (m, 4H). ^{13}C NMR (151 MHz, MeOD) δ = 162.61, 152.63, 139.11, 137.56, 137.34, 132.02, 129.05, 128.84, 126.47, 126.24, 124.24, 121.37, 120.85, 118.56, 111.65, 57.57, 54.65, 52.36, 47.67, 29.40. HPLC/HRAM-MS (ESI [+]) m/z $[M+H^+]^+$ = 422.2047 (100 %). MS (APCI [+]) m/z $[M+H^+]^+$ calculated for $[C_{24}H_{27}N_3O_2S]^+$ = 422.2, found 422.2. M = 458.02 g/mol (HCl salt). mp = 268°C (EtOAc).

6.2 Pharmacological Assays

6.2.1 Cell culture and membrane preparation of CHO cells expressing the human dopamine D_{2s} and D_3 receptors.

All the biological assays were executed in the laboratories of Professor Stark. Cell culture and membrane preparations were performed as reported in this paper with modifications.[434] CHO cells stably expressing the human dopamine D_{2short} or D_3 receptors were cultured in DMEM (with 1% glutamine, 10% FBS, and 1% penicillin/streptomycin for D_2; 1% glutamine, 10% dialysed FBS for D_3). CHO-D_2 cells were collected in PBS buffer, CHO-D_3 cells in medium and centrifuged at 3,000 × g for 10 min at 4 °C. The pellet was resuspended in binding buffer (1 mM $MgCl_2$, 1 mM $CaCl_2$, 5 mM KCl, 120 mM NaCl and 50 mM Tris, pH 7.7), disrupted and centrifuged at 23,000 × g for 30 min (4 °C). The resulting pellet was stored in binding buffer at −80 °C.

6.2.2 Radioligand displacement assays at the human D_{2s} and D_3 receptors.

Adapted from this publication,[241] displacement assays were performed with modifications. Briefly, membrane preparations (D_{2s}: 25 µg/well; D_3: 20 µg/well) were co-incubated with [^{3}H]spiperone (0.2 nM) and the test ligand. Nonspecific binding (NSB) was measured with haloperidol (10 µM) and separation of bound radioligand was performed using VE-water. Assays ran in triplicates at least in three independent experiments. Data was analysed using non-linear regression and equation "one site competition". The K_i values were calculated from the IC_{50} values using the Cheng-Prusoff equation.[386]

7 References

(1) Carlsson, A.; Lindqvist, M.; Magnusson, T.; Waldeck, B. On the Presence of 3-Hydroxy Tiramine. *Science* . **1958**, *180* (4), 688–694. https://doi.org/10.1126/science.127.3296.471.a.

(2) Klein, M. O.; Battagello, D. S.; Cardoso, A. R.; Hauser, D. N.; Bittencourt, J. C.; Correa, R. G. Dopamine: Functions, Signaling, and Association with Neurological Diseases. *Cell. Mol. Neurobiol.* **2019**, *39* (1), 31–59. https://doi.org/10.1007/s10571-018-0632-3.

(3) Fernstrom, J. D.; Fernstrom, M. H. Tyrosine, Phenylalanine, and Catecholamine Synthesis and Function in the Brain. *J. Nutr.* **2007**, *137* (6), 1539S-1547S. https://doi.org/10.1093/jn/137.6.1539s.

(4) Eiden, L. E.; Weihe, E. VMAT2: A Dynamic Regulator of Brain Monoaminergic Neuronal Function Interacting with Drugs of Abuse. *Ann. N. Y. Acad. Sci.* **2011**, *1216* (1), 86–98. https://doi.org/10.1111/j.1749-6632.2010.05906.x.

(5) Udenfriend, S.; Wyngaarden, J. B. Precursors of Adrenal Epinephrine and Norepinephrine in Vivo. *Biochim. Biophys. Acta* **1956**, *20*, 48–52. https://doi.org/10.1016/0006-3002(56)90261-X

(6) Weinshilboum, R. M.; Thoa, N. B.; Johnson, D. G.; Kopin, I. J.; Axelrod, J. Proportional Release of Norepinephrine and Dopamine-ß-Hydroxylase from Sympathetic Nerves. *Science.* **1971**, *174*, 1349–1351. https://doi.org/10.1126/science.174.4016.1349

(7) Guillot, T. S.; Miller, G. W. Protective Actions of the Vesicular Monoamine Transporter 2 (VMAT2) in Monoaminergic Neurons. *Mol. Neurobiol.* **2009**, *2* (39), 149–170. https://doi.org/10.1007/s12035-009-8059-y.

(8) Chen, J.; Song, J.; Yuan, P.; Tian, Q.; Ji, Y.; Ren-patterson, R.; Liu, G.; Sei, Y.; Weinberger, D. R. Orientation and Cellular Distribution of Membrane-Bound Catechol-O-Methyltransferase in Cortical Neurons. *J. Biol. Chem.* **2011**, *286* (40), 34752–34760. https://doi.org/10.1074/jbc.M111.262790.

(9) Meiser, J.; Weindl, D.; Hiller, K. Complexity of Dopamine Metabolism. *Cell Commun. Signal.* **2013**, *11* (34), 1–18.https://doi.org/10.1186/1478-811X-11-34

(10) Napolitano, A.; Manini, P.; Ischia, M. Oxidation Chemistry of Catecholamines and Neuronal Degeneration : An Update. *Curr. Med. Chem.* **2011**, *18* (12), 1832–1845. https://doi.org/10.2174/092986711795496863

(11) Stefani, A.; Pierantozzi, M.; Olivola, E.; Galati, S.; Cerroni, R.; Angelo, V. D.; Hainsworth, A. H.; Saviozzi, V.; Fedele, E.; Liguori, C. Neurochemistry International Homovanillic Acid in CSF of Mild Stage Parkinson ' s Disease Patients Correlates with Motor Impairment. *Neurochem. Int.* **2017**, *105*, 58–63. https://doi.org/10.1016/j.neuint.2017.01.007.

(12) Morimoto, S.; Takao, M.; Hatsuta, H.; Nishina, Y.; Komiya, T.; Sengoku, R.; Nakano, Y.; Uchino, A.;

Sumikura, H.; Saito, Y.; Kanemaru, K.; Murayama, S. Homovanillic Acid and 5-Hydroxyindole Acetic Acid as Biomarkers for Dementia with Lewy Bodies and Coincident Alzheimer's Disease : An Autopsy-Confirmed Study. *PLoS One* **2017**, *12* (2), 1–11. https://doi.org/10.1371/journal.pone.0171524.

(13) Chinta, S. J.; Andersen, J. K. Dopaminergic Neurons. *Int. J. Biochem. Cell Biol.* **2005**, *37* (5), 942–946. https://doi.org/10.1016/j.biocel.2004.09.009.

(14) Vallone, D.; Picetti, R.; Borrelli, E. Structure and Function of Dopamine Receptors. *Neurosci. Biobehav. Rev.* **2000**, *24* (1), 125–132. https://doi.org/10.1016/S0149-7634(99)00063-9.

(15) Haber, S. N. The Primate Basal Ganglia: Parallel and Integrative Networks. *J. Chem. Neuroanat.* **2003**, *26* (4), 317–330. https://doi.org/10.1016/j.jchemneu.2003.10.003.

(16) Correll, C. U.; Abi-Dargham, A.; Howes, O. Emerging Treatments for Schizophrenia. *The Journal of clinical psychiatry*. 2022. https://doi.org/10.4088/JCP.MS19053BR3C.

(17) Davie, C. A. A Review of Parkinson's Disease. *Br. Med. Bull.* **2008**, *86* (1), 109–127. https://doi.org/10.1093/bmb/ldn013.

(18) Wise, R. A. Dopamine, Learning and Motivation. *Nat. Rev. Neurosci.* **2004**, *5* (6), 483–494. https://doi.org/10.1038/nrn1406.

(19) Németh, G.; Csehi, R. Editorial: Novel Antipsychotics within and beyond Clinical Trials: The Treatment of Overlapping Psychiatric Disorders with D_3-D_2 Partial Agonists. *Front. Psychiatry* **2022**, *13*. https://doi.org/10.3389/fpsyt.2022.1038627.

(20) Ben-Jonathan, N.; Hnasko, R. Dopamine as a Prolactin (PRL) Inhibitor. *Endocr. Rev.* **2001**, *22* (6), 724–763. https://doi.org/10.1210/edrv.22.6.0451.

(21) Uhl, G. R. Dopamine Transporter : Basic Science and Human Variation of a Key Molecule for Dopaminergic Function , Locomotion , and Parkinsonism. *Mov. Disord.* **2003**, *18* (7), 71–80. https://doi.org/10.1002/mds.10578.

(22) Floresco, S. B.; West, A. R.; Ash, B.; Moore, H.; Grace, A. A. Afferent Modulation of Dopamine Neuron Firing Differentially Regulates Tonic and Phasic Dopamine Transmission. *Nat. Neurosci.* **2003**, *6* (9), 968–973. https://doi.org/10.1038/nn1103.

(23) Bunzow, J. R.; Van Tol, H. H. M.; Grandy, D. K.; Albert, P.; Salon, J.; Christie, M.; Machida, C. A.; Neve, K. A.; Civelli, O. Cloning and Expression of a Rat D_2 Dopamine Receptor CDNA. *Nature* **1988**, *336* (6201), 783–787. https://doi.org/10.1038/336783a0.

(24) Dearry, A.; Gingrich, J. A.; Falardeau, P.; Fremeau Jr, R. T.; Bates, M. D.; Caron, M. G. Molecular Cloning and Expression of the Gene for a Human D_1 Dopamine Receptor. *Nature* **1990**, *347* (9), 72–75. https://doi.org/10.1038/347072a0

(25) Sokoloff, P.; Giros, B.; Martres, M. P.; Bouthenet, M. L.; Schwartz, J. C. Molecular Cloning and Characterization of a Novel Dopamine Receptor (D_3) as a Target for Neuroleptics. *Nature* **1990**, *347* (6289), 146–151. https://doi.org/10.1038/347146a0.

(26) Van Tol, H. H. M.; Bunzow, J. R.; Guan, H. C.; Sunahara, R. K.; Seeman, P.; Niznik, H. B.; Civelli, O. Cloning of the Gene for a Human Dopamine D_4 Receptor with High Affinity for the Antipsychotic Clozapine. *Nature* **1991**, *350* (6319), 610–614. https://doi.org/10.1038/350610a0.

(27) Sunahara, R. K.; Guan, H. C.; O´Dowd, B. F.; Seeman, P.; Laurier, L. G.; George, S. R.; Torchia, J.; Van Tol, H. H. M.; Niznik, H. B. Cloning of the Gene for a Human Dopamine D_5 Receptor with Higher Affinity for Dopamine than D_1. *Nature* **1991**, *350* (6319), 614–619. https://doi.org/10.1038/350610a0.

(28) Gingrich, J. A.; Caron, M. G. Recent Advances in the Molecular Biology of Dopamine Receptors. *Annu. Rev. Neurosci.* **1993**, 67–90.https://doi.org/10.1146/annurev.ne.16.030193.001503

(29) Jackson, D. M.; Westlind-Danielssont, A. Dopamine Receptors: Molecular Biology, Biochemistry and Behavioural Aspects. *Pharmacol. Ther.* **1994**, *64*, 291–369.https://doi.org/10.1016/0163-7258(94)90041-8

(30) De Mei, C.; Ramos, M.; Iitaka, C.; Borrelli, E. Getting Specialized: Presynaptic and Postsynaptic Dopamine D2 Receptors. *Curr. Opin. Pharmacol.* **2009**, No. 225, 307. https://doi.org/10.1093/nq/s7-IX.225.307-h.

(31) Missale, C.; Nash, S. R.; Robinson, S. W.; Jaber, M.; Caron, M. G.; Nash, S. R.; Robinson, S. W.; Jaber, M.; Dopamine, M. G. C. Dopamine Receptors : From Structure to Function. *Physiol. Rev.* **1998**, *78* (1), 189–225. https://doi.org/10.1152/physrev.1998.78.1.189

(32) O´Dowd, B. F. Structures of Dopamine Receptors. *J. Neurochem.* **1993**, *60* (3), 804–816. https://doi.org/10.1111/j.1471-4159.1993.tb03224.x

(33) Dohlman, H. G.; Caron, M. G.; DeBlasi, A.; Frielle, T.; Lefkowitz, R. J. Role of Extracellular Disulfide-Bonded Cysteines in the Ligand Binding Function of the Beta2-Adrenergic Receptor. *Biochemistry* **1990**, *29* (9), 2335–2342.https://doi.org/10.1021/bi00461a018

(34) Civelli, O.; Bunzow, J. R.; Grandy, D. K. Molecular Diversity of the Dopamine Receptors. *Annu. Rev. Pharmacol. Toxicol.* **1993**, *32*, 281–307.https://doi.org/10.1146/annurev.pa.33.040193.001433

(35) Banks, M. L.; Sprague, J. E. The Dopamine 3 Receptor as a Candidate Biomarker and Therapeutic for Opioid Use Disorder. *Addict. Biol.* **2024**, *29* (2), 1–4. https://doi.org/10.1111/adb.13369.

(36) Freiermuth, C. E.; Kisor, D. F.; Lambert, J.; Braun, R.; Frey, J. A.; Bachmann, D. J.; Bischof, J. J.; Lyons, M. S.; Pantalon, M. V.; Punches, B. E.; Ancona, R.; Sprague, J. E. Genetic Variants Associated With Opioid Use Disorder. *Clin. Pharmacol. Ther.* **2023**, *113* (5), 1089–1095. https://doi.org/10.1002/cpt.2864.

(37) Levran, O.; Peles, E.; Randesi, M.; Correa Da Rosa, J.; Ott, J.; Rotrosen, J.; Adelson, M.; Kreek, M. J. Dopaminergic Pathway Polymorphisms and Heroin Addiction: Further Support for Association of CSNK1E Variants. *Pharmacogenomics* **2014**, *15* (16), 2001–2009. https://doi.org/10.2217/pgs.14.145.

(38) Baik, J. Dopamine Signaling in Reward-Related Behaviors. *Front. Neural Circuits* **2013**, *7* (152), 1–16. https://doi.org/10.3389/fncir.2013.00152.

(39) Agnati, L. F.; Guidolin, D.; Cervetto, C.; Borroto-Escuela, D. O.; Fuxe, K. Role of Iso-Receptors in Receptor Interactions with a Focus on Dopamine Iso-Receptor Complexes. *Rev. Neurosci.* **2016**, *27* (1), 1–25. https://doi.org/10.1515/revneuro-2015-0024.

(40) Wang, E.; Ding, Y.; Flodman, P.; Kidd, J. R.; Kidd, K. K.; Grady, D. L.; Ryder, O. A.; Spence, M. A.; Swanson, J. M.; Moyzis, R. K. The Genetic Architecture of Selection at the Human Dopamine Receptor D_4 (DRD4) Gene Locus. *Am. J. Hum. Genet.* **2004**, *74* (4), 931–944. https://doi.org/10.1086/420854

(41) González, S.; Rangel-barajas, C.; Peper, M.; Lorenzo, R.; Ciruela, F.; Borycz, J.; Ortiz, J.; Lluís, C.; Franco, R.; Mccormick, P. J.; Volkow, N. D.; Rubinstein, M.; Floran, B. Dopamine D_4 Receptor, but Not the ADHD-Associated $D_{4.7}$ Variant, Forms Functional Heteromers with the Dopamine D_{2s} Receptor in the Brain. *Mol. Psychiatry* **2012**, *17* (6), 650–662. https://doi.org/10.1038/mp.2011.93.Dopamine.

(42) Lee, S. P.; O´Dowd, B. F.; George, S. R. Homo- and Hetero-Oligomerization of G Protein-Coupled Receptors. *Life Sci.* **2003**, *74*, 173–180. https://doi.org/10.1016/j.lfs.2003.09.028.

(43) Lee, S. P.; So, C. H.; Rashid, A. J.; Varghese, G.; Cheng, R.; Jose, A.; Dowd, B. F. O.; George, S. R. Dopamine D_1 and D_2 Receptor Co-Activation Generates a Novel Phospholipase C-Mediated Calcium Signal. *J. Biol. Chem.* **2004**, *279* (34), 35671–35678. https://doi.org/10.1074/jbc.M401923200.

(44) Marcellino, D.; Ferre, S.; Casado, V.; Corte, A. Identification of Dopamine D_1-D_3 Receptor Heteromers. *J. Biol. Chem.* **2008**, *283* (38), 26016–26025. https://doi.org/10.1074/jbc.M710349200.

(45) Scarselli, M.; Novi, F.; Schallmach, E.; Lin, R.; Baragli, A.; Colzi, A.; Griffon, N.; Corsini, G. U.; Sokoloff, P.; Levenson, R.; Vogel, Z.; Maggio, R. D_2-D_3 Dopamine Receptor Heterodimers Exhibit Unique Functional Properties. *J. Biol. Chem.* **2001**, *276* (32), 30308–30314. https://doi.org/10.1074/jbc.M102297200.

(46) So, C. H.; Verma, V.; Alijaniaram, M.; Cheng, R.; Rashid, A. J.; Dowd, B. F. O.; George, S. R. Calcium Signaling by Dopamine D_5 Receptor and D_5-D_2 Receptor Hetero-Oligomers Occurs by a Mechanism Distinct from That for Dopamine D_1-D_2 Receptor Hetero-Oligomers. *Mol. Pharmacol.* **2009**, *75* (4), 843–854. https://doi.org/10.1124/mol.108.051805.which.

(47) Chien, E. Y. T.; Liu, W.; Zhao, Q.; Katritch, V.; Han, G. W.; Hanson, M. A.; Shi, L.; Newman, A. H.; Javitch, J. A.; Cherezov, V.; Stevens, R. C. Structure of the Human Dopamine D_3 Receptor in Complex with a D_2/D_3 Selective Antagonist. *Science.* **2010**, *330* (6007), 1091–1095.

https://doi.org/10.1126/science.1197410.

(48) Wang, S.; Wacker, D.; Levit, A.; Che, T.; Betz, R. M.; Mccorvy, J. D.; Venkatakrishnan, A. J.; Huang, X.; Dror, R. O.; Shoichet, B. K.; Roth, B. L. D_4 Dopamine Receptor High-Resolution Structures Enable the Discovery of Selective Agonists. *Science.* **2017**, *386*, 381–386. https://doi.org/10.1126/science.aan5468

(49) Wang, S.; Che, T.; Levit, A.; Shoichet, B. K.; Wacker, D.; Roth, B. L. Structure of the D_2 Dopamine Receptor Bound to the Atypical Antipsychotic Drug Risperidone. *Nature* **2018**. https://doi.org/10.1038/nature25758.

(50) Fan, L.; Tan, L.; Chen, Z.; Qi, J.; Nie, F.; Luo, Z.; Cheng, J.; Wang, S. Haloperidol Bound D_2 Dopamine Receptor Structure Inspired the Discovery of Subtype Selective Ligands. *Nat. Commun.* **2020**, *11* (1), 1–11. https://doi.org/10.1038/s41467-020-14884-y.

(51) Sun, B.; Feng, D.; Chu, M. L. H.; Fish, I.; Lovera, S.; Sands, Z. A.; Kelm, S.; Valade, A.; Wood, M.; Ceska, T.; Kobilka, T. S.; Lebon, F.; Kobilka, B. K. Crystal Structure of Dopamine D_1 Receptor in Complex with G Protein and a Non-Catechol Agonist. *Nat. Commun.* **2021**, *12* (1), 1–9. https://doi.org/10.1038/s41467-021-23519-9.

(52) Zhuang, Y.; Xu, P.; Mao, C.; Zhang, Y.; Zhang, C.; Xu, E. H. Structural Insights into the Human D1 and D_2 Dopamine Receptor Signaling Complexes. *Cell* **2021**, *184* (4), 931–942. https://doi.org/10.1016/j.cell.2021.01.027.

(53) Xu, P.; Huang, S.; Krumm, B. E.; Zhuang, Y.; Mao, C.; Zhang, Y.; Wang, Y.; Huang, X.-P.; Liu, Y.-F.; He, X.; Li, H.; Yin, W.; Jiang, J.; Zhang, Y.; Roth, B. L.; Xu, E. H. Structural Genomics of the Human Dopamine Receptor System. *Cell Res.* **2023**, 5. https://doi.org/10.1038/s41422-023-00808-0.

(54) Yin, J.; Chen, K. M.; Clark, M. J.; Hijazi, M.; Kumari, P.; Bai, X.; Sunahara, R. K.; Barth, P.; Rosenbaum, D. M. Structure of a D_2 Dopamine Receptor – G-Protein Complex in a Lipid Membrane. *Nature* **2020**, *584* (8). https://doi.org/10.1038/s41586-020-2379-5.

(55) Arroyo-Urea, S.; Nazarova, A.; Bonifazi, A.; Battiti, F.; Lam, J.; Newman, A. H.; Vsevolod, K.; Garcia-Nafria, J. Structure of the Dopamine D_3 Receptor Bound to a Bitopic Agonist Reveals a New Speciicity Site in an Expanded Allosteric Pocket. *Res. Sq.* **2023**,12, 1–34. https://doi.org/https://doi.org/10.21203/rs.3.rs-3433207/v1.

(56) Xu, P.; Huang, S.; Mao, C.; Cheng, X.; Zhang, Y.; Xu, E. H. Structures of the Human Dopamine D_3 Receptor-G i Complexes. *Mol. Cell* **2021**, *81* (3), 1–13. https://doi.org/10.1016/j.molcel.2021.01.003.

(57) Zhou, Y.; Cao, C.; He, L.; Wang, X.; Zhang, X. C. Crystal Structure of Dopamine Receptor D_4 Bound to the Subtype Selective Ligand, L745870. *Elife* **2019**, *8*, 1–15. https://doi.org/10.7554/eLife.48822.

(58) Graßl, F.; Bock, L.; Huete-Huerta González, Á.; Schiller, M.; Gmeiner, P.; König, J.; Fromm, M. F.;

Hübner, H.; Heinrich, M. R. Exploring Structural Determinants of Bias among D_4 Subtype-Selective Dopamine Receptor Agonists. *J. Med. Chem.* **2023**, *66* (14), 9710–9730. https://doi.org/10.1021/acs.jmedchem.3c00537.

(59) Beaulieu, J.-M.; Gainetdinov, R. R. The Physiology, Signaling, and Pharmacology of Dopamine Receptors. *Pharmacol Rev* **2011**, *63* (1), 182–217. https://doi.org/10.1124/pr.110.002642.182.

(60) Tritsch, N. X.; Sabatini, B. L. Dopaminergic Modulation of Synaptic Transmission in Cortex and Striatum. *Neuron* **2012**, *76* (1), 33–50. https://doi.org/10.1016/j.neuron.2012.09.023.

(61) Pierce, K. L.; Premont, R. T.; Lefkowitz, R. J.; Hughes, T. H. Seven-Transmembrane Receptors. *Mol. Cell Biol.* **2002**, *3*. https://doi.org/10.1038/nrm908.

(62) Teng, X.; Chen, S.; Wang, Q.; Chen, Z.; Wang, X.; Huang, N.; Zheng, S. Structural Insights into G Protein Activation by D1 Dopamine Receptor. *Sci. Adv.* **2022**, *8* (23). https://doi.org/10.1126/sciadv.abo4158.

(63) Predescu, D. V.; Crețoiu, S. M.; Crețoiu, D.; Pavelescu, L. A.; Suciu, N.; Radu, B. M.; Voinea, S. C. G Protein-Coupled Receptors (Gpcrs)-Mediated Calcium Signaling in Ovarian Cancer: Focus on Gpcrs Activated by Neurotransmitters and Inflammation-Associated Molecules. *Int. J. Mol. Sci.* **2019**, *20* (5568), 1–23. https://doi.org/10.3390/ijms20225568.

(64) Missale, C.; Fiorentini, C.; Collo, G.; Spano, P. The Neurobiology of Dopamine Receptors : Evolution from the Dual Concept to Heterodimer Complexes. *J. Recept. Signal Transduct.* **2010**, *30* (5), 347–354. https://doi.org/10.3109/10799893.2010.506192.

(65) Beaulieu, J.; Espinoza, S.; Gainetdinov, R. R. Dopamine Receptors – IUPHAR Review 13. *Br. J. Pharmacol.* **2015**, *172* (8), 1–23. https://doi.org/10.1111/bph.12906.

(66) Hollinger, S.; Hepler, J. R. Cellular Regulation of RGS Proteins : Modulators and Integrators of G Protein Signaling. *Pharmacol. Rev.* **2002**, *54* (3), 527–559.

(67) Laporte, A.; Miller, W. E.; Kim, K.; Caron, M. G.; Laporte, A. R.; Chem, M. G. J. B. Beta-Arrestin / AP-2 Interaction in G Protein-Coupled Receptor. *J. Biol. Chem.* **2002**, *277* (11), 9247–9254. https://doi.org/10.1074/jbc.M108490200.

(68) Rajagopal, S.; Shenoy, S. K. GPCR Desensitization : Acute and Prolonged Phases. *Cell. Signal.* **2018**, *41* (1), 9–16. https://doi.org/10.1016/j.cellsig.2017.01.024.

(69) Svenningsson, P.; Nishi, A.; Fisone, G.; Girault, J. A.; Nairn, A. C.; Greengard, P. DARPP-32: An Integrator of Neurotransmission. *Annu. Rev. Pharmacol. Toxicol.* **2004**, *44*, 269–296. https://doi.org/10.1146/annurev.pharmtox.44.101802.121415.

(70) Lindskog, M.; Svenningsson, P.; Pozzi, L.; Kim, Y.; Flenberg, A. A.; Bibb, J. A.; Fredholm, B. B.; Nairn, A. C.; Greengard, P.; Fisone, G. Involvement of DARPP-32 Phosphorylation in the Stimulant

Action of Caffeine. *Nature* **2002**, *418* (6899), 774–778. https://doi.org/10.1038/nature00817.

(71) Andersson, M.; Usiello, A.; Borgkvist, A.; Pozzi, L.; Dominguez, C.; Fienberg, A. A.; Svenningsson, P.; Fredholm, B. B.; Borrelli, E.; Greengard, P.; Fisone, G. Cannabinoid Action Depends on Phosphorylation of Dopamine- and CAMP-Regulated Phosphoprotein of 32 KDa at the Protein Kinase a Site in Striatal Projection Neurons. *J. Neurosci.* **2005**, *25* (37), 8432–8438. https://doi.org/10.1523/JNEUROSCI.1289-05.2005.

(72) Usiello, A.; Baik, J.; Rouge-Pont, F.; Picetti, R.; Dierich, A.; LeMeur, M.; Piazza, P. V.; Borrelli, E. Distinct Functions of the Two Isoforms of Dopamine D_2 Receptors. *Nature* **2000**, *408* (9), 199–202. https://doi.org/10.1038/35041572

(73) Sibley, D. R.; Monsma, F. J. Molecular Biology of Dopamine Receptors. *Trends Pharmacol. Sci.* **1992**, *13*, 61–69. https://doi.org/10.1016/0165-6147(92)90025-2

(74) Di Chiara, G.; Bassareo, V. Reward System and Addiction : What Dopamine Does and Doesn ' t Do. *Curr. Opin. Pharmacol.* **2007**, *7*, 69–76. https://doi.org/10.1016/j.coph.2006.11.003.

(75) Koob, G. F.; Volkow, N. D. Neurocircuitry of Addiction. *Neuropsychopharmacology* **2010**, *35*, 217–238. https://doi.org/10.1038/npp.2009.110.

(76) Xu, T.; Yao, W. D1 and D2 Dopamine Receptors in Separate Circuits Cooperate to Drive Associative Long-Term Potentiation in the Prefrontal Cortex. *Proc. Natl. Acad. Sci.* **2010**, *107* (37), 16366–16371. https://doi.org/10.1073/pnas.1004108107.

(77) Iversen, S. D.; Iversen, L. L. Dopamine : 50 Years in Perspective. *Trends Neurosci.* **2007**, *30* (5), 188–193. https://doi.org/10.1016/j.tins.2007.03.002.

(78) Carlsson, A. A Paradigm Shift in Brain Research. *Science.* **2001**, *294* (11), 1021–1024. https://doi.org/10.1126/science.1066969

(79) Frankle, W. G.; Laruelle, M. Neuroreceptor Imaging in Psychiatric Disorders. *Ann. Nucl. Med.* **2002**, *16* (7), 437–446. https://doi.org/10.1007/BF02988639

(80) Willner, P. The Mesolimbic Dopamine System as a Target for Rapid Antidepressant Action. *Int. Clin. Psychopharmacol.***1997**,*12* (3), 7–14. https//intclinpsychopharm/abstract/1997/07003

(81) Nikolaus, S.; Antke, C.; Müller, H. W. In Vivo Imaging of Synaptic Function in the Central Nervous System: II. Mental and Affective Disorders. *Behav. Brain Res.* **2009**, *204* (1), 32–66. https://doi.org/10.1016/j.bbr.2009.06.009.

(82) Volkow, N. D.; Fowler, J. S.; Wang, G. J.; Baler, R.; Telang, F. Imaging Dopamine's Role in Drug Abuse and Addiction. *Neuropharmacology* **2009**, *56* (1), 3–8. https://doi.org/10.1016/j.neuropharm.2008.05.022.

(83) Albert, K. A.; Hemmings, H. C.; Adamo, A. I. B.; Potkin, S. G.; Akbarian, S.; Sandman, C. A.; Cotman, C. W.; Bunney, W. E.; Greengard, P. Evidence for Decreased DARPP-32 in the Prefrontal Cortex of Patients with Schizophrenia. *Arch. Gen. Psychiatry* **2002**, *59* (8), 705–712. https://doi.org/10.1001/archpsyc.59.8.705.

(84) Ishikawa, M.; Mizukami, K.; Iwakiri, M.; Asada, T. Immunohistochemical and Immunoblot Analysis of Dopamine and Cyclic AMP-Regulated Phosphoprotein, Relative Molecular Mass 32,000 (DARPP-32) in the Prefrontal Cortex of Subjects with Schizophrenia and Bipolar Disorder. *Prog. Neuro-Psychopharmacology Biol. Psychiatry* **2007**, *31* (6), 1177–1181. https://doi.org/10.1016/j.pnpbp.2007.04.013.

(85) Feldcamp, L. A.; Souza, R. P.; Romano-Silva, M.; Kennedy, J. L.; Wong, A. H. C. Reduced Prefrontal Cortex DARPP-32 MRNA in Completed Suicide Victims with Schizophrenia. *Schizophr. Res.* **2008**, *103* (1–3), 192–200. https://doi.org/10.1016/j.schres.2008.05.014.

(86) Torres, K. C. L.; Souza, B. R.; Miranda, D. M.; Nicolato, R.; Neves, F. S.; Barros, A. G. A.; Dutra, W. O.; Gollob, K. J.; Correa, H.; Romano-Silva, M. A. The Leukocytes Expressing DARPP-32 Are Reduced in Patients with Schizophrenia and Bipolar Disorder. *Prog. Neuro-Psychopharmacology Biol. Psychiatry* **2009**, *33* (2), 214–219. https://doi.org/10.1016/j.pnpbp.2008.10.020.

(87) Santini, E.; Valjent, E.; Usiello, A.; Carta, M.; Borgkvist, A.; Girault, J.; Herve, D.; Greengard, P.; Fisone, G.; Curie, M. Critical Involvement of CAMP / DARPP-32 and Extracellular Signal-Regulated Protein Kinase Signaling in L -DOPA-Induced Dyskinesia. *J. Neurosci.* **2007**, *27* (26), 6995–7005. https://doi.org/10.1523/JNEUROSCI.0852-07.2007.

(88) Girault, J.; Valjent, E.; Caboche, J.; Herve, D. ERK2 : A Logical and Gate Critical for Drug-Induced Plasticity ? *Curr. Opin. Pharmacol.* **2007**, *7*, 77–85. https://doi.org/10.1016/j.coph.2006.08.012.

(89) Beaulieu, J. M. Not Only Lithium: Regulation of Glycogen Synthase Kinase-3 by Antipsychotics and Serotonergic Drugs. *Int. J. Neuropsychopharmacol.* **2007**, *10* (1), 3–6. https://doi.org/10.1017/S1461145706006857.

(90) Rossi, M.; Fasciani, I.; Marampon, F.; Maggio, R.; Scarselli, M. The First Negative Allosteric Modulator for Dopamine D2 and D3 Receptors, SB269652 May Lead to a New Generation of Antipsychotic Drugs. *Mol. Pharmacol.* **2017**, *91* (6), 586–594. https://doi.org/10.1124/mol.116.107607.

(91) Fuxe, K.; Marcellino, D.; Leo, G.; Agnati, L. F. Molecular Integration via Allosteric Interactions in Receptor Heteromers. A Working Hypothesis. *Curr. Opin. Pharmacol.* **2010**, *10* (1), 14–22. https://doi.org/10.1016/j.coph.2009.10.010.

(92) Ragajopal, S.; Rajagopal, K.; Lefkowitz, R. J. Teaching Old Receptors New Tricks: Biasing Seven-Transmembrane Receptors. *Nat. Rev. Drug Discov.* **2010**, *9* (5), 373–386.

https://doi.org/10.1038/nrd3024.Teaching.

(93) Komatsu, H.; Fukuchi, M.; Habata, Y. Potential Utility of Biased GPCR Signaling for Treatment of Psychiatric Disorders. *Int. J. Mol. Sci.* **2019**, *20* (3207), 1–18. https://doi.org/10.3390/ijms20133207

(94) Gao, Y.; Peterson, S.; Masri, B.; Hougland, T. M.; Adham, N.; Gyertyán, I.; Kiss, B.; Caron, M. G.; El-Mallakh, R. S. Cariprazine Exerts Antimanic Properties and Interferes with Dopamine D2 Receptor Beta-Arrestin Interactions. *Pharmacol. Res. Perspect.* **2015**, *3* (1), 1–10. https://doi.org/10.1002/prp2.73.

(95) Kim, K. M. Unveiling the Differences in Signaling and Regulatory Mechanisms between Dopamine D2 and D3 Receptors and Their Impact on Behavioral Sensitization. *Int. J. Mol. Sci.* **2023**, *24* (6742), 1–22. https://doi.org/10.3390/ijms24076742.

(96) Strange, P. G. Antipsychotic Drugs: Importance of Dopamine Receptors for Mechanisms of Therapeutic Actions and Side Effects. *Pharmacol. Rev.* **2001**, *53* (1), 119–133. https://pharmrev.aspetjournals.org/content/53/1/119

(97) Maramai, S.; Gemma, S.; Brogi, S.; Campiani, G.; Butini, S.; Stark, H.; Brindisi, M. Dopamine D3 Receptor Antagonists as Potential Therapeutics for the Treatment of Neurological Diseases. *Front. Neurosci.* **2016**, *10* (OCT), 1–16. https://doi.org/10.3389/fnins.2016.00451.

(98) Hackling, A. E.; Stark, H. Dopamine D_3 Receptor Ligands with Antagonist Properties. *ChemBioChem* **2002**, *3* (10), 946–961. https://doi.org/10.1002/1439-7633(20021004)3:10<946::AID-CBIC946>3.0.CO;2-5.

(99) Searle, G.; Beaver, J. D.; Comley, R. A.; Bani, M.; Tziortzi, A.; Slifstein, M.; Mugnaini, M.; Griffante, C.; Wilson, A. A.; Merlo-Pich, E.; Houle, S.; Gunn, R.; Rabiner, E. A.; Laruelle, M. Imaging Dopamine D_3 Receptors in the Human Brain with Positron Emission Tomography, [11C]PHNO, and a Selective D_3 Receptor Antagonist. *Biol. Psychiatry* **2010**, *68* (4), 392–399. https://doi.org/10.1016/j.biopsych.2010.04.038.

(100) Levant, B. Differential Distribution of D_3 Dopamine Receptors in the Brains of Several Mammalian Species. *Brain Res.* **1998**, *800* (2), 269–274. https://doi.org/10.1016/S0006-8993(98)00529-0.

(101) Gurevich, E. V.; Joyce, J. N. Dopamine D3 Receptor Is Selectively and Transiently Expressed in the Developing Whisker Barrel Cortex of the Rat. *J. Comp. Neurol.* **2000**, *420* (1), 35–51. https://doi.org/10.1002/(SICI)1096-9861(20000424)420:1<35::AID-CNE3>3.0.CO;2-K.

(102) Clarkson, R. L.; Liptak, A. T.; Gee, S. M.; Sohal, V. S.; Bender, K. J. D_3 Receptors Regulate Excitability in a Unique Class of Prefrontal Pyramidal Cells. *J. Neurosci.* **2017**, *37* (24), 5846–5860. https://doi.org/10.1523/JNEUROSCI.0310-17.2017.

(103) Herroelen, L.; De Backer, J. P.; Wilczak, N.; Flamez, A.; Vauquelin, G.; De Keyser, J.

Autoradiographic Distribution of D3-Type Dopamine Receptors in Human Brain Using [^{3}H]7-Hydroxy-N,N-Di-n-Propyl-2-Aminotetralin. *Brain Res.* **1994**, *648* (2), 222–228. https://doi.org/10.1016/0006-8993(94)91121-5.

(104) Hall, H.; Halldin, C.; Dijkstra, D.; Wikström, H.; Wise, L. D.; Pugsley, T. A.; Sokoloff, P.; Pauli, S.; Farde, L.; Sedvall, G. Autoradiographic Localisation of D_3-Dopamine Receptors in the Human Brain Using the Selective D_3-Dopamine Receptor Agonist (+)-[3H]PD 128907. *Psychopharmacology (Berl).* **1996**, *128* (3), 240–247. https://doi.org/10.1007/s002130050131.

(105) Joyce, J. N.; Janowsky, A.; Neve, K. A. Characterization and Distribution of [125I] Epidepride Dopamine D2 Receptors in Basal Ganglia and Cortex of Human Brain Binding To. *J. Pharmacol. Exp. Ther.* **1991**, *257* (3).https://doi.org/content/257/3/1253

(106) Mukherjee, J.; Yang, Z.; Brown, T.; Lew, R.; Wernick, M.; Ouyang, X.; Yasillo, N.; Chen, C.; Mintzer, R.; Cooper, M. Preliminary Assessment of Extrastriatal Dopamine D-2 Receptor Binding in the Rodent and Nonhuman Primate Brains Using the High Affinity Radioligand , 18 F-Fallypride. *Nucl. Med. Biol.* **1999**, *26*, 519–527. https://doi.org/https://doi.org/10.1016/S0969-8051(99)00012-8.

(107) Marti, R.; Pen, A.; Rivera, A.; Calle, A. D. E. L. A. Differential Regional and Cellular Distribution of Dopamine D2-Like Receptors : An Immunocytochemical Study of Subtype-Specific Antibodies in Rat and Human Brain. *J. Comp. Neurol.* **1998**, *371*, 353–371. https://doi.org/10.1002/(sici)1096-9861(19981221)402:3<353::aid-cne5>3.0.co;2-4

(108) Suzuki, M.; Hurd, Y. L.; Sokoloff, P.; Schwartz, J. D3 Dopamine Receptor MRNA Is Widely Expressed in the Human Brain. *Brain Res.* **1998**, *779*, 58–74. https://doi.org/10.1016/S0006-8993(97)01078-0

(109) Fujisawa, S.; Buzsáki, G. A 4Hz Oscillation Adaptively Synchronizes Prefrontal, VTA, and Hippocampal Activities. *Neuron* **2011**, *72* (1), 153–165. https://doi.org/10.1016/j.neuron.2011.08.018.

(110) Nakajima, S.; Gerretsen, P.; Takeuchi, H.; Caravaggio, F.; Chow, T.; Le Foll, B.; Mulsant, B.; Pollock, B.; Graff-Guerrero, A. The Potential Role of Dopamine D_3 Receptor Neurotransmission in Cognition. *Eur. Neuropsychopharmacol.* **2013**, *23* (8), 799–813. https://doi.org/10.1016/j.euroneuro.2013.05.006.

(111) Boileau, I.; Collo, G. *Therapeutic Applications of Dopamine D3 Receptor Function*; 2023. https://doi.org/https://doi.org/10.1007/978-3-031-23058-5.

(112) Sokoloff, P.; Leriche, L.; Diaz, J.; Louvel, J.; Pumain, R. Direct and Indirect Interactions of the Dopamine D_3 Receptor with Glutamate Pathways: Implications for the Treatment of Schizophrenia. *Naunyn. Schmiedebergs. Arch. Pharmacol.* **2013**, *386* (2), 107–124. https://doi.org/10.1007/s00210-012-0797-0.

(113) Connell, D. P. O.; Vaughan, C. J.; Aherne, A. M.; Botkin, S. J.; Wang, Z.; Felder, R. A.; Carey, R. M. Expression of the Dopamine D_3 Receptor Protein in the Rat Kidney. *Hypertension* **1998**, *32* (5), 886–895. https://doi.org/10.1161/01.HYP.32.5.886.

(114) Franz, D.; Osorio-barrios, F.; Osorio, F.; Ugalde, V.; Lopez, E.; Elgueta, D.; Figueroa, A.; Lladser, A.; Pacheco, R. Dopamine Receptor D_3 Signaling on CD4+ T Cells Favors Th1- and Th17- Mediated Immunity □. *J. Immunol.* **2016**, *196* (10), 4143–4149. https://doi.org/10.4049/jimmunol.1502420.

(115) Elgueta, D.; Contreras, F.; Prado, C.; Montoya, A. Dopamine Receptor D3 Expression Is Altered in CD4 + T-Cells From Parkinson' s Disease Patients and Its Pharmacologic Inhibition Attenuates the Motor Impairment in a Mouse Model. *Front. Immunol.* **2019**, *10*, 1–17. https://doi.org/10.3389/fimmu.2019.00981.

(116) Ustione, A.; Piston, D. W. Dopamine Synthesis and D3 Receptor Activation in Pancreatic ß -Cells Regulates Insulin Secretion and Intracellular [Ca 2+] Oscillations. *Mol. Endocrinol.* **2012**, *26* (11), 1928–1940. https://doi.org/10.1210/me.2012-1226.

(117) Caravaggio, F.; Scifo, E.; Sibille, E. L.; Mota, S. E. H.; Gerretsen, P.; Remington, G.; Gra, A. Expression of Dopamine D2 and D3 Receptors in the Human Retina Revealed by Positron Emission Tomography and Targeted Mass Spectrometry. *Exp. Eye Res.* **2018**, *175*, 32–41. https://doi.org/10.1016/j.exer.2018.06.006.

(118) Reyes-Resina, I.; Awad Alkozi, H.; del Serbadia, A.; Sanchez-Naves, J.; Lillo, J.; Jimenez, J.; Pintor, J.; Navarro, G.; Franco, R. Expression of Melatonin and Dopamine D_3 Receptor Heteromers in Eye Ciliary Body Epithelial Cells and Negative Correlation with Ocular Hypertension. *Cells* **2020**, *9* (1), 152. https://doi.org/doi:10.3390/cells9010152.

(119) Chu, E.; Chu, T. C.; Potter, D. E. Mechanisms and Sites of Ocular Action of 7-Hydroxy-2-Dipropylaminotetralin: A Dopamine3 Receptor Agonist. *J. Pharmacol. Exp. Ther.* **2000**, *293* (3), 710–716. https://doi.org/10.1016/j.bmc.2012.04.055.

(120) Leggio, G. M.; Bucolo, C.; Platania, C. B. M.; Salomone, S.; Drago, F. Current Drug Treatments Targeting Dopamine D3 Receptor. *Pharmacol. Ther.* **2016**, *165*, 164–177. https://doi.org/10.1016/j.pharmthera.2016.06.007.

(121) Tian, G.; Hsieh, C.; Taylor, M.; Youn, J.; Riad, A. A.; Luedtke, R. R.; Mach, R. H. Synthesis of Bitopic Ligands Based on Fallypride and Evaluation of Their Affinity and Selectivity towards Dopamine D2 and D3 Receptors. *Eur. J. Med. Chem.* **2023**, *261* (8), 115751. https://doi.org/10.1016/j.ejmech.2023.115751.

(122) Gross, G.; Wicke, K.; Drescher, K. U. Dopamine D3 Receptor Antagonism - Still a Therapeutic Option for the Treatment of Schizophrenia. *Naunyn. Schmiedebergs. Arch. Pharmacol.* **2013**, *386* (2), 155–166. https://doi.org/10.1007/s00210-012-0806-3.

(123) Kiss, B.; Laszlovszky, I.; Krámos, B.; Visegrády, A.; Bobok, A.; Lévay, G.; Lendvai, B.; Román, V. Neuronal Dopamine D3 Receptors: Translational Implications for Preclinical Research and Cns Disorders. *Biomolecules* **2021**, *11* (1), 1–39. https://doi.org/10.3390/biom11010104.

(124) Vorel, S. R.; Ashby, C. R.; Paul, M.; Liu, X.; Hayes, R.; Hagan, J. J.; Middlemiss, D. N.; Stemp, G.; Gardner, E. L. Dopamine D3 Receptor Antagonism Inhibits Cocaine-Seeking and Cocaine-Enhanced Brain Reward in Rats. *J. Neurosci.* **2018**, *22* (21), 9595–9603. https://doi.org/10.1523/jneurosci.22-21-09595.2002.

(125) Caine, S. B.; Koob, G. F. Modulation of Cocaine Self-Administration in the Rat Through D_3 Dopamine Receptors. *Science.* **1993**, *260* (5115), 1814–1816. https://doi.org/10.1126/science.8099761.

(126) Bordet, R.; Ridray, S.; Carboni, S.; Diaz, J.; Sokoloff, P.; Schwartz, J. C. Induction of Dopamine D_3 Receptor Expression as a Mechanism of Behavioral Sensitization to Levodopa. *Proc. Natl. Acad. Sci. U. S. A.* **1997**, *94* (7), 3363–3367. https://doi.org/10.1073/pnas.94.7.3363.

(127) Bézard, E.; Ferry, S.; Mach, U.; Stark, H.; Leriche, L.; Boraud, T.; Gross, C.; Sokoloff, P. Attenuation of Levodopa-Induced Dyskinesia by Normalizing Dopamine D3 Receptor Function. *Nat. Med.* **2003**, *9* (6), 762–767. https://doi.org/10.1038/nm875.

(128) Guillin, O.; Diaz, J.; Carroll, P.; Griffon, N.; Schwartz, J. C.; Sokoloff, P. BDNF Controls Dopamine D3 Receptor Expression and Triggers Behavioural Sensitization. *Nature* **2001**, *411* (6833), 86–89. https://doi.org/10.1038/35075076.

(129) Solís, O.; Espadas, I.; Del-Bel, E. A.; Moratalla, R. Nitric Oxide Synthase Inhibition Decreases L-DOPA-Induced Dyskinesia and the Expression of Striatal Molecular Markers in Pitx3-/- Aphakia Mice. *Neurobiol. Dis.* **2015**, *73*, 49–59. https://doi.org/10.1016/j.nbd.2014.09.010.

(130) Payer, D. E.; Guttman, M.; Kish, S. J.; Tong, J.; Adams, J. R.; Rusjan, P.; Houle, S.; Furukawa, Y.; Wilson, A. A.; Boileau, I. D3 Dopamine Receptor-Preferring [11C]PHNO PET Imaging in Parkinson Patients with Dyskinesia. *Am. Acad. Neurol.* **2016**, *86* (3), 224–230. https://doi.org/10.1212/WNL.0000000000002285.

(131) Seroogy, K. B.; Lundgren, K. H.; Tran, T. M. D.; Guthrie, K. M.; Isackson, P. J.; Gall, C. M. Dopaminergic Neurons in Rat Ventral Midbrain Express Brain-derived Neurotrophic Factor and Neurotrophin-3 MRNAs. *J. Comp. Neurol.* **1994**, *342* (3), 321–334. https://doi.org/10.1002/cne.903420302.

(132) Leggio, G. M.; Salomone, S.; Bucolo, C.; Platania, C.; Micale, V.; Caraci, F.; Drago, F. Dopamine D3 Receptor as a New Pharmacological Target for the Treatment of Depression. *Eur. J. Pharmacol.* **2013**, *719* (1–3), 25–33. https://doi.org/10.1016/j.ejphar.2013.07.022.

(133) Sokoloff, P.; Le Foll, B. The Dopamine D3 Receptor, a Quarter Century Later. *Eur. J. Neurosci.* **2016**, *45* (1), 2–19. https://doi.org/10.1111/ejn.13390.

(134) Joyce, J. N. Dopamine D_3 Receptor as a Therapeutic Target for Antipsychotic and Antiparkinsonian Drugs. *Pharmacol. Ther.* **2001**, *90*, 231–259. https://doi.org/10.1016/S0163-7258(01)00139-5

(135) Wilson, S. M.; Wurst, M. G.; Whatley, M. F.; Daniels, R. N. Classics in Chemical Neuroscience : Pramipexole. *ACS Chem. Neurosci.* **2020**, *11*, 2506–2512. https://doi.org/10.1021/acschemneuro.0c00332.

(136) Zhu, J.; Chen, M. The Effect and Safety of Ropinirole in the Treatment of Parkinson Disease. *Medicine (Baltimore)*. **2021**, *100* (46), 1–7. https://doi.org/10.1097/MD.0000000000027653

(137) Silindir, M.; Ozer, A. Y. The Benefits of Pramipexole Selection in the Treatment of Parkinson ' s Disease. *Neurol. Sci.* **2014**, *35*, 1505–1511. https://doi.org/10.1007/s10072-014-1891-5.

(138) Varga, L. I.; Ako-Agugua, N.; Colasante, J.; Hertweck, L.; Houser, T.; Smith, J.; Watty, A. A.; Nagar, S.; Raffa, R. B. Critical Review of Ropinirole and Pramipexole – Putative Dopamine D 3 -Receptor Selective Agonists – for the Treatment of RLS. *J. Clin. Pharm. Ther.* **2009**, *34*, 493–505. https://doi.org/10.1111/j.1365-2710.2009.01025.x.

(139) Holloway, R. G. Pramipexole vs Levodopa as Initial Treatment for Parkinson Disease. *Arch. Neurol.* **2004**, *61* (7), 1044–1053. https://doi.org/10.1001/archneur.61.7.1044

(140) Damsma, G.; Bottema, T.; Westerink, B. H. C.; Tepper, P. G.; Dijkstra, D.; Pugsley, T. A.; MacKenzie, R. G.; Heffner, T. G.; Wikström, H. Pharmacological Aspects of R-(+)-7-OH-DPAT, a Putative Dopamine D3 Receptor Ligand. *Eur. J. Pharmacol.* **1993**, *249*, 9–10. https://doi.org/10.1016/0014-2999(93)90533-N

(141) Van Kampen, J. M.; Eckman, C. B. Dopamine D3 Receptor Agonist Delivery to a Model of Parkinson's Disease Restores the Nigrostriatal Pathway and Improves Locomotor Behavior. *J. Neurosci.* **2006**, *26* (27), 7272–7280. https://doi.org/10.1523/JNEUROSCI.0837-06.2006.

(142) Rodrigo, B.; Jorge, A.; Néstor, M.; Damián, C. J.; Luis, C. Á. J.; Fiacro, J.; Gerardo, R. Quinpirole Effects on the Dopaminergic System. *Br. J. Pharmacol. Toxicol.* **2011**, *2* (6), 310–317. https://www.airitilibrary.com/Article/Detail?DocID=20442467-201112-201507070016-201507070016-310-317

(143) Collo, G.; Zanetti, S.; Missale, C.; Spano, P. F. Dopamine D3 Receptor-Preferring Agonists Increase Dendrite Arborization of Mesencephalic Dopaminergic Neurons via Extracellular Signal-Regulated Kinase Phosphorylation. *Eur. J. Neurosci.* **2008**, *28* (7), 1231–1240. https://doi.org/10.1111/j.1460-9568.2008.06423.x.

(144) Laux, G. Amisulpride and Sulpiride in the Treatment of Psychosis. *Neuropsychopharmacotherapy* **2022**, 1943–1952. https://doi.org/10.1007/978-3-030-62059-2_57#DOI

(145) Elek, M.; Djokovic, N.; Frank, A.; Oljacic, S.; Zivkovic, A.; Nikolic, K.; Stark, H. Synthesis, in Silico, and in Vitro Studies of Novel Dopamine D2 and D3 Receptor Ligands. *Arch. Pharm. (Weinheim)*. **2021**, *354* (6). https://doi.org/10.1002/ardp.202000486.

(146) Gonnet, G. H.; Cohen, M. A.; Benner, S. A. Exhaustive Matching of the Entire Protein Sequence Database Dy. *Science* . **1992**, *256*, 1443–1446. https://doi.org/10.1126/science.1604319

(147) Boeckler, F.; Gmeiner, P. Dopamine D3 Receptor Ligands-Recent Advances in the Control of Subtype Selectivity and Intrinsic Activity. *Biochim. Biophys. Acta - Biomembr.* **2007**, *1768* (4), 871–887. https://doi.org/10.1016/j.bbamem.2006.12.001.

(148) Murray, P. J.; Harrison, L. A.; Johnson, M. R.; Robertson, G. M.; Scopes, D. I. C.; Buli, D. R.; Graham, S. E. A.; Hayes, A. G.; Kilpatrick, G. J.; Daas, I. Den; Large, C.; Sheehan, M. J.; Stubbs, C. M.; Turpin, M. P. A Novel series of Arylpiperazines with high affinity and selectivity for the dopamine D_3 receptor. *Bioorganic Med. Chem. Lett.* **1995**, *5* (3), 219–222. https://doi.org/10.1016/0960-894X(95)00011-H

(149) Pilla, M.; Perachon, S.; Sautel, F.; Garrido, F.; Mann, A.; Wermuth, C. G.; Schwartz, J.; Everitt, B. J.; Sokoloff, P. Selective Inhibition of Cocaine- Seeking Behaviour by a Partial Dopamine D_3 Receptor Agonist. *Nature* **1999**, *400*, 371–375. https://doi.org/10.1038/22560

(150) Preti, A. BP-897 Bioprojet. *Curr. Opin. Investig. Drugs* **2000**, *1* (1), 110-115. https://doi.org/10.1111/j.1527-3458.2003.tb00246.x

(151) Yuan, J.; Chen, X.; Brodbeck, R.; Primus, R.; Braun, J.; Wasley, J. W. F.; Thurkauf, A. NGB2904 and NGB2849: two higly selective dopamine D_3 receptor antagonists. *Bioorganic Med. Chem. Lett.* **1998**, *8*, 2715–2718. https://doi.org/10.1016/S0960-894X(98)00469-7

(152) Bettinetti, L.; Schlotter, K.; Hübner, H.; Gmeiner, P. Interactive SAR Studies: Rational Discovery of Super-Potent and Highly Selective Dopamine D_3 Receptor Antagonists and Partial Agonists. *J. Med. Chem.* **2002**, *45* (21), 4594–4597. https://doi.org/10.1021/jm025558r.

(153) Löber, S.; Hübner, H.; Tschammer, N.; Gmeiner, P. Recent Advances in the Search for D 3 - and D 4 -Selective Drugs : Probes , Models and Candidates. *Trends Pharmacol. Sci.* **2011**, *32* (3), 148–157. https://doi.org/10.1016/j.tips.2010.12.003.

(154) Hackling, A.; Ghosh, R.; Perachon, S.; Mann, A.; Höltje, H. D.; Wermuth, C. G.; Schwartz, J. C.; Sippl, W.; Sokoloff, P.; Stark, H. N-(ω)-(4-(2-Methoxyphenyl)Piperazin-1-Yl)Alkyl)Carboxamides as Dopamine D2 and D3 Receptor Ligands. *J. Med. Chem.* **2003**, *46* (18), 3883–3899. https://doi.org/10.1021/jm030836n.

(155) Leopoldo, M.; Berardi, F.; Colabufo, N. A.; De Giorgio, P.; Lacivita, E.; Perrone, R.; Tortorella, V. Structure-Affinity Relationship Study on N-[4-(4-Arylpiperazin-1-Yl)Butyl]Arylcarboxamides as Potent and Selective Dopamine D3 Receptor Ligands. *J. Med. Chem.* **2002**, *45* (26), 5727–5735. https://doi.org/10.1021/jm020952a.

(156) Campiani, G.; Butini, S.; Trotta, F.; Fattorusso, C.; Catalanotti, B.; Aiello, F.; Gemma, S.; Nacci, V.; Novellino, E.; Stark, J. A.; Cagnotto, A.; Fumagalli, E.; Carnovali, F.; Cervo, L.; Mennini, T. Synthesis and Pharmacological Evaluation of Potent and Highly Selective D3 Receptor Ligands: Inhibition of

Cocaine-Seeking Behavior and the Role of Dopamine D3/D2 Receptors. *J. Med. Chem.* **2003**, *46* (18), 3822–3839. https://doi.org/10.1021/jm0211220.

(157) Newman, A. H.; Grundt, P.; Cyriac, G.; Deschamps, J. R.; Taylor, M.; Kumar, R.; Ho, D.; Luedtke, R. R. N-(4-(4-(2,3-Dichloro- or 2-Methoxyphenyl)Piperazin-1-Yl)Butyl) Heterobiarylcarboxamides with Functionalized Linking Chains as High Affinity and Enantioselective D3 Receptor Antagonists. *J. Med. Chem.* **2009**, *52* (8), 2559–2570. https://doi.org/10.1021/jm900095y.

(158) Sasse, B. C.; Mach, U. R.; Leppaenen, J.; Calmels, T.; Stark, H. Hybrid Approach for the Design of Highly Affine and Selective Dopamine D3 Receptor Ligands Using Privileged Scaffolds of Biogenic Amine GPCR Ligands. *Bioorganic Med. Chem.* **2007**, *15* (23), 7258–7273. https://doi.org/10.1016/j.bmc.2007.08.034.

(159) Joyce, J. N.; Millan, M. J. Dopamine D_3 Receptor Antagonists as Therapeutic Agents. *Drug Discov. Today* **2005**, *10* (13), 917–925. https://doi.org/10.1016/S1359-6446(05)03491-4.

(160) Keck, T. M.; Banala, A. K.; Slack, R. D.; Burzynski, C.; Bonifazi, A.; Okunola-Bakare, O. M.; Moore, M.; Deschamps, J. R.; Rais, R.; Slusher, B. S.; Newman, A. H. Using Click Chemistry toward Novel 1,2,3-Triazole-Linked Dopamine D3 Receptor Ligands. *Bioorganic Med. Chem.* **2015**, *23* (14), 4000–4012. https://doi.org/10.1016/j.bmc.2015.01.017.Using.

(161) Belliotti, T. R.; Kesten, S. R.; Rubin, J. R.; Wustrow, D. J.; Georgic, L. M.; Zoski, K. T.; Akunne, H. C.; Wise, L. D. Novel cyclohexyl amides as potent and selective D_3 dopamine receptor ligands. *Bioorganic Med. Chem. Lett.* **1997**, *7* (18), 2403–2408. https://doi.org/10.1016/S0960-894X(97)00443-5

(162) Stemp, G.; Ashmeade, T.; Branch, C. L.; Hadley, M. S.; Hunter, A. J.; Johnson, C. N.; Nash, D. J.; Thewlis, K. M.; Vong, A. K. K.; Austin, N. E.; Jeffrey, P.; Avenell, K. Y.; Boyfield, I.; Hagan, J. J.; Middlemiss, D. N.; Reavill, C.; Riley, G. J.; Routledge, C.; Wood, M. Desing and Synthesis of Trans-N-[4-[2-(6-Cyano-1,2,3,4-Tetrahydroisoquinolin-2-Yl) Ethyl] Cyclohexy]-4-Quinolinecarboxamide(SB-277011): A Potent and Selective Dopamine D_3 Receptor Antagonist with High Oral Bioavailability and CNS Penetration in the Rat. *J. Med. Chem.* **2000**, *43* (9), 1878–1885. https://doi.org/10.1021/jm000090i

(163) Reavill, C.; Taylor, S. G.; Wood, M. D.; Ashmeade, T.; Austin, N. E.; Avenell, K. I. M. Y.; Boyfield, I.; Branch, C. L.; Cilia, J.; Coldwell, M. C.; Hadley, M. S.; Hunter, A. J.; Jeffrey, P.; Jewitt, F.; Johnson, C. N.; Jones, D. N. C.; Medhurst, A. D.; Middlemiss, D. N.; Nash, D. J.; Riley, G. J.; Routledge, C.; Stemp, G.; Thewlis, K. M.; Trail, B.; Vong, A. K. K.; Hagan, J. I. M. J. Pharmacological Actions of a Novel , High-Affinity , and Selective Human Dopamine D_3 Receptor Antagonist , SB-277011-A. *J. Pharmacol. Exp. Ther.* **2000**, *294* (3), 1154–1165. https://doi.org/10.1021/jo960057x.

(164) Thanos, P. K.; Katana, J. M.; Ashby, C. R.; Michaelides, M.; Gardner, E. L.; Heidbreder, C. A.;

Volkow, N. D. The Selective Dopamine D3 Receptor Antagonist SB-277011-A Attenuates Ethanol Consumption in Ethanol Preferring (P) and Non-Preferring (NP) Rats. *Pharmacol. Biochem. Behav.* **2005**, *81*, 190–197. https://doi.org/10.1016/j.pbb.2005.03.013.

(165) Silvano, E.; Millan, M. J.; La Cour, C. M.; Han, Y.; Duan, L.; Griffin, S. A.; Luedtke, R. R.; Aloisi, G.; Rossi, M.; Zazzeroni, F.; Javitch, J. A.; Maggio, R. The Tetrahydroisoquinoline Derivative SB269,652 Is an Allosteric Antagonist at Dopamine D_3 and D_2 Receptors. *Mol. Pharmacol.* **2010**, *78* (5), 925–934. https://doi.org/10.1124/mol.110.065755.

(166) Kiss, B.; Horvath, A.; Nemethy, Z.; Schmidt, E.; Laszlovszky, I.; Bugovics, G.; Fazekas, K.; Hornok, K.; Orosz, S.; Gyertyan, I.; Agai-Csongor, E.; Domany, G.; Tihanyi, K.; Adham, N.; Szombathelyi, Z. Cariprazine (RGH-188), a Dopamine D3 Receptor-Preferring, D3/D2 Dopamine Receptor Antagonist-Partial Agonist Antipsychotic Candidate: In Vitro and Neurochemical Profile. *J. Pharmacol. Exp. Ther.* **2010**, *333* (1), 328–340. https://doi.org/10.1124/jpet.109.160432.

(167) Román, V.; Gyertyán, I.; Sághy, K.; Kiss, B.; Szombathelyi, Z. Cariprazine (RGH-188), a D3-Preferring Dopamine D 3/D2 Receptor Partial Agonist Antipsychotic Candidate Demonstrates Anti-Abuse Potential in Rats. *Psychopharmacology (Berl).* **2013**, *226* (2), 285–293. https://doi.org/10.1007/s00213-012-2906-7.

(168) Brito, A. F.; Moreira, L. K. S.; Menegatti, R.; Costa, E. A. Piperazine Derivatives with Central Pharmacological Activity Used as Therapeutic Tools. *Fundam. Clin. Pharmacol.* **2019**, *33* (1), 13–24. https://doi.org/10.1111/fcp.12408.

(169) Chien, E. Y. T.; Liu, W.; Zhao, Q.; Katritch, V.; Han, G. W.; Michael, A.; Shi, L.; Newman, A. H.; Javitch, J. A.; Cherezov, V.; Stevens, R. C. Structure of the Human Dopamine D3 Receptor in Complex with a D2/D3 Selective Antagonist. *Science (80-.).* **2010**, *330* (6007), 1091–1095. https://doi.org/10.1126/science.1197410.Structure.

(170) Alberts, G. L.; Pregenzer, J. F.; IM, W. BIN. Identification of Transmembrane Regions Critical for Ligand Binding to the Human D_3 Dopamine Receptor Using Various D3/ D1 Transmembrane Chimeras. *Mol. Pharmacol.* **1998**, *54*, 379–388. https://doi.org/10.1124/mol.54.2.379

(171) Shi, L.; Simpson, M. M.; Ballesteros, J. A.; Javitch, J. A. The First Transmembrane Segment of the Dopamine D2 Receptor : Accessibility in the Binding-Site Crevice and Position in the Transmembrane Bundle. *Biochemistry* **2001**, *40* (41), 12339–12348. https://doi.org/10.1021/bi011204a

(172) Guo, W.; Urizar, E.; Kralikova, M.; Carlos, J.; Shi, L.; Filizola, M.; Javitch, J. A. Dopamine D2 Receptors Form Higher Order Oligomers at Physiological Expression Levels. *Eur. Mol. Biol. Organ.* **2008**, *27* (17), 2293–2304. https://doi.org/10.1038/emboj.2008.153.

(173) Adhikari, P.; Xie, B.; Semeano, A.; Bonifazi, A.; Battiti, F. O.; Newman, A. H.; Yano, H.; Shi, L. Chirality of Novel Bitopic Agonists Determines Unique Pharmacology at the Dopamine D_3 Receptor.

Biomolecules **2021**, *11* (570), 1–18. https:// doi.org/10.3390/biom11040570.

(174) Yu, Y.; He, J.; Huang, Z.; Li, Y.; Wu, Y.; Shen, Y. Safety , Tolerability , and Pharmacokinetics of JX11502MA in Chinese Healthy Subjects : Placebo-Controlled Study Following Single-Dose Administration. *Expert Opin. Investig. Drugs* **2024**, *33* (1), 51–62. https://doi.org/10.1080/13543784.2023.2291470.

(175) Chagraoui, A.; Di Giovanni, G.; De Deurwaerdere, P. Neurobiological and Pharmacological Perspectives of D3 Receptors in Parkinson ' s Disease. *Biomolecules* **2022**, *12* (243), 1–34. https://doi.org/https:// doi.org/10.3390/biom12020243.

(176) Galaj, E.; Newman, A. H.; Xi, Z. Dopamine D3 Receptor-Based Medication Development for the Treatment of Opioid Use Disorder : Rationale , Progress , and Challenges. *Neurosci. Biobehav. Rev.* **2020**, *114*, 38–52. https://doi.org/10.1016/j.neubiorev.2020.04.024.

(177) Peng, X.; Wang, Q.; Mishra, Y.; Xu, J.; Reichert, D. E.; Malik, M.; Taylor, M.; Luedtke, R. R.; Mach, R. H. Synthesis, Pharmacological Evaluation and Molecular Modeling Studies of Triazole Containing Dopamine D3 Receptor Ligands. *Bioorganic Med. Chem. Lett.* **2015**, *25* (3), 519–523. https://doi.org/10.1016/j.bmcl.2014.12.023.

(178) Michino, M.; Donthamsetti, P.; Beuming, T.; Banala, A.; Duan, L.; Roux, T.; Han, Y.; Trinquet, E.; Newman, A. H.; Javitch, J. A.; Shi, L. A Single Glycine in Extracellular Loop 1 Is the Critical Determinant for Pharmacological Specificity of Dopamine D2 and D3 Receptors. *Mol. Pharmacol.* **2013**, *84* (6), 854–864. https://doi.org/10.1124/mol.113.087833.

(179) Newman, A. H.; Beuming, T.; Banala, A. K.; Donthamsetti, P.; Pongetti, K.; Labounty, A.; Levy, B.; Cao, J.; Michino, M.; Luedtke, R. R.; Javitch, J. A.; Shi, L. Molecular Determinants of Selectivity and Efficacy at the Dopamine D3 Receptor. *J. Med. Chem.* **2012**, *55* (15), 6689–6699. https://doi.org/10.1021/jm300482h.

(180) Sansom, M. S. P.; Weinstein, H. Hinges , Swivels and Switches : The Role of Prolines in Signalling via Transmembrane Alpha-Helices. *Trends Pharmacol. Sci.* **2000**, *21*, 445–451.

(181) Ballesteros, J. A.; Shi, L. E. I.; Javitch, J. A. Structural Mimicry in G Protein-Coupled Receptors : Implications of the High-Resolution Structure of Rhodopsin for Structure-Function Analysis of Rhodopsin-Like Receptors. *Mol. Pharmacol.* **2001**, *60* (1), 1–19. https://doi.org/10.1016/s0165-6147(00)01553-4

(182) Michino, M.; Beuming, T.; Donthamsetti, P.; Newman, A. H.; Javitch, J. A.; Shi, L. What Can Crystal Structures of Aminergic Receptors Tell Us about Designing Subtype-Selective Ligands ? *Pharmacol. Rev.* **2015**, *23*, 198–213. https://doi.org/10.1124/pr.114.009944

(183) Newman, A. H.; Battiti, F. O.; Bonifazi, A. 2016 Philip S. Portoghese Medicinal Chemistry Lectureship: Designing Bivalent or Bitopic Molecules for G-Protein Coupled Receptors. The Whole Is

Greater Than the Sum of Its Parts. *J. Med. Chem.* **2020**, *63* (5), 1779–1797. https://doi.org/10.1021/acs.jmedchem.9b01105.

(184) Moritz, A. E.; Bonifazi, A.; Guerrero, A. M.; Kumar, V.; Free, R. B.; Lane, J. R.; Verma, R. K.; Shi, L.; Newman, A. H.; Sibley, D. R. Evidence for a Stereoselective Mechanism for Bitopic Activity by Extended-Length Antagonists of the D3Dopamine Receptor. *ACS Chem. Neurosci.* **2020**, *11* (20), 3309–3320. https://doi.org/10.1021/acschemneuro.0c00425.

(185) Lane, J. R.; Donthamsetti, P.; Shonberg, J.; Draper-Joyce, C. J.; Dentry, S.; Michino, M.; Shi, L.; López, L.; Scammells, P. J.; Capuano, B.; Sexton, P. M.; Javitch, J. A.; Christopoulos, A. A New Mechanism of Allostery in a G Protein-Coupled Receptor Dimer. *Nat. Chem. Biol.* **2014**, *10* (9), 745–752. https://doi.org/10.1038/nchembio.1593.

(186) Shonberg, J.; Draper-joyce, C.; Mistry, S. N.; Christopoulos, A.; Scammells, P. J.; Lane, J. R.; Capuano, B. Structure-Activity Study of N-((Trans)-4-(2-(7-Cyano-3,4-Dihydroisoquinolin-2(1H)-Yl)Ethyl)Cyclohexyl)-1H-Indole-2-Carboxamide (SB269652), a Bitopic Ligand That Acts as a Negative Allosteric Modulator of the DOpmaine D2 Receptor. *J. Med. Chem.* **2015**, *58*, 5287–5307. https://doi.org/10.1021/acs.jmedchem.5b00581.

(187) Kopinathan, A.; Draper-Joyce, C.; Szabo, M.; Christopoulos, A.; Scammells, P. J.; Lane, J. R.; Capuano, B. Subtle Modifications to the Indole-2-Carboxamide Motif of the Negative Allosteric Modulator N-((Trans)-4-(2-(7-Cyano-3,4-Dihydroisoquinolin-2(1 H)-Yl)Ethyl)Cyclohexyl)-1 H-Indole-2-Carboxamide (SB269652) Yield Dramatic Changes in Pharmacological Activity . *J. Med. Chem.* **2019**, *62* (1), 371–377. https://doi.org/10.1021/acs.jmedchem.8b00192.

(188) Valant, C.; Lane, J. R.; Sexton, P. M.; Christopoulos, A. The Best of Both Worlds ? Bitopic Orthosteric / Allosteric Ligands of G Protein – Coupled Receptors. *Annu. Rev. Pharmacol. Toxicol.* **2012**, *52*. https://doi.org/10.1146/annurev-pharmtox-010611-134514.

(189) Lane, J. R.; Sexton, P. M.; Christopoulos, A. Bridging the Gap: Bitopic Ligands of G-Protein-Coupled Receptors. *Trends Pharmacol. Sci.* **2013**, *34* (1), 59–66. https://doi.org/10.1016/j.tips.2012.10.003.

(190) Kumar, V.; Moritz, A. E.; Keck, T. M.; Bonifazi, A.; Ellenberger, M. P.; Sibley, C. D.; Free, R. B.; Shi, L.; Lane, J. R.; Sibley, D. R.; Newman, A. H. Synthesis and Pharmacological Characterization of Novel Trans-Cyclopropylmethyl-Linked Bivalent Ligands That Exhibit Selectivity and Allosteric Pharmacology at the Dopamine D3 Receptor (D3R). *J. Med. Chem.* **2017**, *60* (4), 1478–1494. https://doi.org/10.1021/acs.jmedchem.6b01688.

(191) Shah, P.; Westwell, A. D. The Role of Fluorine in Medicinal Chemistry. *J. Enzyme Inhib. Med. Chem.* **2007**, *22* (5), 527–540. https://doi.org/10.1080/14756360701425014.

(192) Zafrani, Y.; Yeffet, D.; Sod-Moriah, G.; Berliner, A.; Amir, D.; Marciano, D.; Gershonov, E.; Saphier, S. Difluoromethyl Bioisostere: Examining the “Lipophilic Hydrogen Bond Donor” Concept. *J. Med.*

Chem. **2017**, *60* (2), 797–804. https://doi.org/10.1021/acs.jmedchem.6b01691.

(193) Meanwell, N. A. Fluorine and Fluorinated Motifs in the Design and Application of Bioisosteres for Drug Design. *J. Med. Chem.* **2018**, *61* (14), 5822–5880. https://doi.org/10.1021/acs.jmedchem.7b01788.

(194) Banala, A. K.; Levy, B. A.; Khatri, S. S.; Furman, C. A.; Roof, R. A.; Mishra, Y.; Gri, S. A.; Sibley, D. R.; Luedtke, R. R.; Newman, A. H. N-(3-Fluoro-4-(4-(2-Methoxy or 2,3-Dichlorophenyl) Piperazine-1-Yl)Butyl) Arylcarboxamides as Selective Dopamine D3 Receptor Ligands: Critical Role of the Carboxamide Linker for D3 Receptor Seletivity. *J. Med. Chem.* **2011**, *54* (2), 3581–3594.

(195) Kumar, V.; Banala, A. K.; Garcia, E. G.; Cao, J.; Keck, T. M.; Bonifazi, A.; Deschamps, J. R.; Newman, A. H. Chiral Resolution and Serendipitous Fluorination Reaction for the Selective Dopamine D3 Receptor Antagonist BAK2-66. *ACS Med. Chem. Lett.* **2014**, *5* (6), 647–651. https://doi.org/10.1021/ml500006v.

(196) Jordan, C. J.; Humburg, B.; Rice, M.; Bi, G. H.; You, Z. B.; Shaik, A. B.; Cao, J.; Bonifazi, A.; Gadiano, A.; Rais, R.; Slusher, B.; Newman, A. H.; Xi, Z. X. The Highly Selective Dopamine D3R Antagonist, R-VK4-40 Attenuates Oxycodone Reward and Augments Analgesia in Rodents. *Neuropharmacology* **2019**, *158*, 107597. https://doi.org/10.1016/j.neuropharm.2019.04.003.

(197) Shaik, A. B.; Kumar, V.; Bonifazi, A.; Guerrero, A. M.; Cemaj, S. L.; Gadiano, A.; Lam, J.; Xi, Z.; Rais, R.; Slusher, B. S.; Newman, A. H. Investigation of Novel Primary and Secondary Pharmacophores and 3 - Substitution in the Linking Chain of a Series of Highly Selective and Bitopic Dopamine D 3 Receptor Antagonists and Partial Agonists. *J. Med. Chem.* **2019**, *62*, 9061–9077. https://doi.org/10.1021/acs.jmedchem.9b00607.

(198) Tamminga, C. A. Partial Dopamine Agonists in the Treatment of Psychosis. *J. Neural Transm.* **2002**, *109* (2), 411–420. https://doi.org/10.2174/1568007024606195.

(199) Mailman, R.; Murthy, V. Third Generation Antipsychotic Drugs: Partial Agonism or Receptor Functional Selectivity? *Curr. Pharm. Des.* **2010**, *16* (5), 488–501. https://doi.org/10.2174/138161210790361461.

(200) *Diagnostic and Statistical Manual of Mental Disorders (5th Edition)*; 2013. https://doi.org/10.1007/978-3-319-95720-3_23.

(201) Rees, E.; O'Donovan, M. C.; Owen, M. J. Genetics of Schizophrenia. *Curr. Opin. Behav. Sci.* **2015**, *2*, 8–14. https://doi.org/10.1016/j.cobeha.2014.07.001.

(202) Avramopoulos, D. Recent Advances in the Genetics of Schizophrenia. *Mol. Neuropsychiatry* **2018**, *10* (4), 35–51. https://doi.org/10.1159/000488679.

(203) Cannon, T. D.; Kaprio, J.; Lönnqvist, J.; Huttunen, M.; Koskenvuo, M. The Genetic Epidemiology of

Schizophrenia in a Finnish Twin Cohort: A Population-Based Modeling Study. *Arch. Gen. Psychiatry* **1998**, *55* (1), 67–74. https://doi.org/10.1001/archpsyc.55.1.67.

(204) Cong, L.; Ran, A. F.; Cox, D.; Lin, S.; Barreto, R.; Habib, N.; Hsu, P. D.; Wu, X.; Jiang, W.; Marraffini, L. A.; Zhang, F. Multiplex Genome Engineering Using CRISPR/Cas Systems. *Science.* **2013**, *339* (2), 819–823. https://doi.org/10.1126/science.1231143

(205) Henssler, J.; Brandt, L.; Müller, M.; Liu, S.; Montag, C.; Sterzer, P.; Heinz, A. Migration and Schizophrenia: Meta-Analysis and Explanatory Framework. *Eur. Arch. Psychiatry Clin. Neurosci.* **2020**, *270* (3), 325–335. https://doi.org/10.1007/s00406-019-01028-7.

(206) Mcdonald, C.; Murray, R. M. Interactive Report Early and Late Environmental Risk Factors for Schizophrenia. *Brain Res. Rev.* **2000**, *31*, 130–137. https://doi.org/10.1016/S0165-0173(99)00030-2

(207) Chiang, M.; Natarajan, R.; Fan, X. Vitamin D in Schizophrenia: A Clinical Review. *Evid. Based. Ment. Health* **2016**, *19* (1), 6–9. https://doi.org/10.1136/eb-2015-102117. https://doi.org/10.1136/eb-2015-102117

(208) Fusar-Poli, P.; Tantardini, M.; De Simone, S.; Ramella-Cravaro, V.; Oliver, D.; Kingdon, J.; Kotlicka-Antczak, M.; Valmaggia, L.; Lee, J.; Millan, M. J.; Galderisi, S.; Balottin, U.; Ricca, V.; McGuire, P. Deconstructing Vulnerability for Psychosis: Meta-Analysis of Environmental Risk Factors for Psychosis in Subjects at Ultra High-Risk. *Eur. Psychiatry* **2017**, *40*, 65–75. https://doi.org/10.1016/j.eurpsy.2016.09.003.

(209) Babulas, V.; Factor-Litvak, P.; Goetz, R.; Schaefer, C. A.; Brown, A. S. Prenatal Exposure to Maternal Genital and Reproductive Infections and Adult Schizophrenia. *Am. J. Psychiatry* **2006**, *163* (5), 927–929. https://doi.org/10.1176/ajp.2006.163.5.927.

(210) Eyles, D. W.; Trzaskowski, M.; Vinkhuyzen, A. A. E.; Mattheisen, M.; Meier, S.; Gooch, H.; Anggono, V.; Cui, X.; Tan, M. C.; Burne, T. H. J.; Jang, S. E.; Kvaskoff, D.; Hougaard, D. M.; Nørgaard-Pedersen, B.; Cohen, A.; Agerbo, E.; Pedersen, C. B.; Børglum, A. D.; Mors, O.; Sah, P.; Wray, N. R.; Mortensen, P. B.; McGrath, J. J. The Association between Neonatal Vitamin D Status and Risk of Schizophrenia. *Sci. Rep.* **2018**, *8* (1), 1–8. https://doi.org/10.1038/s41598-018-35418-z.

(211) McCutcheon, R. A.; Abi-Dargham, A.; Howes, O. D. Schizophrenia, Dopamine and the Striatum: From Biology to Symptoms. *Trends Neurosci.* **2019**, *42* (3), 205–220. https://doi.org/10.1016/j.tins.2018.12.004.

(212) Beck, K.; Hindley, G.; Borgan, F.; Ginestet, C.; McCutcheon, R.; Brugger, S.; Driesen, N.; Ranganathan, M.; D'Souza, D. C.; Taylor, M.; Krystal, J. H.; Howes, O. D. Association of Ketamine with Psychiatric Symptoms and Implications for Its Therapeutic Use and for Understanding Schizophrenia: A Systematic Review and Meta-Analysis. *JAMA Netw. Open* **2020**, *3* (5), 1–20. https://doi.org/10.1001/jamanetworkopen.2020.4693.

(213) Marsman, A.; Van Den Heuvel, M. P.; Klomp, D. W. J.; Kahn, R. S.; Luijten, P. R.; Hulshoff Pol, H. E. Glutamate in Schizophrenia: A Focused Review and Meta-Analysis of 1H-MRS Studies. *Schizophr. Bull.* **2013**, *39* (1), 120–129. https://doi.org/10.1093/schbul/sbr069.

(214) Insel, T. R. Rethinking Schizophrenia. *Nature* **2010**, *468* (7321), 187–193. https://doi.org/10.1038/nature09552.

(215) Leucht, S.; Davis, J. M. Which First-Generation Antipsychotics Should Be "Repurposed" for the Treatment of Schizophrenia. *Eur. Arch. Psychiatry Clin. Neurosci.* **2022**, *272* (1), 1–3. https://doi.org/10.1007/s00406-021-01378-1.

(216) Cerveri, G.; Gesi, C.; Mencacci, C. Pharmacological Treatment of Negative Symptoms in Schizophrenia: Update and Proposal of a Clinical Algorithm. *Neuropsychiatr. Dis. Treat.* **2019**, *15*, 1525–1535. https://doi.org/10.2147/NDT.S201726.

(217) Seeman, P. Atypical Antipsychotics: Mechanism of Action. *Can. J. Psychiatry* **2002**, *47* (1), 27–38.

(218) Roerig, J. L.; Steffen, K. J.; Mitchell, J. E. Atypical Antipsychotic-Induced Weight Gain: Insights into Mechanisms of Action. *CNS Drugs* **2011**, *25* (12), 1035–1059. https://doi.org/10.2165/11596300-000000000-00000.

(219) Hirsch, L.; Patten, S. B.; Bresee, L.; Jette, N.; Pringsheim, T. Second-Generation Antipsychotics and Metabolic Side-Effects: Canadian Population-Based Study. *BJPsych Open* **2018**, *4* (4), 256–261. https://doi.org/10.1192/bjo.2018.33.

(220) Townsend, L. K.; Peppler, W. T.; Bush, N. D.; Wright, D. C. Obesity Exacerbates the Acute Metabolic Side Effects of Olanzapine. *Psychoneuroendocrinology* **2018**, *88* (October 2017), 121–128. https://doi.org/10.1016/j.psyneuen.2017.12.004.

(221) Pirmohamed, M.; Park, K. Mechanism of Clozapine-Induced Agranulocytosis. Current Status of Research and Implications for Drug Development. *CNS Drugs* **1997**, *7* (2), 139–158. https://doi.org/10.2165/00023210-199707020-00005.

(222) Klein Herenbrink, C.; Verma, R.; Lim, H. D.; Kopinathan, A.; Keen, A.; Shonberg, J.; Draper-Joyce, C. J.; Scammells, P. J.; Christopoulos, A.; Javitch, J. A.; Capuano, B.; Shi, L.; Lane, J. R. Molecular Determinants of the Intrinsic Efficacy of the Antipsychotic Aripiprazole. *ACS Chem. Biol.* **2019**, *14* (8), 1780–1792. https://doi.org/10.1021/acschembio.9b00342.

(223) Burris, K. D.; Molski, T. F.; Xu, C.; Ryan, E.; Tottori, K.; Kikuchi, T.; Yocca, F. D.; Molinoff, P. B. Aripiprazole, a Novel Antipsychotic, Is a High-Affinity Partial Agonist at Human Dopamine D2 Receptors. *J. Pharmacol. Exp. Ther.* **2002**, *302* (1), 381–389. https://doi.org/10.1124/jpet.102.033175.

(224) Oshiro, Y.; Sato, S.; Kurahashi, N.; Tanaka, T.; Kikuchi, T.; Tottori, K.; Uwahodo, Y.; Nishi, T. Novel Antipsychotic Agents with Dopamine Autoreceptor Agonist Properties: Synthesis and Pharmacology

of 7-[4-84-Phenyl-1-Piperazinyl)Butoxy]-3,4-Dihydro-2(1H)-Quinolinone Derivatives. *J. Med. Chem.* **1998**, *2623* (94), 658–667. https://doi.org/10.1021/jm940608g

(225) Kiss, B.; Horváth, A.; Némethy, Z.; Schmidt, É.; Laszlovszky, I.; Bugovics, G.; Fazekas, K.; Hornok, K.; Orosz, S.; Gyertyán, I.; Ágai-Csongor, É.; Domány, G.; Tihanyi, K.; Adham, N.; Szombathelyi, Z. Cariprazine (RGH-188), a Dopamine D3 Receptor-Preferring, D 3/D2 Dopamine Receptor Antagonist-Partial Agonist Antipsychotic Candidate: In Vitro and Neurochemical Profile. *J. Pharmacol. Exp. Ther.* **2010**, *333* (1), 328–340. https://doi.org/10.1124/jpet.109.160432.

(226) Natesan, S.; Reckless, G. E.; Barlow, K. B. L.; Kapur, S. Partial Agonists in Schizophrenia – Why Some Work and Others Do Not : Insights from Preclinical Animal Models. *Int. J. Neuropsychopharmacol.* **2011**, *11* (14), 1165–1178. https://doi.org/10.1017/S1461145710001343.

(227) Preda, A.; Shapiro, B. B. A Safety Evaluation of Aripiprazole in the Treatment of Schizophrenia. *Expert Opin. Drug Saf.* **2020**, *19* (12), 1529–1538. https://doi.org/10.1080/14740338.2020.1832990.

(228) Goff, D. C. Brexpiprazole: A New Antipsychotic Following in the Footsteps of Aripiprazole. *Am. J. Psychiatry* **2015**, *172* (9), 820–821. https://doi.org/10.1176/appi.ajp.2015.15060741.

(229) Frankel, J. S.; Schwartz, T. L. Brexpiprazole and Cariprazine: Distinguishing Two New Atypical Antipsychotics from the Original Dopamine Stabilizer Aripiprazole. *Ther. Adv. Psychopharmacol.* **2017**, *7* (1), 29–41. https://doi.org/10.1177/2045125316672136.

(230) Stahl, S. M. Mechanism of Action of Brexpiprazole: Comparison with Aripiprazole. *CNS Spectr.* **2016**, *21* (1), 1–6. https://doi.org/10.1017/S1092852915000954.

(231) Kikuchi, T.; Maeda, K.; Suzuki, M.; Hirose, T.; Futamura, T.; McQuade, R. D. Discovery Research and Development History of the Dopamine D2 Receptor Partial Agonists, Aripiprazole and Brexpiprazole. *Neuropsychopharmacol. Reports* **2021**, *41* (2), 134–143. https://doi.org/10.1002/npr2.12180.

(232) Girgis, R. R.; Slifstein, M.; Souza, D. D.; Lee, Y.; Periclou, A.; Ghahramani, P.; Laszlovszky, I.; Durgam, S.; Kiss, B.; Kapás, M.; Abi-dargham, A.; Rakhit, A. Preferential Binding to Dopamine D3 over D2 Receptors by Cariprazine in Patients with Schizophrenia Using PET with the D3/D2 Receptor Ligand [11C]-(+)-PHNO. *Psychopharmacology (Berl).* **2016**, *233* (3), 3503–3512. https://doi.org/10.1007/s00213-016-4382-y.

(233) Tarzian, M.; Ndrio, M.; Kaja, S.; Beason, E.; Fakoya, A. O. Cariprazine for Treating Schizophrenia, Mania, Bipolar Depression, and Unipolar Depression: A Review of Its Efficacy. *Cureus* **2023**, *15* (5), 1–16. https://doi.org/10.7759/cureus.39309.

(234) Garnock-Jones, K. P. Cariprazine: A Review in Schizophrenia. *CNS Drugs* **2017**, *31* (6), 513–525. https://doi.org/10.1007/s40263-017-0442-z.

(235) Campbell, R. H.; Diduch, M.; Gardner, K. N.; Thomas, C. Review of Cariprazine in Management of Psychiatric Illness. *Ment. Heal. Clin.* **2017**, *7* (5), 221–229. https://doi.org/10.9740/mhc.2017.09.221.

(236) Durgam, S.; Earley, W.; Li, R.; Li, D.; Lu, K.; Laszlovszky, I.; Fleischhacker, W. W.; Nasrallah, H. A. Long-Term Cariprazine Treatment for the Prevention of Relapse in Patients with Schizophrenia : A Randomized, Double-Blind, Placebo-Controlled Trial. *Schizophr. Res.* **2016**, *176* (3), 264–271. https://doi.org/10.1016/j.schres.2016.06.030.

(237) Laszlovszky, I.; Barabássy, Á.; Németh, G. Cariprazine, A Broad-Spectrum Antipsychotic for the Treatment of Schizophrenia: Pharmacology, Efficacy, and Safety. *Adv. Ther.* **2021**, *38* (7), 3652–3673. https://doi.org/10.1007/s12325-021-01797-5.

(238) Patel, K. R.; Cherian, J.; Gohil, K.; Atkinson, D. Schizophrenia: Overview and Treatment Options. *P T* **2014**, *39* (9), 638–645. https://pubmed.ncbi.nlm.nih.gov/25210417/

(239) Stank, L.; Frank, A.; Hagenow, S.; Stark, H. Talipexole Variations as Novel Bitopic Dopamine D2 and D3receptor Ligands. *Medchemcomm* **2019**, *10* (11), 1926–1929. https://doi.org/10.1039/c9md00379g.

(240) Biswas, S.; Hazeldine, S.; Ghosh, B.; Parrington, I.; Kuzhikandathil, E.; Reith, M. E. A.; Dutta, A. K. Bioisosteric Heterocyclic Versions of 7-{[2-(4-Phenyl-Piperazin-1-Yl)Ethyl] Propylamino}-5,6,7,8-Tetrahydronaphthalen-2-Ol: Identification of Highly Potent and Selective Agonists for Dopamine D3 Receptor with Potent in Vivo Activity. *J. Med. Chem.* **2008**, *51* (10), 3005–3019. https://doi.org/10.1021/jm701524h.

(241) Schübler, M.; Sadek, B.; Kottke, T.; Weizel, L.; Stark, H. Synthesis, Molecular Properties Estimations, and Dual Dopamine D2 and D3 Receptor Activities of Benzothiazole-Based Ligands. *Front. Chem.* **2017**, *5* (September), 1–19. https://doi.org/10.3389/fchem.2017.00064.

(242) da Silva Cunha, T. T.; Silva, R. R.; Rodrigues, D. A.; de Sena Murteira Pinheiro, P.; Kronenberger, T.; Sant'Anna, C. M. R.; Noël, F.; Fraga, C. A. M. Design, Synthesis and Pharmacological Evaluation of Novel Conformationally Restricted N-Arylpiperazine Derivatives Characterized as D2/D3 Receptor Ligands, Candidates for the Treatment of Neurodegenerative Diseases. *Biomolecules* **2022**, *12* (8), 1112. https://doi.org/10.3390/biom12081112.

(243) Khatik, G. L.; Kaur, J.; Kumar, V.; Tikoo, K.; Nair, V. A. 1,2,4-Oxadiazoles: A New Class of Anti-Prostate Cancer Agents. *Bioorganic Med. Chem. Lett.* **2012**, *22* (5), 1912–1916. https://doi.org/10.1016/j.bmcl.2012.01.059.

(244) Sakairi, M.; Kogami, M.; Torii, M.; Kataoka, H.; Fujieda, H.; Makino, M.; Kataoka, D.; Okamoto, R.; Miyazawa, T.; Okabe, M.; Inoue, M.; Takahashi, N.; Harada, S.; Watanabe, N. Synthesis and SAR Studies of Bicyclic Amine Series GPR119 Agonists. *Bioorganic Med. Chem. Lett.* **2012**, *22* (15), 5123–5128. https://doi.org/10.1016/j.bmcl.2012.05.117.

(245) Mukherjee, A.; Jayaraman, N. 2,3-Unsaturated Enoses. A Pummerer Rearrangement Route to Sugar

Vinyl Sulfides and Synthesis of 3-Deoxy-3-Alkyl/Arylsulfinyl Pyranosides. *Tetrahedron* **2012**, *68* (42), 8746–8752. https://doi.org/10.1016/j.tet.2012.08.011.

(246) Kim, C.; Traylor, T. G.; Perrin, C. L. MCPBA Epoxidation of Alkenes: Reinvestigation of Correlation between Rate and Ionization Potential. *J. Am. Chem. Soc.* **1998**, *120* (37), 9513–9516. https://doi.org/10.1021/ja981531e.

(247) Kishikawa, K.; Naruse, M.; Kohmoto, S.; Yamamoto, M.; Yamaguchi, K. Investigation of Arene-Arene Interaction in Stereoselective MCPBA Epoxidation. *J. Chem. Soc.* **2001**, No. 4, 462–468. https://doi.org/10.1039/b004098n.

(248) Mello, R.; Alcalde-Aragones, A.; Gonzalez Nunez, M. E.; Asensio, G. Epoxidation of Olefins with a Silica-Supported Peracid. *J. Org. Chem.* **2012**,77, 6409–6413. https://doi.org/10.1021/jo300533b

(249) Sandaroos, R.; Goldani, M. T.; Damavandi, S.; Mohammadi, A. Efficient Asymmetric Baeyer – Villiger Oxidation of Prochiral Cyclobutanones Using New Polymer-Supported and Unsupported Chiral Co (Salen) Complexes. *Indian Acad. Sci.* **2012**, *124* (4), 871–876. https://doi.org/10.1007/s12039-012-0277-6

(250) Krow, G. R. The Baeyer-Villiger Oxidation of Ketones and Aldehydes. In *Organic Reactions*; 1993; 43, 251–310. https://doi.org/10.1002/0471264180.or043.03

(251) Penkett, C. S.; Simpson, I. D. Oxidative Rearrangements of Bicyclic 2-Alkenyl Aziridines. *Tetrahedron Lett.* **2001**, *42* (11), 3029–3032. https://doi.org/10.1016/S0040-4039(01)00362-8

(252) Cope, A. C.; Foster, T. T.; Towle, P. H. Thermal Decomposition of Amine Oxides to Olefins and Dialkylhydroxylamines. *J. Am. Chem. Soc.* **1949**, *71*, 3929–3934. https://foi.org/10.1021/JA01180A014

(253) O´Neil, I. A.; Cleator, E.; Tapolczay, D. J. A Convenient Synthesis of Secondary Hydroxylamines. *Tetrahedron Lett.* **2001**, *42* (8), 8247–8249. https://doi.org/10.1016/S0040-4039(01)01745-2

(254) Fraser, S.; Mikhail, A. A. Synthesis of 1-Hydroxy-L-Proline and Related Cyclic N-Hydroxyamino Acids. Metabolic Disposition of 14C-Labeled 1-Hydroxy-L-Proline in Rodents. *J. Med. Chem.* **1972**, *15* (5), 483–486. https://doi.org/10.1021/jm00275a011

(255) Rubottom, G. M.; Vazquez, M. A.; Pelegrina, D. R. Peracid Oxidation of Trimethylsilyl Enol Ethers: A Facile Alpha-Hydroxylation Procedure. *Tetrahedron Lett.* **1974**, *49*, 4319–4322.

(256) Rubottom, G. M.; Gruber, J. M. M-Chloroperbenzoic Acid Oxidation of 2-Trimethylsilyloxy-1,3-Dienes. Synthesis of Alpha-Hydroxy and Alpha-Acetoxy Enones. *J. Org. Chem.* **1978**, *43* (8), 1599–1602. https://doi.org/10.1016/S0040-4039(01)92153-7

(257) Hussain, H.; Al-Harrasi, A.; Green, I. R.; Ahmed, I.; Abbas, G.; Rehman, N. U. Meta-Chloroperbenzoic Acid (MCPBA): A Versatile Reagent in Organic Synthesis. *RSC Adv.* **2014**, *4* (25), 12882–12917.

https://doi.org/10.1039/c3ra45702h.

(258) Clayden, J.; Greeves, N.; Warren, S. *Organic Chemistry*, 2nd Editio.; 2012; Vol. 7.

(259) Griffin, R. J.; Henderson, A.; Curtin, N. J.; Echalier, A.; Endicott, J. A.; Hardcastle, I. R.; Newell, D. R.; Noble, M. E. M.; Wang, L. Z.; Golding, B. T. Searching for Cyclin-Dependent Kinase Inhibitors Using a New Variant of the Cope Elimination. *J. Am. Chem. Soc.* **2006**, *128* (18), 6012–6013. https://doi.org/10.1021/ja060595j.

(260) Horner, L.; Hoffmann, H.; Wippel, H. G. Phosphinoxyde Als Olefinierungsreagenzien. *Chem. Ber.* **1958**, 61–63. https://doi.org/10.1002/cber.19580910113

(261) Horner, L.; Hoffmann, H.; Wippel, H. G.; Klahre, G. Phosphinoxyde Als Olefinierungsreagenzien. *Chem. Ber.* **1959**, *92*, 2499–2505. https://doi.org/10.1002/cber.19580910113

(262) Wadsworth, W. S.; Emmons, W. D. The Utility of Phosphonate Carbanions in Olefin Synthesis. *J. Am. Chem. Soc.* **1961**, *83* (7), 1731–1736. https://doi.org/10.1021/ja01468a042

(263) Kobayashi, K.; Iii, K. T.; Kogen, H. Recent Topics of the Natural Product Synthesis by Horner – Wadsworth – Emmons Reaction. *Tetrahedron Lett.* **2018**, *59*, 568–582. https://doi.org/10.1016/j.tetlet.2017.12.076.

(264) Castro, F. . J.; Meyer, G.; Zampieri, G. Effects of Sulfur Poisoning on Hydrogen Desorption from Palladium. *J. Alloys Compd.* **2002**, *332*, 612–616. https://doi.org/10.1016/S0925-8388(01)01626-7

(265) Xiong, R.; Ren, W.; Wang, Z.; Zhang, M. Triphenylphosphine as Efficient Antidote for the Sulfur-Poisoning of the Pd / C Hydrogenation Catalyst. *ChemCatChem* **2021**, *13*, 548–552. https://doi.org/10.1002/cctc.202001537.

(266) Yin, B. L.; Cai, C. B.; Lai, J. Q.; Zhang, Z. R.; Huang, L.; Xu, L. W.; Jiang, H. F. Sodium Borohydride-Nickel Chloride-Methanol Catalytic System for Regioselective Reduction of Electron-Rich Conjugated Dienes and Reductive Cleavage of Allyl Esters Involving π-Allylnickel Intermediates. *Adv. Synth. Catal.* **2011**, *353* (18), 3319–3324. https://doi.org/10.1002/adsc.201100612.

(267) Jacobi, P. A.; Lee, K. Total Syntheses of (+) and (-) Stemoamide. *J. Am. Chem. Soc.* **2000**, *122* (2), 4295–4303. https://doi.org/10.1021/ja994214w

(268) Watanabe, S.; Ikishima, S.; Matsuo, T. A Luminescent Metalloreceptor Exhibiting Remarkably High Selectivity for Mg 2 + over Ca 2 +. *J. Am. Chem. Soc.* **2001**, *123* (12), 8402–8403. https://doi.org/10.1021/ja010931q

(269) Venkatesan, A. M.; Davis, J. M.; Grosu, G. T.; Baker, J.; Zask, A.; Levin, J. I.; Ellingboe, J.; Skotnicki, J. S.; DiJoseph, J. F.; Sung, A.; Jin, G.; Xu, W.; McCarthy, D. J.; Barone, D. Synthesis and Structure-Activity Relationships of 4-Alkynyloxy Phenyl Sulfanyl, Sulfinyl, and Sulfonyl Alkyl Hydroxamates as Tumor Necrosis Factor-α Converting Enzyme and Matrix Metalloproteinase Inhibitors. *J. Med.*

Chem. **2004**, *47* (25), 6255–6269. https://doi.org/10.1021/jm040086x.

(270) Bandgar, B. P.; Nikat, S. M.; Wadgaonkar, P. P. The Reduction of Aromatic Oximes to Amines with Borohydride Exchange Resin-Nickel Acetate System. *Synth. Commun.* **2006**, *25* (6), 863–869. https://doi.org/10.1080/00397919508013422.

(271) Setamdideh, D.; Khezri, B.; Mollapour, M. Convenient Reduction of Nitro Compounds to Their Corresponding Amines with Promotion of NaBH4/ Ni(OAc)2.4H2O System in Wet CH3CN. *Orient. J. Chem.* **2011**, *27* (3), 991–996. https://www.proquest.com/scholarly-journals/convenient-reduction-nitro-compounds-their/docview/2122000348/se-2

(272) Demir, A. S.; Akhmedov, I. M.; Sesenoglu, Ö. Transition Metal Compound Mediated Reduction of Alpha-Amino Acids to 1,2-Amino Alcohols with NaBH4 in Water Transition Metal Compound Mediated Reduction of α-Amino Acids to 1,2-Amino Alcohols with NaBH4 in Water. *Turkish J. Chem.* **1999**, *23* (2), 1–5. https://journals.tubitak.gov.tr/chem/vol23/iss2/2?utm_source=journals.

(273) Appel, R. Tertiary Phosphane/Tetrachloromethane, a Versatile Reagent for Chlorination, Dehydration, and P-N Linkage. *Angew. Chemie - Int. Ed.* **1975**, *14* (12), 801–811. https://doi.org/10.1002/anie.197508011

(274) Finkelstein, H. Darstellung Organischer Jodideaus Entsprechenden Bromiden Und Chloriden. *Chem. Ber.* **1910**, *43* (2), 1528–1532. https://doi.org/10.1002/cber.19100430257

(275) Tang, W.; Zhao, J.; Jiang, P.; Xu, X.; Zhao, S.; Tong, Z. Solvent Effects on the Symmetric and Asymmetric SN2 Reactions in the Acetonitrile Solution: A Reaction Density Functional Theory Study. *J. Phys. Chem.* **2020**, *124*, 3114–3122. https://doi.org/10.1021/acs.jpcb.0c00607.

(276) Chen, J.; Lin, J. H.; Xiao, J. C. Halogenation through Deoxygenation of Alcohols and Aldehydes. *Org. Lett.* **2018**, *20* (10), 3061–3064. https://doi.org/10.1021/acs.orglett.8b01058.

(277) Doyle, M. P.; Dellaria, J. F.; Siegfried, B.; Bishop, S. W. Reductive Deamination of Arylamines by Alkyl Nitrites in N,N-Dimethylformamide. A Direct Conversion of Arylamines to Aromatic Hydrocarbons. *J. Org. Chem.* **1977**, *42* (22), 3494–3498. https://doi.org/10.1021/jo00442a009.

(278) Röder, L.; Nicholls, A. J.; Baxendale, I. R. Flow Hydrodediazoniation of Aromatic Heterocycles. *Molecules* **2019**, *24* (10), 1–18. https://doi.org/10.3390/molecules24101996.

(279) Mock, W. L.; Tsay, J. T. Sulfoximine and Sulfodiimine Transition-State Analogue Inhibitors for Carboxypeptidase A. *J. Am. Chem. Soc.* **1989**, *111* (12), 4467–4472. https://doi.org/10.1021/ja00194a049.

(280) Lücking, U. Sulfoximines: A Neglected Opportunity in Medicinal Chemistry. *Angew. Chemie - Int. Ed.* **2013**, *52* (36), 9399–9408. https://doi.org/10.1002/anie.201302209.

(281) Mäder, P.; Kattner, L. Sulfoximines as Rising Stars in Modern Drug Discovery? Current Status and

Perspective on an Emerging Functional Group in Medicinal Chemistry. *J. Med. Chem.* **2020**, *63* (23), 14243–14275. https://doi.org/10.1021/acs.jmedchem.0c00960.

(282) Gais, H.; Miiller, H.; Bund, J.; Scommoda, M.; Brandt, J.; Raabe, G. Regio and Enantioselectove Substitution of Primary Endocyclilc Allylic Sulfoximines with Organocopper and Organocuprate Reagents. The Importance of Iodided for the Allylic Substitution with Organocopper Compounds. *J. Am. Chem. Soc.* **1995**, *117* (9), 2453–2466. https://doi.org/10.1002/(SICI)1099-0690(199807)1998:7<1319::AID-EJOC1319>3.0.CO;2-L

(283) Frings, M.; Thomé, I.; Bolm, C. Synthesis of Chiral Sulfoximine-Based Thioureas and Their Application in Asymmetric Organocatalysis. *Beilstein J. Org. Chem.* **2012**, *8*, 1443–1451. https://doi.org/10.3762/bjoc.8.164.

(284) Reggelin, M.; Zur, C. Sulfoximines: Structures, Properties and Synthetic Applications. *Synthesis (Stuttg).* **2000**, *6* (1), 1–64. https://doi.org/10.1055/s-2000-6217.

(285) Branca, J. C.; Vanier, N. R.; Bordwell, F. G.; Johnson, C. R. Acidities of Sulfoximines and Related Oxosulfonium Cations. Cyclopropyl Effects and Structures of α-Sulfonyl-Type Carbanions. *J. Org. Chem.* **1980**, *45* (19), 3884–3889. https://doi.org/10.1021/jo01307a030.

(286) Zheng, W.; Chen, X.; Chen, F.; He, Z.; Zeng, Q. Syntheses and Transformations of Sulfoximines. *Chem. Rec.* **2020**, 1–22. https://doi.org/10.1002/tcr.202000134.

(287) Lücking, U.; Jautelat, R.; Krüger, M.; Brumby, T.; Lienau, P.; Schäfer, M.; Briem, H.; Schulze, J.; Hillisch, A.; Reichel, A.; Wengner, A. M.; Siemeister, G. The Lab Oddity Prevails: Discovery of Pan-CDK Inhibitor (R)-S-Cyclopropyl-S-(4-{[4-{[(1R,2R)-2-Hydroxy-1-Methylpropyl]Oxy}-5-(Trifluoromethyl)Pyrimidin-2-Yl]Amino}phenyl)Sulfoximide (BAY1000394) for the Treatment of Cancer. *ChemMedChem* **2013**, *8* (7), 1067–1085. https://doi.org/10.1002/cmdc.201300096.

(288) Lücking, U.; Scholz, A.; Lienau, P.; Siemeister, G.; Kosemund, D.; Bohlmann, R.; Briem, H.; Terebesi, I.; Meyer, K.; Prelle, K.; Denner, K.; Bömer, U.; Schäfer, M.; Eis, K.; Valencia, R.; Ince, S.; von Nussbaum, F.; Mumberg, D.; Ziegelbauer, K.; Klebl, B.; Choidas, A.; Nussbaumer, P.; Baumann, M.; Schultz-Fademrecht, C.; Rühter, G.; Eickhoff, J.; Brands, M. Identification of Atuveciclib (BAY 1143572), the First Highly Selective, Clinical PTEFb/CDK9 Inhibitor for the Treatment of Cancer. *ChemMedChem* **2017**, *12* (21), 1776–1793. https://doi.org/10.1002/cmdc.201700447.

(289) Sirvent, J. A.; Lücking, U. Novel Pieces for the Emerging Picture of Sulfoximines in Drug Discovery: Synthesis and Evaluation of Sulfoximine Analogues of Marketed Drugs and Advanced Clinical Candidates. *ChemMedChem* **2017**, *12* (7), 487–501. https://doi.org/10.1002/cmdc.201700044.

(290) Lücking, U. Neglected Sulfur(vi) Pharmacophores in Drug Discovery: Exploration of Novel Chemical Space by the Interplay of Drug Design and Method Development. *Org. Chem. Front.* **2019**, *6* (8), 1319–1324. https://doi.org/10.1039/c8qo01233d.

(291) Lücking, U. New Opportunities for the Utilization of the Sulfoximine Group in Medicinal Chemistry from the Drug Designer ' s Perspective. *Chem. Eur. J.* **2022**, *28* (56), 1–13. https://doi.org/10.1002/chem.202201993.

(292) Zhu, Y.; Loso, M. R.; Watson, G. B.; Sparks, T. C.; Rogers, R. B.; Huang, J. X.; Gerwick, B. C.; Babcock, J. M.; Kelley, D.; Hegde, V. B.; Nugent, B. M.; Renga, J. M.; Denholm, I.; Gorman, K.; Deboer, G. J.; Hasler, J.; Meade, T.; Thomas, J. D. Discovery and Characterization of Sulfoxaflor, a Novel Insecticide Targeting Sap-Feeding Pests. *J. Agric. Food Chem.* **2011**, *59* (7), 2950–2957. https://doi.org/10.1021/jf102765x.

(293) Foote, K. M.; Nissink, J. W. M.; McGuire, T.; Turner, P.; Guichard, S.; Yates, J. W. T.; Lau, A.; Blades, K.; Heathcote, D.; Odedra, R.; Wilkinson, G.; Wilson, Z.; Wood, C. M.; Jewsbury, P. J. Discovery and Characterization of AZD6738, a Potent Inhibitor of Ataxia Telangiectasia Mutated and Rad3 Related (ATR) Kinase with Application as an Anticancer Agent. *J. Med. Chem.* **2018**, *61* (22), 9889–9907. https://doi.org/10.1021/acs.jmedchem.8b01187.

(294) Boulard, E.; Zibulski, V.; Oertel, L.; Lienau, P.; Schäfer, M.; Ganzer, U.; Lücking, U. Increasing Complexity: A Practical Synthetic Approach to Three-Dimensional, Cyclic Sulfoximines and First Insights into Their in Vitro Properties. *Chem. - A Eur. J.* **2020**, *26* (19), 4378–4388. https://doi.org/10.1002/chem.201905461.

(295) Bentley, H. R.; McDermott, E. E.; Pace, J.; Whitehead, J. K.; Moran, T. Action of Nitrogen Trichloride (Agene) on Proteins: Isolation of Crystalline Toxic Factor. *Nature* **1949**, *164*, 438–439. https://doi.org/10.1038/164438a0

(296) Bentley, H. R.; McDermott, E. E.; Whitehead, J. K. Action of Nitrogen Trichloride on Proteins: A Synthsis of the Toxic Factor from Methionine. *Nature* **1950**, *307* (4201), 735. https://doi.org/10.1038/165735b0

(297) Manning, J. M.; Moore, S.; Rowe, W. B.; Meister, A. Identification of L-Methionine s-Sulfoximine as the Diastereoisomer of L-Methionine Sr-Sulfoximine That Inhibits Glutamine Synthetase. *Biochemistry* **1969**, *8* (6), 2681–2685. https://doi.org/10.1021/bi00834a066

(298) Richman, P. G.; Orlowski, M.; Meister, A. Inhibition of γ Glutamylcysteine Synthetase by L Methionine S Sulfoximine. *J. Biol. Chem.* **1973**, *248* (19), 6684–6690. https://doi.org/10.1016/s0021-9258(19)43407-8. https://doi.org/10.1016/S0021-9258(19)43407-8

(299) Hernández-Breijo, B.; Monserrat, J.; Ramírez-Rubio, S.; Cuevas, E. P.; Vara, D.; Díaz-Laviada, I.; Fernández-Moreno, M. D.; Román, I. D.; Gisbert, J. P.; Guijarro, L. G. Preclinical Evaluation of Azathioprine plus Buthionine Sulfoximine in the Treatment of Human Hepatocarcinoma and Colon Carcinoma. *World J. Gastroenterol.* **2011**, *17* (34), 3899–3911. https://doi.org/10.3748/wjg.v17.i34.3899.

(300) Jeannoda, V. R. L.; Valisolalao, J.; Creppy, E. E.; Dirheimer, G. Identification of the Toxic Principle of Cnestis Glabra as Methionine Sulphoximine. *Phytochemistry* **1985**, *24* (4), 854–855. https://doi.org/10.1016/S0031-9422(00)84907-9

(301) Murakoshi, I.; Sekine, T.; Maeshima, K.; Ikegami, F.; Yoshinaga, K.; Fujii, Y.; Okonogi, S. Absolute Configuration of L-Methionine Sulfoximine as a Toxic Principle in Cnestis Palata. *Chem. Pharm. Bull.* **1993**, *41* (2), 388–390. https://doi.org/10.1248/cpb.41.388

(302) Okamura, H.; Bolm, C. Rhodium-Catalyzed Imination of Sulfoxides and Sulfides: Efficient Preparation of N-Unsubstituted Sulfoximines and Sulfilimines. *Org. Lett.* **2004**, *6* (8), 1305–1307. https://doi.org/10.1021/ol049715n.

(303) Dauban, P.; Dodd, R. H. Iminoiodanes and C-N Bond Formation in Organic Synthesis. *Synlett* **2003**, No. 11, 1571–1586. https://doi.org/10.1055/s-2003-41010.

(304) Zhdankin, V. V. *Hypervalent Iodine Chemistry*; 2013. https://doi.org/10.1002/9781118341155.

(305) Han, Y.; Xing, K.; Zhang, J.; Tong, T.; Shi, Y.; Cao, H.; Yu, H.; Zhang, Y.; Liu, D.; Zhao, L. Application of Sulfoximines in Medicinal Chemistry from 2013 to 2020. *Eur. J. Med. Chem.* **2021**, *209* (7), 112885. https://doi.org/10.1016/j.ejmech.2020.112885.

(306) Andresini, M.; Tota, A.; Degennaro, L.; Bull, J. A. Synthesis and Transformations of NH-Sulfoximines. *Chem. Eur. J.* **2021**, *27*, 17293–17321. https://doi.org/10.1002/chem.202102619.

(307) Zhou, T.; Qian, P. F.; Li, J. Y.; Zhou, Y. B.; Li, H. C.; Chen, H. Y.; Shi, B. F. Efficient Synthesis of Sulfur-Stereogenic Sulfoximines via Ru(II)-Catalyzed Enantioselective C-H Functionalization Enabled by Chiral Carboxylic Acid. *J. Am. Chem. Soc.* **2021**, *143* (18), 6810–6816. https://doi.org/10.1021/jacs.1c03111.

(308) Tota, A.; Zenzola, M.; Chawner, S. J.; John-Campbell, S. S.; Carlucci, C.; Romanazzi, G.; Degennaro, L.; Bull, J. A.; Luisi, R. Synthesis of NH-Sulfoximines from Sulfides by Chemoselective One-Pot N- and O-Transfers. *Chem. Commun.* **2017**, *53* (2), 348–351. https://doi.org/10.1039/c6cc08891k.

(309) Zenzola, M.; Doran, R.; Degennaro, L.; Luisi, R.; Bull, J. A. Transfer of Electrophilic NH Using Convenient Sources of Ammonia: Direct Synthesis of NH Sulfoximines from Sulfoxides. *Angew. Chemie - Int. Ed.* **2016**, *55* (25), 7203–7207. https://doi.org/10.1002/anie.201602320.

(310) Zenzola, M.; Doran, R.; Luisi, R.; Bull, J. A. Synthesis of Sulfoximine Carbamates by Rhodium-Catalyzed Nitrene Transfer of Carbamates to Sulfoxides. *J. Org. Chem.* **2015**, *80* (12), 6391–6399. https://doi.org/10.1021/acs.joc.5b00844.

(311) Miao, J.; Richards, N. G. J.; Ge, H. Rhodium-Catalyzed Direct Synthesis of Unprotected NH-Sulfoximines from Sulfoxides. *Chem. Commun.* **2014**, *50* (68), 9687–9689. https://doi.org/10.1039/c4cc04349a.

(312) Bull, J. A.; Degennaro, L.; Luisi, R. Straightforward Strategies for the Preparation of NH-Sulfox-Imines: A Serendipitous Story. *Synlett* **2017**, *28* (19), 2525–2538. https://doi.org/10.1055/s-0036-1590874.

(313) Briggs, E. L.; Tota, A.; Colella, M.; Degennaro, L.; Luisi, R.; Bull, J. A. Synthesis of Sulfonimidamides from Sulfenamides via an Alkoxy-Amino-Λ6-Sulfanenitrile Intermediate. *Angew. Chemie - Int. Ed.* **2019**, *58* (40), 14303–14310. https://doi.org/10.1002/anie.201906001.

(314) Stoss, P.; Satzinger, G. 3-Oxo-Benzo[d]Isothiazol-1-Oxide. *Angew. Chemie - Int. Ed.* **1970**, *83* (2), 83–84. https://doi.org/10.1002/ange.19710830209

(315) Rynbrandt, R. H.; Balgoyen, D. P. Synthesis and Thermal Decomposition of 1-Methyl-1H,3H-1,2-Benzisothiazole 1-Oxide Hydrochloride. *J. Org. Chem.* **1978**, *43* (9), 1824–1825. https://doi.org/10.1021/jo00403a049

(316) Tamura, Y.; Minamikawa, J.; Sumoto, K.; Fujii, S.; Ikeda, M. Synthesis and Some Properties of O-Acyl and O-Nitrophenylhydroxylamines. *J. Org. Chem.* **1973**, *38* (6), 1239–1241. https://doi.org/10.1021/jo00946a045

(317) Johnson, C. R.; Kirchhoff, R. A.; Corkins, G. H. Synthesis of Optically Active Sulfoximines from Optically Active Sulfoxides. *J. Org. Chem.* **1974**, *39* (16), 2458–2459. https://doi.org/10.1021/jo00930a044

(318) Glass, R.; Reineke, K.; Shanklin, M. Diels-Alder Reactions of S Vinyl-S-Arylsulfoximines. *J. Org. Chem.* **1984**, *4* (9), 1527–1533. https://doi.org/10.1021/jo00183a010

(319) Tanaka, R.; Kuniaki, Y. Nucleophilic Attack on Chloro(Phenyl)Ethyne by Azide Ion. *J. Chem. Soc. Chem. Commun.* **1983**, 7, 329–330.https://doi.org/10.1039/C39830000329

(320) Bach, T.; Körber, C. Iron (Mediated Nitrene Transfer from t-Butyloxycarbonyl Azide (BocN3) to Sulfoxides , Sulfides , and Ketene Acetals. *Tetrahedron Lett.* **1998**, *39* (4), 5015–5016. https://doi.org/10.1016/S0040-4039(98)00927-7

(321) Müller, J. F. K.; Vogt, P. Cu(I)-Catalyzed Sulfoximination. *Tetrahedron Lett.* **1998**, *39*, 4805–4806. https://doi.org/10.1016/S0040-4039(98)00925-3

(322) Bach, T.; Körber, C. Fe (II) -Catalyzed Imidation of Allyl Sulfides and Subsequent [2 , 3] -Sigmatropic Rearrangement . Preparation of r -Branched N - Tert -Butyloxycarbonyl (Boc) -Protected N -Allylamines. *J. Org. Chem.* **2000**, *65* (8), 2358–2367. https://doi.org/10.1021/jo991569p

(323) Cren, S.; Kinahan, T. C.; Skinner, C. L.; Tye, H. A Study of the Functional Group Compatibility of Sulfoximination Methods. *Tetrahedron Lett.* **2002**, *43* (2), 2749–2751. https://doi.org/10.1016/S0040-4039(02)00378-7

(324) Tomooka, C. S.; Carreira, E. M. Enantioselective Nitrogen Transfer to Sulfides from Nitridomanganese

(V) Complexes. *Helv. Chim. Acta* **2002**, *85*, 3773–3784.https://doi.org/10.1002/1522-2675(200211)85:11<3773::AID-HLCA3773>3.0.CO;2-O

(325) Tamura, Y.; Uchida, T.; Katsuki, T. Highly Enantioselective (OC) Ru(Salen)-Catalyzed Sulfimidation Using N-Alkoxycarbonyl Azide as Nitrene Precursor. *Tetrahedron Lett.* **2003**, *44*, 3301–3303. https://doi.org/10.1016/S0040-4039(03)00609-9

(326) Södergren, M. J.; Alonso, D. A.; Bedekar, A. V; Andersson, P. G. Preparation and Evaluation of Nitrene Precursors (PhI=NSO2Ar) for the Copper-Catalyzed Aziridination of Olefins. *Tetrahedron Lett.* **1997**, *38* (39), 6897–6900. https://doi.org/10.1016/S0040-4039(97)01589-X

(327) Reith, S.; Demeshko, S.; Battistella, B.; Reckziegel, A.; Schneider, C.; Stoy, A.; Lichtenberg, C.; Meyer, F.; Munz, D.; Werncke, G. Between Imide, Imidyl and Nitrene- an Imido Iron Complex in Two Oxidation States. *Chem. Sci.* **2022**, *13*, 7907–7913. https://doi.org/10.1039/d2sc01088g.

(328) Abdel-Magid, A. F.; Carson, K. G.; Harris, B. D.; Maryanoff, C. A.; Shah, R. D. Reductive Amination of Aldehydes and Ketones with Sodium Triacetoxyborohydride. Studies on Direct and Indirect Reductive Amination Procedures. *J. Org. Chem.* **1996**, *61* (11), 3849–3862. https://doi.org/10.1021/jo960057x.

(329) Mirza-Aghayan, M.; Tavana, M. M.; Rahimifard, M.; Boukherroub, R. Palladium on Activated Carbon Catalyzed Reductive Amination of Aldehydes and Ketones by Triethylsilane. *Appl. Organomet. Chem.* **2014**, *28* (2), 113–115. https://doi.org/10.1002/aoc.3090.

(330) Sanders, M. L.; Donkor, I. O. A Novel Series of Urea-Based Peptidomimetic Calpain Inhibitors. *Bioorganic Med. Chem. Lett.* **2006**, *16* (7), 1965–1968. https://doi.org/10.1016/j.bmcl.2005.12.068.

(331) Shokrolahi, A.; Zali, A.; Keshavarz, M. H. Reductive Amination of Aldehydes and Ketones by NaBH 4 Using Carbon-Based Solid Acid (CBSA) as Catalyst. *Green Chem. Lett. Rev.* **2011**, *4* (3), 195–203. https://doi.org/10.1080/17518253.2010.528051.

(332) de Sena M. Pinheiro, P.; Rodrigues, D. A.; do Couto Maia, R.; Thota, S.; Fraga, C. A. M. The Use of Conformational Restriction in Medicinal Chemistry. *Curr. Top. Med. Chem.* **2019**, *19* (19), 1712–1733. https://doi.org/10.2174/1568026619666190712205025.

(333) Kumari, S.; Carmona, A. V.; Tiwari, A. K.; Trippier, P. C. Amide Bond Bioisosteres: Strategies, Synthesis, and Successes. *J. Med. Chem.* **2020**, *63* (21), 12290–12358. https://doi.org/10.1021/acs.jmedchem.0c00530.

(334) Heravi, M. M.; Ghavidel, M.; Mohammadkhani, L. Beyond a Solvent: Triple Roles of Dimethylformamide in Organic Chemistry. *RSC Adv.* **2018**, *8* (49), 27832–27862. https://doi.org/10.1039/c8ra04985h.

(335) Pearson, R. G. Hard and Soft Acids and Bases. *J. Am. Chem. Soc.* **1963**, *85* (22), 3533–3539.

https://doi.org/10.1021/ja00905a001.

(336) Méndez, F.; Romero, M. de L.; De Proft, F.; Geerlings, P. The Basicity of p -Substituted Phenolates and the Elimination−Substitution Ratio in p -Nitrophenethyl Bromide: A HSAB Theoretical Study. *J. Org. Chem.* **1998**, *63* (17), 5774–5778. https://doi.org/10.1021/jo972212t.

(337) Rana, K. K.; Rana, S. Microwave Reactors: A Brief Review on Its Fundamental Aspects and Applications. *OALib* **2014**, *01* (06), 1–20. https://doi.org/10.4236/oalib.1100686.

(338) Gaba, M.; Dhingra, N. Microwave Chemistry: General Features and Applications. *Indian J. Pharm. Educ. Res.* **2011**, *45* (2), 175–183. https://doi.org/10.1016/j.mtnano.2020.100076

(339) Lidström, P.; Tierney, J.; Wathey, B.; Westman, J. Microwave Assisted Organic Synthesis- A Review. *Tetrahedron* **2001**, *57* (1), 9225–9283. https://doi.org/10.1055/s-2006-925464.

(340) Surati, M. A.; Jauhari, S.; Desai, K. R. A Brief Review: Microwave Assisted Organic Reaction. *Sch. Res. Libr. Arch. Appl. Sci. Res.* **2012**, *2012* (1), 645–661.https://doi.org/10.1016/S0040-4020(01)00906-1

(341) Perreux, L.; Loupy, A. A Tentative Rationalization of Microwave Effects in Organyc Synthesis According to the Reaction Medium, and Mechanistic Considerations. *Tetrahedron* **2001**, *57* (588), 9199–9223. https://doi.org/10.1016/S0040-4020(01)00905-X.

(342) Langa, F.; De La Cruz, P.; De La Hoz, A.; Diaz-Ortiz, A.; Diez-Barra, E. Microwave Irradiation: More than Just a Method for Accelerating Reactions. *Contemp. Org. Synth.* **1996**, *34* (7), 373–386. https://doi.org/10.1039/CO9970400373

(343) Branco, P. D.; Yablonsky, G.; Marin, G. B.; Constales, D. The Switching Point between Kinetic and Thermodynamic Control. *Comput. Chem. Eng.* **2019**, *125*, 606–611. https://doi.org/10.1016/j.compchemeng.2016.06.022.

(344) Kwak, J. M.; Moon, J. S.; Choi, J. I.; Murugan, R. N.; Park, W. K.; Gong, J. Y.; Lee, H. Y.; Koh, H. Y. Construction of a Library of Arylpiperazinyl 1,2,3-Triazole Derivatives as Ligands for Dopamine D3/D4 Receptor. *Bull. Korean Chem. Soc.* **2013**, *34* (11), 3467–3470. https://doi.org/10.5012/bkcs.2013.34.11.3467.

(345) Bajda, M.; Łażewska, D.; Godyń, J.; Zaręba, P.; Kuder, K.; Hagenow, S.; Łątka, K.; Stawarska, E.; Stark, H.; Kieć-Kononowicz, K.; Malawska, B. Search for New Multi-Target Compounds against Alzheimer's Disease among Histamine H3 Receptor Ligands. *Eur. J. Med. Chem.* **2020**, *185*. https://doi.org/10.1016/j.ejmech.2019.111785.

(346) Krause, T.; Baader, S.; Erb, B.; Gooßen, L. J. Atom-Economic Catalytic Amide Synthesis from Amines and Carboxylic Acids Activated in Situ with Acetylenes. *Nat. Commun.* **2016**, *7*, 1–7. https://doi.org/10.1038/ncomms11732.

(347) El-Faham, A.; Albericio, F. Peptide Coupling Reagents, More than a Letter Soup. *Chem. Rev.* **2011**, *111* (11), 6557–6602. https://doi.org/10.1021/cr100048w.

(348) Montalbetti, C. A. G. N.; Falque, V. Amide Bond Formation and Peptide Coupling. *Tetrahedron* **2005**, *61* (740), 10827–10852. https://doi.org/10.1016/j.tet.2005.08.031.

(349) Vrettos, E. I.; Sayyad, N.; Mavrogiannaki, E. M.; Stylos, E.; Kostagianni, A. D.; Papas, S.; Mavromoustakos, T.; Theodorou, V.; Tzakos, A. G. Unveiling and Tackling Guanidinium Peptide Coupling Reagent Side Reactions towards the Development of Peptide-Drug Conjugates. *RSC Adv.* **2017**, *7* (80), 50519–50526. https://doi.org/10.1039/c7ra06655d.

(350) Regan, J.; Breitfelder, S.; Cirillo, P.; Gilmore, T.; Graham, A. G.; Hickey, E.; Klaus, B.; Madwed, J.; Moriak, M.; Moss, N.; Pargellis, C.; Pav, S.; Proto, A.; Swinamer, A.; Tong, L.; Torcellini, C. Pyrazole Urea-Based Inhibitors of P38 MAP Kinase : From Lead Compound to Clinical Candidate. *J. Med. Chem.* **2002**, *41*, 2994–3008. https://doi.org/10.1021/jm020057r

(351) Ghosh, A. K.; Brindisi, M. Urea Derivatives in Modern Drug Discovery and Medicinal Chemistry. *J. Med. Chem.* **2020**, *63*, 2751–2788. https://doi.org/10.1021/acs.jmedchem.9b01541.

(352) Pajouhesh, H.; Lenz, G. R. Medicinal Chemical Properties of Successful Central Nervous System Drugs. *NeuroRx* **2005**, *2* (10), 541–553. https://doi.org/10.1602/neurorx.2.4.541

(353) *Urea: Synthesis, Properties and Uses*; Munoz, C. M., Fernandez, A. M., Eds.; Nova Science Publishers, 2012.

(354) Ganis, P.; Goodman, M. Crystal and Molecular Structure of N,N′-Diethyl-N,N′-Diphenylurea. *Proc. Natl. Acad. Sci.* **1970**, *67* (1), 426–433. https://doi.org/10.1073/pnas.67.1.426.

(355) Zhang, Z.; Schreiner, P. R. (Thio) Urea Organocatalysis — What Can Be Learnt from Anion Recognition ? *Chem. Soc. Rev.* **2009**, *38*, 1187–1198. https://doi.org/10.1039/b801793j.

(356) Serdyuk, O. V; Heckel, C. M.; Tsogoeva, S. B. Bifunctional Primary Amine-Thioureas in Asymmetric Organocatalysis. *Org. Biomol. Chem.* **2013**, *11*, 7051–7071. https://doi.org/10.1039/c3ob41403e.

(357) Groszek, G. A Convenient Method of Synthesis of Unsymmetrical Urea Derivatives. *Org. Process Res. Dev.* **2002**, *6* (6), 759–761. https://doi.org/10.1021/op020055g

(358) Nowick, J. S.; Powell, N. A.; Nguyen, T. M.; Noronha, G. An Improved Method for the Synthesis of Enantiomerically Pure Amino Acid Ester Isocyanates. *J. Org. Chem.* **2019**, *57* (10), 7364–7366. https://doi.org/10.1021/jo00052a069

(359) Lai, E. C. C.; Chang, C. H.; Yang, Y. H. K.; Lin, S. J.; Lin, C. Y. Effectiveness of Sulpiride in Adult Patients with Schizophrenia. *Schizophr. Bull.* **2013**, *39* (3), 673–683. https://doi.org/10.1093/schbul/sbs002.

(360) McKeage, K.; Plosker, G. L. Amisulpride, A Review of Its Use in the Management of Schizophrenia. *CNS Drugs* **2012**, *18* (13), 934–952. https://doi.org/10.1093/ajhp/zxaa292.

(361) Santos Andrade, E. H.; Pan, P. M.; Ramalho Da Silva, P. F.; Gadelha, A. New Insights in the Management of Antipsychotics in the Treatment of Schizophrenia in a Patient with Prolactinoma: A Case Report and Review of the Literature. *Case Rep. Med.* **2010**, *2010*, 1–5. https://doi.org/10.1155/2010/573252.

(362) Pani, L.; Villagrán, J. M.; Kontaxakis, V. P.; Alptekin, K. Practical Issues with Amisulpride in the Management of Patients with Schizophrenia. *Clin. Drug Investig.* **2008**, *28* (8), 465–477. https://doi.org/10.2165/00044011-200828080-00001.

(363) Fideleff, H. L.; Belma, S.; Guitelman, A.; Baigorri, A. M.; Aquilano, D.; Scaglia, H. E. Sulpiride Stimulation of Prolactin Secretion in Adolescents with Gynecomastia: Relation to the Circulating Levels of Estradiol. *Acta Med. Port.* **1980**, *2* (4), 269–273. https://doi.org/10.20344/amp.4170

(364) Komossa, K.; Rummel-Kluge, C.; Hunger, H.; Schmid, F.; Schwarz, S.; Silveira da Mota Neto, J. I.; Kissling, W.; Leucht, S. Amisulpride versus Other Atypical Antipsychotics for Schizophrenia. *Cochrane Database Syst. Rev.* **2014**, No. 2, 1–106. https://doi.org/10.1002/14651858.cd006624.pub2.

(365) Perrone, R.; Berardi, F.; Colabufo, N. A.; Leopoldo, M.; Tortorella, V. N-[2-[4-(4-Chlorophenyl)Piperazin-1-Yl]Ethyl]-3-Methoxybenzamide: A Potent and Selective D4 Ligand. *J. Med. Chem.* **1998**, *41*, 4903–4909. https://doi.org/10.1021/jm981041x

(366) Gadhiya, S.; Cordone, P.; Pal, R. K.; Gallicchio, E.; Wickstrom, L.; Kurtzman, T.; Ramsey, S.; Harding, W. W. New Dopamine D3-Selective Receptor Ligands Containing a 6-Methoxy-1,2,3,4-Tetrahydroisoquinolin-7-Ol Motif. *ACS Med. Chem. Lett.* **2018**, *9* (10), 990–995. https://doi.org/10.1021/acsmedchemlett.8b00229.

(367) Hodgson, H. H. The Sandmeyer Reaction. *Chem. Rev.* **1947**, 251–277. https://doi.org/10.1021/cr60126a003

(368) Akhtar, R.; Fawad, A.; Nasir, Z.; Matloob, R.; Kulsoom, A.; Ali, G. *Recent Trends in the Chemistry of Sandmeyer Reaction : A Review*; Springer International Publishing, 2022; Vol. 26. https://doi.org/10.1007/s11030-021-10295-3.

(369) Yan, Y.; Li, H.; Niu, B.; Zhu, C.; Chen, T.; Liu, Y. Mild and Efficient TBAI-Catalyzed Synthesis of 1,2,3-Benzotriazine- 4- (3 H) -Ones from Tert -Butyl Nitrite and 2-Aminobenzamides under Acid-Free Conditions. *Tetrahedron Lett.* **2016**, *57* (37), 4170–4173. https://doi.org/10.1016/j.tetlet.2016.07.102.

(370) Khaligh, N. G.; Johan, B. M. R.; A, J. J. C. Saccharin and Tert-Butyl Nitrite : Cheap and Efficient Reagents for the Synthesis of 1, 2, 3-Benzotriazine-4- (3 H)-Ones from 2-Aminobenzamides under Metal-Free Conditions. *Aust. J. Chem.* **2018**, *71*, 186–189. https://doi.org/10.1071/CH17590

(371) Barak, D. S.; Mukhopadhyay, S.; Dahatonde, D. J.; Batra, S. NaNO2/I2 as an Alternative Reagent for the Synthesis of 1, 2, 3-Benzotriazin-4-(3H)-Ones from 2-Aminobenzamides. *Tetrahedron Lett.* **2019**, *60* (3), 248–251. https://doi.org/10.1016/j.tetlet.2018.12.025.

(372) McGrory, R.; Faggyas, R. J.; Sutherland, A. Biomolecular Chemistry Triazoles via Stable Arene Diazonium Salts †. *Org. Biomol. Chem.* **2021**, *19* (4), 6127–6140. https://doi.org/10.1039/d1ob00968k.

(373) Subbaiah, M. A. M.; Meanwell, N. A. Bioisosteres of the Phenyl Ring: Recent Strategic Applications in Lead Optimization and Drug Design. *J. Med. Chem.* **2021**, *64* (19), 14046–14128. https://doi.org/10.1021/acs.jmedchem.1c01215.

(374) Ostrowska, K. Coumarin-Piperazine Derivatives as Biologically Active Compounds. *Saudi Pharm. J.* **2020**, *28* (2), 220–232. https://doi.org/10.1016/j.jsps.2019.11.025.

(375) Żołek, T.; Dömötör, O.; Ostrowska, K.; Enyedy, É. A.; Maciejewska, D. Evaluation of Blood-Brain Barrier Penetration and Examination of Binding to Human Serum Albumin of 7-O-Arylpiperazinylcoumarins as Potential Antipsychotic Agents. *Bioorg. Chem.* **2019**, *84* (11), 211–225. https://doi.org/10.1016/j.bioorg.2018.11.034.

(376) Chen, Y.; Wang, S.; Xu, X.; Liu, X.; Yu, M.; Zhao, S.; Liu, S.; Qiu, Y.; Zhang, T.; Liu, B.-F.; Zhang, G. Synthesis and Biological Investigation of Coumarin Piperazine Derivatives as Potential Multireceptor Atypical Antipsychotics. *J. Med. Chem.* **2013**, *56* (8), 4671–4690. https://doi.org/10.1016/j.bmcl.2020.127027.

(377) Chen, Y.; Lan, Y.; Wang, S.; Zhang, H.; Xu, X.; Liu, X.; Yu, M.; Liu, B. F.; Zhang, G. Synthesis and Evaluation of New Coumarin Derivatives as Potential Atypical Antipsychotics. *Eur. J. Med. Chem.* **2014**, *74*, 427–439. https://doi.org/10.1016/j.ejmech.2014.01.012.

(378) Santana, L.; Uriarte, E.; Fall, Y.; Teijeira, M.; Terán, C.; García-Martínez, E.; Tolf, B. R. Synthesis and Structure-Activity Relationships of New Arylpiperazines: Para Substitution with Electron-Withdrawing Groups Decrease Binding to 5-HT1A and D2A Receptors. *Eur. J. Med. Chem.* **2002**, *37* (6), 503–510. https://doi.org/10.1016/S0223-5234(02)01357-0.

(379) Zhang, Q.; Soulère, L.; Queneau, Y. Amide Bioisosteric Replacement in the Design and Synthesis of Quorum Sensing Modulators. *Eur. J. Med. Chem.* **2024**, *273*, 116525. https://doi.org/10.1016/j.ejmech.2024.116525.

(380) Frank, A.; Kiss, D. J.; Keserű, G. M.; Stark, H. Binding Kinetics of Cariprazine and Aripiprazole at the Dopamine D3 Receptor. *Sci. Rep.* **2018**, *8* (1), 1–9. https://doi.org/10.1038/s41598-018-30794-y.

(381) McKinney, M.; Raddatz, R. Practical Aspects of Radioligand Binding. *Curr. Protoc. Pharmacol.* **2006**, No. 1, 1–42. https://doi.org/10.1002/0471141755.ph0103s33.

(382) Bylund, D. B.; Toews, M. L. Radioligand Binding Methods Practical Guide and Tips. *Am. J. Physiol.*

- *Lung Cell. Mol. Physiol.* **1993**, *265* (5), 421–429. https://doi.org/10.1152/ajplung.1993.265.5.l421.

(383) Mendel, C. M.; Mendel, D. B. "Non-Specific" Binding, the Problem and a Solution. *Biochem. J.* **1985**, *228* (1), 269–272. https://doi.org/10.1042/bj2280269

(384) Motulsky, H. J.; Neubig, R. R. *Analyzing Binding Data*; 2010; Vol. 52. https://doi.org/10.1002/0471142301.ns0705s52.

(385) Rosenthal, H. E. A Graphic Method for the Determination Parameters. *Anal. Biochem.* **1967**, *20* (3), 525–532. https://doi.org/10.1016/0003-2697(67)90297-7

(386) Cheng, Y.; Prusoff, W. H. Relationship between the Inhibition Constant (Ki) and the Concentration of Inhibitor Which Causes 50 per Cent Inhibition (I50) of an Enxymatic Reaction. *Biochem. Pharmacol.* **1973**, *22*, 3099–3108. https://doi.org/10.1016/0006-2952(73)90196-2

(387) Cheng, H. C. The Power Issue: Determination of KB or Ki from IC50 - A Closer Look at the Cheng-Prusoff Equation, the Schild Plot and Related Power Equations. *J. Pharmacol. Toxicol. Methods* **2002**, *46* (2), 61–71. https://doi.org/10.1016/S1056-8719(02)00166-1.

(388) Sander, T.; Freyss, J.; Von Korff, M.; Rufener, C. DataWarrior: An Open-Source Program for Chemistry Aware Data Visualization and Analysis. *J. Chem. Inf. Model.* **2015**, *55* (2), 460–473. https://doi.org/10.1021/ci500588j.

(389) Benet, L. Z.; Hosey, C. M.; Ursu, O.; Oprea, T. I. BDDCS, the Rule of 5 and Drugability. *Adv. Drug Deliv. Rev.* **2016**, *101*, 89–98. https://doi.org/10.1016/j.addr.2016.05.007.

(390) Lipinski, C. A.; Lombardo, F.; Dominy, B. W.; Feeney, P. J. Experimental and Computational Approaches to Estimate Solubility and Permeability in Drug Discovery and Development Settings. *Adv. Drug Deliv. Rev.* **1997**, *23* (6), 3–25. https://doi.org/10.1016/S0169-409X(96)00423-1

(391) Lipinski, C. A.; Lombardo, F.; Dominy, B. W.; Feeney, P. J. Experimental and Computational Approaches to Estimate Solubility and Permeability in Drug Discovery and Development Settings. *Adv. Drug Deliv. Rev.* **2012**, *64*, 4–17. https://doi.org/10.1016/j.addr.2012.09.019.

(392) Via, M. A.; Chandra, H.; Takako, A.; Potenza, M. V; Skamagas, M. Bromocriptine Approved as the First Medication to Target Dopamine Activity to Improve Glycemic Control in Patients with Type 2 Diabetes. *Diabetes, Metab. Syndr. Obes. Targets Ther.* **2010**, *3*, 43–48. https://doi.org/10.2147/dmsott.s9575

(393) Deininger, M.; Buchdunger, E.; Druker, B. J. The Development of Imatinib as a Therapeutic Agent for Chronic Myeloid Leukemia. *Am. Soc. Hematol.* **2005**, *105* (7), 2640–2653. https://doi.org/10.1182/blood-2004-08-3097.Supported.

(394) Davis, R.; Coukell, A.; McTavish, D. Fosinopril A Review of Its Pharmacology and Clinical Efficacy in the Management of Heart Failure. *Adis Dug Eval.* **1997**, *54* (1), 103–116.

https://doi.org/10.2165/00003495-199754010-00012

(395) Manto Chagas, C.; Moss, S.; Alisaraie, L. Drug Metabolites and Their Effects on the Development of Adverse Reactions: Revisiting Lipinski's Rule of Five. *Int. J. Pharm.* **2018**, *549* (2), 133–149. https://doi.org/10.1016/j.ijpharm.2018.07.046.

(396) Roskoski Jr., R. Rule of Five Violations among the FDA-Approved Small Molecule Protein Kinase Inhibitors. *Pharmacol. Res.* **2023**, *191* (7), 106774. https://doi.org/10.1016/j.phrs.2023.106774.

(397) Ursu, O.; Rayan, A.; Goldblum, A.; Oprea, T. I. Understanding Drug-Likeness. *Wiley Interdiscip. Rev. Comput. Mol. Sci.* **2011**, *1* (5), 760–781. https://doi.org/10.1002/wcms.52.

(398) Van De Waterbeemd, H.; Camenisch, G.; Folkers, G.; Chretien, J. R.; Raevsky, O. A. Estimation of Blood-Brain Barrier Crossing of Drugs Using Molecular Size and Shape, and H-Bonding Descriptors. *J. Drug Target.* **1998**, *6* (2), 151–165. https://doi.org/10.3109/10611869808997889.

(399) Veber, D. F.; Johnson, S. R.; Cheng, H.-Y.; Smith, B. R.; Ward, K. W.; Kopple, K. D. Molecular Properties That Influence the Oral Bioavailability of Drug Candidates. *J. Med. Chem.* **2002**, *45* (7), 2615–2623. https://doi.org/10.1021/jm020017n

(400) Garcia-Ladona, F. J.; Cox, B. F. BP 897 , a Selective Dopamine D 3 Receptor Ligand with Therapeutic Potential for the Treatment of Cocaine-Addiction. *CNS Drug Rev.* **2003**, *9* (2), 141–158. https://doi.org/10.1111/j.1527-3458.2003.tb00246.x

(401) Oldak, S. E.; Chaparro, M. C.; Jean-paul, L. A. A Brief Review of Cariprazine. *Am. J. Psychiatry* **2024**, *19* (3), 6–8. https://doi.org/10.1176/appi.ajp-rj.2024.190302

(402) Ertl, P.; Rohde, B.; Selzer, P. Fast Calculation of Molecular Polar Surface Area as a Sum of Fragment-Based Contributions and Its Application to the Prediction of Drug Transport Properties. *J. Med. Chem.* **2000**, *43* (20), 3714–3717. https://doi.org/10.1021/jm000942e.

(403) Pires, D. E. V.; Blundell, T. L.; Ascher, D. B. PkCSM: Predicting Small-Molecule Pharmacokinetic and Toxicity Properties Using Graph-Based Signatures. *J. Med. Chem.* **2015**, *58* (9), 4066–4072. https://doi.org/10.1021/acs.jmedchem.5b00104.

(404) Vangveravong, S.; Zhang, Z.; Taylor, M.; Bearden, M.; Xu, J.; Cui, J.; Wang, W.; Luedtke, R. R.; MacH, R. H. Synthesis and Characterization of Selective Dopamine D2 Receptor Ligands Using Aripiprazole as the Lead Compound. *Bioorganic Med. Chem.* **2011**, *19* (11), 3502–3511. https://doi.org/10.1016/j.bmc.2011.04.021.

(405) Leopoldo, M.; Lacivita, E.; Colabufo, N. A.; Berardi, F.; Perrone, R. Synthesis and Binding Profile of Constrained Analogues of N -[4-(4-Arylpiperazin-1-Yl)Butyl]-3-Methoxybenzamides, a Class of Potent Dopamine D3 Receptor Ligands . *J. Pharm. Pharmacol.* **2010**, *58* (2), 209–218. https://doi.org/10.1211/jpp.58.2.0008.

(406) Vamvakopoulou, I. A.; Narine, K. A. D.; Campbell, I.; Dyck, J. R. B.; Nutt, D. J. Mescaline: The Forgotten Psychedelic. *Neuropharmacology* **2023**, *222* (June 2022), 109294. https://doi.org/10.1016/j.neuropharm.2022.109294.

(407) Rickli, A.; Moning, O. D.; Hoener, M. C.; Liechti, M. E. Receptor Interaction Profiles of Novel Psychoactive Tryptamines Compared with Classic Hallucinogens. *Eur. Neuropsychopharmacol.* **2016**, *26* (8), 1327–1337. https://doi.org/10.1016/j.euroneuro.2016.05.001.

(408) Agin-Liebes, G.; Haas, T. F.; Lancelotta, R.; Uthaug, M. V.; Ramaekers, J. G.; Davis, A. K. Naturalistic Use of Mescaline Is Associated with Self-Reported Psychiatric Improvements and Enduring Positive Life Changes. *ACS Pharmacol. Transl. Sci.* **2021**, *4* (2), 543–552. https://doi.org/10.1021/acsptsci.1c00018.

(409) Teran, C.; Santana, L.; Uriarte, E.; Fall, Y.; Unelius, L.; Tolf, B. R. Phenylpiperazine Derivatives with Strong Affinity for 5HT1A, D2A and D3 Receptors. *Bioorg. Med. Chem. Lett.* **1998**, *8*, 3567–3570. https://doi.org/10.1016/S0960-894X(98)00646-5

(410) Procopiou, P. A.; Ancliff, R. A.; Gore, P. M.; Hancock, A. P.; Hodgson, S. T.; Holmes, D. S.; Keeling, S. P.; Looker, B. E.; Parr, N. A.; Rowedder, J. E.; Slack, R. J. The Discovery of Quinoline Based Single-Ligand Human H1and H3receptor Antagonists. *Bioorganic Med. Chem. Lett.* **2016**, *26* (24), 5855–5859. https://doi.org/10.1016/j.bmcl.2016.11.022.

(411) Rueter, J. K.; Nortey, S. O.; Baxter, E. W.; Leo, G. C.; Reitz, A. B. Arylsulfonate Esters in Solid Phase Organic Synthesis. I. Cleavage with Amines, Thiolate, and Imidazole. *Tetrahedron Lett.* **1998**, *39* (9), 975–978. https://doi.org/10.1016/S0040-4039(97)10719-5.

(412) Hussain, H.; Al-Harrasi, A.; Green, I. R.; Ahmed, I.; Abbas, G.; Rehman, N. U. Meta-Chloroperbenzoic Acid (MCPBA): A Versatile Reagent in Organic Synthesis. **2014**. https://doi.org/10.1039/c3ra45702h.

(413) Reuman, M.; Beish, S.; Davis, J.; Batchelor, M. J.; Hutchings, M. C.; Moffat, D. F. C.; Connolly, P. J.; Russell, R. K. Scalable Synthesis of the VEGF-R2 Kinase Inhibitor JNJ-17029259 Using Ultrasound-Mediated Addition of MeLi-CeCl3 to a Nitrile. *J. Org. Chem.* **2008**, *73* (3), 1121–1123. https://doi.org/10.1021/jo7021372.

(414) Silva, R. O.; de Oliveira, A. S.; Nunes Lemes, L. F.; de Camargo Nascente, L.; Coelho do Nascimento Nogueira, P.; Silveira, E. R.; Brand, G. D.; Vistoli, G.; Cilia, A.; Poggesi, E.; Buccioni, M.; Marucci, G.; Bolognesi, M. L.; Romeiro, L. A. S. Synthesis and Structure–Activity Relationships of Novel Arylpiperazines as Potent Antagonists of A1-Adrenoceptor. *Eur. J. Med. Chem.* **2016**, *122*, 601–610. https://doi.org/10.1016/j.ejmech.2016.06.052.

(415) Peng, Y.; Liu, H.; Tang, M.; Cai, L.; Pike, V. Highly Efficient N-Monomethylation of Primary Aryl Amines. *Chinese J. Chem.* **2009**, *27* (7), 1339–1344. https://doi.org/10.1002/cjoc.200990224.

(416) Chen, L.; Huang, G.; Lü, M.; Zhang, Y.; Xu, J.; Bai, S. Amide Derivatives of Gallic Acid : Design ,

Synthesis and Evaluation of Inhibitory Activities against in Vitro α-Synuclein Aggregation. *Bioorganic Med. Chem.* **2020**, *28* (April). https://doi.org/10.1016/j.bmc.2020.115596.

(417) Buscató, E. La; Blöcher, R.; Lamers, C.; Klingler, F. M.; Hahn, S.; Steinhilber, D.; Schubert-Zsilavecz, M.; Proschak, E. Design and Synthesis of Dual Modulators of Soluble Epoxide Hydrolase and Peroxisome Proliferator-Activated Receptors. *J. Med. Chem.* **2012**, *55* (23), 10771–10775. https://doi.org/10.1021/jm301194c.

(418) Li, F.; Liang, X.; Jiang, Z.; Wang, A.; Wang, J.; Chen, C.; Wang, W.; Zou, F.; Qi, Z.; Liu, Q.; Hu, Z.; Cao, J.; Wu, H.; Wang, B.; Wang, L.; Liu, J.; Liu, Q. Discovery of (S)-2-(1-(4-Amino-3-(3-Fluoro-4-Methoxyphenyl)-1 H-Pyrazolo[3,4- d]Pyrimidin-1-Yl)Propyl)-3-Cyclopropyl-5-Fluoroquinazolin-4(3 H)-One (IHMT-PI3Kδ-372) as a Potent and Selective PI3KδInhibitor for the Treatment of Chronic Obstructive Pulmonary. *J. Med. Chem.* **2020**, *63* (22), 13973–13993. https://doi.org/10.1021/acs.jmedchem.0c01544.

(419) Aravapalli, S.; Lai, H.; Teramoto, T.; Alliston, K. R.; Lushington, G. H.; Ferguson, E. L.; Padmanabhan, R.; Groutas, W. C. Inhibitors of Dengue Virus and West Nile Virus Proteases Based on the Aminobenzamide Scaffold. *Bioorganic Med. Chem.* **2012**, *20* (13), 4140–4148. https://doi.org/10.1016/j.bmc.2012.04.055.

(420) Zarei, O.; Azimian, F.; Hamzeh-Mivehroud, M.; Shahbazi Mojarrad, J.; Hemmati, S.; Dastmalchi, S. Design, Synthesis, and Biological Evaluation of Novel Benzo[b]Thiophene-Diaryl Urea Derivatives as Potential Anticancer Agents. *Med. Chem. Res.* **2020**, *29* (8), 1438–1448. https://doi.org/10.1007/s00044-020-02559-8.

(421) Hartz, R. A.; Xu, L.; Sit, S. Y.; Chen, J.; Venables, B. L.; Lin, Z.; Zhang, S.; Li, Z.; Parker, D.; Simmons, T. S.; Jenkins, S.; Hanumegowda, U. M.; Dicker, I.; Krystal, M.; Meanwell, N. A.; Regueiro-Ren, A. Synthesis, Structure-Activity Relationships, and in Vivo Evaluation of Novel C-17 Amine Derivatives Based on GSK3640254 as HIV-1 Maturation Inhibitors with Broad Spectrum Activity. *J. Med. Chem.* **2022**, *65* (23), 15935–15966. https://doi.org/10.1021/acs.jmedchem.2c01618.

(422) Bisceglia, J. A.; Orelli, L. R. Recent Progress in the Horner-Wadsworth-Emmons Reaction. *Curr. Org. Chem.* **2015**, *19* (1113), 744–775. https://doi.org/10.1002/CHIN.201537252

(423) Rodríguez-Franco, M. I.; Fernández-Bachiller, M. I.; Pérez, C.; Castro, A.; Martínez, A. Design and Synthesis of N-Benzylpiperidine-Purine Derivatives as New Dual Inhibitors of Acetyl- and Butyrylcholinesterase. *Bioorganic Med. Chem.* **2005**, *13* (24), 6795–6802. https://doi.org/10.1016/j.bmc.2005.07.019.

(424) Piscitelli, F.; Ligresti, A.; La Regina, G.; Coluccia, A.; Morera, L.; Allarà, M.; Novellino, E.; Di Marzo, V.; Silvestri, R. Indole-2-Carboxamides as Allosteric Modulators of the Cannabinoid CB 1 Receptor. *J. Med. Chem.* **2012**, *55* (11), 5627–5631. https://doi.org/10.1021/jm201485c.

(425) Regueiro-Ren, A.; Swidorski, J. J.; Liu, Z.; Chen, Y.; Sin, N.; Sit, S. Y.; Chen, J.; Venables, B. L.; Zhu, J.; Nowicka-Sans, B.; Protack, T.; Lin, Z.; Terry, B.; Samanta, H.; Zhang, S.; Li, Z.; Easter, J.; Beno, B. R.; Arora, V.; Huang, X. S.; Rahematpura, S.; Parker, D. D.; Haskell, R.; Santone, K. S.; Cockett, M. I.; Krystal, M.; Meanwell, N. A.; Jenkins, S.; Hanumegowda, U.; Dicker, I. B. Design, Synthesis, and SAR of C-3 Benzoic Acid, C-17 Triterpenoid Derivatives. Identification of the HIV-1 Maturation Inhibitor 4-((1 R,3a S,5a R,5b R,7a R,11a S,11b R,13a R,13b R)-3a-((2-(1,1-Dioxidothiomorpholino)Ethyl)Amino)-5a,5b,8,8,11a-Pentamethyl-1. *J. Med. Chem.* **2018**, *61* (16), 7289–7313. https://doi.org/10.1021/acs.jmedchem.8b00854.

(426) Wang, Y.; Huang, D.; Cheng, Y.-X. Structural Optimization , Fungicidal Activities Evaluation , DFT Study and Structure-Activity Relationship of Dopamine Derivatives with Benzothiazole Fragment from Polyrhachis. *Chem. Biodivers.* **2023**, *20*, 1–8. https://doi.org/10.1002/cbdv.202300533.

(427) Katsura, Y.; Inoue, Y.; Tomoi, M.; Takasugi, H. Studies on Antiulcer Drugs. *Chem. Pharm. Bull.* **1992**, *40* (8), 2062–2074. https://doi.org/10.1248/cpb.40.2062

(428) Capaldo, L.; Quadri, L. L.; Merli, D.; Ravelli, D. Photoelectrochemical Cross-Dehydrogenative Coupling of Benzothiazoles with Strong Aliphatic C-H Bonds. *Chem. Commun.* **2021**, *57* (36), 4424–4427. https://doi.org/10.1039/d1cc01012c.

(429) Fujiyoshi, K.; Kawashima, S. A.; Yamatsugu, K.; Kanai, M. A Single-Step Asymmetric Phosphodiester Synthesis from Alco- Hols with Phosphoenolpyruvate Phosphodiester. *Synlett* **2021**, *32*, 1135–1140. https://doi.org/10.1055/a-1509-9275.

(430) Farina, R.; Pisani, L.; Catto, M.; Nicolotti, O.; Gadaleta, D.; Denora, N.; Soto-Otero, R.; Mendez-Alvarez, E.; Passos, C. S.; Muncipinto, G.; Altomare, C. D.; Nurisso, A.; Carrupt, P. A.; Carotti, A. Structure-Based Design and Optimization of Multitarget-Directed 2 H -Chromen-2-One Derivatives as Potent Inhibitors of Monoamine Oxidase B and Cholinesterases. *J. Med. Chem.* **2015**, *58* (14), 5561–5578. https://doi.org/10.1021/acs.jmedchem.5b00599.

(431) Sole, R.; Toldo, S.; Bortoluzzi, M.; Beghetto, V. A Sustainable Route for the Synthesis of Alkyl Arylacetates via Halogen and Base Free Carbonylation of Benzyl Acetates. *Catal. Sci. Technol.* **2022**, *12*, 4561–4571. https://doi.org/10.1039/d2cy00203e.

(432) Li, G.; Dong, H.; Ma, Y.; Shao, K.; Li, Y.; Wu, X.; Wang, S.; Shao, Y.; Zhao, W. Structure-Activity Relationships Study of Neolamellarin A and Its Analogues as Hypoxia Inducible Factor-1 (HIF-1) Inhibitors. *Bioorganic Med. Chem. Lett.* **2019**, *29* (16), 2327–2331. https://doi.org/10.1016/j.bmcl.2019.06.017.

(433) Aechtner, T.; Barry, D. A.; David, E.; Ghellamallah, C.; Harvey, D. F.; De La Houpliere, A.; Knopp, M.; Malaska, M. J.; Pérez, D.; Schärer, K. A.; Siesel, B. A.; Vollhardt, K. P. C.; Zitterbart, R. Cobalt-Mediated [2+2+2] Cycloadditions of Alkynes to Benzo-[b]Furans and Benzo[b]Thiophenes: A

Potential Route toward Morphanoids. *Synth.* **2018**, *50* (5), 1053–1089. https://doi.org/10.1055/s-0036-1589147.

(434) Sokoloff, P.; Andrieux, M.; Besançon, R.; Pilon, C.; Martres, M. P.; Giros, B.; Schwartz, J. C. Pharmacology of Human Dopamine D 3 Receptor Expressed in a Mammalian Cell Line: Comparison with D 2 Receptor. *Eur. J. Pharmacol. Mol. Pharmacol.* **1992**, *225* (4), 331–337. https://doi.org/10.1016/0922-4106(92)90107-7.

ACKNOWLEDGEMENTS

I would like to thank:

- Professor Holger Stark for having believed in me 4 years ago and for having given to me the opportunity of executing my PhD project in his laboratories.
- Professor Constantin Czekelius for evaluating my PhD thesis and for being always available to my questions about chemical challenges during these years.
- Dr. Aleksandra Zivkovic for having determined the purity grade of my compounds.
- Dr Annika Frank and Luisa Leitzbach for having determined the affinity data of my compounds.
- The Italian Erasmus student Erika Saccullo for her support together with Flavia and Maria. They made me feel at home in this cold Germany.
- All the technicians and colleagues, that I met during these years, for having shared time and work with me. Without these people, the workflow in the laboratories would not have been so effective.

I would like to express my deepest gratitude to Will and Jonas, my beloved friends in Germany. Guys, I feel that this experience would have been even harder without you. Especially, you were an enormous support at the beginning of my journey to establish myself in a new country and during the months of pandemic. I will never forget what you have done for me and I will be always grateful for the memories, fun and experiences that we shared together. Thank you.

For Hannah, these words mean nothing in comparison to the real life, but I must say thanks to you also here. I am grateful every day for having met you in my life. I would have never concluded this pathway without you. Thanks to you, I have learned that there is always hope, there is always the sun behind the clouds and that “5 minuten” can change the day or even the life. You are the greatest and kindest human being that I have ever met. Thank you.

Being emotive was never, is never and will be never a problem. Emotions, passion and love are the driving forces of human beings. That´s why, be always proud of the man and of the human being that you have become so far, Cristian.